Damping Models for Structural Vibration

Cambridge University
Engineering Department

A dissertation
submitted to the University of Cambridge
for the Degree of Doctor of Philosophy

by

Sondipon Adhikari
Trinity College, Cambridge

September, 2000

To my Parents

Declaration

This dissertation describes part of the research performed at the Cambridge University Engineering Department between October 1997 and September 2000. It is the result of my own work and includes nothing which is the outcome of work done in collaboration, except where stated. The dissertation contains approximately 63,000 words, 120 figures and 160 references.

Sondipon Adhikari
September, 2000

Abstract

This dissertation reports a systematic study on *analysis* and *identification* of multiple parameter damped mechanical systems. The attention is focused on viscously and non-viscously damped multiple degree-of-freedom linear vibrating systems. The non-viscous damping model is such that the damping forces depend on the past history of motion via convolution integrals over some kernel functions. The familiar viscous damping model is a special case of this general linear damping model when the kernel functions have no memory.

The concept of proportional damping is critically examined and a generalized form of proportional damping is proposed. It is shown that the proportional damping can exist even when the damping mechanism is non-viscous.

Classical modal analysis is extended to deal with general non-viscously damped multiple degree-of-freedom linear dynamic systems. The new method is similar to the existing method with some modifications due to non-viscous effect of the damping mechanism. The concept of (complex) *elastic modes* and *non-viscous modes* have been introduced and numerical methods are suggested to obtain them. It is further shown that the system response can be obtained exactly in terms of these modes. Mode orthogonality relationships, known for undamped or viscously damped systems, have been generalized to non-viscously damped systems. Several useful results which relate the modes with the system matrices are developed.

These theoretical developments on non-viscously damped systems, in line with classical modal analysis, give impetus towards understanding damping mechanisms in general mechanical systems. Based on a first-order perturbation method, an approach is suggested to the identify non-proportional viscous damping matrix from the measured complex modes and frequencies. This approach is then further extended to identify non-viscous damping models. Both the approaches are simple, direct, and can be used with incomplete modal data.

It is observed that these methods yield non-physical results by breaking the symmetry of the fitted damping matrix when the damping mechanism of the original system is significantly different from what is fitted. To solve this problem, approaches are suggested to preserve the symmetry of the identified viscous and non-viscous damping matrix.

The damping identification methods are applied experimentally to a beam in bending vibration with localized constrained layer damping. Since the identification method requires complex modal data, a general method for identification of complex modes and complex frequencies from a set of measured transfer functions have been developed. It is shown that the proposed methods can give useful information about the true damping mechanism of the beam considered for the experiment. Further, it is demonstrated that the damping identification methods are likely to perform quite well even for the case when noisy data is obtained.

The work conducted here clarifies some fundamental issues regarding damping in linear dynamic systems and develops efficient methods for analysis and identification of generally damped linear systems.

Acknowledgements

I am very grateful to my supervisor Prof. Jim Woodhouse for his technical guidance and encouraging association throughout the period of my research work in Cambridge. I would also like to thank Prof R. S. Langley for his interest into my research.

I would like to express my gratitude to the *Nehru Memorial Trust*, London, the *Cambridge Commonwealth Trust, The Committee of Vice-chancellors and Principals*, UK and *Trinity College*, Cambridge for providing the financial support during the period in which this research work was carried out.

I wish to take this opportunity to thank The Old Schools, Cambridge for awarding me the John Wibolt Prize 1999 for my paper (Adhikari, 1999).

I am thankful to my colleagues in the Mechanics Group of the Cambridge University Engineering Department for providing a congenial working atmosphere in the laboratory. I am particularly thankful to David Miller and Simon Smith for their help in setting up the experiment and James Talbot for his careful reading of the manuscript.

I also want to thank my parents for their inspiration, in spite of being far away from me. Finally, I want to thank my wife Sonia – without her constant mental support this work might not come into this shape.

Contents

List of Figures

List of Tables

Nomenclature

Chapters 1 and 2

$\mathbf{C}$	Viscous damping matrix
$\mathfrak{f}(t)$	Forcing vector
$\mathcal{F}$	Dissipation function
$\mathbf{I}_N$	Identity matrix of size N
i	Unit imaginary number, $i = \sqrt{-1}$
$\mathbf{K}$	Stiffness matrix
$\mathcal{L}$	Laglargian of the system
$\mathbf{M}$	Mass matrix
N	Degrees-of-freedom of the system
$\mathbf{O}_N$	Null matrix of size N
$\mathbf{q}(t)$	Vector of the generalized coordinates
Q_{nc_k}	Non-conservative forces
t	Time
$\mathcal{T}$	Kinetic energy of the system
$\mathcal{V}$	Potential energy of the system
$\mathbf{X}$	Matrices of the eigenvectors
$\mathbf{y}(t)$	Modal coordinates
$\mathfrak{z}(t)$	Response vector in the state-space
$\delta(t)$	Dirac-delta function
δ_{jk}	Kroneker-delta function
$\boldsymbol{\mathcal{G}}(t)$	Damping function in the time domain
ω_k	k-th undamped natural frequency
$\boldsymbol{\Omega}$	Diagonal matrix containing ω_k
τ	Dummy time variable

Chapter 3

$\mathbf{D}(s)$	Dynamic stiffness matrix
$\mathbf{G}(s)$	Damping function in the Laplace domain
$\mathbf{G}'(s)$	Damping function (in the Laplace domain) in the modal coordinates
$\mathbf{H}(s)$	Transfer function matrix in the Laplace domain
m	Order of the characteristic polynomial
s	Laplace domain parameter
$\mathbf{z}_j$	j-th eigenvector of the system
$\mathbf{Z}$	Matrix of the eigenvectors
p	Number of non-viscous modes, $p = m - 2N$
Q_j	Q-factors

$\mathbf{q_0}$	Vector of initial displacements
$\dot{\mathbf{q}}_\mathbf{0}$	Vector of initial velocities
$\mathbf{R}_j$	Residue matrix corresponding to the pole s_j
$\mathbf{x}_j$	j-th undamped eigenvector
$\alpha_l^{(j)}$	Constants associated with expansion of j-th elastic modes
s_j	j-th eigenvalue of the system
$\mathbf{\Phi}(s)$	Matrix of the eigenvectors of $\mathbf{D}(s)$
μ	Parameter of the exponential damping model
μ_1, μ_2	Parameters of the GHM damping model
$\nu_k(s)$	k-th eigenvalue of $\mathbf{D}(s)$
$\boldsymbol{\nu}(s)$	Diagonal matrix containing $\nu_k(s)$

Chapter 4

$\mathbf{S}$	Diagonal matrix containing S_k
$\mathbf{\Theta}$	Normalization matrix
$(\bullet)_e$	Elastic modes
$(\bullet)n$	Non-viscous modes
$(\bullet)\prime$	Derivative of $(\bullet)$ with respect to s

Chapters 5, 6 and 7

$\bar{\mathbf{C}}$	Coefficient matrix associated with the non-viscous damping functions
$\mathbf{C}$	Viscous damping matrix
$\mathcal{D}(t)$	Energy dissipation function
$D(\omega)$	Fourier transform of $\mathcal{D}(t)$
$f(t)$	Non-viscous damping functions (not normalized)
$F(\omega)$	Fourier transform of $f(t)$
$F_R(\omega)$	Real part of $F(\omega)$
$F_I(\omega)$	Imaginary part of $F(\omega)$
$\boldsymbol{\mathcal{G}}(t)$	Damping function matrix in the time domain
$g(t)$	Normalized non-viscous damping functions
$\mathbf{G}(\omega)$	Fourier transform of damping function matrix $\boldsymbol{\mathcal{G}}(t)$
$G(\omega)$	Fourier transform of damping function $g(t)$
$G_R(\omega)$	Real part of $G(\omega)$
$G_I(\omega)$	Imaginary part of $G(\omega)$
$\mathbf{G}'(\omega)$	Frequency domain damping function matrix in the modal coordinates
$H_{ij}(\omega)$	Set of measured transfer functions
i	Unit imaginary number, $i = \sqrt{-1}$
$\mathbf{K}$	Stiffness matrix
m_μ	Number of modes used for estimation of $\hat{\mu}$
$\mathbf{M}$	Mass matrix
$\mathcal{M}_k$	k-th moment of $g(t)$
N	Degrees-of-freedom of the system

m	number of measured modes
Q_j	Q-factor for j-th mode
t	Time
T_{min}	Minimum time period for the system
$\mathbf{x}_j$	j-th undamped mode
$\mathbf{X}$	Matrix containing $\mathbf{x}_j$
$\mathbf{y}(t)$	Vector of the generalized coordinates
$\mathbf{z}_j$	j-th complex mode
$\hat{\mathbf{z}}_j$	j-th measured complex mode
$\hat{\mathbf{U}}$	Matrix containing $\hat{\mathbf{z}}_j$
$\hat{\mathbf{u}}_j$	Real part of $\hat{\mathbf{z}}_j$
$\hat{\mathbf{U}}$	Matrix containing $\hat{\mathbf{u}}_j$
$\hat{\mathbf{v}}_j$	Imaginary part of $\hat{\mathbf{z}}_j$
$\hat{\mathbf{V}}$	Matrix containing $\hat{\mathbf{v}}_j$
ω_j	j-th undamped natural frequency
λ_j	j-th complex natural frequency of the system
$\boldsymbol{\varepsilon}_j$	Error vector associated with j-th complex mode
$\alpha_l^{(j)}$	Constants associated with expansion of j-th elastic modes
ζ_j	j-th modal damping factor
μ	Relaxation parameter of the fitted damping model
$\hat{\mu}_j$	Estimated relaxation parameter for j-th mode
μ_1	Constant associated with exponential damping function
μ_2	Constant associated with Gaussian damping function
μ_3, μ_4	Constants associated with double exponential damping function
β_1, β_2	Weights associated with double exponential damping function
β	Normalization constant associated with non-viscous damping function, $f(t) = \beta g(t)$
$\hat{\theta}_j$	Estimated characteristic time constant for j-th mode
$\hat{\theta}(\omega)$	Frequency dependent estimated characteristic time constant
θ	Characteristic time constant
γ	Non-dimensional characteristic time constant
$\hat{(\bullet)}$	Estimated value of $(\bullet)$

Chapter 8

$H_n(\omega)$	Fitted transfer functions
$Y_n(\omega)$	Measured transfer functions
$R_{k_{jn}}$	Transfer function residues
$\varepsilon_n(\omega)$	frequency dependent error corresponding to nth transfer functions
$\mathbf{D}$	Hessian matrix
$\boldsymbol{\mathcal{V}}$	Vector of Q factors and natural frequencies
$\boldsymbol{\nabla}(\bullet)$	Gradient of $(\bullet)$
$\mathbf{M}'$	Mass matrix in the modal coordinates
$\boldsymbol{\Delta}(\bullet)$	Error associated with $(\bullet)$
$(\bullet)_0$	Error-free part of $(\bullet)$

Notations and Symbols

$\mathbb{C}$	Space of complex numbers
$\mathbb{R}$	Space of real numbers
i	Unit imaginary number, $\mathrm{i} = \sqrt{-1}$
$\Re(\bullet)$	Real part of $(\bullet)$
$\Im(\bullet)$	Imaginary part of $(\bullet)$
$\det(\bullet)$	Determinant of $(\bullet)$
adj$(\bullet)$	Adjoint matrix of $(\bullet)$
diag	A diagonal matrix
$\in$	Belongs to
$\forall$	For all
$(\bullet)^T$	Matrix transpose of $(\bullet)$
$(\bullet)^{-1}$	Matrix inverse of $(\bullet)$
$(\bullet)^{-T}$	Inverse transpose of $(\bullet)$
$\dot{(\bullet)}$	Derivative of $(\bullet)$ with respect to t
$(\bullet)^*$	Complex conjugate of $(\bullet)$
$\| \bullet \|$	l_2 matrix norm of $(\bullet)$
$\| \bullet \|$	Absolute value of $(\bullet)$

Abbreviations

DOF	Degrees of freedom
FEM	Finite element method
MDOF	Multiple-degrees-of-freedom system
PSD	Power spectral density
SDOF	Single-degree-of-freedom system

Chapter 1

Introduction

> *It is true that the grasping of truth is not possible without empirical basis. However, the deeper we penetrate and the more extensive and embracing our theories become, the less empirical knowledge is needed to determine those theories.*
>
> Albert Einstein, December 1952.

Problems involving vibration occur in many areas of mechanical, civil and aerospace engineering: wave loading of offshore platforms, cabin noise in aircrafts, earthquake and wind loading of cable stayed bridges and high rise buildings, performance of machine tools – to pick only few random examples. Quite often vibration is not desirable and the interest lies in reducing it by dissipation of vibration energy or *damping*. Characterization of damping forces in a vibrating structure has long been an active area of research in structural dynamics. Since the publication of Lord Rayleigh's classic monograph 'Theory of Sound (1877)', a large body of literature can be found on damping. Although the topic of damping is an age old problem, the demands of modern engineering have led to a steady increase of interest in recent years. Studies of damping have a major role in vibration isolation in automobiles under random loading due to surface irregularities and buildings subjected to earthquake loadings. The recent developments in the fields of robotics and active structures have provided impetus towards developing procedures for dealing with general dissipative forces in the context of structural dynamics. Beside these, in the last few decades, the sophistication of modern design methods together with the development of improved composite structural materials instilled a trend towards lighter structures. At the same time, there is also a constant demand for larger structures, capable of carrying more loads at higher speeds with minimum noise and vibration level as the safety/workability and environmental criteria become more stringent. Unfortunately, these two demands are conflicting and the problem cannot be solved without proper understanding of energy dissipation or damping behaviour. It is the aim of this dissertation is to develop fundamental techniques for the analysis and identification of damped structural systems.

In spite of a large amount of research, understanding of damping mechanisms is quite primitive. A major reason for this is that, by contrast with inertia and stiffness forces, it is not in general clear which *state variables* are relevant to determine the damping forces. Moreover, it seems that

in a realistic situation it is often the structural joints which are more responsible for the energy dissipation than the (solid) material. There have been detailed studies on the material damping (see Bert, 1973) and also on energy dissipation mechanisms in the joints (Earls, 1966, Beards and Williams, 1977). But here difficulty lies in representing all these tiny mechanisms in different parts of the structure in an unified manner. Even in many cases these mechanisms turn out be locally non-linear, requiring an equivalent linearization technique for a global analysis (Bandstra, 1983). A well known method to get rid of all these problems is to use the so called 'viscous damping'. This approach was first introduced by Rayleigh (1877) via his famous 'dissipation function', a quadratic expression for the energy dissipation rate with a symmetric matrix of coefficients, the 'damping matrix'. A further idealization, also pointed out by Rayleigh, is to assume the damping matrix to be a linear combination of the mass and stiffness matrices. Since its introduction this model has been used extensively and is now usually known as 'Rayleigh damping', 'proportional damping' or 'classical damping'. With such a damping model, the *modal analysis* procedure, originally developed for undamped systems, can be used to analyze damped systems in a very similar manner.

In this Chapter, we begin our discussion with classical dynamics of undamped systems. A brief review of literature on currently available damping models, techniques for analysis of damped dynamic systems and methods for identification of damping is presented. Based on this literature review, some open problems have been identified which are discussed in the subsequent Chapters of this dissertation.

From an analytical point of view, models of vibrating systems are commonly divided into two broad classes – discrete, or lumped-parameter models, and continuous, or distributed-parameter models. In real life, however, systems can contain both distributed and lumped parameter models (for example, a beam with a tip mass). Distributed-parameter modelling of vibrating systems leads to *partial-differential equations* as the equations of motion. Exact solutions of such equations are possible only for a limited number of problems with simple geometry, boundary conditions, and material properties (such as constant mass density). For this reason, normally we need some kind of approximate method to solve a general problem. Such solutions are generally obtained through spatial discretization (for example, the Finite Element Method, Zienkiewicz and Taylor, 1991), which amounts to approximating distributed-parameter systems by lumped-parameter systems. Equations of motion of lumped-parameter systems can be shown to be expressed by a set of coupled *ordinary-differential equations*. In this dissertation we mostly deal with such lumped-parameter systems. We also restrict our attention to the linear system behaviour only.

1.1 Dynamics of Undamped Systems

Linear dynamics of undamped systems occupy a central role in vibrational studies of engineering systems. This is also the starting point of the work taken up in this dissertation and here we briefly

outline the classical theory of linear dynamics of undamped systems.

1.1.1 Equation of Motion

Suppose that a system with N degrees of freedom is executing small oscillations around equilibrium points. The theory of small oscillations was studied in detail by Rayleigh (1877). Considering the vector of *generalized coordinates*

$$\mathbf{q} = \{q_1(t), q_2(t), \cdots, q_N(t)\}^T \in \mathbb{R}^N \tag{1.1}$$

the potential energy could be expanded in the form of a Taylor series in the neighborhood of the equilibrium position as (see Meirovitch, 1997, for details)

$$\mathcal{V}(\mathbf{q}) = \mathcal{V}(\mathbf{0}) + \sum_{j=1}^{N} \left(\frac{\partial \mathcal{V}}{\partial q_j}\right)_{\mathbf{q}=\mathbf{0}} q_j + \frac{1}{2}\sum_{j=1}^{N}\sum_{k=1}^{N} \left(\frac{\partial^2 \mathcal{V}}{\partial q_j \partial q_k}\right)_{\mathbf{q}=\mathbf{0}} q_j q_k + \mathcal{O}(\mathbf{q}^3). \tag{1.2}$$

Since the potential energy is defined only to a constant, it may be assumed that $\mathcal{V}(\mathbf{0}) = 0$, and consequently the second order approximation yields

$$\mathcal{V}(\mathbf{q}) = \frac{1}{2}\sum_{j=1}^{N}\sum_{k=1}^{N} K_{jk} q_j q_k \tag{1.3}$$

because second term is zero at equilibrium. Here the *elastic coefficients*

$$K_{jk} = \left(\frac{\partial^2 \mathcal{V}}{\partial q_j \partial q_k}\right)_{\mathbf{q}=\mathbf{0}}. \tag{1.4}$$

Equation (1.3) can also be put in the matrix positive definite quadratic form as

$$\mathcal{V}(\mathbf{q}) = \frac{1}{2}\mathbf{q}^T \mathbf{K} \mathbf{q} \tag{1.5}$$

where $\mathbf{K} \in \mathbb{R}^{N\times N}$, the (linear) *stiffness matrix* of the system, is symmetric and non-negative definite. In a similar way, in the absence of any centripetal and Coriolis forces, the kinetic energy of a system can be expressed as

$$\mathcal{T}(\mathbf{q}) = \frac{1}{2}\sum_{j=1}^{N}\sum_{k=1}^{N} M_{jk}\dot{q}_j \dot{q}_k = \frac{1}{2}\dot{\mathbf{q}}^T \mathbf{M} \dot{\mathbf{q}}. \tag{1.6}$$

In the above expression $\dot{\mathbf{q}}$ is the vector of the generalized velocities and $\mathbf{M} \in \mathbb{R}^{N\times N}$, the *mass matrix* of the system, is a symmetric and positive definite matrix. The equations of motion of free vibration can now be obtained by the application of Lagrange's equation

$$\frac{\mathrm{d}}{\mathrm{d}t}\left(\frac{\partial \mathcal{L}}{\partial \dot{q}_k}\right) - \frac{\partial \mathcal{L}}{\partial q_k} = Q_{\mathrm{nc}_k} + f_k, \quad \forall k = 1, \cdots, N \tag{1.7}$$

where $\mathcal{L} = \mathcal{T} - \mathcal{V}$ is the Lagrangian, Q_{nc_k} are the non-conservative forces and f_k are the applied forces acting on the system. For undamped systems $Q_{\mathrm{nc}_k} = 0, \forall k$. Using the expressions of $\mathcal{V}$ and $\mathcal{T}$ from equation (1.5) and (1.6) and substituting $\mathcal{L}$, from equation (1.7), the equations of motion of an undamped non-gyroscopic system can be obtained as

$$\mathbf{M}\ddot{\mathbf{q}}(t) + \mathbf{K}\mathbf{q}(t) = \mathfrak{f}(t) \tag{1.8}$$

where $\mathfrak{f}(t) \in \mathbb{R}^N$ is the forcing vector. Equation (1.8) represents a set of coupled second-order ordinary-differential equations. The solution of this equation also requires knowledge of the initial conditions in terms of the displacements and velocities of all the coordinates.

1.1.2 Modal Analysis

Rayleigh (1877) has shown that undamped linear systems, equations of motion of which are given by (1.8), are capable of so-called *natural motions*. This essentially implies that all the system coordinates execute harmonic oscillation at a given frequency and form a certain displacement pattern. The oscillation frequency and displacement pattern are called *natural frequencies* and *normal modes*, respectively. The natural frequencies (ω_j) and the mode shapes ($\mathbf{x}_j$) are intrinsic characteristic of a system and can be obtained by solving the associated matrix eigenvalue problem

$$\mathbf{K}\mathbf{x}_j = \omega_j^2 \mathbf{M}\mathbf{x}_j, \quad \forall\, j = 1, \cdots, N. \tag{1.9}$$

Since the above eigenvalue problem is in terms of real symmetric matrices $\mathbf{M}$ and $\mathbf{K}$, the eigenvalues and consequently the eigenvectors are real, that is $\omega_j \in \mathbb{R}$ and $\mathbf{x}_j \in \mathbb{R}^N$. In addition to this, it was also shown by Rayleigh that the undamped eigenvectors satisfy an orthogonality relationship over the mass and stiffness matrices, that is

$$\mathbf{x}_l^T \mathbf{M}\mathbf{x}_j = \delta_{lj} \tag{1.10}$$

$$\text{and} \quad \mathbf{x}_l^T \mathbf{K}\mathbf{x}_j = \omega_j^2 \delta_{lj}, \quad \forall\, l, j = 1, \cdots, N \tag{1.11}$$

where δ_{lj} is the Kroneker delta function. In the above equations the eigenvectors are unity mass normalized, a convention often used in practice. This orthogonality property of the undamped modes is very powerful as it allows to transform a set of coupled differential equations to a set of independent equations. For convenience, we construct the matrices

$$\mathbf{\Omega} = \mathrm{diag}\,[\omega_1, \omega_2, \cdots, \omega_N] \in \mathbb{R}^{N\times N} \tag{1.12}$$

$$\text{and} \quad \mathbf{X} = [\mathbf{x}_1, \mathbf{x}_2, \cdots, \mathbf{x}_N] \in \mathbb{R}^{N\times N} \tag{1.13}$$

where the eigenvalues are arranged such that $\omega_1 < \omega_2$, $\omega_2 < \omega_3, \cdots, \omega_k < \omega_{k+1}$. Use a coordinate transformation

$$\mathbf{q}(t) = \mathbf{X}\mathbf{y}(t). \tag{1.14}$$

Substituting $\mathbf{q}(t)$ in equation (1.8), premultiplying by $\mathbf{X}^T$ and using the orthogonality relationships in (1.12) and (1.13), the equations of motion in the modal coordinates may be obtained as

$$\ddot{\mathbf{y}}(t) + \mathbf{\Omega}^2\mathbf{y}(t) = \tilde{\mathfrak{f}}(t) \tag{1.15}$$

where $\tilde{\mathfrak{f}}(t) = \mathbf{X}^T\mathfrak{f}(t)$ is the forcing function in modal coordinates. Clearly, this method significantly simplifies the dynamic analysis because complex multiple degrees of freedom systems can be treated as collections of single degree of freedom oscillators. This approach of analyzing linear undamped systems is known as *modal analysis*, possibly the most efficient tool for vibration analysis of complex engineering structures.

1.2 Models of Damping

Damping is the dissipation of energy from a vibrating structure. In this context, the term dissipate is used to mean the transformation of energy into the other form of energy and, therefore, a removal of energy from the vibrating system. The type of energy into which the mechanical energy is transformed is dependent on the system and the physical mechanism that cause the dissipation. For most vibrating system, a significant part of the energy is converted into heat.

The specific ways in which energy is dissipated in vibration are dependent upon the physical mechanisms active in the structure. These physical mechanisms are complicated physical process that are not totally understood. The types of damping that are present in the structure will depend on which mechanisms predominate in the given situation. Thus, any mathematical representation of the physical damping mechanisms in the equations of motion of a vibrating system will have to be a generalization and approximation of the true physical situation. As Scanlan (1970) has observed, any mathematical damping model is really only a crutch which does not give a detailed explanation of the underlying physics.

For our mathematical convenience, we divide the elements that dissipate energy into three classes: (a) damping in single degree-of-freedom (SDOF) systems, (b) damping in continuous systems, and (c) damping in multiple degree-of-freedom (MDOF) systems. Elements such as dampers of a vehicle-suspension fall in the first class. Dissipation within a solid body, on the other hand, falls in the second class, demands a representation which accounts for both its intrinsic properties and its spatial distribution. Damping models for MDOF systems can be obtained by discretization of the equations of motion. There have been attempt to mathematically describe the damping in SDOF, continuous and MDOF systems.

1.2.1 Single Degree-of-freedom Systems

Free oscillation of an undamped SDOF system never die out and the simplest approach to introduce dissipation is to incorporate an ideal viscous dashpot in the model. The damping force (F_d) is

assumed to be proportional to the instantaneous velocity, that is

$$F_d = c\,\dot{x} \tag{1.16}$$

and the coefficient of proportionality, c is known as the dashpot-constant or viscous damping constant. The loss factor, which is the energy dissipation per radian to the peak potential energy in the cycle, is widely accepted as a basic measure of the damping. For a SDOF system this loss factor can be given by

$$\eta = \frac{c|\omega|}{k} \tag{1.17}$$

where k is the stiffness. The expression similar to this equation have been discussed by Ungar and Kerwin (1962) in the context of viscoelastic systems. Equation (1.17) shows a linear dependence of the loss factor on the driving frequency. This dependence has been discussed by Crandall (1970) where it has been pointed out that the frequency dependence, observed in practice, is usually not of this form. In such cases one often resorts to an equivalent ideal dashpot. Theoretical objections to the approximately constant value of damping over a range of frequency, as observed in aeroelasticity problems, have been raised by Naylor (1970). On the lines of equation (1.17) one is tempted to define the frequency-dependent dashpot as

$$c(\omega) = \frac{k\eta(\omega)}{|\omega|}. \tag{1.18}$$

This representation, however has some serious physical limitations. Crandall (1970, 1991), Newland (1989) and Scanlan (1970) have pointed out that such a representation violates causality, a principle which asserts that the states of a system at a given point of time can be affected only by the events in the past and not by those of the future.

Now for the SDOF system, the frequency domain description of the equation of motion can be given by

$$\left[-m\omega^2 + \mathrm{i}\omega c(\omega) + k\right] X(\mathrm{i}\omega) = F(\mathrm{i}\omega) \tag{1.19}$$

where $X(\mathrm{i}\omega)$ and $F(\mathrm{i}\omega)$ are the response and excitation respectively, represented in the frequency domain. Note that the dashpot is now allowed to have frequency dependence. Inserting equation (1.18) into (1.19) we obtain

$$\left[-m\omega^2 + k\left\{1 + \mathrm{i}\eta(\omega)\mathrm{sgn}(\omega)\right\}\right] X(\mathrm{i}\omega) = F(\mathrm{i}\omega) \tag{1.20}$$

where $\mathrm{sgn}(\bullet)$ represents the sign function. The 'time-domain' representations of equations (1.19) and (1.20) are often taken as

$$m\ddot{x} + c(\omega)\dot{x} + kx = f \tag{1.21}$$

and

$$m\ddot{x} + kx\left\{1 + \mathrm{i}\eta(\omega)\mathrm{sgn}(\omega)\right\} = f \tag{1.22}$$

respectively. It has been pointed out by Crandall (1970) that these are not the correct Fourier inverses of equations (1.19) and (1.20). The reason is that the inertia, the stiffness and the forcing function are inverted properly, while the damping terms in equations (1.21) and (1.22) are obtained by mixing the frequency-domain and time-domain operations. Crandall (1970) calls (1.21) and (1.22) the 'non-equations' in time domain. It has been pointed out by Newland (1989) that only certain forms of frequency dependence for $\eta(\omega)$ are allowed in order to to satisfy causality. Crandall (1970) has shown that the impulse response function for the ideal hysteretic dashpot (η independent of frequency), is given by

$$h(t) = \frac{1}{\pi k \eta_0} . \frac{1}{t}, \quad -\infty < t < \infty. \tag{1.23}$$

This response function is clearly non-causal since it states that the system responds before the excitation (or the cause) takes place. This non-physical behaviour of the hysteretic damping model is a flaw, and further attempts have been made to cure this problem. Bishop and Price (1986) introduced the band limited hysteretic damper and suggested that it might satisfy the causality requirement. However, Crandall (1991) has further shown that the band-limited hysteretic dashpot is also non-causal. In view of this discussion it can be said that the most of the hysteretic damping model fails to satisfy the casualty condition. Recently, based on the analyticity of the transfer function, Makris (1999) has shown that for causal hysteretic damping the real and imaginary parts of the dynamic stiffness matrix must form a Hilbert transform pair[1]. He has shown that the causal hysteretic damping model is the limiting case of a linear viscoelastic model with nearly frequency-independent dissipation that was proposed by Biot (1958). It was also shown that there is a continuous transition from the linear viscoelastic model to the ideally hysteretic damping model.

The physical mechanisms of damping, including various types of external friction, fluid viscosity, and internal material friction, have been studied rather extensively in some detail and are complicated physical phenomena. However, a certain simplified mathematical formulation of damping forces and energy dissipation can be associated with a class of physical phenomenon. Coulomb damping, for example is used to represent dry friction present in sliding surfaces, such as structural joints. For this kind of damping, the force resisting the motion is assumed to be proportional to the normal force between the sliding surfaces and independent of the velocity except for the sign. The damping force is thus

$$F_d = \frac{\dot{x}}{|\dot{x}|} F_r = \mathrm{sgn}(\dot{x}) F_r \tag{1.24}$$

where F_r is the frictional force. In the context of finding equivalent viscous damping, Bandstra (1983) has reported several mathematical models of physical damping mechanisms in SDOF systems. For example, velocity squared damping, which is present when a mass vibrates in a fluid or

[1]The Hilbert transform relation is known as Kramers-Kronig result.

when fluid is forced rapidly through an orifice. The damping force in this case is

$$F_d = \text{sgn}(\dot{x})a\dot{x}^2; \quad \text{or, more generally} \quad F_d = c\dot{x}|\dot{x}|^{n-1} \tag{1.25}$$

where c is the damping proportionality constant. Viscous damping is a special case of this type of damping. If the fluid flow is relatively slow *i.e.* laminar, then by letting $n = 1$ the above equation reduces to the case of viscous damping (1.16).

1.2.2 Continuous Systems

Construction of damping models becomes more difficult for continuous systems. Banks and Inman (1991) have considered four different damping models for a composite beam. These models of damping are:

1. *Viscous air damping:* For this model the damping operator in the Euler-Bernoulli equation for beam vibration becomes
$$L_1 = \gamma \frac{\partial}{\partial t} \tag{1.26}$$
where γ is the viscous damping constant.

2. *Kelvin-Voigt damping:* For this model the damping operator becomes
$$L_1 = c_d I \frac{\partial^5}{\partial x^4 \partial t} \tag{1.27}$$
where I is the moment of inertia and c_d is the strain-rate dependent damping coefficient. A similar damping model was also used by Manohar and Adhikari (1998) and Adhikari and Manohar (1999) in the context of randomly parametered Euler-Bernoulli beams.

3. *Time hysteresis damping:* For this model the damping operator is assumed as
$$L_1 = \int_{-\infty}^{t} g(\tau) u_{xx}(x, t+\tau) \mathrm{d}\tau \quad \text{where } g(\tau) = \frac{\alpha}{\sqrt{-\tau}} \exp(\beta\tau) \tag{1.28}$$
where α and β are constants. Later, this model will be discussed in detail.

4. Spatial hysteresis damping:
$$L_1 = \frac{\partial}{\partial x}\left[\int_0^L h(x,\xi)\{u_{xx}(x,t) - u_{xt}(\xi,t)\}\mathrm{d}\xi\right] \tag{1.29}$$
The kernel function $h(x, \xi)$ is defined as
$$h(x,\xi) = \frac{a}{b\sqrt{\pi}} \exp[-(x-\xi)^2/2b^2]$$
where b is some constant.

It was observed by them that the spatial hysteresis model combined with a viscous air damping model results in the best quantitative agreement with the experimental time histories. Again, in the context of Euler-Bernoulli beams, Bandstra (1983) has considered two damping models where the damping term is assumed to be of the forms $\{\text{sgn}\, u_t(x,t)\}\, b_1 u^2(x,t)$ and $\{\text{sgn}\, u_t(x,t)\}\, b_2|u(x,t)|$.

1.2.3 Multiple Degrees-of-freedom Systems

The most popular approach to model damping in the context of multiple degrees-of-freedom (MDOF) systems is to assume viscous damping. This approach was first introduced by Rayleigh (1877). By analogy with the potential energy and the kinetic energy, Rayleigh assumed the *dissipation function*, given by

$$\mathcal{F}(\mathbf{q}) = \frac{1}{2}\sum_{j=1}^{N}\sum_{k=1}^{N} C_{jk}\dot{q}_j\dot{q}_k = \frac{1}{2}\dot{\mathbf{q}}^T\mathbf{C}\dot{\mathbf{q}}. \tag{1.30}$$

In the above expression $\mathbf{C} \in \mathbb{R}^{N\times N}$ is a non-negative definite symmetric matrix, known as the viscous damping matrix. It should be noted that not all forms of the viscous damping matrix can be handled within the scope of classical modal analysis. Based on the solution method, viscous damping matrices can be further divided into classical and non-classical damping. Further discussions on viscous damping will follow in Section 1.3.

It is important to avoid the widespread misconception that viscous damping is the *only* linear model of vibration damping in the context of MDOF systems. Any causal model which makes the energy dissipation functional non-negative is a possible candidate for a damping model. There have been several efforts to incorporate non-viscous damping models in MDOF systems. Bagley and Torvik (1983), Torvik and Bagley (1987), Gaul *et al.* (1991), Maia *et al.* (1998) have considered damping modeling in terms of fractional derivatives of the displacements. Following Maia *et al.* (1998), the damping force using such models can be expressed by

$$\mathbf{F}_d = \sum_{j=1}^{l} \mathbf{g}_j D^{\nu_j}[\mathbf{q}(t)]. \tag{1.31}$$

Here $\mathbf{g}_j$ are complex constant matrices and the fractional derivative operator

$$D^{\nu_j}[\mathbf{q}(t)] = \frac{\mathrm{d}^{\nu_j}\mathbf{q}(t)}{\mathrm{d}t^{\nu_j}} = \frac{1}{\Gamma(1-\nu_j)}\frac{\mathrm{d}}{\mathrm{d}t}\int_0^t \frac{\mathbf{q}(t)}{(t-\tau)^{\nu_j}}\mathrm{d}\tau \tag{1.32}$$

where ν_j is a fraction and $\Gamma(\bullet)$ is the Gamma function. The familiar viscous damping appears as a special case when $\nu_j = 1$. We refer the readers to the review papers by Slater *et al.* (1993), Rossikhin and Shitikova (1997) and Gaul (1999) for further discussions on this topic. The physical justification for such models, however, is far from clear at the present time.

Possibly the most general way to model damping within the linear range is to consider non-viscous damping models which depend on the past history of motion via convolution integrals over some kernel functions. A *modified dissipation function* for such damping model can be defined as

$$\mathcal{F}(\mathbf{q}) = \frac{1}{2}\sum_{j=1}^{N}\sum_{k=1}^{N} \dot{q}_k\int_0^t \mathcal{G}_{jk}(t-\tau)\dot{q}_j(\tau)\mathrm{d}\tau = \frac{1}{2}\dot{\mathbf{q}}^T\int_0^t \boldsymbol{\mathcal{G}}(t-\tau)\dot{\mathbf{q}}(\tau)\mathrm{d}\tau. \tag{1.33}$$

Here $\boldsymbol{\mathcal{G}}(t) \in \mathbb{R}^{N\times N}$ is a symmetric matrix of the damping kernel functions, $\mathcal{G}_{jk}(t)$. The kernel functions, or others closely related to them, are described under many different names in the literature of different subjects: for example, retardation functions, heredity functions, after-effect functions, relaxation functions *etc*. In the special case when $\boldsymbol{\mathcal{G}}(t-\tau) = \mathbf{C}\,\delta(t-\tau)$, where $\delta(t)$ is the Dirac-delta function, equation (1.33) reduces to the case of viscous damping as in equation (1.30). The damping model of this kind is a further generalization of the familiar viscous damping. By choosing suitable kernel functions, it can also be shown that the fractional derivative model discussed before is also a special case of this damping model. Thus, as pointed by Woodhouse (1998), this damping model is the most general damping model within the scope of a linear analysis.

Golla and Hughes (1985), McTavis and Hughes (1993) have used damping model of the form (1.33) in the context of viscoelastic structures. The damping kernel functions are commonly defined in the frequency/Laplace domain. Conditions which $\mathbf{G}(s)$, the Laplace transform of $\boldsymbol{\mathcal{G}}(t)$, must satisfy in order to produce dissipative motion were given by Golla and Hughes (1985). Several authors have proposed several damping models and they are summarized in Table 1.1.

Damping functions	Author, Year
$G(s) = \sum_{k=1}^{n} \dfrac{a_k s}{s+b_k}$	Biot (1955, 1958)
$G(s) = as\int_0^\infty \dfrac{\gamma(\rho)}{s+\rho}\mathrm{d}\rho$, $\gamma(\rho) = \begin{cases} \dfrac{1}{\beta-\alpha} & \alpha \le \gamma \le \beta \\ 0 & \text{otherwise} \end{cases}$	Buhariwala (1982)
$G(s) = \dfrac{E_1 s^\alpha - E_0 b s^\beta}{1+bs^\beta}$, $0<\alpha<1, \quad 0<\beta<1$	Bagley and Torvik (1983)
$sG(s) = G^\infty\left[1+\sum_k \alpha_k \dfrac{s^2+2\xi_k\omega_k s}{s^2+2\xi_k\omega_k s+\omega_k^2}\right]$	Golla and Hughes (1985) and McTavis and Hughes (1993)
$G(s) = 1+\sum_{k=1}^{n}\dfrac{\Delta_k s}{s+\beta_k}$	Lesieutre and Mingori (1990)
$G(s) = c\dfrac{1-e^{-st_0}}{st_0}$	Adhikari (1998)
$G(s) = c\dfrac{1+2(st_0/\pi)^2-e^{-st_0}}{1+2(st_0/\pi)^2}$	Adhikari (1998)

Table 1.1: Summary of damping functions in the Laplace domain

1.2.4 Other Studies

Another major source of damping in a vibrating structure is the structural joints, see Tan (1997) for a recent review. Here, a major part of the energy loss takes place through air-pumping. The air-pumping phenomenon is associated with damping when air is entrapped in pockets in the vicinity of a vibrating surface. In these situations, the entrapped air is 'squeezed out' and 'sucked-in'

through any available hole. Dissipation of energy takes place in the process of air flow and culomb-friction dominates around the joints. This damping behaviour has been studied by many authors in some practical situations, for example by Cremer and Heckl (1973). Earls (1966) has obtained the energy dissipation in a lap joint over a cycle under different clamping pressure. Beards and Williams (1977) have noted that significant damping can be obtained by suitably choosing the fastening pressure at the interfacial slip in joints.

Energy dissipation within the material is attributed to a variety of mechanisms such as thermoelasticity, grainboundary viscosity, point-defect relaxation etc (see Lazan, 1959, 1968, Bert, 1973). Such effects are in general called material damping. In an imperfect elastic material, the stress-strain curve forms a closed hysteresis loop rather that a single line upon a cyclic loading. Much effort has been devoted by numerous investigators to develop models of hysteretic restoring forces and techniques to identify such systems. For a recent review on this literature we refer the readers to Chassiakos *et al.* (1998). Most of these studies are motivated by the observed fact that the energy dissipation from materials is only a weak function of frequency and almost directly proportional to x^n. The exponent on displacement for the energy dissipation of material damping ranges from 2 to 3, for example 2.3 for mild steel (Bandstra, 1983). In this context, another large body of literature can be found on composite materials where many researchers have evaluated a material's specific damping capacity (SDC). Baburaj and Matsukai (1994) and the references therein give an account of research that has been conducted in this area.

1.3 Modal Analysis of Viscously Damped Systems

Equations of motion of a viscously damped system can be obtained from the Lagrange's equation (1.7) and using the Rayleigh's dissipation function given by (1.30). The non-conservative forces can be obtained as

$$Q_{\mathrm{nc}_k} = -\frac{\partial \mathcal{F}}{\partial \dot{q}_k}, \quad k = 1, \cdots, N \tag{1.34}$$

and consequently the equations of motion can expressed as

$$\mathbf{M}\ddot{\mathbf{q}}(t) + \mathbf{C}\dot{\mathbf{q}}(t) + \mathbf{K}\mathbf{q}(t) = \mathfrak{f}(t). \tag{1.35}$$

The aim is to solve this equation (together with the initial conditions) by modal analysis as described in Section 1.1.2. Using the transformation in (1.14), premultiplying equation (1.35) by $\mathbf{X}^T$ and using the orthogonality relationships in (1.12) and (1.13), equations of motion of a damped system in the modal coordinates may be obtained as

$$\ddot{\mathbf{y}}(t) + \mathbf{X}^T\mathbf{C}\mathbf{X}\dot{\mathbf{y}}(t) + \mathbf{\Omega}^2\mathbf{y}(t) = \tilde{\mathfrak{f}}(t). \tag{1.36}$$

Clearly, unless $\mathbf{X}^T\mathbf{C}\mathbf{X}$ is a diagonal matrix, no advantage can be gained by employing modal analysis because the equations of motion will still be coupled. To solve this problem, it it common

to assume *proportional damping*, that is **C** is simultaneously diagonalizable with **M** and **K**. Such damping model allows to analyze damped systems in very much the same manner as undamped systems. Later, Caughey and O'Kelly (1965) have derived the condition which the system matrices must satisfy so that viscously damped linear systems possess classical normal modes. In Chapter 2, the concept of proportional damping or classical damping will be analyzed in more detail.

Modes of proportionally damped systems preserve the simplicity of the real normal modes as in the undamped case. Unfortunately there is no physical reason why a general system should behave like this. In fact practical experience in modal testing shows that most real-life structures do not do so, as they possess complex modes instead of real normal modes. This implies that in general linear systems are non-classically damped. When the system is non-classically damped, some or all of the N differential equations in (1.36) are coupled through the $\mathbf{X}^T\mathbf{C}\mathbf{X}$ term and can not be reduced to N second-order uncoupled equation. This coupling brings several complication in the system dynamics – the eigenvalues and the eigenvectors no longer remain real and also the eigenvectors do not satisfy the classical orthogonality relationship as given by equations (1.10) and (1.11). The methods for solving this kind of problem follow mainly two routes, the state-space method and the methods in configuration space or 'N-space'. A brief discussion of these two approaches is taken up in the following sections.

1.3.1 The State-Space Method

The state-space method is based on transforming the N second-order coupled equations into a set of $2N$ first-order coupled equations by augmenting the displacement response vectors with the velocities of the corresponding coordinates (see Newland, 1989). Equation (1.35) can be recast as

$$\dot{\mathfrak{z}}(t) = \mathbf{A}\mathfrak{z}(t) + \mathbf{p}(t) \tag{1.37}$$

where $\mathbf{A} \in \mathbb{R}^{2N\times 2N}$ is the system matrix, $\mathbf{p}(t) \in \mathbb{R}^{2N}$ the force vector and $\mathfrak{z}(t) \in \mathbb{R}^{2N}$ is the response vector in the state-space given by

$$\mathbf{A} = \begin{bmatrix} \mathbf{O}_N & \mathbf{I}_N \\ -\mathbf{M}^{-1}\mathbf{K} & -\mathbf{M}^{-1}\mathbf{C} \end{bmatrix}, \quad \mathfrak{z}(t) = \begin{Bmatrix} \mathbf{q}(t) \\ \dot{\mathbf{q}}(t) \end{Bmatrix}, \quad \text{and} \quad \mathbf{p}(t) = \begin{Bmatrix} 0 \\ -\mathbf{M}^{-1}\mathfrak{f}(t). \end{Bmatrix} \tag{1.38}$$

In the above equation $\mathbf{O}_N$ is the $N \times N$ null matrix and $\mathbf{I}_N$ is the $N \times N$ identity matrix. The eigenvalue problem associated with the above equation is in term of an asymmetric matrix now. Uncoupling of equations in the state-space is again possible and has been considered by many authors, for example, Meirovitch (1980), Newland (1989) and Veletsos and Ventura (1986). This analysis was further generalized by Newland (1987) for the case of systems involving singular matrices. In the formulation of equation (1.37) the matrix **A** is no longer symmetric, and so eigenvectors are no longer orthogonal with respect to it. In fact, in this case, instead of an orthogonality relationship, one obtains a biorthogonality relationship, after solving the adjoint eigenvalue problem. The complete procedure for uncoupling the equations now involves solving two eigenvalue

problems, each of which is double the size of an eigenvalue problem in the modal space. The details of the relevant algebra can be found in Meirovitch (1980, 1997). It should be noted that these solution procedures are exact in nature. One disadvantage of such an exact method is that it requires significant numerical effort to determine the eigensolutions. The effort required is evidently intensified by the fact that the eigensolutions of a non-classically damped system are complex. From the analyst's view point another disadvantage is the lack of physical insight afforded by this method which is intrinsically numerical in nature.

Another variation of the state-space method available in the literature is through the use of 'Duncan form'. This approach was introduced by Foss (1958) and later several authors, for example, Béliveau (1977), Nelson and Glasgow (1979), Vigneron (1986), Suarez and Sing (1987, 1989), Sestieri and Ibrahim (1994) and Ren and Zheng (1997) have used this approach to solve a wide range of interesting problems. The advantage of this approach is that the system matrices in the state-space retain symmetry as in the configuration space.

1.3.2 Methods in Configuration Space

It has been pointed out that the state-space approach towards the solution of equation of motion in the context of linear structural dynamics is not only computationally expensive but also fails to provide the physical insight which modal analysis in configuration space or N-space offers. The eigenvalue problem associated with equation (1.35) can be represented by the $\lambda-$matrix problem (Lancaster, 1966)

$$s_j^2\mathbf{M}\mathbf{u}_j + s_j\mathbf{C}\mathbf{u}_j + \mathbf{K}\mathbf{u}_j = \mathbf{0} \tag{1.39}$$

where $s_j \in \mathbb{C}$ is the j-th latent root (eigenvalue) and $\mathbf{u}_j \in \mathbb{C}^N$ is the j-th latent vector (eigenvector). The eigenvalues, s_j, are the roots of the characteristic polynomial

$$\det\left[s^2\mathbf{M} + s\mathbf{C} + \mathbf{K}\right] = 0. \tag{1.40}$$

The order of the polynomial is $2N$ and the roots appear in complex conjugate pairs. Several authors have studied non-classically damped linear systems by approximate methods. In this section we briefly review the existing methods for this kind of analysis.

Approximate Decoupling Method

Consider the equations of motion of a general viscously damped system in the modal coordinates given by (1.36). Earlier it has been mentioned that due to non-classical nature of the damping this set of N differential equations are coupled through the $\mathbf{C}' = \mathbf{X}^T\mathbf{C}\mathbf{X}$ term. An usual approach in this case is simply to ignore the off-diagonal terms of the modal damping matrix $\mathbf{C}'$ which couple the equations of motion. This approach is termed the decoupling approximation. For large-scale systems, the computational effort in adopting the decoupling approximation is an order of magnitude smaller than the methods of complex modes. The solution of the decoupled equation would

be close to the exact solution of the coupled equations if the non-classical damping terms are sufficiently small. Analysis of this question goes back to Rayleigh (1877). A preliminary discussion on this topic can be found in Meirovitch (1967, 1997). Thomson *et al.* (1974) have studied the effect of neglecting off-diagonal entries of the modal damping matrix through numerical experiments and have proposed a method for improved accuracy. Warburton and Soni (1977) have suggested a criterion for such a diagonalization so that the computed response is acceptable. Using the frequency domain approach, Hasselsman (1976) proposed a criterion for determining whether the equations of motion might be considered practically decoupled if non-classical damping exists. The criterion suggested by him was to have adequate frequency separation between the natural modes.

Using matrix norms, Shahruz and Ma (1988) have tried to find an optimal diagonal matrix $\mathbf{C}_d$ in place of $\mathbf{C}'$. An important conclusion emerging from their study is that if $\mathbf{C}'$ is diagonally dominant, then among all approximating diagonal matrices $\mathbf{C}_d$, the one that minimizes the error bound is simply the diagonal matrix obtained by omitting the off-diagonal elements of $\mathbf{C}'$. Using a time-domain analysis Shahruz (1990) has rigorously proved that if $\mathbf{C}_d$ is obtained form $\mathbf{C}'$ by neglecting the off-diagonal elements of $\mathbf{C}'$, then the error in the solution of the approximately decoupled system will be small as long as the off-diagonal elements of $\mathbf{C}'$ are not too large.

Ibrahimbegovic and Wilson (1989) have developed a procedure for analyzing non-pro- portionally damped systems using a subspace with a vector basis generated from the mass and stiffness matrices. Their approach avoids the use of complex eigensolutions. An iterative approach for solving the coupled equations is developed by Udwadia and Esfandiari (1990) based on updating the forcing term appropriately. Felszeghy (1993) presented a method which searches for another coordinate system in the neighborhood of the normal coordinate system so that in the new coordinate system removal of coupling terms in the equations of motion produces a minimum bound on the relative error introduced in the approximate solution. Hwang and Ma (1993) have shown that the error due to the decoupling approximation can be decomposed into an infinite series and can be summed exactly in the Laplace domain. They also concluded that by solving a small number of additional coupled equations in an iterative fashion, the accuracy of the approximate solution can be greatly enhanced. Felszeghy (1994) developed a formulation based on biorthonormal eigenvector for modal analysis of non-classically damped discrete systems. The analytical procedure take advantage of simplification that arises when the modal analysis of the motion separated into a classical and non-classical modal vector expansion.

From the above mentioned studies it has been believed that either frequency separation between the normal modes (Hasselsman, 1976), often known as ‘Hasselsman’s criteria’, or some form of diagonal dominance (Shahruz and Ma, 1988), in the modal damping matrix $\mathbf{C}'$ is sufficient for neglecting modal coupling. In contrast to these widely accepted beliefs Park *et al.* (1992a,b, 1994) have shown using Laplace transform methods that within the practical range of engineering applications neither the diagonal dominance of the modal damping matrix nor the frequency separation between the normal modes would be sufficient for neglecting modal coupling. They have

also given examples when the effect of modal coupling may even increase following the previous criterion.

In the context of approximate decoupling, Shahruz and Srimatsya (1997) have considered error vectors in modal and physical coordinates, say denoted by $\mathbf{e_N}(\bullet)$ and $\mathbf{e_P}(\bullet)$ respectively. They have shown that based on the norm (denoted here as $\| \ (\bullet) \ \|$) of these error vectors three cases may arise:

1. $\| \ \mathbf{e_N}(\bullet) \ \|$ is small (respectively, large) and $\| \ \mathbf{e_P}(\bullet) \ \|$ is small (respectively, large)
2. $\| \ \mathbf{e_N}(\bullet) \ \|$ is large but $\| \ \mathbf{e_P}(\bullet) \ \|$ is small
3. $\| \ \mathbf{e_N}(\bullet) \ \|$ is small but $\| \ \mathbf{e_P}(\bullet) \ \|$ is large

From this study, especially in view of case 3, it is clear that the error norms based on the modal coordinates are not reliable to use in the actual physical coordinates. However, they have given conditions when $\| \ \mathbf{e_N}(\bullet) \ \|$ will lead to a reliable estimate of $\| \ \mathbf{e_P}(\bullet) \ \|$. For a flexible structure with light damping, Gawronski and Sawicki (1997) have shown that neglecting off-diagonal terms of the modal damping matrix in most practical cases imposes negligible errors in the system dynamics. They also concluded that the requirement of diagonal dominance of the damping matrix is not necessary in the case of small damping, which relaxes the criterion earlier given by Shahruz and Ma (1988).

In order to quantify the extent of non-proportionality, several authors have proposed 'non-proportionality indices'. Parter and Sing (1986) and Nair and Sing (1986) have developed several indices based on modal phase difference, modal polygon areas, relative magnitude of coupling terms in the modal damping matrix, system response, Nyquist plot *etc*. Recently, based on the idea related to the modal polygon area, Bhaskar (1999) has proposed two more indices of non-proportionality. Another index based on driving frequency and elements of the modal damping matrix is given by Bellos and Inman (1990). Bhaskar (1992, 1995) has proposed a non-proportionality index based on the error introduced by ignoring the coupling terms in the modal damping matrix. Tong *et al.* (1992, 1994) have developed an analytical index for quantification of non-proportionality for discrete vibrating systems. It has been shown that the fundamental nature of non-proportionality lies in finer decompositions of the damping matrix. Shahruz (1995) have shown that the analytical index given by Tong *et al.* (1994) solely based on the damping matrix can lead to erroneous results when the driving frequency lies close to a system natural frequency. They have suggested that a suitable index for non-proportionality should include the damping matrix and natural frequencies as well as the excitation vector. Prells and Friswell (2000) have shown that the (complex) modal matrix of a non-proportionally damped system depends on an orthonormal matrix, which represents the phase between different degrees of freedom of the system. For proportionally damped systems this matrix becomes an identity matrix and consequently they have used this orthonormal matrix as an indicator of non-proportionality. Recently, Liu *et al.* (2000) has

proposed three indices to measure the damping non-proportionality. The first index measures the correlation between the real and imaginary parts of the complex modes, the second index measures the magnitude of the imaginary parts of the complex modes and the third index quantifies the degree of modal coupling. These indices are based on the fact that the complex modal matrix can be decomposed to a product of a real and and complex matrix.

Complex Modal Analysis

Other than the approximate decoupling methods, another approach towards the analysis of non-proportionally damped linear systems is to use complex modes. Since the original contribution of Caughey and O'Kelly (1965), many papers have been written on complex modes. Several authors, for example, Mitchell (1990), Imregun and Ewins (1995) and Lallement and Inman (1995), have given reviews on this subject. Placidi *et al.* (1991) have used a series expansion of complex eigenvectors into the subspace of real modes, in order to identify normal modes from complex eigensolutions. In the context of modal analysis Liang *et al.* (1992) have posed and analyzed the question of whether the existence of complex modes is an indicator of non-proportional damping and how a mode is influenced by damping. Analyzing the errors in the use of modal coordinates, Sestieri and Ibrahim (1994) and Ibrahim and Sestieri (1995) have concluded that the complex mode shapes are not necessarily the result of high damping. The complexity of the mode shapes is the result of particular damping distributions in the system and depends upon the proximity of the mode shapes. Liu and Sneckenberger (1994) have developed a complex mode theory for a linear vibrating deficient system based on the assumption that it has a complete set of eigenvectors. Complex mode superposition methods have been used by Oliveto and Santini (1996) in the context of soil structure interaction problems. Balmès (1997) has proposed a method to find normal modes and the associated non-proportional damping matrix from the complex modes. He has also shown that a set of complex modes is complete if it verifies a defined properness condition which is used to find complete approximations of identified complex modes. Garvey *et al.* (1995) have given a relationship between real and imaginary parts of complex modes for general systems whose mass, stiffness and damping can be expressed by real symmetric matrices. They have also observed that the relationship becomes most simple when all roots are complex and the real part of all the roots have same sign. Recently Bhaskar (1999) has analyzed complex modes in detail and addressed the problem of visualizing the deformed modes shapes when the motion is not synchronous.

While the above mentioned works concentrate on the properties of the complex modes, several authors have considered the problem of determination of complex modes in the N-space. Cronin (1976) has obtained an approximate solution for a non-classically damped system under harmonic excitation by perturbation techniques. Clough and Mojtahedi (1976) considered several methods of treating generally damped systems, and concluded that the proportional damping approximation may give unreliable results for many cases. Similarly, Duncan and Taylor (1979) have shown that significant errors can be incurred when dynamic analysis of a non-proportionally damped sys-

tem is based on a truncated set of modes, as is commonly done in modelling continuous systems. Meirovitch and Ryland (1985) have used a perturbation approach to obtain left and right eigenvectors of damped gyroscopic systems. Chung and Lee (1986) applied perturbation techniques to obtain the eigensolutions of damped systems with weakly non-classical damping. Cronin (1990) has developed an efficient perturbation-based series method to solve the eigenproblem for dynamic systems having non-proportional damping matrix. To illustrate the general applicability of this method, Peres-Da-Silva *et al.* (1995) have applied it to determine the eigenvalues and eigenvectors of a damped gyroscopic system. In the context of non-proportionally damped gyroscopic systems Malone *et al.* (1997) have developed a perturbation method which uses an undamped gyroscopic system as the unperturbed system. Based on a small damping assumption, Woodhouse (1998) has given the expression for complex natural frequencies and mode shapes of non-proportionally damped linear discrete systems with viscous and non-viscous damping. More recently, based on the idea related to the first-order perturbation method, Adhikari (2000) has proposed an expression of complex modes in terms of classical normal modes.

Response Bounds and Frequency Response

In the two previous subsections we have mainly discussed on the eigensolutions of non-classically damped systems. In this subsection we briefly consider the problem of obtaining dynamic response of such systems. Nicholson (1987b) and Nicholson and Baojiu (1996) have reviewed the literature on stable response of non-classically damped mechanical systems. Nicholson (1987a) gave upper bounds for the response of non-classically damped systems under impulsive loads and step loads. Yae and Inman (1987) have obtained bound on the displacement response of non-proportionally damped discrete systems in terms of physical parameters of the system and input. They also have observed that the larger the deviation from proportional damping the less accurate their results become.

Bellos and Inman (1990) have given a procedure for computing the transfer functions of a non-proportionally damped discrete system. Their method was based on Laplace transformation of the equation of motion in modal coordinates. A fairly detailed survey of the previous research is made in Bellos and Inman (1990). Yang (1993) has developed a iterative procedure for calculation of the transfer functions of non-proportionally damped systems. Bhaskar (1995) has analyzed the behaviour of errors in calculating frequency response function when the off-diagonal terms of modal damping matrix are neglected. It has been shown that the exact response can be expressed by an infinite Taylor series and the approximation of ignoring the off-diagonal terms of modal damping matrix is equivalent to retaining one term of the series.

Finally, it should be noted that frequency responses of viscously damped systems with non-proportional damping can be obtained *exactly* in terms of the complex frequencies and complex modes in the configuration space, see for example Lancaster (1966, Section 7.5) and Géradin and Rixen (1997, pp. 126-128). Similar expressions are also derived by Fawzy and Bishop (1976),

Vigneron (1986) and Woodhouse (1998). This in turn requires determination of complex modes in the configuration space.

1.4 Analysis of Non-viscously Damped Systems

In Section 1.2.3 it was pointed out that the most general way to model (non-viscous) damping within the scope of linear theory is through the use of the modified dissipation function given by equation (1.33). Equations of motion of such non-viscously damped systems can be obtained from the Lagrange's equation (1.7). The non-conservative forces can be obtained as

$$Q_{\mathrm{nc}_k} = -\frac{\partial \mathcal{F}}{\partial \dot{q}_k} = -\sum_{j=1}^{N} \int_0^t \mathcal{G}_{jk}(t-\tau)\dot{q}_j(\tau)\mathrm{d}\tau, \quad k = 1, \cdots, N \tag{1.41}$$

and consequently the equations of motion can be expressed as

$$\mathbf{M}\ddot{\mathbf{q}}(t) + \int_0^t \boldsymbol{\mathcal{G}}(t-\tau)\dot{\mathbf{q}}(\tau)\mathrm{d}\tau + \mathbf{K}\mathbf{q}(t) = \mathfrak{f}(t). \tag{1.42}$$

This is a set of coupled second-order integro-differential equation. The presence of the 'integral' term in the equations of motion complicates the analysis. Unlike the viscously damped systems, the concept of 'proportional damping' cannot easily be formulated for such systems. The question of the existence of classical normal modes in such systems, *i.e.*, if proportional damping can occur in such systems, will be discussed in Chapter 2.

Equations similar to (1.42) occur in many different subjects. Bishop and Price (1979) have considered equations of motion similar to (1.42) in the context of *ship dynamics*. The convolution term appeared in order to represent the fluid forces and moments. They have discussed the eigenvalue problem associated with equation (1.42) and presented an orthogonality relationship for the right and left eigenvectors. They have also given an expression for the system response due to sinusoidal excitation. Their results were not very efficient because the orthogonality relationship of the eigenvectors were not utilized due to the difficulty associated with the form of the orthogonality equation, which itself became frequency dependent.

Equations of motion like (1.42) also arise in the dynamics of *viscoelastic structures*. Golla and Hughes (1985), McTavis and Hughes (1993) have proposed a method to obtain such equations using a time-domain finite-element formulation. Their approach (the GHM method), which introduces additional dissipation coordinates corresponding to the internal dampers, increases the size of the problem. Dynamic responses of the system were obtained by using the eigensolutions of the augmented problem in the state-space. Muravyov (1997, 1998) has proposed a method to obtain the time and frequency-domain description of the response by introducing additional coordinates like the GHM method. To reduce the order of the problem, recently Park *et al.* (1999) and Friswell and Inman (1999) have proposed a state-space approach which employs a modal truncation and uses an iterative approach to obtain the eigensolutions. Using a first-order perturbation approach,

Woodhouse (1998) has obtained expressions for the eigensolutions and transfer functions of system (1.42). His method, although it avoids the state-space representations and additional dissipation coordinates, is valid for small damping terms only.

1.5 Identification of Viscous Damping

In Section 1.3 we have discussed several methods for *analysis* of viscously damped linear dynamic systems. In this section we focus our attention on the methodologies available for identification of viscous damping parameters from experimental measurements.

1.5.1 Single Degree-of-freedom Systems Systems

Several methods are available for identifying the viscous damping parameters for single degree of freedom systems for linear and non-linear damping models (see Nashif *et al.*, 1985). For linear damping models these methods can be broadly described as:

1. *Methods based on transient response of the system:* This is also known as logarithmic decrement method: if q_i and q_{i+i} are heights of two subsequent peaks then the damping ratio ζ can be obtained as
$$\delta = \log_e \left(\frac{q_i}{q_{i+i}} \right) \approx 2\pi\zeta \tag{1.43}$$
For applicability of this method the decay must be exponential.

2. *Methods based on harmonic response of the system:* These methods are based on calculating the half power points and bandwidth from the frequency response curve. It can be shown that the damping factor ζ can be related to a peak of the normalized frequency response curve by
$$|H|_{\max} \approx \frac{1}{2\zeta} \tag{1.44}$$

3. *Methods based on energy dissipation:* Consider the force-deflection behaviour of a spring-mass-damper (equivalent to a block of material) under sinusoidal loading at some particular frequency. In steady-state, considering conservation of energy, energy loss per cycle (Δu_{cyc}) can be calculated by equating it with the input power. Here it can be shown that the damping factor ζ can be related as
$$2\zeta = \frac{\Delta u_{\text{cyc}}}{2\pi U_{\max}} \tag{1.45}$$
where $U_{\max}$ is maximum energy of the system.

The above mentioned methods, although developed for single-degree-of-freedom systems, can be used for separate modes of multiple degree of freedom systems, for example a cantilever beam vibrating in the first mode. Recently Chassiakos *et al.* (1998) proposed an on-line parameter identification technique for a single degree of freedom hysteretic system.

1.5.2 Multiple Degrees-of-freedom Systems

For multiple degree-of-freedom systems, most of the common methods for experimental determination of the damping parameters use the proportional damping assumption. A typical procedure can be described as follows (see Ewins, 1984, for details):

1. Measure a set of transfer functions $H_{ij}(\omega)$ at a set of grid points on the structure.
2. Obtain the natural frequencies ω_k by a pole-fitting method.
3. Evaluate the modal half-power bandwidth $\Delta\omega_k$ from the frequency response functions, then the Q-factor $Q_k = \frac{\omega_k}{\Delta\omega_k}$ and the modal damping factor $\zeta_k = \frac{1}{2Q_k}$.
4. Determine the modal amplitude factors a_k to obtain the mode shapes, $\mathbf{u}_k$.
5. Finally reconstruct some transfer functions to verify the accuracy of the evaluated parameters.

Such a procedure does not provide reliable information about the nature or spatial distribution of the damping, though the reconstructed transfer functions may match the measured ones well.

The next stage, followed by many researchers, is to attempt to obtain the full viscous damping matrix from the experimental measurements. Pilkey and Inman (1998) have given a recent survey on methods of viscous damping identification. These methods can be divided into two basic categories (Fabunmi *et al.*, 1988): (a) damping identification from modal testing and analysis, and (b) direct damping identification from the forced response measurements.

The modal testing and analysis method seeks to determine the modal parameters, such as natural frequencies, damping ratio and mode shapes, from the measured transfer functions, and then fit a damping matrix to these data. In one of the earliest works, Lancaster (1961) has given an expression from which the damping matrix can be constructed from complex modes and frequencies. Unfortunately this expression relies on having all the modes, which is almost impossible in practice. For this reason, several authors have proposed identification methods by considering the modal data to be incomplete or noisy. Hasselsman (1972) has proposed a perturbation method to identify a non-proportional viscous damping matrix from complex modes and frequencies. Béliveau (1976) has proposed a method which uses eigensolutions, phase angles and damping ratios to identify the parameters of viscous damping matrix. His method utilizes a Bayesian framework based on eigensolution perturbation and a Newton-Raphson scheme. Ibrahim (1983b) uses the higher order analytical modes together with the experimental set of complex modes to compute improved mass, stiffness and damping matrices. Minas and Inman (1991) have proposed a method for viscous damping identification in which it is assumed that the mass and stiffness are *a priori* known and modal data, obtained from experiment, allowed to be incomplete. Starek and Inman (1997) have proposed an inverse vibration problem approach in which it is assumed that the damping matrix has an *a priori* known structure. Their method yields a positive-definite damping matrix

but requires the full set of complex modes. Pilkey and Inman (1997) have developed an iterative method for damping matrix identification by using Lancaster's (1961) algorithm. This method requires experimentally identified complex eigensolutions and the mass matrix. Alvin *et al.* (1997) have proposed a method in which a correction was applied to the proportionally damped matrix by means of an error minimization approach. Recently Halevi and Kenigsbuch (1999) have proposed a method for updating the damping matrix by using the reference basis approach in which error and incompleteness of the measured modal data were taken into account. As an intermediate step, their method corrects the imaginary parts of the measured complex modes which are more inaccurate than their corresponding real parts.

Direct damping identification methods attempt to fit the equations of motion to the measured forced response data at several time/frequency points. Caravani and Thomson (1974) have proposed a least-square error minimization approach to obtain the viscous damping matrix. Their method uses measured frequency response at a set of chosen frequency points and utilizes an iterative method to successively improve the identified parameters. Fritzen (1986) has used the instrumental variable method for identification of the mass, damping and stiffness matrices. It was observed that the identified values are less sensitive to noise compared to what obtained from least-square approach. Fabunmi *et al.* (1988) has presented a damping matrix identification scheme that uses forced response data in the frequency domain and assumes that the mass and stiffness matrices are known. Mottershead (1990) has used the inverse of the frequency response functions to modify the system matrices so that the modified model varies minimally from an initial finite-element model. Using a different approach, Roemer and Mook (1992) have developed methods in the time domain for simultaneous identification of the mass, damping and stiffness matrices. It was observed that the identified damping matrix has larger relative error than that of the mass and stiffness matrices. Chen *et al.* (1996a) have proposed a frequency domain technique for identification of the system matrices in which the damping matrix was determined independently. It was shown that separate identification of the damping matrix improves the result as relative magnitude of the damping matrix is less than those of the mass and stiffness matrices. Later, Baruch (1997) has proposed a similar approach in which the damping matrix was identified separately from the mass and stiffness matrices.

1.6 Identification of Non-viscous Damping

Unlike viscous damping, there is very little available in the literature which discusses generic methodologies for identification of non-viscous damping. Most of the methods proposed in the literature are system-specific. Banks and Inman (1991) have considered the problem of estimating damping parameters in a non-proportionally damped beam. They have taken four different models of damping: viscous air damping, Kelvin-Voigt damping, time hysteresis damping and spatial hysteresis damping, and used a spline inverse procedure to form a least-square fit to the experimen-

tal data. A procedure for obtaining hysteretic damping parameters in free-hanging pipe systems is given by Fang and Lyons (1994). Assuming material damping is the only source of damping they have given a theoretical expression for the loss factor of the n-th mode. Their theory predicts higher modal damping ratios in higher modes. Maia *et al.* (1997) have emphasized the need for development of identification methodologies of general damping models and indicated several difficulties that might arise. Recently, Dalenbring (1999) has proposed a method for identification of (exponentially decaying) damping functions from the measured frequency response functions and finite element displacement modes. A limitation of this method is that it neglects the effect of modal coupling, that is, the identified non-viscous damping model is effectively proportional.

1.7 Open Problems

From the discussions based on the existing literature it is clear that in spite of extensive research effort, many questions regarding damped dynamic systems are still to be answered. These questions can be broadly divided as follows:

1. What damping model has to be used for a given structure, *i.e.*, viscous or non-viscous, and if non-viscous then what kind of model should it be?

2. How can conventional modal analysis be extended to systems with non-viscous damping?

3. How is it possible to determine the damping parameters by conventional modal testing if a system is non-viscous?

The first question is a major issue, and in the context of general vibration analysis, has been 'settled' by assuming viscous damping, although has been pointed out in the literature that in general it will not be the correct model. The last two questions are related to each other in the sense that for identification of the non-viscous damping parameters a reliable method of modal analysis is also required.

Most of the techniques for detecting damping in a structure either consider the structure to be viscously damped or *a priori* assume some particular non-viscous model of damping and try to fit its parameters with regard to some specific structure. This *a priori* selection of damping no doubt hides the physics of the system and there has not been any indication in the literature on how to find a damping model by doing conventional vibration testing. However another relevant question in this context is whether this *a priori* selection of damping model matters from an engineering point of view: it may be possible that a pre-assumed damping model with a 'correct' set of parameters may represent the system response quite well, although the actual physical mechanism behind the damping may be different. These issues will be discussed in this dissertation. Next, the works taken up in this dissertation is outlined briefly.

1.8 Outline of the Dissertation

Motivated by the existing gaps and open problems identified in the last section, a systematic study on *analysis* and *identification* of damped discrete linear dynamic systems has been carried out in this dissertation. In Section 1.2 it has been brought out that the convolution integral model is the most general damping model for multiple-degrees-of-freedom linear systems. Attention is specifically focused on this kind of general damping model. However, for comparing and establishing the relationship with the current literature, viscously damped systems are also discussed. The dissertation is divided into nine chapters and two Appendices.

In Chapter 2, the concept of classical damping, well known for viscously damped systems, is extended to non-viscously damped discrete linear systems. The convolution integral model is assumed for non-viscous damping. Conditions for the existence of classical normal modes in such non-viscously damped systems are discussed. Several numerical examples are provided to illustrate the derived results.

Chapter 3 is aimed at extending classical modal analysis to treat lumped-parameter non-viscously damped linear dynamic systems. The nature of the eigenvalues and eigenvectors are discussed under certain simplified but physically realistic assumptions concerning the system matrices and kernel functions. A numerical method for calculation of the eigenvectors is suggested. The transfer function matrix of the system is derived in terms of the eigenvectors of the second-order system. Exact closed-form expressions for the dynamic response due to general forces and initial conditions are derived.

In Chapter 4, the mode-orthogonality relationships, known for undamped or viscously damped systems, have been generalized to such non-viscously damped systems. Some expressions are suggested for the normalization of the eigenvectors. A number of useful results which relate the system matrices with the eigensolutions have been established.

The above mentioned studies give a firm basis for modal analysis of non-viscously damped systems. Motivated by these results, from Chapter 5 onwards, studies on damping identification are considered. Chapter 5 considers identification of viscous damping under circumstances when the actual damping model in the structure is non-viscous. A method is presented to obtain a full (non-proportional) viscous damping matrix from complex modes and complex natural frequencies. It is assumed that the damping is ‘small’ so that a first order perturbation method is applicable. The proposed method and several related issues are discussed by considering numerical examples based on a linear array of damped spring-mass oscillators. It is shown that the method can predict the spatial location of damping with good accuracy, and also give some indication of the correct mechanism of damping.

From the studies in Chapter 5 it is observed that when a system is non-viscously damped, an identified equivalent viscous damping model does not accurately represent the damping behaviour. This demands new methodologies to identify non-viscous damping models. Chapter 6 takes a

first step, by outlining a procedure for identifying a damping model involving an exponentially-decaying relaxation function. The method uses experimentally identified complex modes and complex natural frequencies, together with the knowledge of mass matrix for the system. The proposed method and several related issues are discussed by considering numerical examples of a linear array of damped spring-mass oscillators. It is shown that good estimates can be obtained for the exponential time constant and the spatial distribution of the damping.

In some cases the identified damping matrix become non-symmetric, which in a way is a non-physical result because the original system is reciprocal. In Chapter 7, methods are developed to identify damping models which preserve the symmetry of the system. Both viscous and non-viscous models are considered. The procedures are based on a constrained error minimization approach and they use experimentally identified complex modes and complex natural frequencies. The proposed methods are supported by suitable numerical examples.

Experimental verification of the damping identification techniques developed in this dissertation is considered in Chapter 8. First, extraction of complex modes and frequencies from a set of measured transfer functions is considered as all the damping identification procedures rely heavily on these complex modal parameters. A general methodology based on linear-nonlinear least-square approach is proposed. The experimental structure is comprised of a beam with localized constrained layer damping. It is demonstrated that the proposed approach for damping identification can indeed predict the nature of the damping with good accuracy. Through an error analysis, it is further shown that the proposed method is likely to be robust in the presence of noisy data, as the identified damping matrix is less sensitive to the imaginary parts of the complex modes, on which any measurement noise has highest effect.

Finally, Chapter 9 presents the conclusions emerging from the studies taken up in this dissertation and makes a few suggestions for further research.

Chapter 2

The Nature of Proportional Damping

2.1 Introduction

Modal analysis is the most popular and efficient method for solving engineering dynamic problems. The concept of modal analysis, as introduced by Rayleigh (1877), was originated from the linear dynamics of *undamped systems*. It was shown (see Section 1.1.2 for details) that the undamped modes or *classical normal modes* satisfy an orthogonality relationship over the mass and stiffness matrices and uncouple the equations of motion, *i.e.*, If $\mathbf{X} \in \mathbb{R}^{N\times N}$ is the modal matrix then $\mathbf{X}^T\mathbf{M}\mathbf{X}$ and $\mathbf{X}^T\mathbf{K}\mathbf{X}$ are both diagonal matrices. This significantly simplifies the dynamic analysis because complex multiple degree-of-freedom (MDOF) systems can be treated as a collection of single degree-of-freedom oscillators.

Real-life systems are however, not undamped, but possess some kind of energy dissipation mechanism or damping. In order to apply modal analysis of undamped systems to damped systems, it is common to assume the proportional damping, a special case of viscous damping. The proportional damping model expresses the damping matrix as a linear combination of the mass and stiffness matrices, that is

$$\mathbf{C} = \alpha_1\mathbf{M} + \alpha_2\mathbf{K} \tag{2.1}$$

where α_1, α_2 are real scalars. This damping model is also known as 'Rayleigh damping' or 'classical damping'. Modes of classically damped systems preserve the simplicity of the real normal modes as in the undamped case. Caughey and O'Kelly (1965) have derived the condition which the system matrices must satisfy so that viscously damped linear systems possess classical normal modes. They have also proposed an (series) expression for the damping matrix in terms of the mass and stiffness matrices so that the system can be decoupled by the undamped modal matrix and have shown that the Rayleigh damping is a special case of this general expression. In this chapter a more general expression of the damping matrix is proposed so that the system possess classical normal modes.

There are no physical reasons to believe that viscous damping is the only linear damping model. It is perfectly possible for the damping forces to depend on values of other quantities. In the last

chapter (see Section 1.2.3) it was concluded that the convolution integral model is the most general linear damping model. Since the concept of classical or proportional damping is defined in the context of viscously damped systems, it is not clear whether such a concept exists for this kind of non-viscously damped systems. In this chapter we address the question – under what conditions can such non-viscously damped systems be 'classically damped'? *i.e.*, under what conditions such non-viscously damped systems possess classical normal modes?

2.2 Viscously Damped Systems

The equations of motion of free vibration of a viscously damped system can be expressed by

$$\mathbf{M}\ddot{\mathbf{q}}(t) + \mathbf{C}\dot{\mathbf{q}}(t) + \mathbf{K}\mathbf{q}(t) = \mathbf{0}. \tag{2.2}$$

In this case the equations of motion are characterized by *three* real symmetric matrices which brings additional complication compared to the undamped systems where the equations of motion are characterized by two matrices. We require a non-zero matrix $\mathbf{X} \in \mathbb{R}^{N\times N}$ such that it simultaneously diagonalizes $\mathbf{M}$, $\mathbf{C}$ and $\mathbf{K}$ under a congruence transformation. This requirement restricts the admissible forms of these matrices as discussed below.

2.2.1 Existence of Classical Normal Modes

Caughey and O'Kelly (1965) have proved that a damped linear system of the form (2.2) can possess classical normal modes if and only if the system matrices satisfy the relationship $\mathbf{K}\mathbf{M}^{-1}\mathbf{C} = \mathbf{C}\mathbf{M}^{-1}\mathbf{K}$. This is an important result on modal analysis of viscously damped systems and is now well known. However, this result does not immediately generalize to systems with singular mass matrices (see Newland, 1989, Chapter 6). This *apparent* restriction in Caughey and O'Kelly's result may be removed by considering the fact that the properties (and roles) of all the three system matrices are identical and can be treated on equal basis. In view of this, a modified version of Caughey and O'Kelly's theorem can be stated as following:

Theorem 2.1. *If* $\mathbf{M}$, $\mathbf{C}$ *and* $\mathbf{K}$ *are positive definite matrices and there exist a nonsingular* $\mathbf{X} \in \mathbb{R}^{N\times N}$ *such that* $\mathbf{X}^T\mathbf{M}\mathbf{X}$, $\mathbf{X}^T\mathbf{C}\mathbf{X}$ *and* $\mathbf{X}^T\mathbf{K}\mathbf{X}$ *are all real diagonal matrices then the following are equivalent*

$$(a)\,\mathbf{K}\mathbf{M}^{-1}\mathbf{C} = \mathbf{C}\mathbf{M}^{-1}\mathbf{K}, \quad (b)\,\mathbf{M}\mathbf{K}^{-1}\mathbf{C} = \mathbf{C}\mathbf{K}^{-1}\mathbf{M}, \quad (c)\,\mathbf{M}\mathbf{C}^{-1}\mathbf{K} = \mathbf{K}\mathbf{C}^{-1}\mathbf{M}.$$

Proof. We have to prove that: (1) from the given condition (a), (b) and (c) follows, (2) from (a), (b) and (c) the given condition follows – in total all the six statements proposed in the theorem. For notational brevity define $\mathfrak{Z} = \{\mathbf{M}, \mathbf{C}, \mathbf{K}\}$ as a ordered collection of the system property matrices. Instead of proving all the six statements separately, first we will prove that ' *there exist a* $\mathbf{X}$ *such that* $\mathbf{X}^T\mathfrak{Z}_k\mathbf{X}$ *is a real diagonal if and only if there exist an* $i, 1 \le i \le 3$ *such that* $\mathfrak{Z}_j\mathfrak{Z}_i^{-1}\mathfrak{Z}_m = \mathfrak{Z}_m\mathfrak{Z}_i^{-1}\mathfrak{Z}_j$ *for all* $j, m = 1, 2, 3 \neq i$' and then will come back to our main result.

Consider the 'if' part first: Let $\mathfrak{Z}_i$ is the positive definite matrix, then there exist a $\mathbf{V}$ such that $\mathfrak{Z}_i^{-1} = \mathbf{V}\mathbf{V}^T$. From the given condition $\mathfrak{Z}_j\mathfrak{Z}_i^{-1}\mathfrak{Z}_m = \mathfrak{Z}_m\mathfrak{Z}_i^{-1}\mathfrak{Z}_j$ we have $\mathfrak{Z}_j(\mathbf{V}\mathbf{V}^T)\mathfrak{Z}_m = \mathfrak{Z}_m(\mathbf{V}\mathbf{V}^T)\mathfrak{Z}_j$ or $(\mathbf{V}^T\mathfrak{Z}_j\mathbf{V})(\mathbf{V}^T\mathfrak{Z}_m\mathbf{V}) = (\mathbf{V}^T\mathfrak{Z}_m\mathbf{V})(\mathbf{V}^T\mathfrak{Z}_j\mathbf{V})$. This implies that $(\mathbf{V}^T\mathfrak{Z}_j\mathbf{V})$, $\forall j$, are symmetric matrices and also pairwise commutative. So there exist a orthogonal $\mathbf{Q}$ such that $\mathbf{Q}^T(\mathbf{V}^T\mathfrak{Z}_j\mathbf{V})\mathbf{Q}$ is diagonal $\forall j$. The 'if' part follows by selecting $\mathbf{X} = \mathbf{V}\mathbf{Q}$.

To prove the 'only if' part, suppose $(\mathbf{X}^T\mathfrak{Z}_i\mathbf{X}) = \mathbf{\Lambda}_i$ is a diagonal matrix with its elements $\lambda_{i_r} > 0$, $\forall r$. So $\mathbf{\Lambda}_i^{-1/2}(\mathbf{X}^T\mathfrak{Z}_i\mathbf{X})\mathbf{\Lambda}_i^{-1/2} = \mathbf{I}$, from which one has $\mathfrak{Z}_i = \mathbf{X}^{-T}\mathbf{\Lambda}_i^{1/2}\mathbf{\Lambda}_i^{1/2}\mathbf{X}^{-1}$ or $\mathfrak{Z}_i^{-1} = \mathbf{X}\mathbf{\Lambda}_i^{-1/2}\mathbf{\Lambda}_i^{-1/2}\mathbf{X}^T$. Now from the given condition $(\mathbf{X}^T\mathfrak{Z}_j\mathbf{X}) = \mathbf{\Lambda}_j$ is a diagonal matrix $\forall j \neq i$, or $\mathbf{\Lambda}_i^{-1/2}(\mathbf{X}^T\mathfrak{Z}_j\mathbf{X})\mathbf{\Lambda}_i^{-1/2} = \mathbf{\Lambda}_{j/i}$ a diagonal matrix. Similar expression for $\mathbf{\Lambda}_{m/i}$ can also be obtained by considering that $(\mathbf{X}^T\mathfrak{Z}_m\mathbf{X})$ is diagonal. Since two diagonal matrix always commute we have $\mathbf{\Lambda}_{j/i}\mathbf{\Lambda}_{m/i} = \mathbf{\Lambda}_{m/i}\mathbf{\Lambda}_{j/i}$, $\forall j, m \neq i$ or

$$\mathbf{\Lambda}_i^{-1/2}\mathbf{X}^T\mathfrak{Z}_j\mathbf{X}\mathbf{\Lambda}_i^{-1/2}\,\mathbf{\Lambda}_i^{-1/2}\mathbf{X}^T\mathfrak{Z}_m\mathbf{X}\mathbf{\Lambda}_i^{-1/2} = \mathbf{\Lambda}_i^{-1/2}\mathbf{X}^T\mathfrak{Z}_m\mathbf{X}\mathbf{\Lambda}_i^{-1/2}\,\mathbf{\Lambda}_i^{-1/2}\mathbf{X}^T\mathfrak{Z}_j\mathbf{X}\mathbf{\Lambda}_i^{-1/2}.$$

Using the expression of $\mathfrak{Z}_i^{-1}$ obtained before, the above equation results $\mathfrak{Z}_j\mathfrak{Z}_i^{-1}\mathfrak{Z}_m = \mathfrak{Z}_m\mathfrak{Z}_i^{-1}\mathfrak{Z}_j$, $\forall j, m \neq i$.

Since in this proof l, m, i are all arbitrary and $\mathfrak{Z}_i^{-1}$ exist $\forall i = 1, 2, 3$ all the six statements proposed in the theorem have been proved by successive change of indices. □

This result may be alternatively proved by following Caughey and O'Kelly's approach and interchanging **M**, **K** and **C** successively. If a system is $(\bullet)$-singular then the condition(s) involving $(\bullet)^{-1}$ have to be disregarded and remaining condition(s) have to be used. Thus, for a positive definite system, along with Caughey and O'Kelly's result (condition (a) of the theorem), there exist two other equivalent criterion to judge whether a damped system can possess classical normal modes. It is important to note that these three conditions are equivalent and simultaneously valid but in general *not* the same.

Example 2.1. Assume that a system's mass, stiffness and damping matrices are given by

$$\mathbf{M} = \begin{bmatrix} 1.0 & 1.0 & 1.0 \\ 1.0 & 2.0 & 2.0 \\ 1.0 & 2.0 & 3.0 \end{bmatrix} \quad \text{and} \quad \mathbf{K} = \begin{bmatrix} 2 & -1 & 0.5 \\ -1 & 1.2 & 0.4 \\ 0.5 & 0.4 & 1.8 \end{bmatrix} \quad \text{and} \quad \mathbf{C} = \begin{bmatrix} 15.25 & -9.8 & 3.4 \\ -9.8 & 6.48 & -1.84 \\ 3.4 & -1.84 & 2.22 \end{bmatrix}.$$

It may be verified that all the system matrices are positive definite. The mass-normalized undamped modal matrix is obtained as

$$\mathbf{X} = \begin{bmatrix} 0.4027 & -0.5221 & -1.2511 \\ 0.5845 & -0.4888 & 1.1914 \\ -0.1127 & 0.9036 & -0.4134 \end{bmatrix}. \tag{2.3}$$

Since Caughey and O'Kelly's condition

$$\mathbf{K}\mathbf{M}^{-1}\mathbf{C} = \mathbf{C}\mathbf{M}^{-1}\mathbf{K} = \begin{bmatrix} 125.45 & -80.92 & 28.61 \\ -80.92 & 52.272 & -18.176 \\ 28.61 & -18.176 & 7.908 \end{bmatrix}$$

is satisfied, the system possess classical normal modes and that $\mathbf{X}$ given in equation (2.3) is the modal matrix. Because the system is positive definite the other two conditions,

$$\mathbf{M}\mathbf{K}^{-1}\mathbf{C} = \mathbf{C}\mathbf{K}^{-1}\mathbf{M} = \begin{bmatrix} 2.0 & -1.0 & 0.5 \\ -1.0 & 1.2 & 0.4 \\ 0.5 & 0.4 & 1.8 \end{bmatrix}$$

and

$$\mathbf{M}\mathbf{C}^{-1}\mathbf{K} = \mathbf{K}\mathbf{C}^{-1}\mathbf{M} = \begin{bmatrix} 4.1 & 6.2 & 5.6 \\ 6.2 & 9.73 & 9.2 \\ 5.6 & 9.2 & 9.6 \end{bmatrix}$$

are also satisfied. Thus all three conditions described in theorem 2.1 are simultaneously valid although none of them are the same. So, if any one of the three conditions proposed in Theorem 2.1 is satisfied, a viscously damped positive definite system possesses classical normal modes.

Example 2.2. Suppose for a system

$$\mathbf{M} = \begin{bmatrix} 7.0584 & 1.3139 \\ 1.3139 & 0.2446 \end{bmatrix}, \quad \mathbf{K} = \begin{bmatrix} 3.0 & -1.0 \\ -1.0 & 4.0 \end{bmatrix} \quad \text{and} \quad \mathbf{C} = \begin{bmatrix} 1.0 & -1.0 \\ -1.0 & 3.0 \end{bmatrix}.$$

It may be verified that the mass matrix is singular for this system. For this reason, Caughey and O'Kelly's criteria is not applicable. But, as the other two conditions in theorem 2.1,

$$\mathbf{M}\mathbf{K}^{-1}\mathbf{C} = \mathbf{C}\mathbf{K}^{-1}\mathbf{M} = \begin{bmatrix} 1.6861 & 0.3139 \\ 0.3139 & 0.0584 \end{bmatrix}$$

and

$$\mathbf{M}\mathbf{C}^{-1}\mathbf{K} = \mathbf{K}\mathbf{C}^{-1}\mathbf{M} = \begin{bmatrix} 29.5475 & 5.5 \\ 5.5 & 1.0238 \end{bmatrix}$$

are satisfied all three matrices can be diagonalized by a congruence transformation using the undamped modal matrix

$$\mathbf{X} = \begin{bmatrix} 0.9372 & -0.1830 \\ 0.3489 & 0.9831 \end{bmatrix}.$$

2.2.2 Generalization of Proportional Damping

Obtaining a damping matrix from 'first principles' as with the mass and stiffness matrices is not possible for most systems. For this reason, assuming $\mathbf{M}$ and $\mathbf{K}$ are known, we often want to find $\mathbf{C}$ in terms of $\mathbf{M}$ and $\mathbf{K}$ such that the system still possesses classical normal modes. Of course, the earliest work along this line is the proportional damping shown in equation (2.1) by Rayleigh (1877). It may be verified that, for positive definite systems, expressing $\mathbf{C}$ in such a way will always satisfy all three conditions given by theorem 2.1. Caughey (1960) proposed that a *sufficient* condition for the existence of classical normal modes is: if $\mathbf{M}^{-1}\mathbf{C}$ can be expressed in a series involving powers of $\mathbf{M}^{-1}\mathbf{K}$. His result generalized Rayleigh's result, which turns out to be the first two terms of the series. Later, Caughey and O'Kelly (1965) proved that the series representation of damping

$$\mathbf{C} = \mathbf{M}\sum_{j=0}^{N-1} \alpha_j \left[\mathbf{M}^{-1}\mathbf{K}\right]^j \tag{2.4}$$

is the *necessary and sufficient* condition for existence of classical normal modes for systems without any repeated roots. This series is now known as the 'Caughey series' and is possibly the most general form of damping under which the system will still possess classical normal modes.

Here, a further generalized and useful form of proportional damping will be proposed. We assume that the system is positive definite. Consider the conditions (a) and (b) of theorem 2.1; premultiplying (a) by $\mathbf{M}^{-1}$ and (b) by $\mathbf{K}^{-1}$ one has

$$\begin{aligned} \left(\mathbf{M}^{-1}\mathbf{K}\right)\left(\mathbf{M}^{-1}\mathbf{C}\right) &= \left(\mathbf{M}^{-1}\mathbf{C}\right)\left(\mathbf{M}^{-1}\mathbf{K}\right) \quad \text{or} \quad \mathbf{AB} = \mathbf{BA} \\ \left(\mathbf{K}^{-1}\mathbf{M}\right)\left(\mathbf{K}^{-1}\mathbf{C}\right) &= \left(\mathbf{K}^{-1}\mathbf{C}\right)\left(\mathbf{K}^{-1}\mathbf{M}\right) \quad \text{or} \quad \mathbf{A}^{-1}\mathbf{D} = \mathbf{D}\mathbf{A}^{-1} \end{aligned} \tag{2.5}$$

where $\mathbf{A} = \mathbf{M}^{-1}\mathbf{K}$, $\mathbf{B} = \mathbf{M}^{-1}\mathbf{C}$ and $\mathbf{D} = \mathbf{K}^{-1}\mathbf{C}$. Notice that we did not consider the condition (c) of theorem 2.1. Premultiplying (c) by $\mathbf{C}^{-1}$, one would obtain a similar commutative condition but it would involve $\mathbf{C}$ terms in both the matrices, from which any meaningful expression of $\mathbf{C}$ in terms of $\mathbf{M}$ and $\mathbf{K}$ can not be deduced. For this reason only the above two commutative relationships will be considered. It is well known that for any two matrices $\mathbf{A}$ and $\mathbf{B}$, if $\mathbf{A}$ commutes with $\mathbf{B}$, $f(\mathbf{A})$ also commutes with $\mathbf{B}$ where $f(z)$ is any *analytic function* of the variable z. Thus, in view of the commutative relationships represented by equation (2.5), one can use almost *all* well known functions to represent $\mathbf{M}^{-1}\mathbf{C}$ in terms of $\mathbf{M}^{-1}\mathbf{K}$ and also $\mathbf{K}^{-1}\mathbf{C}$ in terms of $\mathbf{K}^{-1}\mathbf{M}$, that is, representations like $\mathbf{C} = \mathbf{M}f(\mathbf{M}^{-1}\mathbf{K})$ and $\mathbf{C} = \mathbf{K}f(\mathbf{K}^{-1}\mathbf{M})$ are valid for any analytic $f(z)$. Adding these two quantities and also taking $\mathbf{A}$ and $\mathbf{A}^{-1}$ in the argument of the function as (trivially) $\mathbf{A}$ and $\mathbf{A}^{-1}$ always commute we can express the damping matrix in the form of

$$\mathbf{C} = \mathbf{M}f_1\left(\mathbf{M}^{-1}\mathbf{K}, \mathbf{K}^{-1}\mathbf{M}\right) + \mathbf{K}f_2\left(\mathbf{M}^{-1}\mathbf{K}, \mathbf{K}^{-1}\mathbf{M}\right) \tag{2.6}$$

such that the system possesses classical normal modes. Further, postmultiplying condition (a) of theorem 2.1 by $\mathbf{M}^{-1}$ and (b) by $\mathbf{K}^{-1}$ one has

$$\begin{aligned} \left(\mathbf{K}\mathbf{M}^{-1}\right)\left(\mathbf{C}\mathbf{M}^{-1}\right) &= \left(\mathbf{C}\mathbf{M}^{-1}\right)\left(\mathbf{K}\mathbf{M}^{-1}\right) \\ \left(\mathbf{M}\mathbf{K}^{-1}\right)\left(\mathbf{C}\mathbf{K}^{-1}\right) &= \left(\mathbf{C}\mathbf{K}^{-1}\right)\left(\mathbf{M}\mathbf{K}^{-1}\right). \end{aligned} \tag{2.7}$$

Following a similar procedure we can express the damping matrix in the form

$$\mathbf{C} = f_3\left(\mathbf{K}\mathbf{M}^{-1}, \mathbf{M}\mathbf{K}^{-1}\right)\mathbf{M} + f_4\left(\mathbf{K}\mathbf{M}^{-1}, \mathbf{M}\mathbf{K}^{-1}\right)\mathbf{K} \tag{2.8}$$

for which system (2.2) possesses classical normal modes. The functions $f_i,\ i = 1, \cdots, 4$ can have very general forms– they may consist of an arbitrary number of multiplications, divisions, summations, subtractions or powers of any other functions or can even be functional compositions. Thus, any conceivable form of analytic functions that are valid for scalars can be used in equations (2.6) and (2.8). In a natural way, common restrictions applicable to scalar functions are also valid, for example logarithm of a negative number is not permitted. Although the functions $f_i,\ i = 1, \cdots, 4$ are general, the expression of $\mathbf{C}$ in (2.6) or (2.8) gets restricted because of the special nature of the *arguments* in the functions. As a consequence, $\mathbf{C}$ represented in (2.6) or (2.8) does not

cover the whole $\mathbb{R}^{N\times N}$, which is well known that many damped systems do not possess classical normal modes.

Rayleigh's result (2.1) can be obtained directly from equation (2.6) or (2.8) as a very special − one could almost say trivial − case by choosing each matrix function f_i as real scalar times an identity matrix. The damping matrix expressed in equation (2.6) or (2.8) provides a new way of interpreting the 'Rayleigh damping' or 'proportional damping' where the identity matrices (always) associated in the right or left side of **M** and **K** are replaced by arbitrary matrix functions f_i with proper arguments. This kind of damping model will be called *generalized proportional damping*. We call the representation in equation (2.6) *right-functional form* and that in equation (2.8) *left-functional form*. Caughey series (2.4) is an example of right functional form. Note that if **M** or **K** is singular then the argument involving its corresponding inverse has to be removed from the functions.

All analytic functions have power series form via Taylor expansion. It is also known that for any $\mathbf{A}\in\mathbb{R}^{N\times N}$, all $\mathbf{A}^k$, for integer $k>N$, can be expressed as a linear combination of $\mathbf{A}^j, j\leq(N-1)$ by a recursive relationship using the Cayley-Hamilton theorem. For this reason the expression of **C** in (2.6) or (2.8) can in turn be expressed in the form of Caughey series (2.4). However, since all f_i can have very general forms, such a representation may not be always straight forward. For example, if $\mathbf{C}=\mathbf{M}(\mathbf{M}^{-1}\mathbf{K})^e$ the system possesses normal modes, but it is neither a direct member of the Caughey series (2.4) nor is it a member of the series involving rational fractional powers given by Caughey (1960) as e is an irrational number. However, we know that $e=1+\frac{1}{1!}+\cdots+\frac{1}{r!}+\cdots\infty$, from which we can write $\mathbf{C}=\mathbf{M}(\mathbf{M}^{-1}\mathbf{K})(\mathbf{M}^{-1}\mathbf{K})^{\frac{1}{1!}}\cdots(\mathbf{M}^{-1}\mathbf{K})^{\frac{1}{r!}}\cdots\infty$, which can in principle be represented by the Caughey series. It is easy to verify that, from a practical point of view, this representation is not simple and requires truncation of the series up to some finite number of terms. Hence, **C** expressed in the form of equation (2.6) or (2.8) is a more convenient representation of the Caughey series and we say that *viscously damped positive definite systems possess classical normal modes if and only if* **C** *can be represented by equation (2.6) or (2.8)*.

Example 2.3. It will be shown that the linear dynamic system satisfying the following equations of free vibration

$$\begin{aligned}\mathbf{M}\ddot{\mathbf{q}}+\Big[&\mathbf{M}e^{-\left(\mathbf{M}^{-1}\mathbf{K}\right)^2/2}\sinh(\mathbf{K}^{-1}\mathbf{M}\ln(\mathbf{M}^{-1}\mathbf{K})^{2/3})\\&+\mathbf{K}\cos^2(\mathbf{K}^{-1}\mathbf{M})\sqrt[4]{\mathbf{K}^{-1}\mathbf{M}}\tan^{-1}\frac{\sqrt{\mathbf{M}^{-1}\mathbf{K}}}{\pi}\Big]\dot{\mathbf{q}}+\mathbf{K}\mathbf{q}=\mathbf{0}\end{aligned}\tag{2.9}$$

possesses classical normal modes and can be analyzed using modal analysis. Here **M** and **K** are the same as example 2.1.

Direct calculation shows $\mathbf{C}=\begin{bmatrix}-67.9188 & -104.8208 & -95.9566\\ -104.8208 & -161.1897 & -147.7378\\ -95.9566 & -147.7378 & -135.2643\end{bmatrix}$. Using the modal ma-

trix calculated before in equation (2.3), we obtain

$$\mathbf{X}^T\mathbf{C}\mathbf{X} = \begin{bmatrix} -88.9682 & 0.0 & 0.0 \\ 0.0 & 0.0748 & 0.0 \\ 0.0 & 0.0 & 0.5293 \end{bmatrix},$$

a diagonal matrix. Analytically the modal damping ratios can be obtained as

$$2\xi_j\omega_j = e^{-\omega_j^4/2}\sinh\left(\frac{1}{\omega_j^2}\ln\frac{4}{3}\omega_j\right) + \omega_j^2\cos^2\left(\frac{1}{\omega_j^2}\right)\frac{1}{\sqrt{\omega_j}}\tan^{-1}\frac{\omega_j}{\pi}. \tag{2.10}$$

A natural question which arises in the context of the generalized proportional damping is how to obtain the damping functions f_i from experimental modal analysis. The following numerical example shows how one might obtain these damping functions.

Example 2.4. Suppose Figure 2.1 shows modal damping ratios as a function of frequency obtained by conducting simple vibration testing on a structural system. The damping ratio is such that, within the frequency range considered, it shows very low values in the low frequency region, high values in the mid frequency region and again low values in the high frequency region. We want to

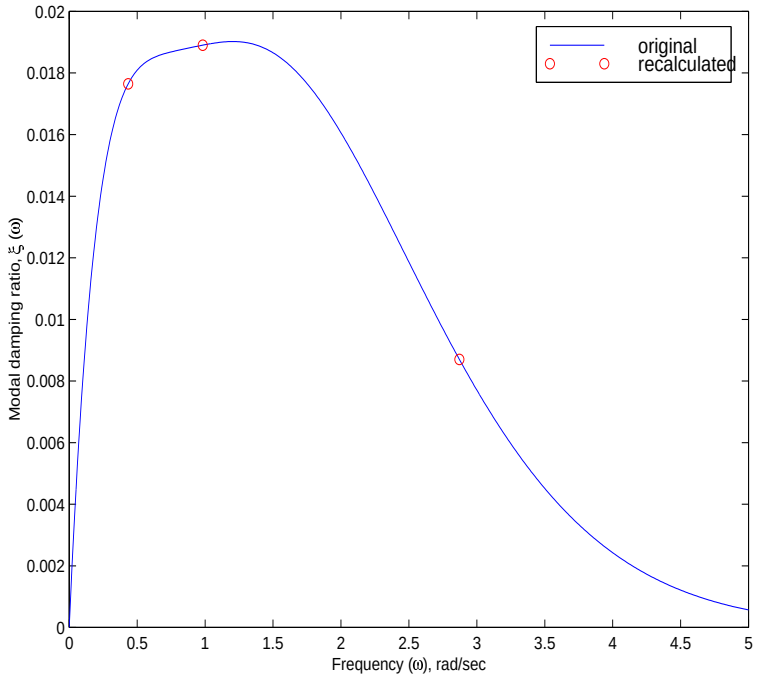

Figure 2.1: Curve of modal damping ratios (simulated)

find a damping model which shows this kind of behaviour. The first step is to identify the function which produces this curve. Here this (continuous) curve was simulated using the equation

$$\xi(\omega) = \frac{1}{15}\left(e^{-2.0\omega} - e^{-3.5\omega}\right)\left(1 + 1.25\sin\frac{\omega}{7\pi}\right)\left(1 + 0.75\omega^3\right). \tag{2.11}$$

From the above equation, the modal damping ratios in terms of the discrete natural frequencies, can be obtained by

$$2\xi_j\omega_j = \frac{2\omega_j}{15}\left(e^{-2.0\omega_j} - e^{-3.5\omega_j}\right)\left(1 + 1.25\sin\frac{\omega_j}{7\pi}\right)\left(1 + 0.75\omega_j^3\right). \tag{2.12}$$

In the light of the previous example, identifying the damping matrix which will produce the above damping ratio is straightforward (see the relationship between equation (2.9) and (2.10)). We view equation (2.12) as a function of ω_j^2 and simply replace ω_j^2 by $\mathbf{M}^{-1}\mathbf{K}$ and any constant terms by that constant times $\mathbf{I}$ to obtain the damping matrix. Using the right functional form in this case one has

$$\begin{aligned}\mathbf{C} =& \frac{2}{15}\mathbf{M}\sqrt{\mathbf{M}^{-1}\mathbf{K}}\left[e^{-2.0\sqrt{\mathbf{M}^{-1}\mathbf{K}}} - e^{-3.5\sqrt{\mathbf{M}^{-1}\mathbf{K}}}\right] \\ &\times \left[\mathbf{I} + 1.25\sin\left(\frac{1}{7\pi}\sqrt{\mathbf{M}^{-1}\mathbf{K}}\right)\right]\left[\mathbf{I} + 0.75(\mathbf{M}^{-1}\mathbf{K})^{3/2}\right]\end{aligned} \tag{2.13}$$

as the identified damping matrix. Using the numerical values of $\mathbf{M}$ and $\mathbf{K}$ from example 2.1 we obtain

$$\mathbf{C} = \begin{bmatrix} 2.3323 & 0.9597 & 1.4255 \\ 0.9597 & 3.5926 & 3.7624 \\ 1.4255 & 3.7624 & 7.8394 \end{bmatrix} \times 10^{-2}. \tag{2.14}$$

If we recalculate the damping ratios from the above constructed damping matrix, it will produce three points corresponding to the three natural frequencies which will exactly match with our initial curve as shown in figure 2.1. The method outlined here can produce a very accurate estimate of the damping matrix if the modal damping ratio function is known. When an exact expression of $\xi(\omega)$ is not known, all polynomial fitting methods can be employed to approximate $\xi(\omega)$ and corresponding to the fitted function one can construct a damping matrix by the procedure outlined here. As an example, if $2\xi_j\omega_j$ can be represented in a Fourier series by $2\xi_j\omega_j = \frac{a_0}{2} + \sum_{r=1}^{\infty}\left[a_r\cos\left(\frac{2\pi r\omega_j}{\Omega}\right) + b_r\sin\left(\frac{2\pi r\omega_j}{\Omega}\right)\right]$ then the damping matrix can be expanded as $\mathbf{C} = \frac{a_0}{2}\mathbf{I} + \mathbf{M}\sum_{r=1}^{\infty}\left[a_r\cos\left(2\pi r\Omega^{-1}\sqrt{\mathbf{M}^{-1}\mathbf{K}}\right) + b_r\sin\left(2\pi r\Omega^{-1}\sqrt{\mathbf{M}^{-1}\mathbf{K}}\right)\right]$ in a Fourier series.

2.3 Non-viscously Damped Systems

In Section 1.2.3 a class of non-viscous linear damping models where the damping forces depend on the past history of motion via convolution integrals was considered. Equations of motion governing free vibration of a linear system with such damping can be expressed by the following coupled integro-differential equations

$$\mathbf{M}\ddot{\mathbf{q}}(t) + \int_{-\infty}^{t} \boldsymbol{\mathcal{G}}(t,\tau)\,\dot{\mathbf{q}}(\tau)\,\mathrm{d}\tau + \mathbf{K}\mathbf{q}(t) = \mathbf{0}. \tag{2.15}$$

Here $\boldsymbol{\mathcal{G}}(t,\tau) \in \mathbb{R}^{N\times N}$ is the matrix of kernel functions. It is also assumed that $\boldsymbol{\mathcal{G}}(t,\tau)$ is a symmetric matrix so that reciprocity holds. Often the kernel depends upon the difference $(t-\tau)$ only: then, $\boldsymbol{\mathcal{G}}(t,\tau) = \boldsymbol{\mathcal{G}}(t-\tau)$. In a special case when $\boldsymbol{\mathcal{G}}(t,\tau) = \mathbf{C}\,\delta(t-\tau)$, where $\delta(t)$ is the Dirac-delta function, equation (2.15) reduces to equation (2.2). Most of the current research considers system (2.15) in its *general* form. For this reason an exact analysis becomes computationally expensive and almost intractable for large systems (see Chapter 3 for further discussions). Here we

are interested in whether such non-viscously damped systems can exhibit 'proportional damping' or 'classical damping', similar to the viscously damped case, so that a simplified analysis method can be adopted.

2.3.1 Existence of Classical Normal Modes

It is required to find out the conditions when there exist a non-zero $\mathbf{X} \in \mathbb{R}^{N\times N}$ which diagonalizes equation (2.15) by a congruence transformation. Unlike the viscously damped case where all the system matrices were constant and symmetric, here the system dynamics is characterized by two constant symmetric matrices and one symmetric matrix containing real functions. The problem of simultaneous diagonalization of Hermitian matrices with functional entries through constant complex transformations has been discussed by Chakrabarti *et al.* (1978). In view of their results and our earlier result (theorem 2.2) on viscously damped systems, the conditions for existence of classical normal modes in system (2.15) can be described as follows:

Theorem 2.2. *If* $\mathbf{M}$, $\mathbf{K}$ *and* $\boldsymbol{\mathcal{G}}(t,\tau), \forall t,\tau$ *are positive definite matrices and there exist a non-zero* $\mathbf{X} \in \mathbb{R}^{N\times N}$ *such that* $\mathbf{X}^T\mathbf{M}\mathbf{X}$, $\mathbf{X}^T\mathbf{K}\mathbf{X}$ *and* $\mathbf{X}^T\boldsymbol{\mathcal{G}}(t,\tau)\mathbf{X}, \forall t,\tau$ *are all real diagonal matrices then the following are equivalent*

(a) $\mathbf{K}\mathbf{M}^{-1}\boldsymbol{\mathcal{G}}(t,\tau) = \boldsymbol{\mathcal{G}}(t,\tau)\mathbf{M}^{-1}\mathbf{K}$,

(b) $\mathbf{M}\mathbf{K}^{-1}\boldsymbol{\mathcal{G}}(t,\tau) = \boldsymbol{\mathcal{G}}(t,\tau)\mathbf{K}^{-1}\mathbf{M}$,

(c) $\mathbf{M}\boldsymbol{\mathcal{G}}^{-1}(t,\tau)\mathbf{K} = \mathbf{K}\boldsymbol{\mathcal{G}}^{-1}(t,\tau)\mathbf{M}, \forall t,\tau$.

A rigorous proof of this theorem can be constructed following the proof of theorem 2.1 together with the results established by Chakrabarti *et al.* (1978). Intuitively, if $\boldsymbol{\mathcal{G}}(t,\tau)$ is a sufficiently smooth matrix function then one can obtain a sequence $\boldsymbol{\mathcal{G}}_{jk} = \boldsymbol{\mathcal{G}}(t_j,\tau_k) \in \mathbb{R}^{N\times N}, \forall j,k = 1,2,\cdots,\infty$, where all $\boldsymbol{\mathcal{G}}_{jk}$ are symmetric. Use of theorem 2.1 for all $j,k = 1,2,\cdots,\infty$ essentially leads to the result of this theorem.

Example 2.5. Consider a system whose equation of motion can be described by (2.15) with

$$\mathbf{M} = \begin{bmatrix} 2 & -1 \\ -1 & 3 \end{bmatrix}, \quad \mathbf{K} = \begin{bmatrix} 1 & -2 \\ -2 & 5 \end{bmatrix}$$

and

$$\boldsymbol{\mathcal{G}}(t,\tau) = \begin{bmatrix} 1.0177e^{-\mu_1\hat{\tau}} + 0.3517e^{-\mu_2\hat{\tau}^2/2} & -1.7724e^{-\mu_1\hat{\tau}} - 0.5364e^{-\mu_2\hat{\tau}^2/2} \\ -1.7724e^{-\mu_1\hat{\tau}} - 0.5364e^{-\mu_2\hat{\tau}^2/2} & 4.4749e^{-\mu_1\hat{\tau}} + 1.3688e^{-\mu_2\hat{\tau}^2/2} \end{bmatrix}, \quad \text{where} \quad \hat{\tau} = t-\tau$$

and μ_1, μ_2 are constants. Note that $\mathbf{M}$, $\mathbf{K}$ and $\boldsymbol{\mathcal{G}}(t,\tau)$ are positive definite. It may be easily verified that all the three conditions outlined in Theorem 2.2 are satisfied. For this reason the undamped modal matrix

$$\mathbf{X} = \begin{bmatrix} 0.7710 & -0.0743 \\ 0.3124 & 0.5499 \end{bmatrix}$$

which diagonalizes $\mathbf{M}$ and $\mathbf{K}$ also diagonalizes $\boldsymbol{\mathcal{G}}(t,\tau)$ as

$$\mathbf{X}^T\boldsymbol{\mathcal{G}}(t,\tau)\mathbf{X} = \begin{bmatrix} 0.1879e^{-\mu_1\hat{\tau}} + 0.0843e^{-\mu_2\hat{\tau}^2/2} & 0.0 \\ 0.0 & 1.5037e^{-\mu_1\hat{\tau}} + 0.4597e^{-\mu_2\hat{\tau}^2/2} \end{bmatrix}$$

is a diagonal matrix $\forall t,\tau$.

2.3.2 Generalization of Proportional Damping

We can now follow the approach similar to the viscously damped case for obtaining an expression of the damping function in terms of $\mathbf{M}$ and $\mathbf{K}$ so that system (2.15) possesses classical normal modes. From results (a) and (b) of theorem 2.2, the conditions for existence of classical normal modes can be expressed as

$$\mathbf{A}\boldsymbol{\mathcal{B}}(t,\tau) = \boldsymbol{\mathcal{B}}(t,\tau)\mathbf{A} \quad \text{and} \quad \mathbf{A}^{-1}\boldsymbol{\mathcal{D}}(t,\tau) = \boldsymbol{\mathcal{D}}(t,\tau)\mathbf{A}^{-1}, \quad \forall t,\tau \tag{2.16}$$

where $\mathbf{A} = \mathbf{M}^{-1}\mathbf{K}$, $\boldsymbol{\mathcal{B}}(t,\tau) = \mathbf{M}^{-1}\boldsymbol{\mathcal{G}}(t,\tau)$ and $\boldsymbol{\mathcal{D}}(t,\tau) = \mathbf{K}^{-1}\boldsymbol{\mathcal{G}}(t,\tau)$. In view of this commutative condition we say system (2.15) possesses classical normal modes if and only if

$$\boldsymbol{\mathcal{G}}(t,\tau) = \mathbf{M}\mathcal{F}_1\left(\mathbf{M}^{-1}\mathbf{K}, \mathbf{K}^{-1}\mathbf{M}, t, \tau\right) + \mathbf{K}\mathcal{F}_2\left(\mathbf{M}^{-1}\mathbf{K}, \mathbf{K}^{-1}\mathbf{M}, t, \tau\right) \tag{2.17}$$

where $\mathcal{F}_i(z_1, z_2, t, \tau),\ i = 1, 2$ are any real $z_1 z_2$-analytic functions such that $\left|\int_{-\infty}^{\infty} \mathcal{F}_i(z_1, z_2, t, \tau)\,\mathrm{d}\tau\right| < \infty,\ \forall z_1, z_2, t$. This representation of damping is the right-functional form. Following a similar approach to that outlined for the viscous damping case, one can also have the left-functional form as

$$\boldsymbol{\mathcal{G}}(t,\tau) = \mathcal{F}_3\left(\mathbf{K}\mathbf{M}^{-1}, \mathbf{M}\mathbf{K}^{-1}, t, \tau\right)\mathbf{M} + \mathcal{F}_4\left(\mathbf{K}\mathbf{M}^{-1}, \mathbf{M}\mathbf{K}^{-1}, t, \tau\right)\mathbf{K}. \tag{2.18}$$

This is possibly the most general class of damping that can be treated within the scope of classical modal analysis. The representation of $\mathbf{C}$ in equation (2.6) and (2.8) can be obtained as a special case when $\mathcal{F}_i(z_1, z_2, t, \tau) = f_i(z_1, z_2)\delta(t-\tau)$. This in turn relates equation (2.17) and (2.18) to the Rayleigh's representation and Caughey series.

Example 2.6. It will be shown that the linear dynamic system satisfying the following equations of motion of free vibration

$$\mathbf{M}\ddot{\mathbf{q}} + \int_{-\infty}^{t} \left[\mathbf{M}(\mathbf{K}^{-1}\mathbf{M})^{-\pi/4}e^{-\mu(t-\tau)} + e^{-\sqrt{\mathbf{K}\mathbf{M}^{-1}}}\mathbf{K}\delta(t-\tau)\right]\dot{\mathbf{q}}(\tau)\,\mathrm{d}\tau + \mathbf{K}\mathbf{q} = \mathbf{0}$$

possesses classical normal modes. Here $\mathbf{M}$ and $\mathbf{K}$ are the same as example 2.1 and μ is a constant.

Introduce the transformation $\mathbf{y}(t) = \mathbf{X}\mathbf{q}(t)$ where the mass normalized modal matrix $\mathbf{X}$ is given as before in equation (2.3). From direct calculation, equations of motion in the modal coordinates may be obtained as

$$\begin{aligned}\mathbf{I}\ddot{\mathbf{y}} + \int_{-\infty}^{t} \begin{bmatrix} 0.2695 & 0.0 & 0.0 \\ 0.0 & 0.9732 & 0.0 \\ 0.0 & 0.0 & 5.2433 \end{bmatrix} e^{-\mu(t-\tau)}\dot{\mathbf{y}}(\tau)\,\mathrm{d}\tau \\ + \begin{bmatrix} 0.1220 & 0.0 & 0.0 \\ 0.0 & 0.3615 & 0.0 \\ 0.0 & 0.0 & 0.4668 \end{bmatrix}\dot{\mathbf{y}} + \begin{bmatrix} 0.1883 & 0.0 & 0.0 \\ 0.0 & 0.9660 & 0.0 \\ 0.0 & 0.0 & 8.2457 \end{bmatrix}\mathbf{y} = \mathbf{0}.\end{aligned}$$

The above equations are uncoupled and can be solved in the frequency domain adopting similar procedures to those used for viscously damped systems.

2.4 Conclusions

Conditions for the existence of classical normal modes in viscously and non-viscously damped linear multiple degree-of-freedom systems have been discussed. The non-viscous damping mechanism is such that it depends on the past history of the velocities via convolution integrals over some kernel functions. Caughey and O'Kelly's (1965) criteria for the existence of classical normal modes in viscously damped systems is extended to non-viscously damped systems and systems with a singular mass matrix. By introducing the concept of generalized proportional damping we have extended the applicability of classical damping. The generalized proportional damping expresses the damping in terms of *any* non-linear function involving time and specially arranged mass and stiffness matrices so that the system still posses classical normal modes. This enables to analyze more general class of non-viscously damped discrete linear dynamic systems using classical modal analysis.

Chapter 3

Dynamics of Non-viscously Damped Systems

3.1 Introduction

In the last chapter, the concept of proportional damping was extended to non-viscously damped systems. Conditions for existence of proportional damping in non-viscously damped systems were derived. It is clear that these conditions are purely mathematical in nature and there is no reason why a general linear system should obey such conditions. Thus, in general, non-viscously damped systems are non-proportionally damped. The central theme of this chapter is to analyze non-viscously damped multiple-degrees-of-freedom linear systems with non-proportional damping. We rewrite the equations of motion of forced vibration of an N-degrees-of-freedom linear system with non-viscous damping as

$$\mathbf{M}\ddot{\mathbf{q}}(t) + \int_0^t \boldsymbol{\mathcal{G}}(t-\tau)\dot{\mathbf{q}}(\tau)\mathrm{d}\tau + \mathbf{K}\mathbf{q}(t) = \mathbf{f}(t). \tag{3.1}$$

The *initial conditions* associated with the above equation are

$$\begin{aligned} \mathbf{q}(0) &= \mathbf{q_0} \in \mathbb{R}^N \\ \text{and} \quad \dot{\mathbf{q}}(0) &= \dot{\mathbf{q}}_\mathbf{0} \in \mathbb{R}^N. \end{aligned} \tag{3.2}$$

In Section 1.4 currently available methods for analyzing such systems were discussed. Majority of the available methods employ additional dissipation coordinates and then use the state-space formalism. This approach not only computationally more involved but also physical insight is lost in such approach. For this reason, we develop procedures which avoid this approach and is consistent with traditional modal analysis.

The nature of eigenvalues and eigenvectors is discussed under certain simplified but physically realistic assumptions on the system matrices and kernel functions. A series expansion method for the determination of complex eigenvectors is proposed. The transfer function matrix of the system is derived in term of these eigenvectors. Exact closed-form expressions are derived for the transient response and the response due to non-zero initial conditions. Applications of the proposed method

and related numerical issues are discussed using a non-viscously damped three-degrees-of-freedom system.

3.2 Eigenvalues and Eigenvectors

Considering free vibration, that is $\mathbf{f}(t) = \mathbf{q_0} = \dot{\mathbf{q}}_\mathbf{0} = \mathbf{0}$, and taking the Laplace transform of the equations of motion (3.1) one has

$$s^2\mathbf{M}\bar{\mathbf{q}} + s\mathbf{G}(s)\bar{\mathbf{q}} + \mathbf{K}\bar{\mathbf{q}} = \mathbf{0}. \tag{3.3}$$

Here $\bar{\mathbf{q}}(s) = \mathcal{L}[\mathbf{q}(t)] \in \mathbb{C}^N$, $\mathbf{G}(s) = \mathcal{L}[\boldsymbol{\mathcal{G}}(t)] \in \mathbb{C}^{N\times N}$ and $\mathcal{L}[\bullet]$ denotes the Laplace transform. In the context of structural dynamics, $s = \mathrm{i}\omega$, where $\mathrm{i} = \sqrt{-1}$ and $\omega \in \mathbb{R}^+$ denotes the frequency. It is assumed that: (a) $\mathbf{M}^{-1}$ exists, and (b) *all* the eigenvalues of $\mathbf{M}^{-1}\mathbf{K}$ are distinct and positive. Because $\boldsymbol{\mathcal{G}}(t)$ is a real function, $\mathbf{G}(s)$ is also a real function of the parameter s. We assume that $\mathbf{G}(s)$ is such that the motion is dissipative. Conditions which $\mathbf{G}(s)$ must satisfy in order to produce dissipative motion were given by Golla and Hughes (1985). Several physically realistic mathematical forms of the elements of $\mathbf{G}(s)$ were given in Table 1.1. For the linear viscoelastic case it can be shown that (see Bland, 1960, Muravyov, 1997), in general, the elements of $\mathbf{G}(s)$ can be represented as

$$G_{jk}(s) = \frac{p_{jk}(s)}{q_{jk}(s)} \tag{3.4}$$

where $p_{jk}(s)$ and $q_{jk}(s)$ are finite-order polynomials in s. Here, we do not assume any specific functional form of $G_{jk}(s)$ but assume that $|G_{jk}(s)| < \infty$ when $s \to \infty$. This in turn implies that the elements of $\mathbf{G}(s)$ are at the most of order $1/s$ in s or constant, as in the case of viscous damping. The eigenvalues, s_j, associated with equation (3.3) are roots of the characteristic equation

$$\det\left[s^2\mathbf{M} + s\mathbf{G}(s) + \mathbf{K}\right] = 0. \tag{3.5}$$

If the elements of $\mathbf{G}(s)$ have simple forms, for example – as in equation (3.4), then the characteristic equation becomes a polynomial equation of finite order. In other cases the characteristic equation can be expressed as a polynomial equation by expanding $\mathbf{G}(s)$ in a Taylor series. However, the order of the equation will be infinite in those cases. For practical purposes the Taylor expansion of $\mathbf{G}(s)$ can be truncated to a finite series to make the characteristic equation a polynomial equation of finite order. Such equations can be solved using standard numerical methods (see Press *et al.*, 1992, Chapter 9). Suppose the order of the characteristic polynomial is m. In general m is more than $2N$, that is $m = 2N + p;\ p \geq 0$. Thus, although the system has N degrees-of-freedom, the number of eigenvalues is more than $2N$. This is a major difference between the non-viscously damped systems and the viscously damped systems where the number of eigenvalues is exactly $2N$, including any multiplicities.

A general analysis on the nature of the eigenvalues of non-viscously damped systems is beyond the scope of this chapter. It is assumed that *all* m eigenvalues are distinct. We further restrict

our attention to a special case when, among the m eigenvalues, $2N$ appear in complex conjugate pairs[1]. Under such assumptions it is easy to show that the remaining p eigenvalues become purely real. The mathematical conditions which **M**, **K** and $\mathbf{G}(s)$ must satisfy in order to produce such eigenvalues will not be obtained but a physical justification will follow shortly. For convenience the eigenvalues are arranged as

$$s_1, s_2, \cdots, s_N, s_1^*, s_2^*, \cdots, s_N^*, s_{2N+1}, \cdots, s_m \tag{3.6}$$

where $(\bullet)^*$ denotes complex conjugation.

The eigenvalue problem associated with equation (3.1) can be defined from (3.3) as

$$\mathbf{D}(s_j)\mathbf{z}_j = \mathbf{0}, \quad \text{for } j = 1, \cdots, m \tag{3.7}$$

where

$$\mathbf{D}(s_j) = s_j^2\mathbf{M} + s_j\,\mathbf{G}(s_j) + \mathbf{K} \tag{3.8}$$

is the *dynamic stiffness matrix* corresponding to the j-th eigenvalue and $\mathbf{z}_j$ is the j-th eigenvector. Here $(\bullet)^T$ denotes the matrix transpose. From equation (3.7) it is clear that, when s_j appear in complex conjugate pairs, $\mathbf{z}_j$ also appear in complex conjugate pairs, and when s_j is real $\mathbf{z}_j$ is also real. Corresponding to the $2N$ complex conjugate pairs of eigenvalues, the N eigenvectors together with their complex conjugates will be called *elastic modes*. These modes are related to the N modes of vibration of the structural system. Physically, the assumption of '$2N$ complex conjugate pairs of eigenvalues' implies that all the elastic modes are oscillatory in nature, that is, they are sub-critically damped. The modes corresponding to the 'additional' p eigenvalues will be called *non-viscous modes*. These modes are induced by the non-viscous effect of the damping mechanism. For stable passive systems the non-viscous modes are over-critically damped (*i.e.*, negative real eigenvalues) and not oscillatory in nature. Non-viscous modes, or similar to these, are known by different names in the literature of different subjects, for example, 'wet modes' in the context of ship dynamics (Bishop and Price, 1979) and 'damping modes' in the context of viscoelastic structures (McTavis and Hughes, 1993). Determination of the eigenvectors is considered next.

3.2.1 Elastic Modes

Once the eigenvalues are known, $\mathbf{z}_j, \forall j = 1, \cdots, 2N$ can be obtained from equation (3.7) by fixing any one element and inverting the matrix $\mathbf{D}(s_j) \in \mathbb{C}^{N\times N}$. Note that inversion of an $(N-1)\times(N-1)$ complex matrix is required for calculation of every $\mathbf{z}_j$. Although the method is exact, it is computationally expensive and does not offer much physical insight. Here we propose an alternative method based on Neumann expansion approach which utilizes the familiar undamped eigenvectors discussed in Section 1.1.2.

[1]Because $\mathcal{G}(t)$ is real, $\mathbf{G}^*(s) = \mathbf{G}(s^*)$. Using this and taking complex conjugation of (3.3) it is clear that $s^{*^2}\mathbf{M}\bar{\mathbf{q}} + s^*\mathbf{G}(s^*)\bar{\mathbf{q}} + \mathbf{K}\bar{\mathbf{q}} = \mathbf{0}$, *i.e.*, if s satisfies equation (3.3) then so does s^*.

Neumann Expansion Method

For distinct undamped eigenvalues (ω_l^2), $\mathbf{x}_l$, $\forall\, l = 1, \cdots, N$, form a *complete* set of vectors. For this reason, $\mathbf{z}_j$ can be expanded as a complex linear combination of $\mathbf{x}_l$. Thus, an expansion of the form

$$\mathbf{z}_j = \sum_{l=1}^{N} \alpha_l^{(j)} \mathbf{x}_l \tag{3.9}$$

may be considered. Now, without any loss of generality, we can assume that $\alpha_j^{(j)} = 1$ (normalization) which leaves us to determine $\alpha_l^{(j)}, \forall l \neq j$. Substituting the expansion of $\mathbf{z}_j$, from equation (3.7) one obtains

$$\sum_{l=1}^{N} s_j^2 \alpha_l^{(j)} \mathbf{M}\mathbf{x}_l + s_j \alpha_l^{(j)} \mathbf{G}(s_j)\mathbf{x}_l + \alpha_l^{(j)} \mathbf{K}\mathbf{x}_l = \mathbf{0}. \tag{3.10}$$

Premultiplying above equation by $\mathbf{x}_k^T$ and using the orthogonality property of the undamped eigenvectors described by (1.10) and (1.11) one obtains

$$s_j^2 \alpha_k^{(j)} + s_j \sum_{l=1}^{N} \alpha_l^{(j)} G'_{kl}(s_j) + \omega_k^2 \alpha_k^{(j)} = 0, \quad \forall k = 1, \cdots, N \tag{3.11}$$

where $G'_{kl}(s_j) = \mathbf{x}_k^T \mathbf{G}(s_j)\mathbf{x}_l$. The j-th equation of this set obtained by setting $k = j$ is a trivial case because $\alpha_j^{(j)} = 1$ has already been assumed. From the above set of equations, excluding this trivial case, one has

$$\begin{aligned} s_j^2 \alpha_k^{(j)} + s_j \left(G'_{kj}(s_j) + \alpha_k^{(j)} G'_{kk}(s_j) + \sum_{l \neq k \neq j}^{N} \alpha_l^{(j)} G'_{kl}(s_j) \right) + \omega_k^2 \alpha_k^{(j)} = 0, \\ \forall k = 1, \cdots, N; \neq j. \end{aligned} \tag{3.12}$$

These equations can be combined into a matrix form as

$$\left[\mathbf{P}^{(j)} - \mathbf{Q}^{(j)} \right] \hat{\mathbf{a}}^{(j)} = {\mathbf{g}_\mathbf{u}}^{(j)}. \tag{3.13}$$

In the above equation:

$$\begin{aligned} \mathbf{P}^{(j)} = \operatorname{diag} \Bigg[\frac{s_j^2 + s_j G'_{11}(s_j) + \omega_1^2}{-s_j}, \cdots, {}^{\{j-\text{th term deleted}\}}, \\ \cdots, \frac{s_j^2 + s_j G'_{NN}(s_j) + \omega_N^2}{-s_j} \Bigg] \in \mathbb{C}^{(N-1)\times(N-1)}, \end{aligned} \tag{3.14}$$

the trace-less matrix

$$\mathbf{Q}^{(j)} = \begin{bmatrix} 0 & G'_{12}(s_j) & \cdots & \{j-\text{th term deleted}\} & \cdots & G'_{1N}(s_j) \\ G'_{21}(s_j) & 0 & \vdots & \vdots & \vdots & G'_{2N}(s_j) \\ \vdots & \vdots & \vdots & \{j-\text{th term deleted}\} & \vdots & \vdots \\ \vdots & \vdots & \vdots & \vdots & \vdots & \vdots \\ G'_{N1}(s_j) & G'_{N2}(s_j) & \cdots & \{j-\text{th term deleted}\} & \cdots & 0 \end{bmatrix} \in \mathbb{C}^{(N-1)\times(N-1)}, \tag{3.15}$$

$$\mathbf{g_u}^{(j)} = \left\{G'_{1j}(s_j), G'_{2j}(s_j), \cdots, ^{\{j-\text{th term deleted}\}}, \cdots, G'_{Nj}(s_j)\right\}^T \in \mathbb{C}^{(N-1)} \tag{3.16}$$

and

$$\hat{\mathbf{a}}^{(j)} = \left\{\alpha_1^{(j)}, \alpha_2^{(j)}, \cdots, ^{\{j-\text{th term deleted}\}}, \cdots, \alpha_N^{(j)}\right\}^T \in \mathbb{C}^{(N-1)} \tag{3.17}$$

is the vector of unknown $\alpha_k^{(j)}, \forall k \neq j$. From equation (3.13), $\hat{\mathbf{a}}^{(j)}$ has to be determined by performing the associated matrix inversion and is achieved by using the Neumann expansion method. Now, using the Neumann expansion we have

$$\begin{aligned}\hat{\mathbf{a}}^{(j)} &= \left[\mathbf{I}_{N-1} - \mathbf{P}^{(j)^{-1}}\mathbf{Q}^{(j)}\right]^{-1}\left\{\mathbf{P}^{(j)^{-1}}\mathbf{g_u}^{(j)}\right\} \\ &= \left[\mathbf{I}_{N-1} + \mathbf{R_u}^{(j)} + \mathbf{R_u}^{(j)^2} + \mathbf{R_u}^{(j)^3} + \cdots\right]\mathbf{a}_0^{(j)}\end{aligned} \tag{3.18}$$

where $\mathbf{I}_{N-1}$ is a $(N-1)\times(N-1)$ identity matrix,

$$\mathbf{R_u}^{(j)} = \mathbf{P}^{(j)^{-1}}\mathbf{Q}^{(j)} \in \mathbb{C}^{(N-1)\times(N-1)} \tag{3.19}$$

and

$$\mathbf{a}_0^{(j)} = \mathbf{P}^{(j)^{-1}}\mathbf{g_u}^{(j)} \in \mathbb{C}^{(N-1)}. \tag{3.20}$$

Because $\mathbf{P}^{(j)}$ is a diagonal matrix, its inversion can be carried out analytically and subsequently the closed-form expressions of $\mathbf{R_u}^{(j)}$ and $\mathbf{a}_0^{(j)}$ can be obtained as

$$R_{u_{kl}}^{(j)} = \frac{-s_j G'_{kl}(s_j)\,(1-\delta_{kl})}{\omega_k^2 + s_j^2 + s_j G'_{kk}(s_j)}, \quad \forall k, l \neq j \tag{3.21}$$

$$a_{0_l}^{(j)} = \frac{-s_j G'_{lj}(s_j)}{\omega_l^2 + s_j^2 + s_j G'_{ll}(s_j)}, \quad \forall l \neq j. \tag{3.22}$$

This makes further calculations involving these quantities simpler. From equation (3.18), $\hat{\mathbf{a}}^{(j)}$ can be calculated in an efficient way as one can write

$$\hat{\mathbf{a}}^{(j)} = \mathbf{a}_0^{(j)} + \mathbf{a}_1^{(j)} + \mathbf{a}_2^{(j)} + \cdots + \mathbf{a}_k^{(j)} + \cdots \tag{3.23}$$

where

$$\mathbf{a}_1^{(j)} = \mathbf{R_u}^{(j)}\mathbf{a}_0^{(j)},\ \mathbf{a}_2^{(j)} = \mathbf{R_u}^{(j)}\mathbf{a}_1^{(j)},\ \cdots\ \mathbf{a}_k^{(j)} = \mathbf{R_u}^{(j)}\mathbf{a}_{k-1}^{(j)}. \tag{3.24}$$

This implies that all the $\mathbf{a}_k^{(j)}$ can be obtained using successive matrix-vector multiplications only. Noting that $\hat{\mathbf{a}}^{(j)}$ is the vector of $\alpha_k^{(j)}, \forall k \neq j$, substitution of it in equation (3.9) will give the elastic modes. It is easy to see that by taking more terms in the series represented by (3.23), one can obtain the elastic modes to any desired accuracy provided the complex matrix power series $\mathbf{I}_{N-1} + \mathbf{R_u}^{(j)} + \mathbf{R_u}^{(j)^2} + \mathbf{R_u}^{(j)^3} + \cdots$ is convergent. Convergence of this series will be addressed later.

From the preceding formulation one may verify that, corresponding to the complex conjugate pairs of the eigenvalues, the eigenvectors also appear in complex conjugate pairs. For many engineering problems it is often observed that the damping forces are not very 'big' and that by retaining only a few terms in the series expression (3.23) will result in an acceptable accuracy. Closed-form approximate expressions for the elastic modes obtained by retaining one and two terms of these series are given in Section 3.2.3. These expressions might be useful whenever we find that the entries of the damping kernel-functions are small compared to those of $\mathbf{M}$ and $\mathbf{K}$.

Convergence of the Neumann Series

For the validity of the series expressions for $\hat{\mathbf{a}}^{(j)}$ in (3.23) it is required that the series

$$\mathbf{S_u} = \mathbf{I}_{N-1} + \mathbf{R_u}^{(j)} + \mathbf{R_u}^{(j)^2} + \mathbf{R_u}^{(j)^3} + \cdots \tag{3.25}$$

should be convergent. We develop following conditions for convergence.

Condition 1. *The complex matrix power series* $\mathbf{S_u}$ *converges if, and only if, for all the eigenvalues* $\sigma_l^{(j)}$ *of the matrix* $\mathbf{R_u}^{(j)}$*, the inequality* $|\sigma_l^{(j)}| < 1$ *holds.*

Although this condition is both necessary and sufficient, checking convergence for all $j = 1, \cdots, N$ is often not feasible. So we look for a sufficient condition which is relatively easy to check and which ensures convergence for all $j = 1, \cdots, N$.

Condition 2. *The complex matrix power series* $\mathbf{S_u}$ *converges for any* s_j, ω_j *if* $\mathbf{G}'(s_j)$ *is a diagonally dominant matrix.*

Proof. Since a matrix norm is always greater than or equal to its maximum eigenvalue, it follows from condition 1 that convergence of the series is guaranteed if $\| \mathbf{R_u}^{(j)} \| < 1$. Writing the sum of absolute values of entries of $\mathbf{R_u}^{(j)}$ results in the following inequality as the required sufficient condition for convergence

$$\sum_{\substack{k=1\\k\neq j}}^{N}\sum_{\substack{l=1\\l\neq j}}^{N}\left|\frac{s_j G'_{kl}(s_j)}{\omega_k^2 + s_j^2 + s_j G'_{kk}(s_j)}\right|(1-\delta_{lk}) < 1. \tag{3.26}$$

Dividing both numerator and denominator by s_j the above inequality can be written as

$$\sum_{\substack{k=1\\k\neq j}}^{N}\sum_{\substack{l=1\\l\neq i\neq k}}^{N}\frac{|G'_{kl}(s_j)|}{|1/s_j\left(\omega_k^2 + s_j^2\right) + G'_{kk}(s_j)|} < 1. \tag{3.27}$$

Taking the maximum for all $k \neq j$ this condition can further be represented as

$$\max_{k\neq j}\frac{\sum_{\substack{l=1\\l\neq j,k}}^{N}|G'_{kl}(s_j)|}{|1/s_j\left(\omega_k^2 + s_j^2\right) + G'_{kk}(s_j)|} < 1. \tag{3.28}$$

It is clear that (3.28) always holds if

$$\sum_{\substack{l=1 \\ l\neq j\neq k}}^{N} |G'_{kl}(s_j)| < |G'_{kk}(s_j)|, \quad \forall k \neq j; \tag{3.29}$$

which in turn implies that, for all $j = 1 \cdots N$, the inequality $\| \mathbf{R_u}^{(j)} \| < 1$ holds if $\mathbf{G}'(s_j)$ is a diagonally dominant matrix. It is important to note that the diagonal dominance of $\mathbf{G}'(s_j)$ is only a sufficient condition and the lack of it does not necessarily prevent convergence of $\mathbf{S_u}$. □

3.2.2 Non-viscous Modes

When $2N < j \leq m$, the eigenvalues become real and consequently from equation (3.8) we observe that $\mathbf{D}(s_j) \in \mathbb{R}^{N\times N}$. The non-viscous modes can be obtained from equation (3.7) by fixing any one element of the eigenvectors. Since $\mathbf{D}(s_j) \in \mathbb{R}^{N\times N}$, from equations (3.7) it is easy to see that $\mathbf{z}_j \in \mathbb{R}^N$. Partition $\mathbf{z}_j$ as

$$\mathbf{z}_j = \begin{Bmatrix} \mathbf{z_1}_j \\ \mathbf{z_2}_j \end{Bmatrix}. \tag{3.30}$$

We select $\mathbf{z_1}_j = 1$ so that $\mathbf{z_2}_j \in \mathbb{R}^{(N-1)}$ has to be determined from equations (3.7). Further, partition $\mathbf{D}(s_j)$ as

$$\mathbf{D}(s_j) = \begin{bmatrix} \mathbf{D_{11}}(s_j) & \mathbf{D_{12}}(s_j) \\ \mathbf{D_{21}}(s_j) & \mathbf{D_{22}}(s_j) \end{bmatrix} \tag{3.31}$$

where $\mathbf{D_{11}}(s_j) \in \mathbb{R}$, $\mathbf{D_{12}}(s_j) \in \mathbb{R}^{1\times(N-1)}$, $\mathbf{D_{21}}(s_j) \in \mathbb{R}^{(N-1)\times 1}$ and $\mathbf{D_{22}}^{(j)} \in \mathbb{R}^{(N-1)\times(N-1)}$. In view of (3.31) and recalling that $\mathbf{z_1}_j = 1$, from equation (3.7) we can have

$$\begin{aligned} \mathbf{D_{22}}(s_j)\mathbf{z_2}_j &= -\mathbf{D_{21}}(s_j) \\ \text{or} \quad \mathbf{z_2}_j &= -\left[\mathbf{D_{22}}(s_j)\right]^{-1} \mathbf{D_{21}}(s_j). \end{aligned} \tag{3.32}$$

It may be noted that determination of the non-viscous modes is computationally more demanding than the elastic modes because inversion of an $(N-1)\times(N-1)$ real matrix is associated with each eigenvector. However, for most physically realistic non-viscous damping models it appears that the number of non-viscous modes is not very high and also the contribution of them to the global dynamic response is not very significant (see the example section). For this reason, calculation of the first few non-viscous modes may be sufficient from a practical point view.

3.2.3 Approximations and Special Cases

The expression of the elastic modes derived in Section 3.2.1 is quite general. In this section we consider some special cases and approximation of this general expression which are of practical interest.

Light Non-proportionally Damped Systems

For light non-proportionally damped systems, the off-diagonal entries of the modal damping function matrix is small compared to the diagonal entries, that is $G'_{kl}(s_j) \leq G'_{kk}(s_j)$, $\forall k \neq l, s_j$. For this reason higher order terms in the series expression (3.23) can be neglected.

The expression for the elastic modes obtained by taking one term in the series (3.23) is close to the one obtained from the first-order perturbation analysis. Considering the j-th set of equation (3.11) and neglecting the second-order terms involving $\alpha_k^{(j)}$ and $G'_{kl}(s_j)$, $\forall k \neq l$, and also noting that $\alpha_j^{(j)} = 1$, one obtains

$$\begin{aligned} & s_j^2 + s_j G'_{jj}(s_j) + \omega_j^2 \approx 0 \\ \text{or} \quad & s_j \approx \pm \mathrm{i}\omega_j - G'_{jj}(\pm \mathrm{i}\omega_j)/2 \\ & = \mathrm{i}\omega_j - G'_{jj}(\mathrm{i}\omega_j)/2, \quad -\mathrm{i}\omega_j - G'_{jj}(-\mathrm{i}\omega_j)/2. \end{aligned} \tag{3.33}$$

This is the first-order approximate expression for the complex eigenvalues of system (3.1) corresponding to the elastic modes. A similar result was also obtained by Woodhouse (1998). In deriving this expression the assumption has been made that $\mathbf{G}(s_j) \approx \mathbf{G}(\mathrm{i}\omega_j)$. Since the off-diagonal elements of $\mathbf{G}(s_j)$ is assumed small, it is expected that this approximation will not result in significant errors. Note that, as $\boldsymbol{\mathcal{G}}(t)$ is a real function, $G'_{jj}(\bullet)$ satisfies the property

$$G'_{jj}(-\mathrm{i}\omega_j) = G'^{*}_{jj}(\mathrm{i}\omega_j). \tag{3.34}$$

Using this relationship it may be confirmed that the eigenvalues corresponding to the elastic modes, approximately given by equation (3.33), appear in complex conjugate pairs.

To obtain approximate expression for the eigenvectors, one simply considers only the first term of the series (3.23) and substitutes $\hat{\mathbf{a}}^{(j)}$ in equation (3.9) to obtain

$$\mathbf{z}_j \approx \mathbf{x}_j - \sum_{\substack{k=1 \\ k\neq j}}^{N} \frac{s_j G'_{kj}(s_j)\mathbf{x}_k}{\omega_k^2 + s_j^2 + s_j G'_{kk}(s_j)}. \tag{3.35}$$

Now, retaining the first two terms of the series expression (3.23) and substituting $\hat{\mathbf{a}}^{(j)}$ in equation (3.9) one obtains

$$\begin{aligned} \mathbf{z}_j \approx \mathbf{x}_j & - \sum_{\substack{k=1 \\ k\neq j}}^{N} \frac{s_j G'_{kj}(s_j)\mathbf{x}_k}{\omega_k^2 + s_j^2 + s_j G'_{k}(s_j)} \\ & + \sum_{\substack{k=1 \\ k\neq j}}^{N} \sum_{\substack{l=1 \\ l\neq j\neq k}}^{N} \frac{s_j^2 G'_{kl}(s_j) G'_{lj}(s_j)\mathbf{x}_k}{\left(\omega_k^2 + s_j^2 + s_j G'_{kk}(s_j)\right)\left(\omega_l^2 + s_j^2 + s_j G'_{ll}(s_j)\right)}. \end{aligned} \tag{3.36}$$

The above equation is second-order approximate expressions for the eigenvectors corresponding to the elastic modes of system (3.1). Finally, note that no such simple expressions can be obtained for the non-viscous modes unless some specific forms for the kernel function are assumed.

Viscously Damped Systems With Light Non-proportional Damping

Eigensolutions of viscously damped systems consist of only the elastic modes. All the results derived for elastic modes can be applied to viscously damped systems by considering the fact that the matrix of the damping functions, $\mathbf{G}(s)$, is a constant matrix. Say $\mathbf{G}(s) = \mathbf{C}, \forall s$, where $\mathbf{C} \in \mathbb{R}^{N\times N}$ is the viscous damping matrix.

Using this simplification, from equation (3.33), the approximate eigenvalues (appear in complex conjugate pairs) can be obtained as

$$s_j \approx \pm \mathrm{i}\omega_j - C'_{jj}/2 = -C'_{jj}/2 + \mathrm{i}\omega_j, \quad -C'_{jj}/2 - \mathrm{i}\omega_j. \tag{3.37}$$

From equation (3.35), the first-order approximate expressions of eigenvectors may be obtained as

$$\mathbf{z}_j \approx \mathbf{x}_j - \sum_{\substack{k=1\\k\neq j}}^{N} \frac{s_j C'_{kj}\mathbf{x}_k}{\omega_k^2 + s_j^2 + s_j C'_{kk}}. \tag{3.38}$$

Similarly, from equation (3.36), the second-order approximate expressions of eigenvectors may be obtained as

$$\mathbf{z}_j \approx \mathbf{x}_j - \sum_{\substack{k=1\\k\neq j}}^{N} \frac{s_j C'_{kj}\mathbf{x}_k}{\omega_k^2 + s_j^2 + s_j C'_k} + \sum_{\substack{k=1\\k\neq j}}^{N}\sum_{\substack{l=1\\l\neq j\neq k}}^{N} \frac{s_j^2 C'_{kl} C'_{lj}\mathbf{x}_k}{\left(\omega_k^2 + s_j^2 + s_j C'_{kk}\right)\left(\omega_l^2 + s_j^2 + s_j C'_{ll}\right)}. \tag{3.39}$$

3.3 Transfer Function

The transfer function (matrix) of a system completely defines its input-output relationship in *steady-state*. It is well known that for any linear system, if the forcing function is harmonic, that is $\mathbf{f}(t) = \bar{\mathbf{f}}\exp[st]$ with $s = \mathrm{i}\omega$ and amplitude vector $\bar{\mathbf{f}} \in \mathbb{R}^N$, the steady-state response will also be harmonic at frequency $\omega \in \mathbb{R}^+$. So we seek a solution of the form $\mathbf{q}(t) = \bar{\mathbf{q}}\exp[st]$, where $\bar{\mathbf{q}} \in \mathbb{C}^N$ is the response vector in the frequency domain. Substitution of $\mathbf{q}(t)$ and $\mathbf{f}(t)$ in equation (3.1) gives

$$s^2\mathbf{M}\bar{\mathbf{q}} + s\,\mathbf{G}(s)\bar{\mathbf{q}} + \mathbf{K}\bar{\mathbf{q}} = \bar{\mathbf{f}} \quad \text{or} \quad \mathbf{D}(s)\bar{\mathbf{q}} = \bar{\mathbf{f}}. \tag{3.40}$$

Here the *dynamic stiffness matrix*

$$\mathbf{D}(s) = s^2\mathbf{M} + s\,\mathbf{G}(s) + \mathbf{K} \ \in \mathbb{C}^{N\times N}. \tag{3.41}$$

From equation (3.40) the response vector $\bar{\mathbf{q}}$ can be obtained as

$$\bar{\mathbf{q}} = \mathbf{D}^{-1}(s)\bar{\mathbf{f}} = \mathbf{H}(s)\bar{\mathbf{f}} \tag{3.42}$$

where

$$\mathbf{H}(s) = \mathbf{D}^{-1}(s) \in \mathbb{C}^{N\times N} \tag{3.43}$$

is the transfer function matrix. From this equation one further has

$$\mathbf{H}(s) = \frac{\text{adj}\,[\mathbf{D}(s)]}{\det\,[\mathbf{D}(s)]}. \tag{3.44}$$

The *poles* of $\mathbf{H}(s)$, denoted by s_j, are the eigenvalues of the system. Because it is assumed that *all* the m eigenvalues are distinct, each pole is a *simple pole*. The matrix inversion in (3.42) is difficult to carry out in practice because of the singularities associated with the poles. Moreover, such an approach would be an expensive numerical exercise and may not offer much physical insight. For these reasons, we seek a solution analogous to the classical modal series solution of the undamped or proportionally damped systems.

From the residue theorem it is known that any complex function can be expressed in terms of the poles and *residues*, that is, the transfer function has the form

$$\mathbf{H}(s) = \sum_{j=1}^{m} \frac{\mathbf{R}_j}{s - s_j}. \tag{3.45}$$

Here

$$\mathbf{R}_j = \operatorname*{res}_{s=s_j} [\mathbf{H}(s)] \stackrel{\text{def}}{=} \lim_{s \to s_j} (s - s_j)\,[\mathbf{H}(s)] \tag{3.46}$$

is the residue of the transfer function matrix at the pole s_j. It may be noted that equation (3.45) is equivalent to expressing the right hand side of equation (3.44) in the partial-fraction form. Here we try to obtain the residues, that is the coefficients in the partial-fraction form, in terms of the system eigenvectors.

3.3.1 Eigenvectors of the Dynamic Stiffness Matrix

It turns out that the eigenvectors of the dynamic stiffness matrix play an important role in determining the residues of the transfer function matrix. For any given $s \in \mathbb{C}$, the eigenvalue problem associated with the dynamic stiffness matrix can be expressed by

$$\mathbf{D}(s)\boldsymbol{\phi}_k(s) = \nu_k(s)\boldsymbol{\phi}_k(s), \quad \forall\, k = 1, \cdots, N. \tag{3.47}$$

In the preceding equation the eigenvalues $\nu_k(s) \in \mathbb{C}$ are the roots of the characteristic equation

$$\det\,[\mathbf{D}(s) - \nu(s)\mathbf{I}_N] = 0 \tag{3.48}$$

and $\boldsymbol{\phi}_k(s) \in \mathbb{C}^N$ is the k-th eigenvector of $\mathbf{D}(s)$. The symbols $\nu_k(s)$ and $\boldsymbol{\phi}_k(s)$ indicate functional dependence of these quantities on the complex parameter s. Such a continuous dependence is expected whenever $\mathbf{D}(s)$ is a sufficiently smooth matrix function of s. It should be noted that because $\mathbf{D}(s)$ is an $N \times N$ complex matrix for a fixed s, the number of eigenvalues (and consequently the eigenvectors) must be N. Further, it can be shown that, for distinct eigenvalues, $\boldsymbol{\phi}_k(s)$ also satisfy an orthogonality relationship although $\mathbf{z}_k$ do not enjoy any such simple relationship. We normalize $\boldsymbol{\phi}_k(s)$ such that

$$\boldsymbol{\phi}_j^T(s)\boldsymbol{\phi}_k(s) = \delta_{kj}, \quad \forall\, k, j = 1, \cdots, N \tag{3.49}$$

In view of the above relationship, from equation (3.47) we have

$$\boldsymbol{\phi}_j^T(s)\mathbf{D}(s)\boldsymbol{\phi}_k(s) = \nu_k(s)\delta_{kj}, \quad \forall\, k, j = 1, \cdots, N \tag{3.50}$$

or in the matrix form

$$\boldsymbol{\Phi}^T(s)\mathbf{D}(s)\boldsymbol{\Phi}(s) = \boldsymbol{\nu}(s). \tag{3.51}$$

Here

$$\boldsymbol{\Phi}(s) = [\boldsymbol{\phi}_1(s), \boldsymbol{\phi}_2(s), \cdots, \boldsymbol{\phi}_N(s)] \in \mathbb{C}^{N\times N}, \tag{3.52}$$

$$\text{and} \quad \boldsymbol{\nu}(s) = \text{diag}\,[\nu_1(s), \nu_2(s), \cdots, \nu_N(s)] \in \mathbb{C}^{N\times N}. \tag{3.53}$$

It is possible to establish the relationships between the original eigenvalue problem of the system defined by equation (3.7) and that by equation (3.47). Consider the case when the parameter s approaches any one of the system eigenvalues, say s_j. Since *all* the $\nu_k(s)$ are assumed to be distinct, for nontrivial eigenvectors, comparing equations (3.7) and (3.47) we can conclude that one and only one of the $\nu_k(s)$ must be zero when $s \to s_j$ (see Yang and Wu, 1998). Suppose that the r-th eigenvalue of the eigenvalue problem (3.47) is zero when $s \to s_j$. It is also clear that the eigenvector in (3.47) corresponding to the r-th eigenvalue also approaches the eigenvector in (3.7) as $s \to s_j$. Thus, when $s = s_j$ one has

$$\nu_r(s_j) = 0 \quad \text{and} \quad \nu_k(s_j) \neq 0, \forall k = 1, \cdots, N; \neq r \tag{3.54}$$

and also

$$\boldsymbol{\phi}_r(s_j) = \mathbf{z}_j. \tag{3.55}$$

These equations completely relate the eigensolutions of (3.7) with (3.47). Now, these relationships will be utilized to obtain the residues of the transfer function matrix.

3.3.2 Calculation of the Residues

From equation (3.51) one has

$$\mathbf{D}^{-1}(s) = \boldsymbol{\Phi}(s)\boldsymbol{\nu}^{-1}(s)\boldsymbol{\Phi}^T(s). \tag{3.56}$$

Using the expression of the transfer function in equation (3.43) and noting that $\boldsymbol{\nu}(s)$ is a diagonal matrix, we may expand the right-hand side of the above equation to obtain

$$\mathbf{H}(s) = \mathbf{D}^{-1}(s) = \sum_{k=1}^{N} \frac{\boldsymbol{\phi}_k(s)\boldsymbol{\phi}_k^T(s)}{\nu_k(s)}. \tag{3.57}$$

Separation of the r-th term in the above sum yields

$$\mathbf{H}(s) = \frac{\boldsymbol{\phi}_r(s)\boldsymbol{\phi}_r^T(s)}{\nu_r(s)} + \left[\sum_{\substack{k=1 \\ k\neq r}}^{N} \frac{\boldsymbol{\phi}_k(s)\boldsymbol{\phi}_k^T(s)}{\nu_k(s)}\right]. \tag{3.58}$$

Clearly, when $s \to s_j$, the second term of the right-hand side of equation (3.58) is analytic because according to equation (3.54) $\nu_k(s_j) \neq 0, \forall k = 1, \cdots, N; \neq r$. Now, from equation (3.46) the residue at $s = s_j$ may be obtained as

$$\begin{aligned}
\mathbf{R}_j &\stackrel{\text{def}}{=} \lim_{s\to s_j}(s-s_j)\left\{\frac{\boldsymbol{\phi}_r(s)\boldsymbol{\phi}_r^T(s)}{\nu_r(s)} + \left[\sum_{\substack{k=1\\k\neq r}}^{N}\frac{\boldsymbol{\phi}_k(s)\boldsymbol{\phi}_k^T(s)}{\nu_k(s)}\right]\right\} \\
&= \lim_{s\to s_j}(s-s_j)\frac{\boldsymbol{\phi}_r(s)\boldsymbol{\phi}_r^T(s)}{\nu_r(s)} \\
&= \frac{\boldsymbol{\phi}_r(s)\boldsymbol{\phi}_r^T(s)|_{s=s_j}}{\frac{\partial\nu_r(s)}{\partial s}|_{s=s_j}} + \lim_{s\to s_j}\frac{(s-s_j)\frac{\partial}{\partial s}\left[\boldsymbol{\phi}_k(s)\boldsymbol{\phi}_k^T(s)\right]}{\frac{\partial\nu_r(s)}{\partial s}} \quad \text{(using l'Hôspital's rule)} \\
&= \frac{\mathbf{z}_j\mathbf{z}_j^T}{\frac{\partial\nu_r(s)}{\partial s}|_{s=s_j}} \quad \text{(by equation (3.55))}.
\end{aligned} \tag{3.59}$$

The denominator in the above expression for the residues, $\frac{\partial\nu_r(s)}{\partial s}|_{s=s_j}$, is still unknown. Now, consider the r-th eigenvalue problem associated with the dynamic stiffness matrix. Differentiation of equation (3.47) for $k = r$ with respect to s yields

$$\frac{\partial\mathbf{D}(s)}{\partial s}\boldsymbol{\phi}_r(s) + \mathbf{D}(s)\frac{\partial\boldsymbol{\phi}_r(s)}{\partial s} = \frac{\partial\nu_r(s)}{\partial s}\boldsymbol{\phi}_r(s) + \nu_r(s)\frac{\partial\boldsymbol{\phi}_r(s)}{\partial s}. \tag{3.60}$$

Premultiplying the above equation by $\boldsymbol{\phi}_r^T(s)$ and rearranging one obtains

$$\boldsymbol{\phi}_r^T(s)\frac{\partial\mathbf{D}(s)}{\partial s}\boldsymbol{\phi}_r(s) + \left[\boldsymbol{\phi}_r^T(s)\mathbf{D}(s) - \boldsymbol{\phi}_r^T(s)\nu_r(s)\right]\frac{\partial\boldsymbol{\phi}_r(s)}{\partial s} = \boldsymbol{\phi}_r^T(s)\frac{\partial\nu_r(s)}{\partial s}\boldsymbol{\phi}_r(s). \tag{3.61}$$

Taking transpose of equation (3.47) it follows that the second term of the left-hand side of the above equation is zero. Using the normalizing condition in (3.49) and letting $s \to s_j$, from equation (3.61) we have

$$\frac{\partial\nu_r(s)}{\partial s}|_{s=s_j} = \mathbf{z}_j^T\frac{\partial\mathbf{D}(s)}{\partial s}|_{s=s_j}\mathbf{z}_j = \mathbf{z}_j^T\frac{\partial\mathbf{D}(s_j)}{\partial s_j}\mathbf{z}_j. \tag{3.62}$$

The term $\dfrac{\partial\mathbf{D}(s_j)}{\partial s_j}$ can be obtained by differentiating equation (3.41) as

$$\frac{\partial\mathbf{D}(s_j)}{\partial s_j} = 2s_j\mathbf{M} + \mathbf{G}(s_j) + s_j\frac{\partial\mathbf{G}(s_j)}{\partial s_j}. \tag{3.63}$$

Using (3.59) and (3.62) one finally obtains the residue as

$$\mathbf{R}_j = \frac{\mathbf{z}_j\mathbf{z}_j^T}{\mathbf{z}_j^T\frac{\partial\mathbf{D}(s_j)}{\partial s_j}\mathbf{z}_j}. \tag{3.64}$$

The above equation completely relates the transfer function residues to the eigenvalues and eigenvectors of the system. Recalling that, among the m eigenvalues $2N$ appear in complex conjugate

pairs, from equation (3.45) the transfer function matrix may be obtained as

$$\mathbf{H}(\mathrm{i}\omega) = \sum_{j=1}^{N} \left[\frac{\gamma_j \mathbf{z}_j \mathbf{z}_j^T}{\mathrm{i}\omega - s_j} + \frac{\gamma_j^* \mathbf{z}_j^* \mathbf{z}_j^{*T}}{\mathrm{i}\omega - s_j^*} \right] + \sum_{j=2N+1}^{m} \frac{\gamma_j \mathbf{z}_j \mathbf{z}_j^T}{\mathrm{i}\omega - s_j}, \tag{3.65}$$

where

$$\gamma_j = \frac{1}{\mathbf{z}_j^T \frac{\partial \mathbf{D}(s_j)}{\partial s_j} \mathbf{z}_j}. \tag{3.66}$$

The transfer function matrix has two parts, the first part is due to the elastic modes, and the second part is due to the non-viscous modes. Using a first-order perturbation method, Woodhouse (1998, equation (35)) has obtained an expression of the transfer functions similar to equation (3.65). However, the non-viscous part of the transfer functions has not been obtained by him.

3.3.3 Special Cases

The expression for the transfer function matrix in equation (3.65) is a natural generalization for the familiar expressions for the transfer function matrix of undamped or viscously damped systems. Transfer functions for several useful special cases may be obtained from (3.65) as follows:

1. *Undamped systems*: In this case $\mathbf{G}(s) = 0$ results the order of the characteristic polynomial $m = 2N$; s_j is purely imaginary so that $s_j = \mathrm{i}\omega_j$ where $\omega_j \in \mathbb{R}$ are the undamped natural frequencies and $\mathbf{z}_j = \mathbf{x}_j \in \mathbb{R}^N$. In view of the mass normalization relationship in (1.10), $\gamma_j = \frac{1}{2\mathrm{i}\omega_j}$ and equation (3.65) leads to

$$\mathbf{H}(\mathrm{i}\omega) = \sum_{j=1}^{N} \frac{1}{2\mathrm{i}\omega_j} \left[\frac{1}{\mathrm{i}\omega - \mathrm{i}\omega_j} - \frac{1}{\mathrm{i}\omega + \mathrm{i}\omega_j} \right] \mathbf{x}_j \mathbf{x}_j^T = \sum_{j=1}^{N} \frac{\mathbf{x}_j \mathbf{x}_j^T}{\omega_j^2 - \omega^2}. \tag{3.67}$$

2. *Viscously-damped systems with non-proportional damping* (see, Lancaster, 1966, Vigneron, 1986, Géradin and Rixen, 1997): In this case $m = 2N$ and $\gamma_j = \frac{1}{\mathbf{z}_j^T [2s_j \mathbf{M} + \mathbf{C}] \mathbf{z}_j}$. These reduce expression (3.65) to

$$\mathbf{H}(\mathrm{i}\omega) = \sum_{j=1}^{N} \left[\frac{\gamma_j \mathbf{z}_j \mathbf{z}_j^T}{\mathrm{i}\omega - s_j} + \frac{\gamma_j^* \mathbf{z}_j^* \mathbf{z}_j^{*T}}{\mathrm{i}\omega - s_j^*} \right]. \tag{3.68}$$

3.4 Dynamic Response

The steady-state response due to harmonic loads or the response due to broad-band random excitation can be obtained directly from the expression of the transfer function matrix in equation (3.65). In this section we consider the system response due to transient loads and initial conditions in the time and frequency domains.

Taking the Laplace transform of equation (3.1) and considering the initial conditions in (3.2) we have

$$\begin{aligned} & s^2\mathbf{M}\bar{\mathbf{q}} - s\mathbf{M}\mathbf{q_0} - \mathbf{M}\dot{\mathbf{q}}_\mathbf{0} + s\,\mathbf{G}(s)\bar{\mathbf{q}} - \mathbf{G}(s)\mathbf{q_0} + \mathbf{K}\bar{\mathbf{q}} = \bar{\mathbf{f}}(s) \\ \text{or} \quad & \left[s^2\mathbf{M} + s\,\mathbf{G}(s) + \mathbf{K}\right]\bar{\mathbf{q}} = \bar{\mathbf{f}}(s) + \mathbf{M}\dot{\mathbf{q}}_\mathbf{0} + \left[s\mathbf{M} + \mathbf{G}(s)\right]\mathbf{q_0}. \end{aligned} \tag{3.69}$$

Using the expression for the transfer function derived before, the response vector $\bar{\mathbf{q}}$ may be obtained as

$$\bar{\mathbf{q}} = \sum_{j=1}^{m} \frac{\gamma_j \mathbf{z}_j \mathbf{z}_j^T}{s - s_j} \left\{\bar{\mathbf{f}}(s) + \mathbf{M}\dot{\mathbf{q}}_\mathbf{0} + \left[s\mathbf{M} + \mathbf{G}(s)\right]\mathbf{q_0}\right\}. \tag{3.70}$$

This can be simplified further to

$$\bar{\mathbf{q}}(\mathrm{i}\omega) = \sum_{j=1}^{m} \frac{\gamma_j A_j(\mathrm{i}\omega)}{\mathrm{i}\omega - s_j}\mathbf{z}_j \tag{3.71}$$

where the frequency-dependent complex scalar

$$A_j(\mathrm{i}\omega) = \mathbf{z}_j^T\bar{\mathbf{f}}(\mathrm{i}\omega) + \mathbf{z}_j^T\mathbf{M}\dot{\mathbf{q}}_\mathbf{0} + \mathrm{i}\omega\mathbf{z}_j^T\mathbf{M}\mathbf{q_0} + \mathbf{z}_j^T\mathbf{G}(\mathrm{i}\omega)\mathbf{q_0}. \tag{3.72}$$

The summation in equation (3.71) may be split into two different parts – the first part would correspond to the $2N$ complex conjugate pairs of elastic modes and the second part would be the contribution of the non-viscous modes.

The response in the time domain due to any forcing function can be obtained using a convolution integral over the *impulse response function*. From the expression of the transfer function in equation (3.65), the impulse response function matrix $\mathbf{h}(t) \in \mathbb{R}^{N\times N}$ may be obtained as

$$\mathbf{h}(t) = \sum_{j=1}^{N}\left[\gamma_j\mathbf{z}_j\mathbf{z}_j^T e^{s_j t} + \gamma_j^*\mathbf{z}_j^*\mathbf{z}_j^{*^T} e^{s_j^* t}\right] + \sum_{j=2N+1}^{m} \gamma_j\mathbf{z}_j\mathbf{z}_j^T e^{s_j t}. \tag{3.73}$$

The response due to the initial conditions may also be obtained by taking the inverse transform of equation (3.70). First, simplify equation (3.70) to obtain

$$\bar{\mathbf{q}}(s) = \sum_{j=1}^{m}\gamma_j\left[\frac{\mathbf{z}_j^T\bar{\mathbf{f}}(s) + \mathbf{z}_j^T\mathbf{G}(s)\mathbf{q_0}}{s - s_j} + \frac{\mathbf{z}_j^T\mathbf{M}\dot{\mathbf{q}}_\mathbf{0}}{s - s_j} + \left(1 + \frac{s_j}{s - s_j}\right)\mathbf{z}_j^T\mathbf{M}\mathbf{q_0}\right]\mathbf{z}_j. \tag{3.74}$$

From the above, one has

$$\mathbf{q}(t) = \mathcal{L}^{-1}[\bar{\mathbf{q}}(s)] = \sum_{j=1}^{N}\left[\gamma_j a_j(t)\mathbf{z}_j + \gamma_j^* a_j^*(t)\mathbf{z}_j^*\right] + \sum_{j=2N+1}^{m}\gamma_j a_j(t)\mathbf{z}_j \tag{3.75}$$

where the time-dependent scalar coefficients

$$a_j(t) = \int_0^t e^{s_j(t-\tau)}\left\{\mathbf{z}_j^T\mathbf{f}(\tau) + \mathbf{z}_j^T\boldsymbol{\mathcal{G}}(\tau)\mathbf{q_0}\right\}\mathrm{d}\tau + e^{s_j t}\left\{\mathbf{z}_j^T\mathbf{M}\dot{\mathbf{q}}_\mathbf{0} + s_j\mathbf{z}_j^T\mathbf{M}\mathbf{q_0}\right\}; \quad \forall t > 0. \tag{3.76}$$

The expression of the system response, either the frequency-domain description in equation (3.71) or the time-domain description in equation (3.75), is similar to the classical modal superposition result for undamped or proportionally damped systems usually obtained using the mode-orthogonality relationships. Thus, the formulation presented here is a generalization of the classical result where the real normal modes are appropriately replaced by the elastic modes and the non-viscous modes. Also note that we have not used any orthogonality relationship – the expression of the transfer function residue in equation (3.64) allows us to express the response in terms of superposition of individual modes even when the equations of motion cannot be decoupled.

3.5 Summary of the Method

Following the procedure outlined so far one can obtain the eigensolutions and dynamic response of non-viscously damped linear systems. Here we briefly summarize the steps to be followed in order to obtain the eigenvalues, eigenvectors and dynamic response of non-viscously damped linear systems:

1. Evaluate the natural frequencies ω_j and eigenvectors $\mathbf{x}_j$ of the undamped system from $\mathbf{K}\mathbf{x}_j = \omega_j^2 \mathbf{M}\mathbf{x}_j$ for all $j = 1, \cdots, N$. Normalize so that $\mathbf{x}_l^T \mathbf{M}\mathbf{x}_j = \delta_{lj}$.

2. Obtain the eigenvalues by solving the (say m-th order) characteristic equation $\det\left[s^2\mathbf{M} + s\mathbf{G}(s) + \mathbf{K}\right] = 0$. For convenience, arrange the eigenvalues as $s_1, s_2, \cdots, s_N, s_1^*, s_2^*, \cdots, s_N^*, s_{2N+1}, s_{2N+2}, \cdots, s_m$.

3. Set up the $\mathbf{G}'(s_j)$ matrix using $G'_{kl}(s_j) = \mathbf{x}_k^T \mathbf{G}(s_j)\mathbf{x}_l$. Calculate the matrices ${\mathbf{R}_\mathbf{u}}^{(j)}$ using

$$R^{(j)}_{u_{k_1 l_1}} = \frac{-s_j G'_{kl}(s_j)\,(1 - \delta_{k_1 l_1})}{\omega_k^2 + s_j^2 + s_j G'_{kk}(s_j)}. \tag{3.77}$$

   In order to keep the dimension of ${\mathbf{R}_\mathbf{u}}^{(j)}$ to $(N-1) \times (N-1)$, the subscript k_1 is expressed as $k_1 = k - \mathcal{U}_{(k,j)}$. Here the function $\mathcal{U}_{(k,j)}$ is defined as

$$\mathcal{U}_{(k,j)} = \begin{cases} 0 & \text{if} \quad k < j, \\ 1 & \text{if} \quad k > j, \\ \text{not defined} & \text{if} \quad k = j. \end{cases} \tag{3.78}$$

4. Obtain the vectors $\mathbf{a}_0^{(j)}$ using

$$a^{(j)}_{0_{l_1}} = \frac{-s_j G'_{lj}(s_j)}{\omega_l^2 + s_j^2 + s_j G'_{ll}(s_j)}. \tag{3.79}$$

5. Select the number of terms, say n, and calculate $\mathbf{a}_k^{(j)} = {\mathbf{R}_\mathbf{u}}^{(j)} \mathbf{a}_{k-1}^{(j)}$ for all $k = 1, \cdots, n$. Subsequently obtain the complex constants $\hat{\mathbf{a}}^{(j)} = \sum_{k=1}^{n} \mathbf{a}_{k-1}^{(j)}$.

6. Determine the *elastic modes* as $\mathbf{u}_j = \mathbf{x}_j + \sum_{\substack{l=1 \\ l \neq j}}^{N} \hat{a}_{l_1}^{(j)} \mathbf{x}_{l_1}$ for all $j = 1, \cdots, N$.

7. For $2N < j < 2N + p$, obtain the dynamic stiffness matrix $\mathbf{D}(s_j) = s_j^2 \mathbf{M} + s_j \mathbf{G}(s_j) + \mathbf{K}$. Partition as $\mathbf{D}(s_j) = \begin{bmatrix} \mathbf{D_{11}}(s_j) & \mathbf{D_{12}}(s_j) \\ \mathbf{D_{21}}(s_j) & \mathbf{D_{22}}(s_j) \end{bmatrix}$ where $\mathbf{D_{11}}(s_j) \in \mathbb{R}$, $\mathbf{D_{12}}(s_j) \in \mathbb{R}^{1\times(N-1)}$, $\mathbf{D_{21}}(s_j) \in \mathbb{R}^{(N-1)\times 1}$ and $\mathbf{D_{22}}^{(j)} \in \mathbb{R}^{(N-1)\times(N-1)}$.

8. Calculate $\mathbf{z_2}_j = -\left[\mathbf{D_{22}}(s_j)\right]^{-1} \mathbf{D_{21}}(s_j)$. Now obtain the *non-viscous* modes as $\mathbf{u}_j = \left\{1, \mathbf{z_2}_j\right\}$ for all $j = 2N + 1, \cdots m$.

9. Finally, using the eigensolutions, calculate the response either in the frequency domain from equation (3.71) or alternatively, in the time domain from equation (3.75).

This procedure is general, simple, direct and provides better physical insights as the familiar N-space eigenvectors are only used. The approach also offers reduction in computational effort because it neither uses the state-space formalism nor utilizes additional dissipation coordinates. Applications of the proposed method are illustrated next.

3.6 Numerical Examples

3.7 The System

We consider a three degree-of-freedom system to illustrate the proposed method. Figure 3.1 shows the example taken together with the numerical values considered for mass and stiffness properties. A similar system with viscous damping has been studied by Newland (1989, see pages 148-151). Damping is associated only with the middle mass, and the kernel function corresponding to this

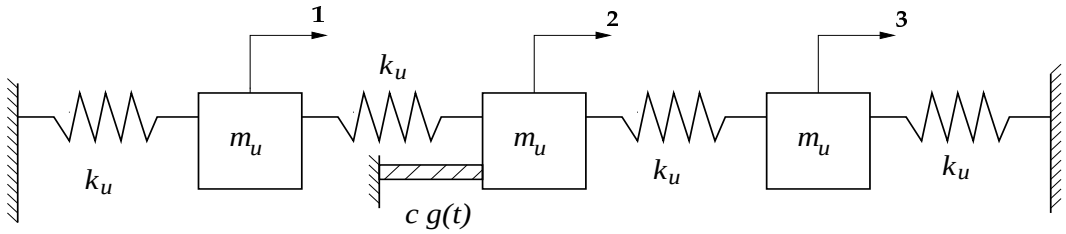

Figure 3.1: Three degree-of-freedom non-viscously damped system, $m_u = 1$ kg, $k_u = 1$ N/m

damper has the form

$$\mathcal{G}_{22}(t) = c\, g(t) \tag{3.80}$$

where c is a damping coefficient and $g(t)$ is the damping function. Two different forms of $g(t)$ available in the literature will be considered here. For the first model (exponential)

$$g(t) = \mu e^{-\mu t}; \quad \mu, t \geq 0 \tag{3.81}$$

and for the second model (double exponential)

$$g(t) = \frac{1}{2}\left(\mu_1 e^{-\mu_1 t} + \mu_2 e^{-\mu_2 t}\right); \quad \mu_1, \mu_2, t \geq 0. \tag{3.82}$$

The exponential function in (3.81) is possibly the simplest physically realistic non-viscous damping model. This function, often known as a 'relaxation function', was introduced by Biot (1955). It has been used extensively in the context of viscoelastic systems. In Chapter 6 a method will be proposed to identify such damping models using modal testing. The double exponential damping function, known as the GHM model, was introduced by Golla and Hughes (1985) and McTavis and Hughes (1993). Identification of GHM model has been discussed by Friswell *et al.* (1997). Both damping functions have been scaled so as to have unit area when integrated to infinity. This makes them directly comparable with the viscous model in which the corresponding damping function would be a unit delta function, $g(t) = \delta(t)$, and the coefficient c would be the usual viscous damping coefficient. The difference between a delta function and $g(t)$ given by equations (3.81) and (3.82) is that at $t = 0$ they start with finite values of μ and $1/2\,(\mu_1 + \mu_2)$ respectively. Thus, the values of μ, μ_1 and μ_2 give a notion of *non-viscousness* – if they are large the damping behaviour will be near-viscous, and vice versa.

The mass and stiffness matrices and the damping matrix in the Laplace domain for the problem can be obtained as:

$$\mathbf{M} = \begin{bmatrix} m_u & 0 & 0 \\ 0 & m_u & 0 \\ 0 & 0 & m_u \end{bmatrix}, \tag{3.83}$$

$$\mathbf{K} = \begin{bmatrix} 2k_u & -k_u & 0 \\ -k_u & 2k_u & -k_u \\ 0 & -k_u & 2k_u \end{bmatrix} \tag{3.84}$$

and

$$\mathbf{G}(s) = \begin{bmatrix} 0 & 0 & 0 \\ 0 & cG(s) & 0 \\ 0 & 0 & 0 \end{bmatrix}. \tag{3.85}$$

Here $G(s)$ is the Laplace transform of $g(t)$. Next, the eigensolutions and the dynamic response of the system are discussed for the two functional forms of $g(t)$.

3.7.1 Example 1: Exponential Damping

Eigensolutions

We assume $c = 0.3$, as considered by Newland (1989, page 149) for the equivalent viscously damped system. From equation (3.81) one obtains

$$G(s) = \frac{1}{s + \mu}. \tag{3.86}$$

Using this expression, the characteristic equation can be simplified as

$$\begin{aligned} & m_u^3 s^7 + m_u^3 \mu\, s^6 + \left(2\, m_u^2 k_u + m_u\left(\mu\, c m_u + 4\, m_u k_u\right)\right) s^5 + 6\, k_u m_u^2 \mu\, s^4 \\ & + \left(2\, k_u\left(\mu\, c m_u + 4\, m_u k_u\right) + m_u\left(2\,\mu\, c k_u + 2\, {k_u}^2\right)\right) s^3 + 10\, {k_u}^2 m_u \mu\, s^2 \\ & + 2\, k_u\left(2\,\mu\, c k_u + 2\, {k_u}^2\right) s + 4\, {k_u}^3 \mu = 0. \end{aligned} \tag{3.87}$$

The order of the above polynomial, $m = 7$. Since the system has three degrees of freedom there are three elastic modes corresponding to the three modes of vibration. The number of the non-viscous modes, $p = m - 2N = 1$.

It is of interest to us to understand the effect of 'non-viscousness' on the eigensolutions. Figure 3.2 shows the locus of the third eigenvalue, that is s_3, plotted as a function of μ. It is interesting to observe that the locus is much more sensitive in the region of lower values of μ (*i.e.*, when damping is significantly non-viscous) compared to that in the region of higher values. The eigenvalue of the corresponding viscously damped system is also plotted (marked by *) in the same diagram. Note that, the non-viscous damping mechanism approaches the viscous damping when $\mu > \approx 50.0$. Similar behaviour has been observed (results not shown here) for the locus of s_1 also. The second mode, in which the middle mass remains stationary, is not effected by damping.

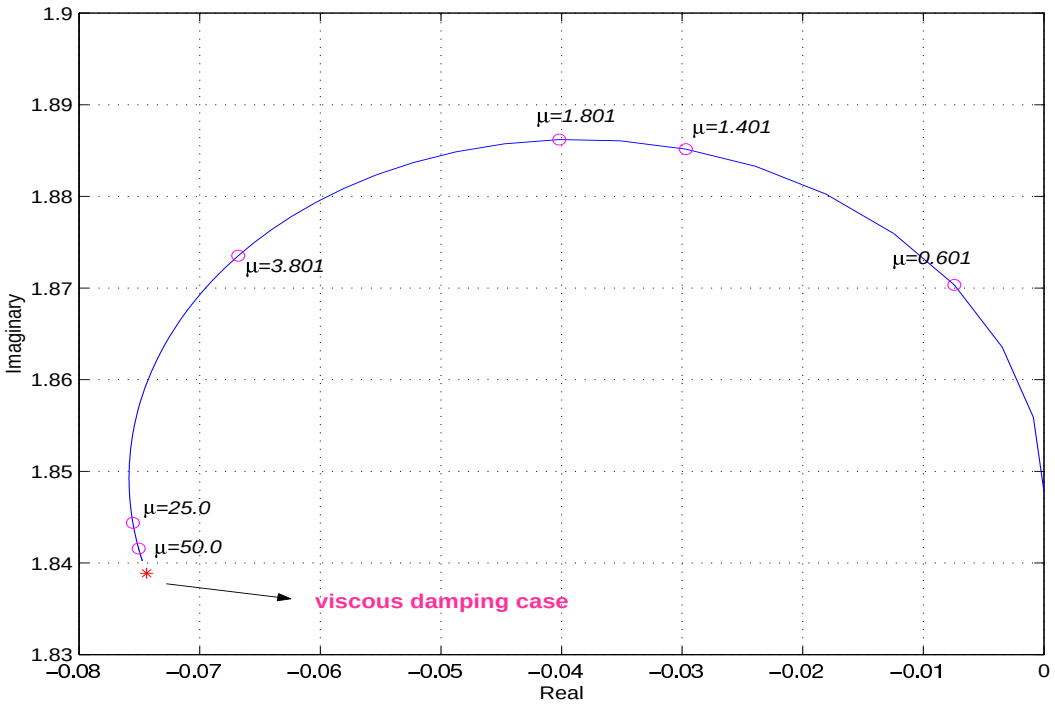

Figure 3.2: Root-locus plot showing the locus of the third eigenvalue (s_3) as a function of μ

The eigenvectors of the system, *i.e.*, the three elastic modes (together with their complex conjugates) and one non-viscous mode can be obtained in a straight forward manner by following the steps outlined in the previous section. We select two representative values of μ – one when

μ is large (*i.e.*, near viscous case) and the other when μ is small. The undamped eigenvalues and eigenvectors are obtained as

$$\{\omega_1, \omega_2, \omega_3\} = \{0.7654, 1.4142, 1.8478\} \tag{3.88}$$

and

$$[\mathbf{x}_1, \mathbf{x}_2, \mathbf{x}_3] = \begin{bmatrix} 0.5 & 0.7071 & -0.5 \\ 0.7071 & 0.0 & 0.7071 \\ 0.5 & -0.7071 & -0.5 \end{bmatrix}. \tag{3.89}$$

Using these results, when $\mu = 50.0$, for the elastic modes we have

$$\{s_1, s_2, s_3\} = \{-0.0757 + 0.7659\mathrm{i}, 1.4142\mathrm{i}, -0.0751 + 1.8416\mathrm{i}\} \tag{3.90}$$

and

$$[\mathbf{z}_1, \mathbf{z}_2, \mathbf{z}_3] = \begin{bmatrix} 0.4983 + 0.0204\mathrm{i} & 0.7071 & -0.5002 + 0.0491\mathrm{i} \\ 0.7095 - 0.0289\mathrm{i} & 0.0 & 0.7069 + 0.0694\mathrm{i} \\ 0.4983 + 0.0204\mathrm{i} & -0.7071 & -0.5002 + 0.0491\mathrm{i} \end{bmatrix}. \tag{3.91}$$

The above calculation is performed by retaining five terms in the series (3.23). It may be verified that, because μ is large (about 27 times of the maximum natural frequency), the results obtained are close to the viscously damped case (see Newland, 1989, page 149). For the one non-viscous mode we obtain

$$s_7 = -49.6984 \quad \text{and} \quad \mathbf{z}_7 = \begin{Bmatrix} 1.0 \\ 2.4719 \times 10^3 \\ 1.0 \end{Bmatrix} \tag{3.92}$$

Because s_7 is purely real and negative this mode is non-oscillatory (over critically damped) and stable.

When $\mu = 0.5$ the damping is significantly non-viscous. For this case, performing similar calculations for the elastic modes one has

$$\{s_1, s_2, s_3\} = \{-0.0207 + 0.8\mathrm{i}, 1.4142\mathrm{i}, -0.0053 + 1.8671\mathrm{i}\} \tag{3.93}$$

and

$$[\mathbf{z}_1, \mathbf{z}_2, \mathbf{z}_3] = \begin{bmatrix} 0.4983 + 0.0204\mathrm{i} & 0.7071 & -0.5002 + 0.0491\mathrm{i} \\ 0.6787 + 0.0112\mathrm{i} & 0.0 & 0.7442 - 0.0630\mathrm{i} \\ 0.4983 + 0.0204\mathrm{i} & -0.7071 & -0.5002 + 0.0491\mathrm{i} \end{bmatrix}. \tag{3.94}$$

These values are not significantly different from those obtained for $\mu = 50.0$ in (3.91). For this problem the elastic modes are not very sensitive to the damping mechanism. However, we emphasize that this fact *cannot* be generalized to all systems. For the non-viscous mode one has

$$s_7 = -0.4480 \quad \text{and} \quad \mathbf{z}_7 = \begin{Bmatrix} 1.0 \\ 2.2007 \\ 1.0 \end{Bmatrix}. \tag{3.95}$$

These values are, however, quite different from those obtained for $\mu = 50.0$ in (3.92). It is difficult to physically visualize the nature of the non-viscous modes in general. These modes are intrinsic

to the dampers and we do not have sufficient generalized coordinates to represent them properly. Nevertheless, they yield non-zero residues in the system transfer functions and thus contribute to the global dynamic response.

Dynamic Response Analysis

The problem of stationary random vibration analysis of the system is considered here. Suppose the system is subjected to a band-limited Gaussian *white noise* at the third DOF. We are interested in the resulting displacement of the system at the third DOF (*i.e.*, $\mathbf{z}_3$). The power spectral density (PSD) of the response (see Nigam, 1983, for details) can be given by

$$S_{uu}(\mathrm{i}\omega) = |H_{33}(\mathrm{i}\omega)|^2 S_{ff}(\mathrm{i}\omega) \tag{3.96}$$

where

$$S_{ff}(\mathrm{i}\omega) = \begin{cases} 1 & \text{if} \quad 0 < \omega \leq 2.5\,\text{rad/sec} \\ 0 & \text{otherwise} \end{cases}. \tag{3.97}$$

In Figure 3.3 the PSD of $\mathbf{z}_3$ that is $|H_{33}(\mathrm{i}\omega)|^2$ is plotted for the cases when $\mu = 50.0$ and $\mu = 0.5$. These results are obtained by direct application of equation (3.65). From the diagram observe that the damping is less for the case when $\mu = 0.5$ than when $\mu = 50.0$. Also note the (horizontal) shift in the position of the natural frequencies. These features may also be observed in the loot locus diagram as shown in Figure 3.2. To understand the effect of 'non-viscosity', in the same diagram we have plotted the non-viscous term (the second term) appearing in equation (3.65) for both values of μ. For this problem the non-viscous part is quite small and becomes smaller at higher frequencies. Observe that when $\mu = 0.5$, that is when damping is significantly non-viscous, the value of the non-viscous part of the response is more than that when $\mu = 50.0$. This plot also clearly demonstrates that the non-viscous part of the response is *not* oscillatory in nature.

3.7.2 Example 2: GHM Damping

Taking the Laplace transform of equation (3.82) one obtains

$$G(s) = \frac{(\mu_1 + \mu_2)/2\, s + \mu_1\mu_2}{s^2 + (\mu_1 + \mu_2)\, s + \mu_1\mu_2}. \tag{3.98}$$

Using this equation, together with the expressions of the system matrices given by equations (3.83) – (3.85), it can be shown that the order of the characteristic polynomial, $m = 8$. Thus, the number of the non-viscous modes, $p = m - 2N = 2$. In this section we focus our attention on the numerical accuracy of the formulation developed in this chapter.

Regarding the numerical values of the damping parameters, we assume $c = 0.5$, $\mu_1 = 1$ and $\mu_2 = 3$. Small values of μ_1 and μ_2 indicate that the damping mechanism is strongly non-viscous. Solving the characteristic equation, exact eigenvalues corresponding to the three elastic modes can be obtained as

$$\{s_1, s_2, s_3\} = \{-0.0994 + 0.8180\mathrm{i}, 1.4142\mathrm{i}, -0.0687 + 1.9025\mathrm{i}\} \tag{3.99}$$

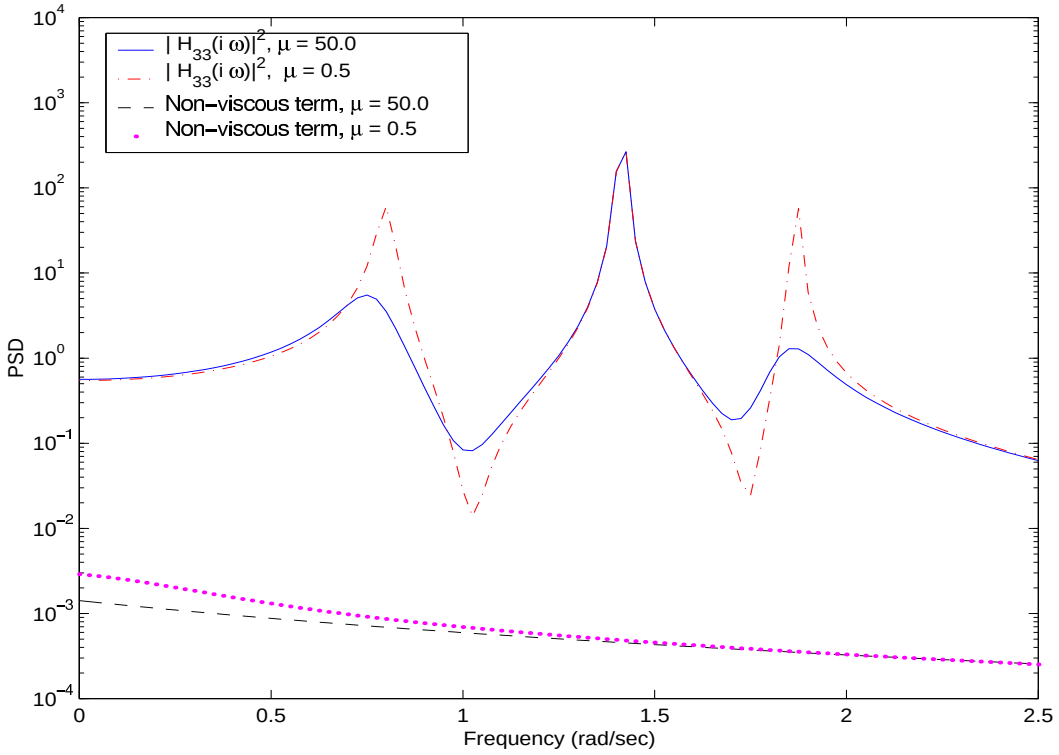

Figure 3.3: Power spectral density function of the displacement at the third DOF ($\mathbf{z}_3$)

and their complex conjugate pairs. Eigenvalues corresponding to the two non-viscous modes are found to be

$$\{s_7, s_8\} = \{-2.7901, -0.8738\}. \tag{3.100}$$

Eigenvalues corresponding to the elastic modes can also be obtained approximately by equation (3.33) in Section 3.2.3. Recall that only the undamped eigensolutions are required in order to apply this equation. Approximate eigenvalues using equation (3.33) are calculated as

$$\{s_1, s_2, s_3\}_{\text{approx}} = \{-0.0981 - 0.8105\text{i}, 1.4142\text{i}, -0.0595 - 1.9018\text{i}\}. \tag{3.101}$$

It is useful to compare the exact and approximate eigenvalues in the light of the Q-factors. In this problem the second mode is not damped, so $Q_2 = \infty$. For the first and third modes we obtain $Q_1 = 4.1164$ and $Q_3 = 13.8540$. Small values of Q-factor indicate that these modes are quite heavily damped. Comparing equations (3.99) and (3.101) it may be observed that the approximate values are quite close to the exact one even when damping is reasonably high.

In order to check the numerical accuracy of the eigenvectors, first the exact values are calculated by the matrix inversion method. For the elastic modes we obtain

$$[\mathbf{z}_1, \mathbf{z}_2, \mathbf{z}_3] = \begin{bmatrix} 0.5114 + 0.0299\text{i} & 0.7071 & -0.4639 + 0.0403\text{i} \\ 0.6905 - 0.0431\text{i} & 0.0 & 0.7596 + 0.0562\text{i} \\ 0.5114 + 0.0299\text{i} & -0.7071 & -0.4639 + 0.0403\text{i} \end{bmatrix} \tag{3.102}$$

and their complex conjugates. For the two non-viscous modes one has

$$[\mathbf{z}_7, \mathbf{z}_8] = \begin{bmatrix} 1.0000 & 1.0000 \\ 9.7847 & 2.7636 \\ 1.0000 & 1.0000 \end{bmatrix}. \tag{3.103}$$

Approximate eigenvectors corresponding to the elastic modes, calculated by equation (3.35), are obtained as

$$[\mathbf{z}_1, \mathbf{z}_2, \mathbf{z}_3]_{\text{approx}} = \begin{bmatrix} 0.5114 + 0.0299\text{i} & 0.7071 & -0.4639 + 0.0403\text{i} \\ 0.6910 - 0.0422\text{i} & 0.0 & 0.7582 + 0.0569\text{i} \\ 0.5114 + 0.0299\text{i} & -0.7071 & -0.4639 + 0.0403\text{i} \end{bmatrix}. \tag{3.104}$$

The above values are equivalent to performing the calculation by retaining only one term in the series (3.23). Also recall that the approximate values are obtained from the undamped eigensolutions only. Comparing equation (3.102) and (3.104) it is clear that the results obtained from the approximate method match the exact solutions to an excellent accuracy.

As a final check on the formulation developed in this chapter, we compare the transfer function obtained from equation (3.65) with the exact transfer function calculated by inversion of the dynamic stiffness matrix. Figure 3.4 shows such a comparison for $H_{33}(\text{i}\omega)$. Approximate natural frequencies and modes given by (3.101) and (3.104) are used and also the non-viscous term in equation (3.65) is neglected in order to calculate the approximate transfer function. Thus, in turn, the approximate transfer function in Figure 3.4 is obtained only by proper 'post-processing' of the undamped eigensolutions. From this figure it may be observed that, except in a few places, the approximate transfer function is reasonably close to the exact one. This analysis demonstrates the usefulness of the proposed method.

3.8 Conclusions

The problem of dynamic analysis of non-viscously damped multiple-degrees-of-freedom linear systems has been considered. The assumed non-viscous damping model is such that the damping forces depend on the past history of motion via convolution integrals over some kernel functions. It has been assumed that, in general, the mass and stiffness matrices as well as the matrix of the kernel functions cannot be simultaneously diagonalized by any linear transformation. The analysis is, however, restricted to systems with non-repetitive eigenvalues and non-singular mass matrices.

The system eigenvalues were obtained by solving the characteristic equation. It turns out that, unlike viscously damped systems, the order of the characteristic equation for an N-degrees-of-freedom system is more than $2N$. As a consequence, the number of modes become more than $2N$ and they were grouped into two types – (a) elastic modes and (b) non-viscous modes. It is assumed that the elastic modes appear in complex conjugate pairs, that is, they are sub-critically damped. The elastic modes, which consist of N eigenvectors together with their complex conjugate pairs, correspond to N modes of vibration of the structural system. These N eigenvectors

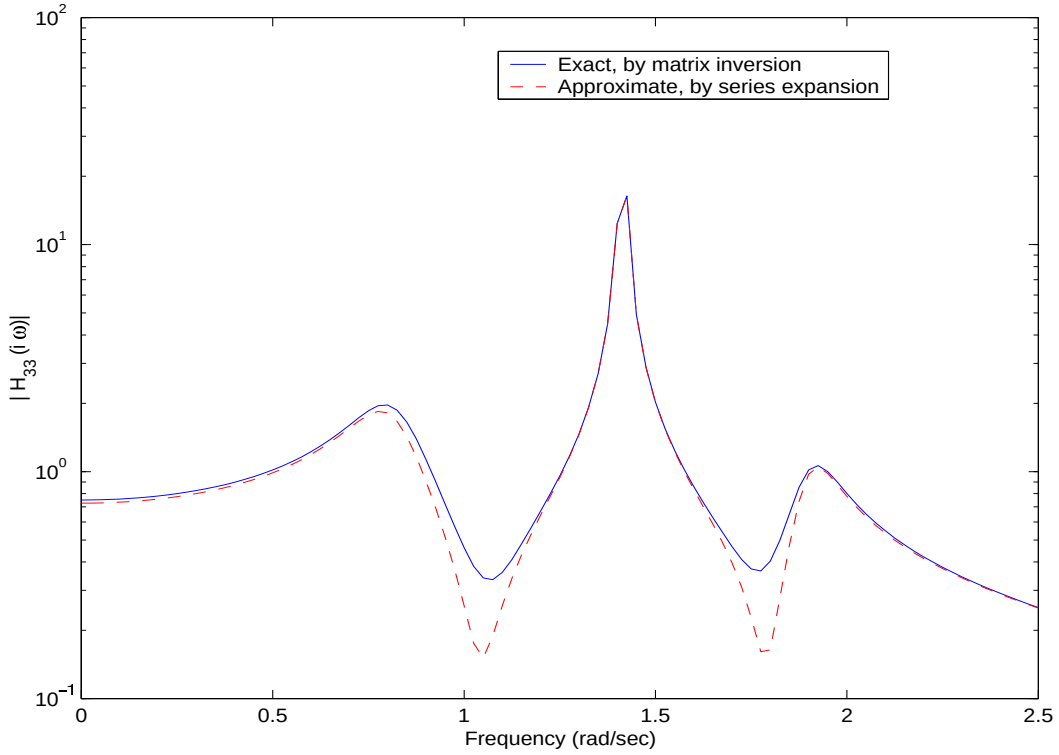

Figure 3.4: Transfer function $H_{33}(\mathrm{i}\omega)$

were expressed as a complex linear combination of the (real) eigenvectors of the corresponding undamped system. The vector of these complex constants were further determined from a series obtained by the Neumann expansion method. Based on this analysis, some approximate formulas for the eigenvalues and eigenvectors were suggested and their accuracy were verified using numerical examples. The non-viscous modes, which occur due to the non-viscous damping mechanism, are real, over critically damped and non-oscillatory in nature. These modes were obtained by inversion of a partition of the dynamic stiffness matrix evaluated at the corresponding eigenvalues.

The transfer function matrix of the system was derived in terms of the eigenvalues and eigenvectors of the second-order system. Exact closed-form expressions of the response due to arbitrary forcing functions and initial conditions were obtained. The response can be expressed as a sum of two parts, one that arises in usual viscously damped systems and the other that occurs due to non-viscous damping mechanisms. Through an example it was shown that the non-viscous part of the response is purely dissipative and non-oscillatory in nature.

The method developed here is analogous to classical modal analysis where undamped natural frequencies and modes have to be appropriately replaced by elastic modes and non-viscous modes of the non-conservative system. The method presented offers a reduction in computational effort because neither the first-order formalisms nor the additional dissipation coordinates are employed. Moreover, this approach also provides better physical insight as familiar N-space eigenvectors are utilized.

Chapter 4

Some General Properties of the Eigenvectors

4.1 Introduction

In the last chapter, the eigenvalues, eigenvectors and transfer functions associated with multiple-degrees-of-freedom non-viscously damped systems have been discussed. A method was outlined to obtain the eigenvectors and dynamic response of the system. Although the method is analogous to classical modal analysis, unlike the classical modes, very little is known about qualitative properties of the modes of non-viscously damped systems. Purpose of this chapter is to develop some basic relationships satisfied by the eigensolutions and the system matrices of (3.1). Specifically we have focused our attention to the normalization and orthogonality relationship of the eigenvectors.

4.2 Nature of the Eigensolutions

The eigenvalue problem associated with equation (3.1) can be defined as

$$\left[s_j^2\mathbf{M} + s_j\,\mathbf{G}(s_j) + \mathbf{K}\right]\mathbf{z}_j = \mathbf{0} \quad \text{or} \quad \mathbf{D}(s_j)\mathbf{z}_j = \mathbf{0},\ \forall\, k = 1, \cdots, m \tag{4.1}$$

where the *dynamic stiffness matrix*

$$\mathbf{D}(s) = s^2\mathbf{M} + s\,\mathbf{G}(s) + \mathbf{K}\ \in \mathbb{C}^{N\times N}. \tag{4.2}$$

Here $\mathbf{z}_j$ is the j-th eigenvector and s_j is the j-th eigenvalue. In general the number of eigenvalues, $m = 2N + p;\ p \geq 0$. It is assumed that *all* m eigenvalues are distinct. It should be noted that eigenvalue problems of this kind are not similar to the eigenvalue problems arise in the context of Lambda-matrices (Lancaster, 1966) because $\mathbf{G}(s)$ is not a constant matrix. We consider the damping to be 'non-proportional', that is, the mass and stiffness matrices as well as the matrix of the kernel functions cannot be simultaneously diagonalized by any linear transformation. It is assumed that $|G_{jk}(s)| < \infty$ when $s \to \infty$. This in turn implies that the elements of $\mathbf{G}(s)$ are at

the most of order $1/s$ in s or constant, as in the case of viscous damping. Construct the diagonal matrix containing the eigenvalues as

$$\mathbf{S} = \text{diag}\,[s_1, s_2, \cdots, s_m] \in \mathbb{C}^{m\times m} \tag{4.3}$$

and the matrix containing the eigenvectors (the modal matrix) as

$$\mathbf{Z} = [\mathbf{z}_1, \mathbf{z}_2, \cdots, \mathbf{z}_m] \in \mathbb{C}^{N\times m}. \tag{4.4}$$

Next, we consider the normalization relationship of the eigenvectors.

4.3 Normalization of the Eigenvectors

Premultiplying equation (4.1) by $\mathbf{z}_k^T$, applying equation (4.1) for k-th set and postmultiplying by $\mathbf{z}_j$ and subtracting one from the other we obtain

$$\mathbf{z}_k^T \left[\left(s_j^2 - s_k^2\right)\mathbf{M} + s_j\mathbf{G}(s_j) - s_k\mathbf{G}(s_k)\right]\mathbf{z}_j = 0. \tag{4.5}$$

Since s_j and s_k are distinct for different j and k, the above equation can be divided by $(s_j - s_k)$ to obtain

$$\mathbf{z}_k^T \left[(s_j + s_k)\,\mathbf{M} + \frac{s_j\mathbf{G}(s_j) - s_k\mathbf{G}(s_k)}{s_j - s_k}\right]\mathbf{z}_j = 0,\ \forall j, k; j \neq k. \tag{4.6}$$

This equation may be regarded as the orthogonality relationship of the eigenvectors. It is easy to verify that, in the undamped limit equation (4.6) degenerates to the familiar mass orthogonality relationship of the undamped eigenvectors. However, this orthogonality relationship is not very useful because it is expressed in terms of the natural frequencies. A frequency-independent orthogonality relationship of the eigenvectors will be derived later in this chapter. Assuming $\delta_s = s_j - s_k$, rewrite equation (4.6) as

$$\mathbf{z}_k^T \left[(\delta_s + 2s_k)\,\mathbf{M} + \frac{(s_k + \delta_s)\,\mathbf{G}(s_k + \delta_s) - s_k\mathbf{G}(s_k)}{\delta_s}\right]\mathbf{z}_j = 0. \tag{4.7}$$

Consider the case when $s_j \longrightarrow s_k$, that is, $\delta_s \longrightarrow 0$. For this limiting case, equation (4.7) reads

$$\mathbf{z}_k^T \left[2s_k\mathbf{M} + \frac{\partial\,[s\mathbf{G}(s)]}{\partial s}\Big|_{s_k}\right]\mathbf{z}_k = \theta_k \tag{4.8}$$

$$\text{or}\quad \mathbf{z}_k^T\left[2s_k\mathbf{M} + \mathbf{G}(s_k) + s_k\mathbf{G}'(s_k)\right]\mathbf{z}_k = \theta_k, \tag{4.9}$$

$$\forall k = 1, \cdots, m$$

for some non-zero $\theta_k \in \mathbb{C}$. Equation (4.9) is the normalization relationship for the eigenvectors of the non-viscously damped system (3.1). From the expression of the dynamic stiffness matrix in (4.2), the normalization condition in equation (4.9) can also be expressed as

$$\mathbf{z}_k^T\mathbf{D}'(s_k)\mathbf{z}_k = \theta_k, \quad \forall k = 1, \cdots, m. \tag{4.10}$$

Equation (4.9), and consequently equation (4.10), can be regarded as the generalization of the 'mass normalization' relationship used in structural dynamics. In the undamped limit when $\mathbf{G}(s)$ is a null matrix, equation (4.9) reduces to the familiar mass normalization relationship for the undamped eigenvectors. For viscously damped systems (see Section 4.7 for details), relationship analogous to (4.9) was obtained, for example, by Sestieri and Ibrahim (1994) using state-space approach and, by Fawzy and Bishop (1976) and Fawzy (1977) using second-order equations of motion. We define the *normalization matrix*, $\mathbf{\Theta}$, as

$$\mathbf{\Theta} = \text{diag}\,[\theta_1, \theta_2, \cdots, \theta_m] \in \mathbb{C}^{m\times m}. \tag{4.11}$$

Numerical values of θ_k can be selected in various ways:

- Choose $\theta_k = 2s_k, \forall k$ that is $\mathbf{\Theta} = 2\mathbf{S}$. This reduces to $\mathbf{z}_k^T\mathbf{M}\mathbf{z}_k = 1, \forall k$ when the damping is zero. This is consistent with the unity modal mass convention, often used in experimental modal analysis and finite element methods.

- Choose $\theta_k = 1 + 0i, \forall k$, that is, $\mathbf{\Theta} = \mathbf{I}_m$. Theoretical analysis becomes easiest with this normalization. However, as pointed out by Fawzy (1977) and Vigneron (1986) in the context of viscously damped systems, this normalization is inconsistent with undamped or classically damped modal theories.

4.4 Orthogonality of the Eigenvectors

The orthogonality relationship of the eigenvectors given by equation (4.6) is not very useful because it is expressed in terms of the eigenvalues of the system. In this section, we will develop an orthogonality relationship which is independent of the eigenvalues. Expressions equivalent to the orthogonality relationships of the undamped eigenvectors with respect to the mass and stiffness matrices will also be established. In order to derive these results, first recall the expression of the transfer function matrix derived in Section 3.3. In the pole-residue form the inverse of the dynamic stiffness matrix (transfer function matrix) can be expressed as

$$\mathbf{D}^{-1}(s) = \frac{\text{adj}\,[\mathbf{D}(s)]}{\det\,[\mathbf{D}(s)]} = \sum_{j=1}^{m} \frac{\mathbf{R}_j}{s - s_j}. \tag{4.12}$$

Here $\mathbf{R}_j$, the residue of $\mathbf{D}^{-1}(s)$ at the pole s_j obtained from equation (3.64) as

$$\mathbf{R}_j = \frac{\mathbf{z}_j\mathbf{z}_j^T}{\mathbf{z}_j^T \frac{\partial \mathbf{D}(s_j)}{\partial s_j}\mathbf{z}_j} \in \mathbb{C}^{N\times N}. \tag{4.13}$$

Interestingly, observe that denominator of left-hand side of the above equation is exactly the same as the normalization condition given by equation (4.10). Now, using equations (4.10) and (4.13) one finally obtains the residues as

$$\mathbf{R}_j = \frac{\mathbf{z}_j\mathbf{z}_j^T}{\theta_j}. \tag{4.14}$$

For undamped systems, *i.e.*, when $\mathbf{G}(s) = \mathbf{O}_N, \forall\, s$, the eigenvectors satisfy familiar orthogonality relationship over the mass and stiffness matrices as given by equations (1.10) and (1.11). For viscously damped systems (with non-proportional damping), equivalent relationships may be obtained by converting the equations of motion into the state-space form (see Sestieri and Ibrahim, 1994). The eigenproblem in the state-space form is essentially similar to the undamped eigenproblem except that the size of the problem gets doubled, and the eigensolutions become complex. Thus, from the analysis point of view, the state-space approach offers significant advantage for viscously damped systems. Unfortunately, for non-viscously damped systems, no advantage can be gained by adopting the state-space formalism as at least one of the system matrices will not be a constant matrix. For this reason, and also realizing that the state-space eigenvectors are not physically appealing, we kept the analysis in the second-order form. One of our main result regarding the orthogonality of the eigenvectors is the following:

Theorem 4.1. *The modal matrix of a non-viscously damped system,* $\mathbf{Z} \in \mathbb{C}^{N\times m}$*, satisfy the orthogonality relationship* $\mathbf{Z}\boldsymbol{\Theta}^{-1}\mathbf{Z}^T = \mathbf{O}_N$.

Proof. From equations (4.12) and (4.14) one obtains

$$\frac{\text{adj}\,[\mathbf{D}(s)]}{\det\,[\mathbf{D}(s)]} = \sum_{j=1}^{m} \frac{1}{s-s_j}\frac{\mathbf{z}_j\mathbf{z}_j^T}{\theta_j}. \tag{4.15}$$

Multiplying both side of the above equation by s and taking limit as $s \to \infty$ we obtain

$$\lim_{s\to\infty} s\frac{\text{adj}\,[\mathbf{D}(s)]}{\det\,[\mathbf{D}(s)]} = \lim_{s\to\infty}\sum_{j=1}^{m} \frac{s}{s-s_j}\frac{\mathbf{z}_j\mathbf{z}_j^T}{\theta_j} = \sum_{j=1}^{m}\frac{\mathbf{z}_j\mathbf{z}_j^T}{\theta_j}. \tag{4.16}$$

It is easy to observe that the order of the elements of $\text{adj}\,[\mathbf{D}(s)]$ is at the most $(m-2)$ in s. Since the order of the determinant, $\det\,[\mathbf{D}(s)]$, is m, after taking the limit every element of the left-hand side of equation (4.16) reduces to zero. Thus, in the limit, the left-hand side of equation (4.16) approaches to an $N \times N$ null matrix. Finally, writing equation (4.16) in the matrix form we obtain

$$\mathbf{Z}\boldsymbol{\Theta}^{-1}\mathbf{Z}^T = \mathbf{O}_N \tag{4.17}$$

and the theorem is proved. □

The result of this theorem is quite general and it does not depend on the nature of the system property matrices. The only requirement of this theorem is that the system must have $m \geq 2N$ distinct eigenvalues. Clearly, the undamped systems as well as the viscously damped systems are also covered as special cases. In the context of viscously damped systems (see Section 4.7 for details), similar result has been derived by Fawzy and Bishop (1976) by considering the normalization matrix $\boldsymbol{\Theta}$ as the identity matrix. Later Fawzy (1977) generalized this result for the case when $\boldsymbol{\Theta}$ is not an identity matrix. The result obtained in theorem 4.1 can be viewed as a further generalization of these results to the non-viscously damped systems. Next, we consider the relationship between the eigensolutions and the mass matrix.

Theorem 4.2. *The modal matrix of a non-viscously damped system,* $\mathbf{Z} \in \mathbb{C}^{N\times m}$*, satisfy the relationship* $\mathbf{Z}\boldsymbol{\Theta}^{-1}\mathbf{S}\mathbf{Z}^T = \mathbf{M}^{-1}$.

Proof. First consider the function $s\mathbf{D}^{-1}(s)$. Following the approach outlined in Section 3.3.2 and using the residue theorem one obtains

$$s\mathbf{D}^{-1}(s) = \sum_{j=1}^{m} \frac{\mathbf{Q}_j}{s - s_j}. \tag{4.18}$$

Here the residues $\mathbf{Q}_j$ can be obtained as

$$\mathbf{Q}_j \stackrel{\text{def}}{=} \lim_{s\to s_j} (s - s_j)\left[s\mathbf{D}^{-1}(s)\right] = s_j \frac{\mathbf{z}_j\mathbf{z}_j^T}{\theta_j}. \tag{4.19}$$

Using the expression of the dynamic stiffness matrix in equation (4.2) we can deduce

$$\lim_{s\to\infty} \frac{\mathbf{D}(s)}{s^2} = \lim_{s\to\infty} \left[\mathbf{M} + \frac{\mathbf{G}(s)}{s} + \frac{\mathbf{K}}{s^2}\right] = \mathbf{M}. \tag{4.20}$$

Taking the inverse of the above equation results

$$\lim_{s\to\infty} \left[s^2\mathbf{D}^{-1}(s)\right] = \mathbf{M}^{-1}. \tag{4.21}$$

Now, multiplying equation (4.18) by s and taking limit as $s \to \infty$ we obtain

$$\lim_{s\to\infty} \left[s^2\mathbf{D}^{-1}(s)\right] = \lim_{s\to\infty} \sum_{j=1}^{m} \frac{s}{s - s_j} \frac{s_j\mathbf{z}_j\mathbf{z}_j^T}{\theta_j} = \sum_{j=1}^{m} \frac{s_j\mathbf{z}_j\mathbf{z}_j^T}{\theta_j}. \tag{4.22}$$

Casting the right-hand side of the above equation in the matrix form and equating it with (4.21) results

$$\mathbf{Z}\boldsymbol{\Theta}^{-1}\mathbf{S}\mathbf{Z}^T = \mathbf{M}^{-1} \tag{4.23}$$

and the theorem is proved. □

Since $\boldsymbol{\Theta}$ and $\mathbf{S}$ are diagonal matrices, they commute in product. For this reason the above result can also be expressed as $\mathbf{Z}\mathbf{S}\boldsymbol{\Theta}^{-1}\mathbf{Z}^T = \mathbf{M}^{-1}$. For viscously damped systems, similar result has been derived by Fawzy and Bishop (1976) by considering the normalization matrix $\boldsymbol{\Theta}$ as the identity matrix. It might be thought that by taking the inverse of equation (4.23) and rearranging, the conventional mass-orthogonality relationship

$$\mathbf{Z}^T\mathbf{M}\mathbf{Z} = \mathbf{S}^{-1}\boldsymbol{\Theta} \tag{4.24}$$

could be obtained. We emphasize that the representation of equation (4.23) in the form of equation (4.24) is *not* always possible. To show this, premultiply equation (4.24) by $\mathbf{Z}\boldsymbol{\Theta}^{-1}$ to obtain

$$\mathbf{Z}\boldsymbol{\Theta}^{-1}\mathbf{Z}^T\mathbf{M}\mathbf{Z} = \mathbf{Z}\boldsymbol{\Theta}^{-1}\mathbf{S}^{-1}\boldsymbol{\Theta} = \mathbf{Z}\mathbf{S}^{-1}. \tag{4.25}$$

Due to theorem 4.1, the left-hand side of equation (4.25) is a null matrix, while its right-hand side is not. Thus (4.24) cannot be a valid equation. However, for a special case, when the system is undamped, the modal matrix $\mathbf{Z}$ can be expressed by a square matrix and equation (4.23) can be represented by the classical mass-orthogonality relationship in (4.24). Thus, theorem 4.2 provides the result equivalent to the classical mass-orthogonality relationship for general cases.

Like the mass-orthogonality relationship of the eigenvectors, the orthogonality relationship with respect to the stiffness matrix can also be obtained. Assuming that $\mathbf{K}^{-1}$ exists we have the following:

Theorem 4.3. *The modal matrix of a non-viscously damped system,* $\mathbf{Z} \in \mathbb{C}^{N\times m}$*, satisfy the relationship* $\mathbf{Z}\boldsymbol{\Theta}^{-1}\mathbf{S}^{-1}\mathbf{Z}^T = -\mathbf{K}^{-1}$.

Proof. Using the expression of the dynamic stiffness matrix in equation (4.2) we can easily deduce

$$\lim_{s\to 0} \mathbf{D}(s) = \mathbf{K}. \tag{4.26}$$

Taking the inverse of the above equation results

$$\lim_{s\to 0} \mathbf{D}^{-1}(s) = \mathbf{K}^{-1}. \tag{4.27}$$

From equations (4.12) and (4.14) one obtains

$$\mathbf{D}^{-1}(s) = \sum_{j=1}^{m} \frac{1}{s - s_j} \frac{\mathbf{z}_j \mathbf{z}_j^T}{\theta_j}. \tag{4.28}$$

Taking the limit as $s \to 0$ in equation (4.28) we obtain

$$\lim_{s\to 0} \mathbf{D}^{-1}(s) = \sum_{j=1}^{m} \frac{1}{-s_j} \frac{\mathbf{z}_j \mathbf{z}_j^T}{\theta_j}. \tag{4.29}$$

Casting the right-hand side of the preceding equation in the matrix form and equating it with (4.27) results

$$\mathbf{Z}\boldsymbol{\Theta}^{-1}\mathbf{S}^{-1}\mathbf{Z}^T = -\mathbf{K}^{-1} \tag{4.30}$$

and the theorem is proved. □

4.5 Relationships Between the Eigensolutions and Damping

In the last section, some direct relationships have been established between the mass and stiffness matrices and the eigensolutions. In this section we try to establish the relationships between the damping matrix and the eigensolutions. A major difficulty in this regard is that, unlike the mass and stiffness matrices, the damping matrix, $\mathbf{G}(s)$, is a function of s. To simplify the problem we consider only two limiting cases, (a) when $s \to \infty$, and (b) when $s \to 0$. Suppose

$$\lim_{s\to\infty} \mathbf{G}(s) = \mathbf{G}_\infty \in \mathbb{R}^{N\times N} \tag{4.31}$$

$$\text{and} \quad \lim_{s\to 0} \mathbf{G}(s) = \mathbf{G}_0 \in \mathbb{R}^{N\times N}, \tag{4.32}$$

where $\|\mathbf{G}_\infty\|$, $\|\mathbf{G}_0\| < \infty$.

4.5.1 Relationships in Terms of $\mathbf{M}^{-1}$

Casting equation (4.28) into the matrix form one obtains

$$\mathbf{D}^{-1}(s) = \mathbf{Z}\boldsymbol{\Theta}^{-1}\left(s\mathbf{I}_m - \mathbf{S}\right)^{-1}\mathbf{Z}^T. \tag{4.33}$$

The preceding equation can be expanded as

$$\begin{aligned}\mathbf{D}^{-1}(s) &= \frac{1}{s}\mathbf{Z}\boldsymbol{\Theta}^{-1}\left(\mathbf{I}_m - \frac{\mathbf{S}}{s}\right)^{-1}\mathbf{Z}^T \\ &= \frac{1}{s}\left(\mathbf{Z}\boldsymbol{\Theta}^{-1}\mathbf{Z}^T\right) + \frac{1}{s^2}\left(\mathbf{Z}\boldsymbol{\Theta}^{-1}\mathbf{S}\mathbf{Z}^T\right) \\ &\quad + \frac{1}{s^3}\left(\mathbf{Z}\boldsymbol{\Theta}^{-1}\mathbf{S}^2\mathbf{Z}^T\right) + \frac{1}{s^4}\left(\mathbf{Z}\boldsymbol{\Theta}^{-1}\mathbf{S}^3\mathbf{Z}^T\right) + \cdots\end{aligned} \tag{4.34}$$

Now, rewrite the expression of the dynamic stiffness matrix in equation (4.2) as

$$\mathbf{D}(s) = s^2\mathbf{M}\left[\mathbf{I}_N + \frac{\mathbf{M}^{-1}}{s}\left(\mathbf{G}(s) + \frac{\mathbf{K}}{s}\right)\right]. \tag{4.35}$$

Taking the inverse of this equation and expanding the right-hand side one obtains

$$\begin{aligned}\mathbf{D}^{-1}(s) = &\left[\mathbf{I}_N - \frac{\mathbf{M}^{-1}}{s}\left(\mathbf{G}(s) + \frac{\mathbf{K}}{s}\right)\right. \\ &\left. + \left\{\frac{\mathbf{M}^{-1}}{s}\left(\mathbf{G}(s) + \frac{\mathbf{K}}{s}\right)\right\}^2 - \cdots\right]\frac{\mathbf{M}^{-1}}{s^2}.\end{aligned} \tag{4.36}$$

Equation (4.36) can be further simplified to obtain

$$\begin{aligned}\mathbf{D}^{-1}(s) = &\frac{\mathbf{M}^{-1}}{s^2} + \frac{1}{s^3}\left(-\mathbf{M}^{-1}\mathbf{G}(s)\mathbf{M}^{-1}\right) \\ &+ \frac{1}{s^4}\left(\mathbf{M}^{-1}\left[\mathbf{G}(s)\mathbf{M}^{-1}\mathbf{G}(s) - \mathbf{K}\right]\mathbf{M}^{-1}\right) + \cdots\end{aligned} \tag{4.37}$$

Comparing equations (4.34) and (4.37) it is clear that their right-hand sides are equal. Theorems 1 and 2 can be alternatively proved by multiplying these equations by s and s^2 respectively and taking the limit as $s \to \infty$. Observe that, the coefficients associated with the corresponding (negative) powers of s in the series expressions (4.34) and (4.37) cannot be equated because $\mathbf{G}(s)$ is also a function of s. However, in the limit when $s \to \infty$, the variation of $\mathbf{G}(s)$ becomes negligible as by equation (4.31) it approaches to $\mathbf{G}_\infty$. Considering the second term of the right-hand side of equation (4.37), equating it with the corresponding term of equation (4.34) and taking the limit as $s \to \infty$ one obtains

$$\mathbf{Z}\boldsymbol{\Theta}^{-1}\mathbf{S}^2\mathbf{Z}^T = -\mathbf{M}^{-1}\mathbf{G}_\infty\mathbf{M}^{-1}. \tag{4.38}$$

It must be noted that this procedure cannot be extended to further lower order terms as all of them would be effected by the functional variation of $\mathbf{G}(s)$ from previous terms.

Were the system viscously damped $\mathbf{G}(s)$ would be a constant matrix and equating the coefficients associated with different powers of s one could obtain several relationships between the eigensolutions and the system matrices. Considering the first few terms in the series expressions (4.34) and (4.37), some such relationships are reported in Section 4.7.

4.5.2 Relationships in Terms of $\mathbf{K}^{-1}$

We rewrite equation (4.33) as

$$\mathbf{D}^{-1}(s) = -\mathbf{Z}\boldsymbol{\Theta}^{-1}\mathbf{S}^{-1}\left(\mathbf{I}_m - s\mathbf{S}^{-1}\right)^{-1}\mathbf{Z}^T. \tag{4.39}$$

Expanding equation (4.39) one obtains

$$\begin{aligned}\mathbf{D}^{-1}(s) = &-\mathbf{Z}\boldsymbol{\Theta}^{-1}\mathbf{S}^{-1}\mathbf{Z}^T - s\left(\mathbf{Z}\boldsymbol{\Theta}^{-1}\mathbf{S}^{-2}\mathbf{Z}^T\right)\\ &- s^2\left(\mathbf{Z}\boldsymbol{\Theta}^{-1}\mathbf{S}^{-3}\mathbf{Z}^T\right) - s^3\left(\mathbf{Z}\boldsymbol{\Theta}^{-1}\mathbf{S}^{-4}\mathbf{Z}^T\right) - \cdots\end{aligned} \tag{4.40}$$

The expression of the dynamic stiffness matrix in equation (4.2) can be rearranged as

$$\mathbf{D}(s) = \mathbf{K}\left[\mathbf{I}_N + s\left(s\mathbf{K}^{-1}\mathbf{M} + \mathbf{K}^{-1}\mathbf{G}(s)\right)\right]. \tag{4.41}$$

Taking the inverse of equation (4.41) and expanding the right-hand side one obtains

$$\begin{aligned}\mathbf{D}^{-1}(s) = \Big[&\mathbf{I}_N - s\left(s\mathbf{K}^{-1}\mathbf{M} + \mathbf{K}^{-1}\mathbf{G}(s)\right)\\ &+ \left\{s\left(s\mathbf{K}^{-1}\mathbf{M} + \mathbf{K}^{-1}\mathbf{G}(s)\right)\right\}^2 - \cdots\Big]\mathbf{K}^{-1}.\end{aligned} \tag{4.42}$$

The preceding equation can be further simplified to obtain

$$\begin{aligned}\mathbf{D}^{-1}(s) =&\mathbf{K}^{-1} + s\left(-\mathbf{K}^{-1}\mathbf{G}(s)\mathbf{K}^{-1}\right)\\ &+ s^2\left(\mathbf{K}^{-1}\left[\mathbf{G}(s)\mathbf{K}^{-1}\mathbf{G}(s) - \mathbf{M}\right]\mathbf{K}^{-1}\right) + \cdots\end{aligned} \tag{4.43}$$

Comparing the right-hand side of equations (4.40) and (4.43), theorem 4.3 can be proved alternatively by taking the limit as $s \to 0$. Considering the second term of the right-hand side of equation (4.43), equating it with the second term of equation (4.40) and taking the limit as $s \to 0$ one obtains

$$\mathbf{Z}\boldsymbol{\Theta}^{-1}\mathbf{S}^{-2}\mathbf{Z}^T = \mathbf{K}^{-1}\mathbf{G}_0\mathbf{K}^{-1}. \tag{4.44}$$

Again, note that this approach cannot be extended to the higher order terms as all of them would be effected by the functional variation of $\mathbf{G}(s)$ from previous terms.

4.6 System Matrices in Terms of the Eigensolutions

Theorems 4.2, 4.3 and equations (4.38), (4.44) allow us to represent the system property matrices explicitly in terms of the eigensolutions. This might be useful in system identification problems

where the eigensolutions of a structure can be measured from experiments. Using the eigensolutions we define two matrices

$$\mathbf{P}_1 = \mathbf{Z}\boldsymbol{\Theta}^{-1}\mathbf{S}\mathbf{Z}^T \tag{4.45}$$

$$\text{and} \quad \mathbf{P}_2 = \mathbf{Z}\boldsymbol{\Theta}^{-1}\mathbf{S}^{-1}\mathbf{Z}^T. \tag{4.46}$$

Using these equations, from equation (4.23) one obtains the mass matrix as

$$\mathbf{M} = \mathbf{P}_1^{-1}. \tag{4.47}$$

Similarly from equation (4.30) the stiffness matrix can be obtained as

$$\mathbf{K} = -\mathbf{P}_2^{-1}. \tag{4.48}$$

The damping matrix in the Laplace domain, $\mathbf{G}(s)$, can be obtained only at the two limiting values when $s \to \infty$, and $s \to 0$. From equations (4.38) and (4.44) one obtains

$$\mathbf{G}_\infty = -\mathbf{P}_1^{-1}\left[\mathbf{Z}\boldsymbol{\Theta}^{-1}\mathbf{S}^2\mathbf{Z}^T\right]\mathbf{P}_1^{-1} \tag{4.49}$$

$$\text{and} \quad \mathbf{G}_0 = \mathbf{P}_2^{-1}\left[\mathbf{Z}\boldsymbol{\Theta}^{-1}\mathbf{S}^{-2}\mathbf{Z}^T\right]\mathbf{P}_2^{-1}. \tag{4.50}$$

These results, however, do not give any indication regarding the functional behaviour of $\mathbf{G}(s)$ between these two extreme values.

4.7 Eigenrelations for Viscously Damped Systems

Viscously damped systems arise as a special case of the more general non-viscously damped systems when the damping matrix become a constant matrix, that is, $\mathbf{G}(s) = \mathbf{C} \in \mathbb{R}^{N\times N}, \forall\, s$. Here, several relationships satisfied by the eigensolutions and the system matrices will be derived for this special case.

For viscously damped systems the order of the characteristic polynomial $m = 2N$, and consequently the modal matrix $\mathbf{Z} \in \mathbb{C}^{N\times 2N}$ and the diagonal matrices $\mathbf{S}, \boldsymbol{\Theta} \in \mathbb{C}^{2N\times 2N}$. From equation (4.9), the normalization relationship reads

$$\mathbf{z}_k^T\left[2s_k\mathbf{M} + \mathbf{C}\right]\mathbf{z}_k = \theta_k, \quad \forall k = 1, \cdots, 2N. \tag{4.51}$$

Now, consider the series expansion of $\mathbf{D}^{-1}(s)$ given by equations (4.34) and (4.37). Equating the coefficients of $1/s$ we obtain the mode orthogonality relationship

$$\mathbf{Z}\boldsymbol{\Theta}^{-1}\mathbf{Z}^T = \mathbf{O}_N. \tag{4.52}$$

This relationship was also derived by Fawzy (1977). Now, equating the coefficients of $1/s^2, \cdots, 1/s^5$ in the right hand sides of equations (4.34) and (4.37), several relationships involving the eigensolutions and $\mathbf{M}^{-1}$, $\mathbf{C}$ and $\mathbf{K}$ may be obtained:

$$\mathbf{Z}\boldsymbol{\Theta}^{-1}\mathbf{S}\mathbf{Z}^T = \mathbf{M}^{-1} \tag{4.53}$$

$$\mathbf{Z}\boldsymbol{\Theta}^{-1}\mathbf{S}^2\mathbf{Z}^T = -\mathbf{M}^{-1}\mathbf{C}\mathbf{M}^{-1} \tag{4.54}$$

$$\mathbf{Z}\boldsymbol{\Theta}^{-1}\mathbf{S}^3\mathbf{Z}^T = \mathbf{M}^{-1}\left[\mathbf{C}\mathbf{M}^{-1}\mathbf{C} - \mathbf{K}\right]\mathbf{M}^{-1} \tag{4.55}$$

and

$$\mathbf{Z}\boldsymbol{\Theta}^{-1}\mathbf{S}^{4}\mathbf{Z}^{T} = \mathbf{M}^{-1}\left[\mathbf{K}\mathbf{M}^{-1}\mathbf{C} + \mathbf{C}\mathbf{M}^{-1}\mathbf{K} - \mathbf{C}\mathbf{M}^{-1}\mathbf{C}\mathbf{M}^{-1}\mathbf{C}\right]\mathbf{M}^{-1}. \tag{4.56}$$

This procedure can be extended to obtain further higher order terms involving $\mathbf{S}$.

Similarly, equating the coefficients of $s^0, \cdots, s^3$ in the right-hand sides of equations (4.40) and (4.43), several relationships involving the eigensolutions and $\mathbf{K}^{-1}$, $\mathbf{C}$ and $\mathbf{M}$ may be obtained:

$$\mathbf{Z}\boldsymbol{\Theta}^{-1}\mathbf{S}^{-1}\mathbf{Z}^{T} = -\mathbf{K}^{-1} \tag{4.57}$$

$$\mathbf{Z}\boldsymbol{\Theta}^{-1}\mathbf{S}^{-2}\mathbf{Z}^{T} = \mathbf{K}^{-1}\mathbf{C}\mathbf{K}^{-1} \tag{4.58}$$

$$\mathbf{Z}\boldsymbol{\Theta}^{-1}\mathbf{S}^{-3}\mathbf{Z}^{T} = \mathbf{K}^{-1}\left[\mathbf{M} - \mathbf{C}\mathbf{K}^{-1}\mathbf{C}\right]\mathbf{K}^{-1} \tag{4.59}$$

and

$$\mathbf{Z}\boldsymbol{\Theta}^{-1}\mathbf{S}^{-4}\mathbf{Z}^{T} = \mathbf{K}^{-1}\left[\mathbf{C}\mathbf{K}^{-1}\mathbf{C}\mathbf{K}^{-1}\mathbf{C} - \mathbf{M}\mathbf{K}^{-1}\mathbf{C} + \mathbf{C}\mathbf{K}^{-1}\mathbf{M}\right]\mathbf{K}^{-1}. \tag{4.60}$$

This procedure can be extended to obtain further lower order terms involving $\mathbf{S}$. Employing a different approach, and considering the normalization matrix $\boldsymbol{\Theta}$ as the identity matrix, Fawzy and Bishop (1976) obtained expressions similar to equations (4.53) – (4.55) and (4.57) – (4.59). Thus, the relationships derived here extend their results to generally normalized eigenvectors.

4.8 Numerical Examples

4.8.1 The System

A three-degree-of-freedom system, similar to what considered in Section 3.7, is used to illustrate the results derived in this chapter. The mass and stiffness matrices are assumed to be

$$\mathbf{M} = \begin{bmatrix} 3 & 0 & 0 \\ 0 & 3 & 0 \\ 0 & 0 & 3 \end{bmatrix} \tag{4.61}$$

$$\text{and} \quad \mathbf{K} = \begin{bmatrix} 4 & -2 & 0 \\ -2 & 4 & -2 \\ 0 & -2 & 4 \end{bmatrix}. \tag{4.62}$$

Numerical values for these matrices are taken by assuming $m_u = 3$ and $k_u = 2$ in the example considered in Section 3.7. The matrix of the damping functions is assumed to be of the form

$$\boldsymbol{\mathcal{G}}(t) = \begin{bmatrix} 0 & 0 & 0 \\ 0 & 1.5g(t) & 0 \\ 0 & 0 & 0 \end{bmatrix} \tag{4.63}$$

where

$$g(t) = \delta(t) + \left(\mu_1 e^{-\mu_1 t} + \mu_2 e^{-\mu_2 t}\right); \quad \mu_1, \mu_2 > 0. \tag{4.64}$$

The damping matrix in the Laplace domain, $\mathbf{G}(s)$, can be obtained by taking the Laplace transform of equation (4.63). The Laplace transform of $g(t)$ given by (4.64) can be obtained as

$$G(s) = 1 + \frac{(\mu_1 + \mu_2)\ s + 2\mu_1\mu_2}{s^2 + (\mu_1 + \mu_2)\, s + \mu_1\mu_2}. \tag{4.65}$$

This damping model is a linear combination of the viscous model and the GHM model considered in the last chapter. Regarding the numerical values of the damping parameters, we assume $\mu_1 = 1.5$ and $\mu_2 = 0.1$.

4.8.2 Eigenvalues and Eigenvectors

Using equation (4.65), together with the expressions of the system matrices given by equations (4.61) – (4.63), it can be shown that the order of the characteristic polynomial, $m = 8$. It has been mentioned that (for lightly damped systems), among the m eigenvalues, $2N = 6$ appear in complex conjugate pairs (elastic modes) and the rest $p = m - 2N = 2$ eigenvalues become purely real (non-viscous modes).

Solving the characteristic equation, the diagonal matrix containing the eigenvalues can be expressed as

$$\mathbf{S} = \mathrm{diag}\left[\mathbf{s}_e, \mathbf{s}_e^*, \mathbf{s}_n\right] \in \mathbb{C}^{8\times 8}. \tag{4.66}$$

Here, the eigenvalues corresponding to the three elastic modes are

$$\mathbf{s}_e = \left\{-0.2632 + 0.7363\mathrm{i}, 1.1547\mathrm{i}, -0.2392 + 1.5177\mathrm{i}, \right\}. \tag{4.67}$$

The eigenvalues corresponding to the two non-viscous modes are found to be

$$\mathbf{s}_n = \left\{-1.0029, -0.0921\right\}. \tag{4.68}$$

Since these eigenvalues are purely real and negative, it implies that the non-viscous modes are stable and non-oscillatory in nature (*i.e.*, over critically damped).

The eigenvectors can be obtained by applying the procedure outlined in the last chapter. The matrix of eigenvectors can be expressed as

$$\mathbf{Z} = \left[\mathbf{Z}_e, \mathbf{Z}_e^*, \mathbf{Z}_n\right] \in \mathbb{C}^{3\times 8} \tag{4.69}$$

Here, $\mathbf{Z}_e$, the matrix of eigenvectors corresponding to the three elastic modes, is

$$\mathbf{Z}_e = \begin{bmatrix} 1 & 1 & 1 \\ 1.2908 - 0.5814\mathrm{i} & 0 & -1.3690 - 1.0893\mathrm{i} \\ 1 & -1 & 1 \end{bmatrix}. \tag{4.70}$$

The matrix of eigenvectors corresponding to the two non-viscous modes is calculated as

$$\mathbf{Z}_n = \begin{bmatrix} 1 & 1 \\ 3.5088 & 2.0127 \\ 1 & 1 \end{bmatrix}. \tag{4.71}$$

Using the eigenvectors given by equations (4.70) – (4.71), the normalization matrix $\boldsymbol{\Theta}$ can be obtained from equation (4.9) as

$$\boldsymbol{\Theta} = \mathrm{diag}\left[\boldsymbol{\theta}_e, \boldsymbol{\theta}_e^*, \boldsymbol{\theta}_n\right]. \tag{4.72}$$

Here

$$\boldsymbol{\theta}_e = \{0.0223 + 0.1180\mathrm{i}, 0.1386\mathrm{i}, -0.2756 + 0.2359\mathrm{i}\} \tag{4.73}$$

and

$$\boldsymbol{\theta}_n = \{1.0075, 9.8738\}\,. \tag{4.74}$$

4.8.3 Orthogonality Relationships

Using $\mathbf{Z}$ and $\boldsymbol{\Theta}$ one can easily verify that the mode orthogonality relationship given by theorem 4.1 is satisfied, that is,

$$\mathbf{Z}\boldsymbol{\Theta}^{-1}\mathbf{Z}^T = \mathbf{O}_3. \tag{4.75}$$

Now, in the line of theorem 4.2 we calculate

$$\mathbf{Z}\boldsymbol{\Theta}^{-1}\mathbf{S}\mathbf{Z}^T = \begin{bmatrix} 0.3333 & 0 & 0 \\ 0 & 0.3333 & 0 \\ 0 & 0 & 0.3333 \end{bmatrix} = \mathbf{M}^{-1}. \tag{4.76}$$

Similarly, following theorem 4.3 one obtains

$$-\mathbf{Z}\boldsymbol{\Theta}^{-1}\mathbf{S}^{-1}\mathbf{Z}^T = \begin{bmatrix} 0.375 & 0.250 & 0.125 \\ 0.250 & 0.500 & 0.250 \\ 0.125 & 0.250 & 0.375 \end{bmatrix} = \mathbf{K}^{-1}. \tag{4.77}$$

4.8.4 Relationships With the Damping Matrix

Taking the Laplace transform of equation (4.63) and considering the limiting cases as $s \to \infty$, and $s \to 0$ one obtains

$$\mathbf{G}_\infty = \begin{bmatrix} 0 & 0 & 0 \\ 0 & 1.5 & 0 \\ 0 & 0 & 0 \end{bmatrix} \tag{4.78}$$

$$\text{and} \quad \mathbf{G}_0 = \begin{bmatrix} 0 & 0 & 0 \\ 0 & 4.5 & 0 \\ 0 & 0 & 0 \end{bmatrix}. \tag{4.79}$$

Note that the matrices $\mathbf{P}_1$ and $\mathbf{P}_2$, defined in equations (4.45) and (4.46) respectively, can be directly obtained from (4.76) and (4.77). Using these matrices, the truth of equations (4.49) and (4.50), which relate $\mathbf{G}_\infty$ and $\mathbf{G}_0$ to the eigensolutions, can be verified. Thus, the damping matrix, $\mathbf{G}(s)$, can be reconstructed from the eigensolutions for the cases when $s \to \infty$, and $s \to 0$.

4.9 Conclusions

In this chapter we have developed several eigenrelations for non-viscously damped multiple-degrees-of-freedom linear dynamic systems. It has been assumed that, in general, the mass and

stiffness matrices as well as the matrix of the kernel functions cannot be simultaneously diagonalized by any linear transformation. The analysis is, however, restricted to systems with non-repetitive eigenvalues and non-singular mass matrices. Relationships regarding the normalization and the orthogonality of the (complex) eigenvectors have been established (theorem 4.1). Expressions equivalent to the orthogonality of the undamped modes over the mass and stiffness matrices have been proposed (theorems 4.2 and 4.3). It was shown that the classical relationships can be obtained as special cases of these general results. Based on these results, we have shown that the mass and stiffness matrices can be uniquely expressed in terms of the eigensolutions. The damping matrix, $\mathbf{G}(s)$, cannot be reconstructed using this approach because it is not a constant matrix. However, we have provided expressions which relate the damping matrix to the eigensolutions for the cases when $s \to \infty$, and $s \to 0$. Whenever applicable, viscously damped counterparts of the newly developed results were provided.

Chapter 5

Identification of Viscous Damping

5.1 Introduction

In Chapters 3 and 4, a systematic study on modal analysis of generally damped linear systems has been carried out. The results based on these studies give a firm basis for further analysis, to use the details of the measured vibration data to learn more about the underlying damping mechanisms. It was shown that non-viscously damped systems have two types of modes, (a) elastic modes, and (b) non-viscous modes. The elastic modes correspond to the 'modes of vibration' of a linear system. The non-viscous modes occur due to the non-viscous damping mechanism and they are not oscillatory in nature. For an underdamped system, that is a system whose all modes are vibrating, the elastic modes are complex (appear in complex conjugate pairs) and non-viscous modes are real. For an N-degrees-of-freedom non-viscously damped systems there are exactly N pairs of elastic modes. The number of non-viscous modes depends on the nature of the damping mechanisms. Conventional viscously damped systems are special cases of non-viscously damped systems when the damping kernel functions have no 'memory'. Modes of viscously damped systems consist of only (complex) elastic modes as non-viscous modes do not appear in such systems. Elastic modes can be real only if the damping is proportional, that is only if the conditions derived in Theorem 2.2 are satisfied.

There is no physical reason why a general system should follow the mathematical conditions for existence of real normal modes. In fact practical experience in modal testing shows that most real-life structures do not do so, as they possess complex modes instead of real normal modes. As Sestieri and Ibrahim (1994) have put it ' ... it is ironic that the real modes are in fact not real at all, in that in practice they do not exist, while complex modes are those practically identifiable from experimental tests. This implies that real modes are pure abstraction, in contrast with complex modes that are, therefore, the only reality!' For this reason it is legitimate to consider only complex modes for further developments. However, consideration of complex modes in experimental modal analysis has not been very popular among researchers. In fact many publications, for example Ibrahim (1983a), Chen *et al.* (1996b) and Balmès (1997), discuss how to obtain the 'best' real normal modes from identified complex modes.

The works in the previous chapters made it clear that the standard procedure of experimental modal analysis actually measured 'modes' when complex results were obtained. The justification of the method in the standard texts (*eg*., Ewins, 1984) is based on assuming viscous damping, and begs the question of how one might tell in practice whether a viscous model is applicable to a given structure, let alone of how to proceed if a viscous model is not supported by the measurements. These are the central questions to be addressed in this study. The works in the earlier chapters showed that the expression for vibration transfer functions in terms of mode shapes and natural frequencies, familiar from undamped systems, carries over almost unchanged to systems with completely general linear damping. One simply replaces the mode shapes with corresponding complex elastic modes and non-viscous modes, and the natural frequencies with their corresponding values. This result shows that experimental modal analysis can indeed measure the correct complex modes of a structure, since the pole-fitting strategy normally used is based on the validity of this transfer function expression. Here we emphasize that by conducting conventional modal testing procedure it is only possible to obtain the elastic modes as the non-viscous modes do not produce any 'peak' in the measured transfer functions (see Section 8.2 for further discussions). This is however, not a very big limitation since it was shown before that the effect of non-viscous modes is not very significant on the vibration response. For this reason, in what follows next, the non-viscous modes will *not* be considered. Beside this we also assume that the damping is light so that the first-order perturbation method can be applied.

There are good arguments to support the principle of reciprocity when the physical mechanism of damping arises from linear viscoelastic behaviour within some or all of the material of which the structure is built. The 'correspondence principle' of linear viscoelasticity applies to such problems under rather general conditions (see *eg*., Fung, 1965), and since the undamped problem satisfies reciprocity, then the damped one will also do so. However, the case is less obvious for damping associated with structural joints, often the dominant source of damping in practice. The mechanisms of such damping are frequently non-linear when examined in detail, but empirically the overall result frequently satisfies normal experimental tests of linearity. The question of whether such systems should be expected to satisfy reciprocity remains open. For the purpose of the present investigation, reciprocity will be assumed in all cases.

These facts gives us the confidence to ask some general questions of interest:

1. From experimentally determined complex modes can one identify the underlying damping mechanism? Is it viscous or non-viscous? Can the correct model parameters be found experimentally?

2. Is it possible to establish experimentally the *spatial distribution* of damping?

3. Is it possible that more than one damping model with corresponding 'correct' sets of parameters may represent the system response equally well, so that the identified model becomes non-unique?

4. Does the selection of damping model matter from an engineering point of view? Which aspects of behaviour are wrongly predicted by an incorrect damping model?

This chapter and following two address these questions. The analysis is restricted to linear systems with light damping: we assume throughout the validity of the first-order perturbation results. The initial aim is to consider what can be learned about these questions in principle, so procedures will be illustrated by applying them to simulated transfer functions, with no noise. The issue of how the usefulness of any procedure might be limited in practice by measurement noise will be deferred to later studies. This chapter will concentrate on the fitting of viscous models to 'measured' transfer functions, and on establishing the symptoms by which a non-viscous model might be recognized. In Section 5.2 we briefly review the theory of determination of complex frequencies and modes based on the first-order perturbation method. In Section 5.3 an algorithm is given for fitting a non-proportional viscous damping model, using the complex modes and complex frequencies. In Section 5.4 numerical examples are given to illustrate the fitting procedure. Some implications of these results for damping identification are summarized in Section 5.5. In Chapter 6, the procedures are generalized to some non-viscous models of damping, and the discussion extended to this more general case.

5.2 Background of Complex Modes

Dynamics of viscously damped systems has been discussed in details in Section 1.3. Complex modes arise in viscously damped systems provided the damping is non-proportional. Expressions of complex modes can be obtained as a special case of the general analysis presented in Section 3.2.1. One such special case when the damping is lightly non-proportional is discussed in Section 3.2.3. In this section we consider a further special case when the damping is light so that the first-order perturbation method can be applied. First-order perturbation results can be obtained from the results in Section 3.2.3 as follows.

Suppose $\lambda_j, \mathbf{z}_j$ is the j-th complex natural frequency and complex mode shape. In the context of the notations used in Section 3.2.3, $s_j = \mathrm{i}\lambda_j$. Using this, from equation (3.37) approximate expression for the complex natural frequencies can be obtained as

$$\lambda_j \approx \pm\omega_j + \mathrm{i}C'_{jj}/2. \tag{5.1}$$

From equation (3.38), the first-order approximate expression of the complex eigenvectors is

$$\mathbf{z}_j \approx \mathbf{x}_j + \mathrm{i}\sum_{\substack{k=1\\k\neq j}}^{N} \frac{\omega_j C'_{kj}}{(\omega_j^2 - \omega_k^2)}\mathbf{x}_k. \tag{5.2}$$

In the above expressions $C'_{kl} = \mathbf{x}_k^T \mathbf{C} \mathbf{x}_l$ are the elements of the damping matrix in modal coordinates. These results were obtained by Rayleigh (1877, see Section 102, equation 5 and 6). The

above equation shows (up to first order approximation) that the real parts of the complex modes are the same as the undamped modes and that the off-diagonal terms of the modal damping matrix are responsible for the imaginary parts.

5.3 Identification of Viscous Damping Matrix

Currently available methods for identification of viscous damping matrix in the context of linear multiple-degrees-of-freedom systems have been discussed in Section 1.5.2. These methods range form the simplest case, that is proportional damping, to more general non-proportional damping case. Several practical issues, for example, effect of measurement noise, incomplete modal data, consistency with FE models, *etc*. have been discussed. However, all these methods are based on the assumption that the damping mechanism of the structure is viscous, and their efficacy when the damping mechanism is not viscous is largely unexplored. Here we propose a method to obtain the full non-proportional viscous damping matrix from complex modal data, in a way which will generalize very naturally to the fitting of non-viscous damping models in Chapter 6. The perturbation expression from the previous section is used as the basis of the fitting procedure, and it is assumed that the damping is sufficiently light to justify this.

Approximate complex natural frequencies and mode shapes for a system with light viscous damping can be obtained from the expressions given in equations (5.1) and (5.2). Write

$$\hat{\mathbf{z}}_j = \hat{\mathbf{u}}_j + \mathrm{i}\hat{\mathbf{v}}_j \tag{5.3}$$

where $\hat{\mathbf{z}}_j \in \mathbb{C}^N$ is the *measured* j-th complex mode, and N denotes the number of measurement points on the structure. Suppose that the number of modes to be considered in the study is m: in general $m \neq N$, usually $N \geq m$. If the measured complex mode shapes are consistent with a viscous damping model then from equation (5.1) the real part of each complex natural frequency gives the undamped natural frequency:

$$\hat{\omega}_j = \Re\left(\hat{\lambda}_j\right), \tag{5.4}$$

where $\hat{\lambda}_j$ denotes the j-th complex natural frequency measured from the experiment. Similarly from equation (5.2), the real part of each complex mode $\hat{\mathbf{u}}_j$ immediately gives the corresponding undamped mode and the mass orthogonality relationship (1.10) will be automatically satisfied. Now from equation (5.2), expand the imaginary part of $\hat{\mathbf{z}}_j$ as a linear combination of $\hat{\mathbf{u}}_j$:

$$\hat{\mathbf{v}}_j = \sum_{k=1}^{m} B_{kj}\hat{\mathbf{u}}_k; \quad \text{where } B_{kj} = \frac{\hat{\omega}_j C'_{kj}}{\hat{\omega}_j^2 - \hat{\omega}_k^2}. \tag{5.5}$$

With $N \geq m$ this relation cannot be satisfied exactly in general. Then the constants B_{kj} should be calculated such that the error in representing $\hat{\mathbf{v}}_j$ by such a sum is minimized. Note that in the above sum we have included the $k = j$ term although in the original sum in equation (5.2) this term was

absent. This is done to simplify the mathematical formulation to be followed, and has no effect on the result. Our interest lies in calculating C'_{kj} from B_{kj} through the relationship given by the second part of the equation (5.5), and indeed for $k = j$ we would obtain $C'_{kj} = 0$. The diagonal terms C'_{jj} are instead obtained from the imaginary part of the complex natural frequencies:

$$C'_{jj} = 2\Im(\hat{\lambda}_j). \tag{5.6}$$

The error from representing $\hat{\mathbf{v}}_j$ by the series sum (5.5) can be expressed as

$$\boldsymbol{\varepsilon}_j = \hat{\mathbf{v}}_j - \sum_{k=1}^{m} B_{kj}\hat{\mathbf{u}}_k. \tag{5.7}$$

To minimize the error a Galerkin approach can be adopted. The undamped mode shapes $\hat{\mathbf{u}}_l, \forall l = 1, \cdots, m$, are taken as 'weighting functions'. Using the Galerkin method on $\boldsymbol{\varepsilon}_j \in \mathbb{R}^N$ for a fixed j one obtains

$$\hat{\mathbf{u}}_l^T \boldsymbol{\varepsilon}_j = 0; \qquad \forall l = 1, \cdots m. \tag{5.8}$$

Combining equations (5.7) and (5.8) yields

$$\hat{\mathbf{u}}_l^T \left\{ \hat{\mathbf{v}}_j - \sum_{k=1}^{m} B_{kj}\hat{\mathbf{u}}_k \right\} = 0 \quad \text{or} \quad \sum_{k=1}^{m} W_{lk}\, B_{kj} = D_{lj}; \qquad l = 1, \cdots, m \tag{5.9}$$

with $W_{lk} = \hat{\mathbf{u}}_l^T \hat{\mathbf{u}}_k$ and $D_{lj} = \hat{\mathbf{u}}_l^T \hat{\mathbf{v}}_j$. Since W_{kl} is $j-$independent, for all $j = 1, \cdots m$ the above equations can be combined in matrix form

$$\mathbf{W}\,\mathbf{B} = \mathbf{D} \tag{5.10}$$

where $\mathbf{B} \in \mathbb{R}^{m\times m}$ is the matrix of unknown coefficients to be found, $\mathbf{W} = \hat{\mathbf{U}}^T\hat{\mathbf{U}} \in \mathbb{R}^{m\times m}$ and $\mathbf{D} = \hat{\mathbf{U}}^T\hat{\mathbf{V}} \in \mathbb{R}^{m\times m}$ with

$$\begin{aligned} \hat{\mathbf{U}} &= [\hat{\mathbf{u}}_1, \hat{\mathbf{u}}_2, \cdots \hat{\mathbf{u}}_m] \in \mathbb{R}^{N\times m} \\ \hat{\mathbf{V}} &= [\mathbf{v}_1, \hat{\mathbf{v}}_2, \cdots \hat{\mathbf{v}}_m] \in \mathbb{R}^{N\times m}. \end{aligned} \tag{5.11}$$

Now $\mathbf{B}$ can be obtained by carrying out the matrix inversion associated with equation (5.10) as

$$\mathbf{B} = \mathbf{W}^{-1}\mathbf{D} = \left[\hat{\mathbf{U}}^T\hat{\mathbf{U}}\right]^{-1}\hat{\mathbf{U}}^T\hat{\mathbf{V}}. \tag{5.12}$$

From the $\mathbf{B}$ matrix, the coefficients of the modal damping matrix can be derived from

$$C'_{kj} = \frac{(\hat{\omega}_j^2 - \hat{\omega}_k^2)B_{kj}}{\hat{\omega}_j}; \qquad k \neq j \tag{5.13}$$

The above two equations together with equation (5.6) completely define the modal damping matrix $\mathbf{C}' \in \mathbb{R}^{m\times m}$. If $\hat{\mathbf{U}} \in \mathbb{R}^{N\times N}$ is the *complete* undamped modal matrix then the damping matrices in the modal coordinates and original coordinates are related by $\mathbf{C}' = \hat{\mathbf{U}}^T\mathbf{C}\hat{\mathbf{U}}$. Thus given $\mathbf{C}'$, the damping matrix in the original coordinates can be easily obtained by the inverse transformation as

$\mathbf{C} = \mathbf{U}^{T^{-1}}\mathbf{C}'\hat{\mathbf{U}}^{-1}$. For the case when the full modal matrix is not available, that is $\hat{\mathbf{U}} \in \mathbb{R}^{N\times m}$ is not a square matrix, a pseudoinverse is required in order to obtain the damping matrix in the original coordinates. The damping in the original coordinates is then given by

$$\mathbf{C} = \left[\left(\hat{\mathbf{U}}^T\hat{\mathbf{U}}\right)^{-1}\hat{\mathbf{U}}^T\right]^T \mathbf{C}' \left[\left(\mathbf{U}^T\hat{\mathbf{U}}\right)^{-1}\hat{\mathbf{U}}^T\right]. \tag{5.14}$$

It is clear from the above equations that we need only the complex natural frequencies and mode shapes to obtain **C**. The method is very simple and does not require much computational time. Another advantage is that neither the estimation of mass and stiffness matrices nor the full set of modal data is required to obtain an estimate of the full damping matrix. Using a larger number of modes will of course produce better results with higher spatial resolution. In summary, this procedure can be described by the following steps:

1. Measure a set of transfer functions $H_{ij}(\omega)$.
2. Choose the number m of modes to be retained in the study. Determine the complex natural frequencies $\hat{\lambda}_j$ and complex mode shapes $\hat{\mathbf{z}}_j$ from the transfer functions, for all $j = 1, \cdots m$. Obtain the complex mode shape matrix $\hat{\mathbf{Z}} = [\hat{\mathbf{z}}_1, \hat{\mathbf{z}}_2, \cdots \hat{\mathbf{z}}_m] \in \mathbb{C}^{N\times m}$.
3. Estimate the 'undamped natural frequencies' as $\hat{\omega}_j = \Re(\hat{\lambda}_j)$.
4. Set $\hat{\mathbf{U}} = \Re\left[\hat{\mathbf{Z}}\right]$ and $\hat{\mathbf{V}} = \Im\left[\hat{\mathbf{Z}}\right]$, from these obtain $\mathbf{W} = \hat{\mathbf{U}}^T\hat{\mathbf{U}}$ and $\mathbf{D} = \hat{\mathbf{U}}^T\hat{\mathbf{V}}$. Now denote $\mathbf{B} = \mathbf{W}^{-1}\mathbf{D}$.
5. From the **B** matrix get $C'_{kj} = \dfrac{(\hat{\omega}_j^2 - \hat{\omega}_k^2)B_{kj}}{\hat{\omega}_j}$ for $k \neq j$ and $C'_{jj} = 2\Im(\hat{\lambda}_j)$.
6. Finally, carry out the transformation $\mathbf{C} = \left[\left(\hat{\mathbf{U}}^T\mathbf{U}\right)^{-1}\hat{\mathbf{U}}^T\right]^T \mathbf{C}' \left[\left(\hat{\mathbf{U}}^T\hat{\mathbf{U}}\right)^{-1}\hat{\mathbf{U}}^T\right]$ to get the damping matrix in physical coordinates.

It should be observed that even if the measured transfer functions are reciprocal, this procedure does not necessarily yield a symmetric damping matrix. If we indeed obtain a non-symmetric damping matrix then it may be deduced that the physical law behind the damping mechanism in the structure is not viscous. This fact is illustrated by example in the next section. Under those circumstances, if an accurate model for the damping in the structure is needed then a non-viscous model of some kind must be fitted to the measured data. Some examples of such models and algorithms for fitting them will be illustrated in the next chapter.

5.4 Numerical Examples

There is a major difference in emphasis between this study and other related studies on damping identification reported in the literature. Most of the methods assume from the outset that the

system is viscously damped (see the review paper by Pilkey and Inman, 1998) and then formulate the theory to identify a viscous damping matrix. Here, we wish to investigate how much one can learn by fitting a viscous damping model when the actual system is non-viscously damped, as one must expect to be the case for most practical systems. It is far from clear in practice what kind of non-viscous damping behaviour a system might exhibit. We defer that question for the moment, and instead study by simulation a system which has a known non-viscous damping model. Two different physically realistic non-viscous damping models are considered in this study. They are applied to a system consisting of a linear array of spring-mass oscillators and dampers.

This simple system gives us a useful basis to carry out numerical investigations. Complex natural frequencies and modes can be calculated for the model system using the procedure outlined in Section 3.2, then treated like experimental data obtained from a modal testing procedure, and used for identifying a viscous damping model by the procedure described in the previous section. Note that in a true experimental environment the measured complex natural frequencies and mode shapes will be contaminated by noise. Since the simulation data are noise-free the results obtained using them are 'ideal', the best one can hope using this approach. Once promising algorithms have been identified in this way, the influence of noise in degrading the performance will have to be addressed.

Figure 5.1 shows the model systems. N masses, each of mass m_u, are connected by springs of stiffness k_u. The mass matrix of the system has the form $\mathbf{M} = m_u \mathbf{I}_N$ where $\mathbf{I}_N$ is the $N \times N$ identity matrix. The stiffness matrix of the system is

$$\mathbf{K} = k_u \begin{bmatrix} 2 & -1 & & & & & \\ -1 & 2 & -1 & & & & \\ & \ddots & \ddots & \ddots & & & \\ & & -1 & 2 & -1 & & \\ & & & & \ddots & \ddots & \\ & & & & & -1 & 2 \end{bmatrix} . \tag{5.15}$$

Certain of the masses of the system shown in Figure 5.1(a) have dissipative elements connecting them to the ground. In this case the damping force depends only on the absolute motion of the individual masses. Such damping will be described as 'locally reacting' by analogy with usage in the theory of fluid-loaded structures (see *eg*. Crighton, 1985). For the system shown in Figure 5.1(b), by contrast, dissipative elements are connected between certain adjacent pairs of masses. In this case the damping force depends on the relative motion of the two adjacent masses, and will be called 'non-locally reacting'.

The dissipative elements shown in Figure 5.1 will be taken to be linear, but not to be simple viscous dashpots. For any such element, the force developed between the two ends will depend on the history of the relative motion of the two ends. The dependence can be written in terms of a convolution integral. Using the mass and the stiffness matrices described before, the equations of

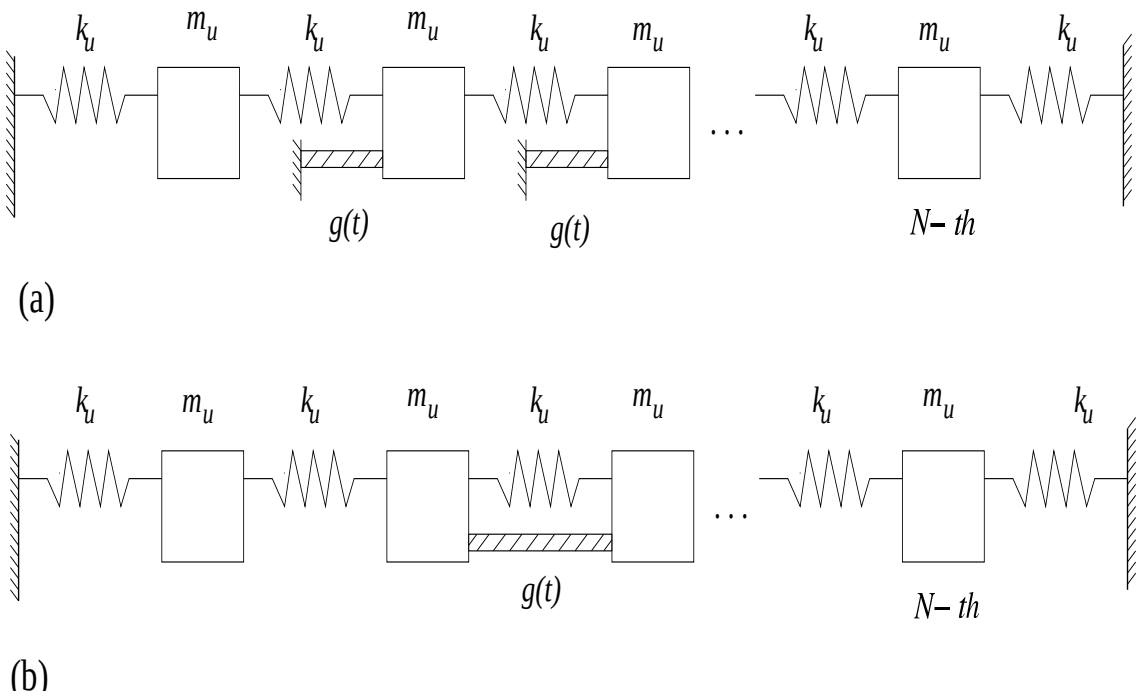

Figure 5.1: Linear array of N spring-mass oscillators, $N = 30$, $m_u = 1\,Kg$, $k_u = 4 \times 10^3 N/m$

motion can thus be expressed in the form

$$\mathbf{M}\ddot{\mathbf{q}}(t) + \bar{\mathbf{C}} \int_{-\infty}^{t} g(t-\tau)\, \dot{\mathbf{q}}(\tau)\, \mathrm{d}\tau + \mathbf{K}\mathbf{q}(t) = \mathbf{0} \tag{5.16}$$

where $g(t)$ is the damping function (assumed to have the same form for all the damping elements in the system) and $\bar{\mathbf{C}}$ is the associated coefficient matrix which depends on the distribution of the dampers. Two specific damping models will be considered, defined by two different forms of $g(t)$:

$$\text{MODEL 1:} \qquad g^{(1)}(t) = \mu_1 e^{-\mu_1 t}; \quad t \geq 0 \tag{5.17}$$

$$\text{MODEL 2:} \qquad g^{(2)}(t) = 2\sqrt{\frac{\mu_2}{\pi}} e^{-\mu_2 t^2}; \quad t \geq 0 \tag{5.18}$$

where μ_1 and μ_2 are constants. Any physically realistic damping model must satisfy a condition of positive energy dissipation at all frequencies. A sufficient condition to guarantee this, satisfied by both models considered here, will be described in Chapter 6.

It is convenient to normalize the functions to make comparisons between models meaningful. Both functions have already been scaled so as to have unit area when integrated to infinity. This makes them directly comparable with the viscous model, in which the corresponding damping function would be a unit delta function, $g(t) = \delta(t)$, and the coefficient matrix $\bar{\mathbf{C}}$ would be the usual damping matrix. It is also convenient to define a characteristic time constant θ_j for each damping function, via the first moment of $g^{(j)}(t)$:

$$\theta_j = \int_0^{\infty} t\, g^{(j)}(t)\, \mathrm{d}t \tag{5.19}$$

For the two damping models considered here, evaluating the above integral gives $\theta_1 = \frac{1}{\mu_1}$ and $\theta_2 = \frac{1}{\sqrt{\pi}\mu_2}$. For viscous damping $\theta_j = 0$. The characteristic time constant of a damping function gives a convenient measure of 'width': if it is close to zero the damping behaviour will be near-viscous, and vice versa. To establish an equivalence between the two damping models we can choose that they have the same time constant, so that $\frac{1}{\mu_1} = \frac{1}{\sqrt{\pi}\mu_2}$.

For the system with locally reacting damping shown in Figure 5.1(a), $\bar{\mathbf{C}} = c\bar{\mathbf{I}}$ where c is a constant and $\bar{\mathbf{I}}$ is a block identity matrix which is non-zero only between the s-th and $(s+l)$-th entries along the diagonal, so that 's' denotes the first damped mass and $(s+l)$ the last one. For the system with non-locally reacting damping shown in Figure 5.1(b), $\bar{\mathbf{C}}$ has a similar pattern to the stiffness matrix given by equation (5.15), but non-zero only for terms relating to the block between s and $(s+l)$. For the numerical calculations considered here, we have taken $N = 30$, $s = 8$ and $(s+l) = 17$.

For the purpose of numerical examples, the values $m_u = 1$ kg, $k_u = 4 \times 10^5$ N/m have been used. The resulting undamped natural frequencies then range from near zero to approximately 200 Hz. For damping models, the value $c = 25$ has been used, and various values of the time constant θ have been tested. These are conveniently expressed as a fraction of the period of the highest undamped natural frequency:

$$\theta = \gamma T_{min} \tag{5.20}$$

When γ is small compared with unity the damping behaviour can be expected to be essentially viscous, but when γ is of order unity non-viscous effects should become significant.

The complex natural frequencies and mode shapes can now be calculated from the analysis presented in Section 3.2. We can then follow the steps outlined in the previous section to obtain an equivalent viscous damping which represents these 'measured' data most accurately.

5.4.1 Results for Small γ

When $\gamma = 0.02$ both damping models should show near-viscous behaviour. First consider the system shown in Figure 5.1(a) with locally reacting damping. Figure 5.2 shows the fitted viscous damping matrix $\mathbf{C}$ for damping model 2, calculated using the complete set of 30 modes. The fitted matrix identifies the damping in the system very well. The high portion of the plot corresponds to the spatial location of the dampers. The off-diagonal terms of the identified damping matrix are very small compared to the diagonal terms, indicating correctly that the damping is locally reacting.

It is useful to understand the effect of modal truncation on the damping identification procedure. In practice, one might expect to be able to use only the first few modes of the system to identify the damping matrix. Figures 5.3 and 5.4 shows the fitted viscous damping matrix using, respectively, the first 20 and the first 10 modes only. The quality of the fitted damping matrix gradually deteriorates as the number of modes used to fit the damping matrix is reduced, but still the

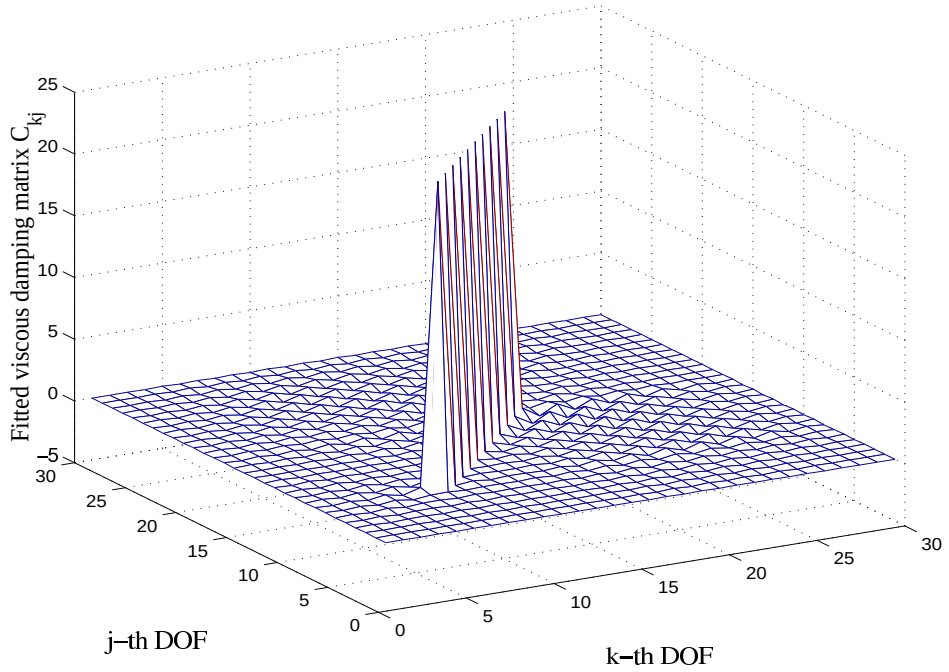

Figure 5.2: Fitted viscous damping matrix for the local case, $\gamma = 0.02$, damping model 2

identified damping matrix shows a reasonable approximation to the true behaviour. The spatial resolution of the identified damping is limited by that of the set of modes used, and some off-diagonal activity is seen in the fitted matrix. Since for this system the mode shapes are approximately sinusoidal, we can recognize the effects of modal truncation as analogous to Gibbs phenomenon in a truncated Fourier series.

Now consider the system shown in Figure 5.1(b) with non-locally reacting damping. Figure 5.5 shows the fitted viscous damping matrix for damping model 2, using the full set of modes. Again, the fitted matrix identifies the damping in the system quite well. The high portion of the plot corresponds to the spatial location of the dampers. The negative off-diagonal terms in the identified damping matrix indicate that the damping is non-locally reacting, and the pattern is recognizably that of equation (5.15). The extent of noise away from the three diagonals is rather higher than was the case in Figure 5.2. This is not very surprising. The pattern of terms along a row of the matrix corresponding to a damped position was, in the former case, a discrete approximation to a delta function. In the latter case it is an approximation to the second derivative of a delta function. The modal expansion, approximately a Fourier series, will thus have a much larger contribution from the higher modes, which are the first to be affected by the non-zero width of the damping function. A higher level of noise is the inevitable result.

One consequence of the distinction between local and non-local damping is illustrated in Figure 5.6. The modal Q-factors are plotted for the two cases studied, for the full set of 30 modes. Locally-reacting damping (solid line) produces a Q-factor roughly proportional to mode number. The particular non-local damping chosen here shows the opposite trend, with Q-factors roughly

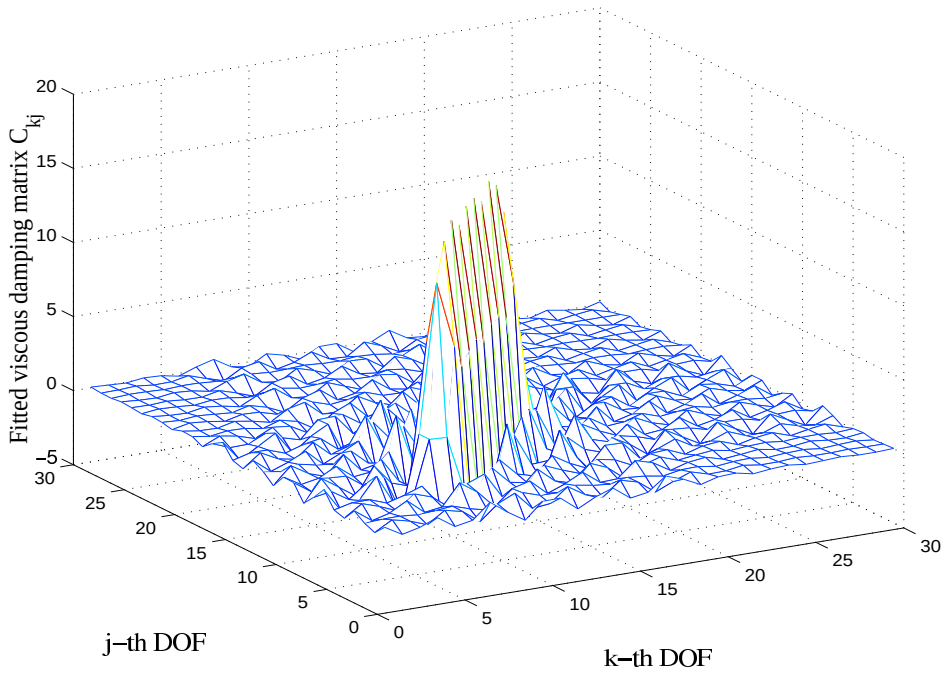

Figure 5.3: Fitted viscous damping matrix using first 20 modes for the local case, $\gamma = 0.02$, damping model 2

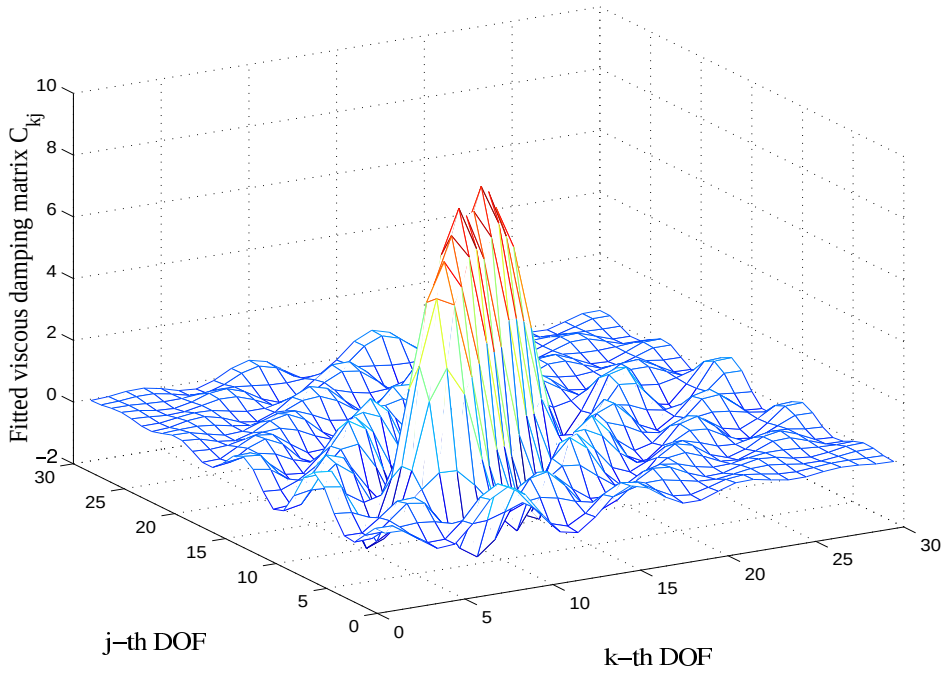

Figure 5.4: Fitted viscous damping matrix using first 10 modes for the local case, $\gamma = 0.02$, damping model 2

inversely proportional to mode number (dashed line). Both trends can be understood in terms of Rayleigh damping. If the damping extended over the entire structure rather that being limited to a finite patch, then the local-reacting damping would correspond to a dissipation matrix proportional to the mass matrix, while the non-local damping would correspond to a dissipation matrix propor-

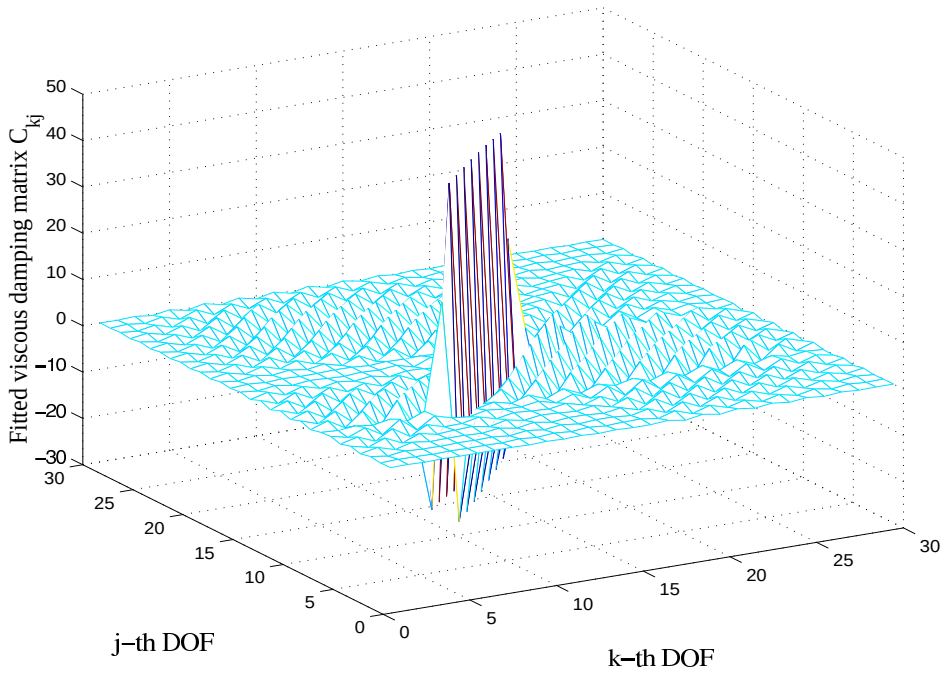

Figure 5.5: Fitted viscous damping matrix for the non-local case, $\gamma = 0.02$, damping model 2

tional to the stiffness matrix. The trends of modal Q-factor with frequency would then be exactly proportional and inversely proportional, respectively. Limiting the damping to a part of the structure has evidently not disturbed this pattern very much. The variation with frequency has translated into a variation with mode number: the mode number relates rather directly to wavenumber for this simple system, and the physical origins of the different trends of Q-factors lies in dependence on wavelength, rather than on frequency as such.

When the fitting procedure is repeated using the alternative damping model of equation (5.17) the results are sufficiently similar that they are not reproduced here. Since the time constant is so short, both damping models are near to viscous damping and the detailed difference in their functional behaviour does not influence the results significantly. In summary, we can say that when the time constant for a damping model is small the proposed identification method works quite well regardless of the functional form of the damping mechanism. The spatial location of damping is revealed clearly, and whether it is locally or non-locally reacting. Modal truncation blurs the results, but does not invalidate the identification process.

5.4.2 Results for Larger γ

When γ is larger the two non-viscous damping models depart from the viscous damping model, each in its own way. For the value $\gamma = 0.5$, Figure 5.7 shows the result of running the fitting procedure for damping model 1 (equation (5.17)) with locally-reacting damping and the full set of modes, similar to Figure 5.2. Figure 5.8 shows the corresponding fitted viscous damping matrix $\mathbf{C}$ for damping model 2 (equation (5.18)). In both cases it may be noted that although we have

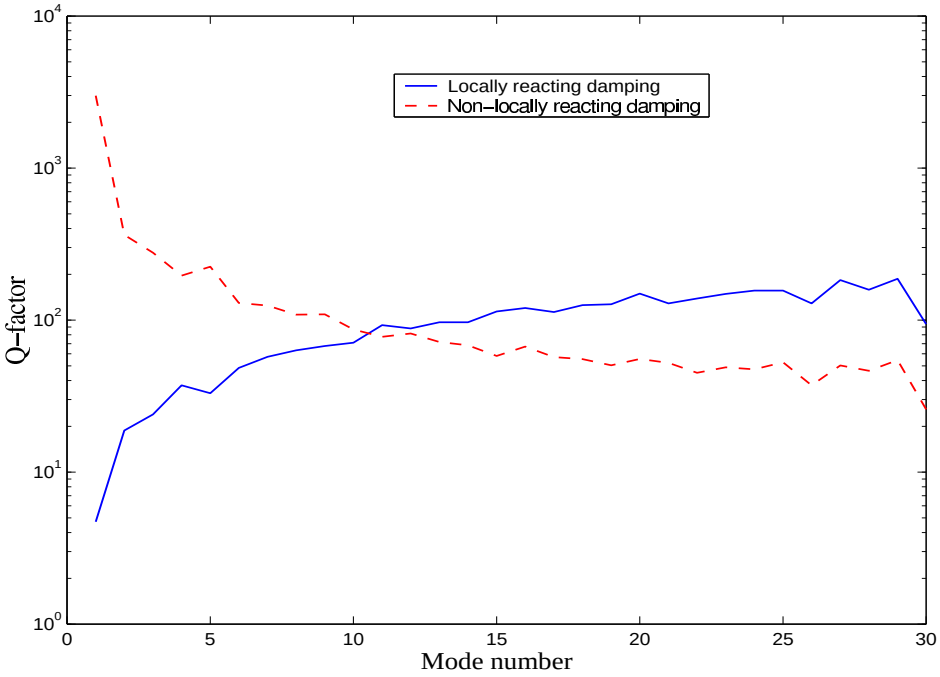

Figure 5.6: Modal Q-factors, $\gamma = 0.02$, damping model 2

started with a locally reacting damping model, which means the matrix is non-zero only along the diagonal, the non-zero values in the off-diagonal terms show that the fitted viscous damping is, in a sense, not locally reacting. Nevertheless, the spatial distribution of the damping is well identified, and perhaps one might be able to guess that the underlying mechanism was locally-reacting from the fact that the significantly non-zero elements all have positive values, with a clear peak centered on the diagonal of the matrix. This remark remains true even for larger values of γ. We give just one example: Figure 5.9 shows the fitted dissipation matrix for $\gamma = 2$. Most of the matrix elements are now significantly non-zero, but the pattern shows the same general features as Figure 5.7. The high values, along the main diagonal of the matrix, still correctly identify the spatial distribution of the damping.

Figures 5.10,5.11 show the fitted results corresponding to Figures 5.7,5.8, using the non-local damping model. Similar remarks can be made as for the locally-reacting case. The spatial distribution of the damping is revealed quite clearly and correctly. The non-local nature of the damping is hinted at by the strong negative values on either side of the main diagonal of the matrix. In both cases, there is an obvious echo of the pattern seen in Figure 5.5 and equation (5.15).

To give a different insight into the behaviour of the various damping models it is useful to see the pattern of modal damping factors. In Figure 5.12, the modal Q-factors are plotted for the two damping models with $\gamma = 0.5$, in the local-reacting case. Figure 5.13 shows the corresponding results for the non-locally reacting case. For locally-reacting damping the Q-factors rise with mode number, for both damping models. For the non-local case the Q-factors fall initially. For damping model 1 and these particular parameter values the Q-factors are then approximately constant, while

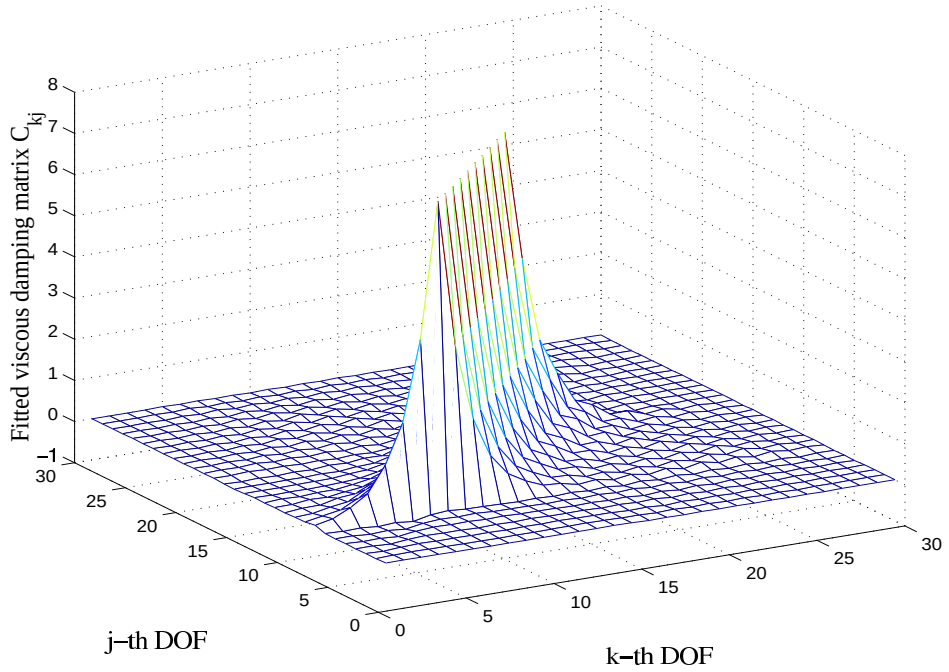

Figure 5.7: Fitted viscous damping matrix for the local case, $\gamma = 0.5$, damping model 1

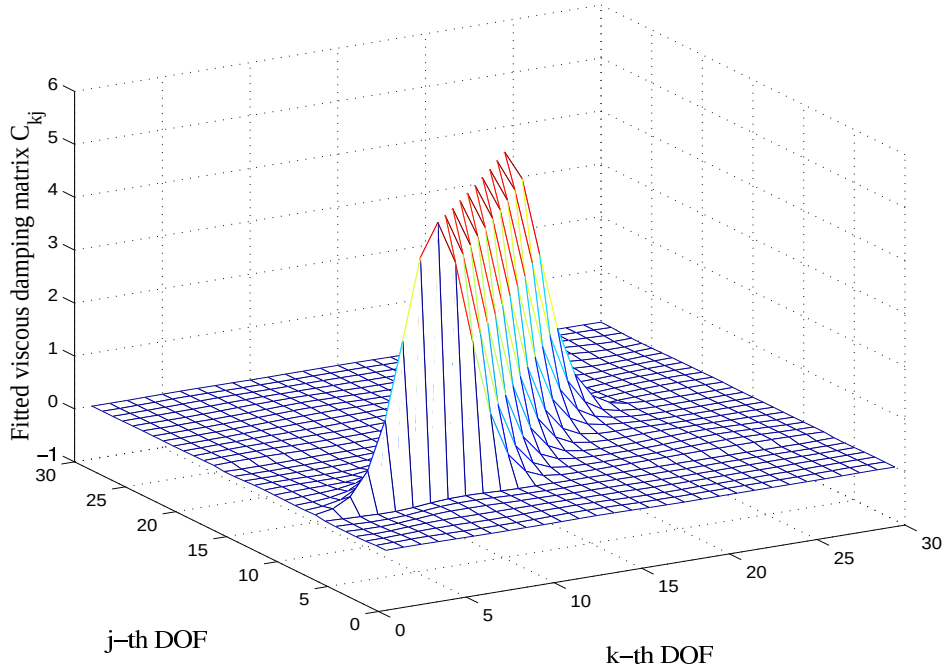

Figure 5.8: Fitted viscous damping matrix for the local case, $\gamma = 0.5$, damping model 2

for damping mode 2 they rise again after a while, reaching very high values at high mode numbers. In terms of physical plausibility, damping model 1 in the non-local configuration gives the closest match to the common practical experience that modal damping factors are approximately constant. However, physical plausibility is not a major issue here, where the aim is to test the procedure under a wide range of circumstances.

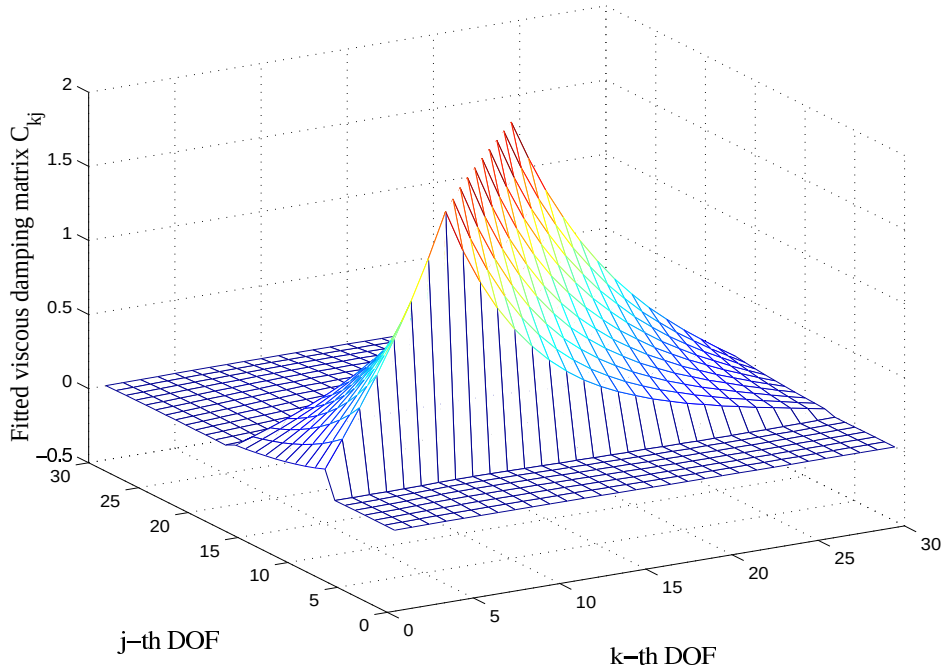

Figure 5.9: Fitted viscous damping matrix for the local case, $\gamma = 2.0$, damping model 1

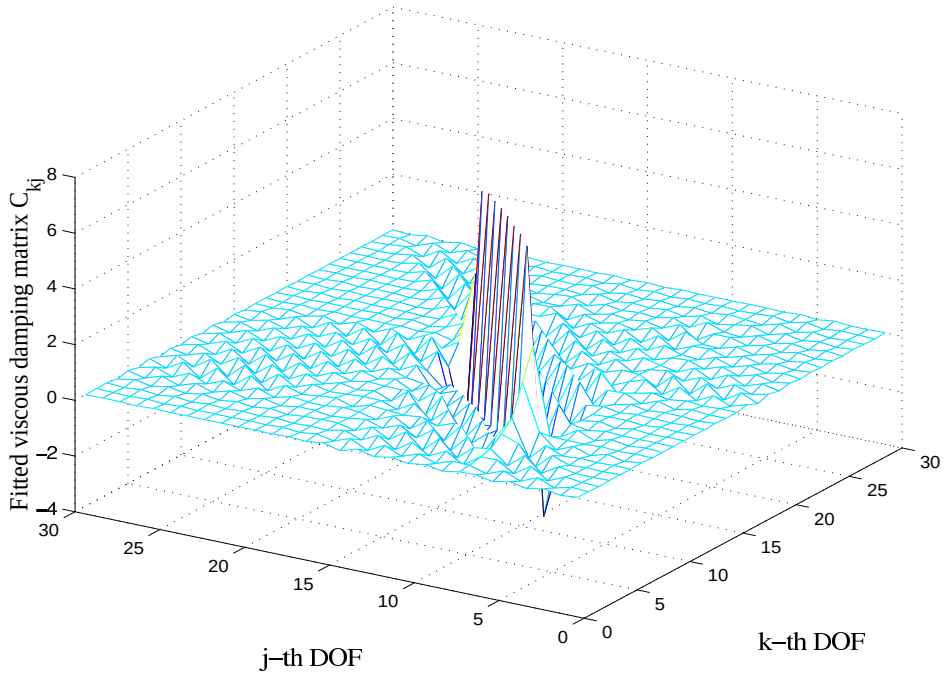

Figure 5.10: Fitted viscous damping matrix for the non-local case, $\gamma = 0.5$, damping model 1

To judge the numerical accuracy of the fitted viscous damping it is useful to reconstruct transfer functions. It is easy to do this, by inverting the dynamic stiffness matrix using the fitted viscous damping matrix. A typical transfer function $H_{kj}(\omega)$, for $k = 11$ and $j = 24$ is shown in Figure 5.14, based on locally-reacting damping using damping model 1. It is clear that the reconstructed transfer function agrees well with the original one. This is to be expected: the fitting procedure

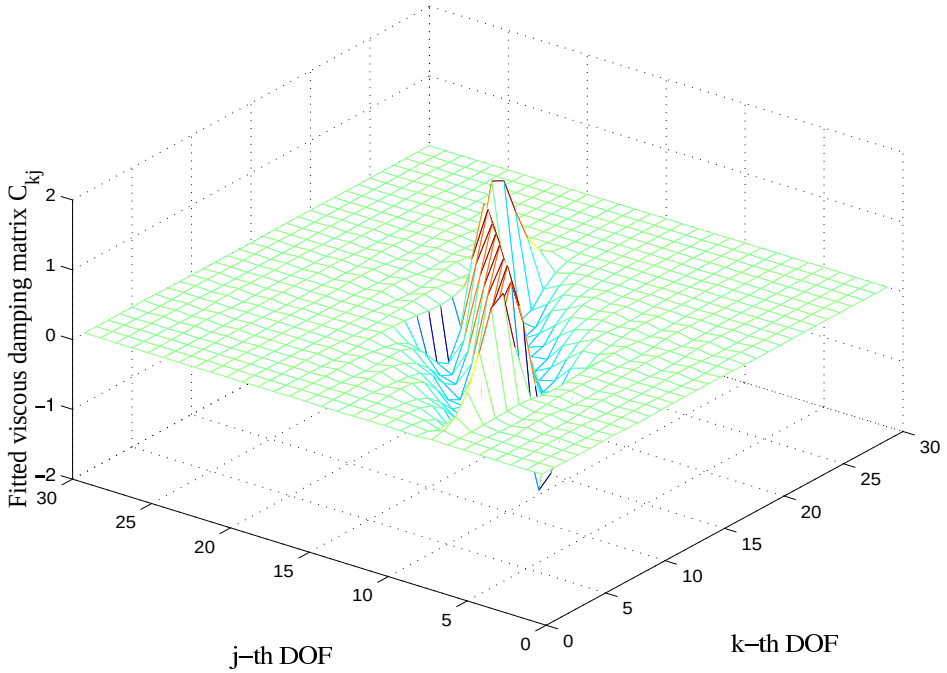

Figure 5.11: Fitted viscous damping matrix for the non-local case, $\gamma = 0.5$, damping model 2

outlined in the previous section is exact, within the the approximations of the small-damping perturbation theory, provided the full set of modes is used. The full set of poles and their residues are correctly reproduced — this is the essential contrast between this approach and one which fits only proportional damping, for which the poles can be correct but the residues cannot (because they will be real, not complex). This result has a far-reaching implication: an incorrect damping model (the fitted viscous damping) with a different spatial distribution from the true locally-reacting model can reproduce accurately the full set of transfer functions. This means that by measuring transfer functions it is not possible to identify uniquely the governing mechanism.

However, it should be noted that in all cases of Figures 5.7−5.11 the fitted damping matrix is not symmetric. This is, in some sense, a non-physical result. In view of this non-symmetry, it is interesting to check the reciprocity of the transfer functions. In Figure 5.14 the reciprocal transfer function $H_{jk}(\omega)$ is also plotted, as a dashed line. It is not visible as a separate line in the figure, because it matches $H_{kj}(\omega)$ to good accuracy. This plot demonstrates that the non-symmetry of the fitted viscous damping in the spatial coordinate does not necessarily affect the reciprocity of the transfer functions. Instead, we should regard non-symmetry of a fitted dissipation matrix as evidence that the true damping model is not viscous. To obtain a correct physical description of the damping, a non-viscous model should be fitted instead. This idea is developed in Chapter 6.

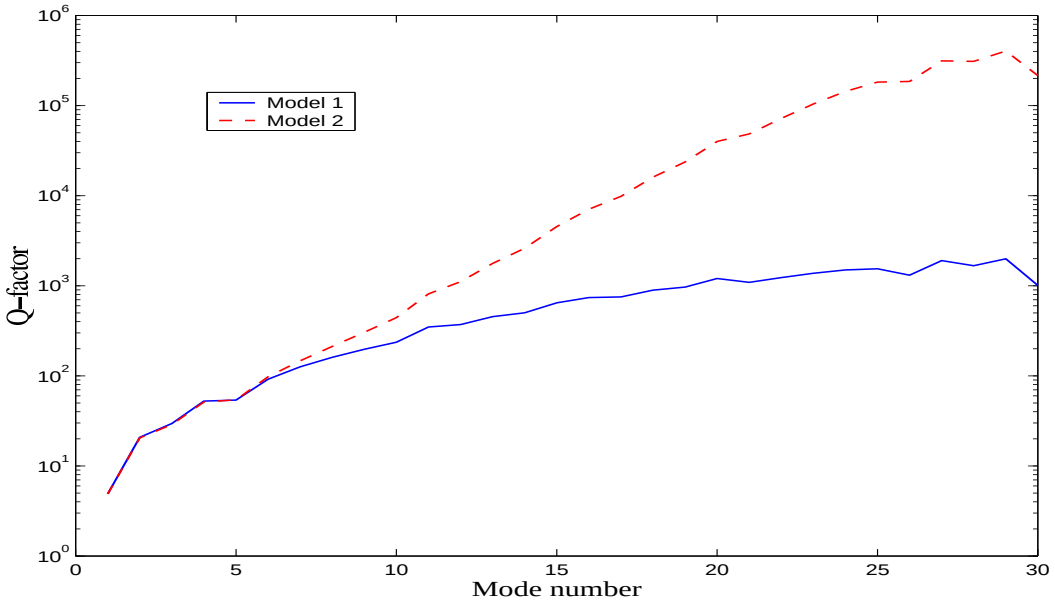

Figure 5.12: Modal Q-factors for the local case, $\gamma = 0.5$

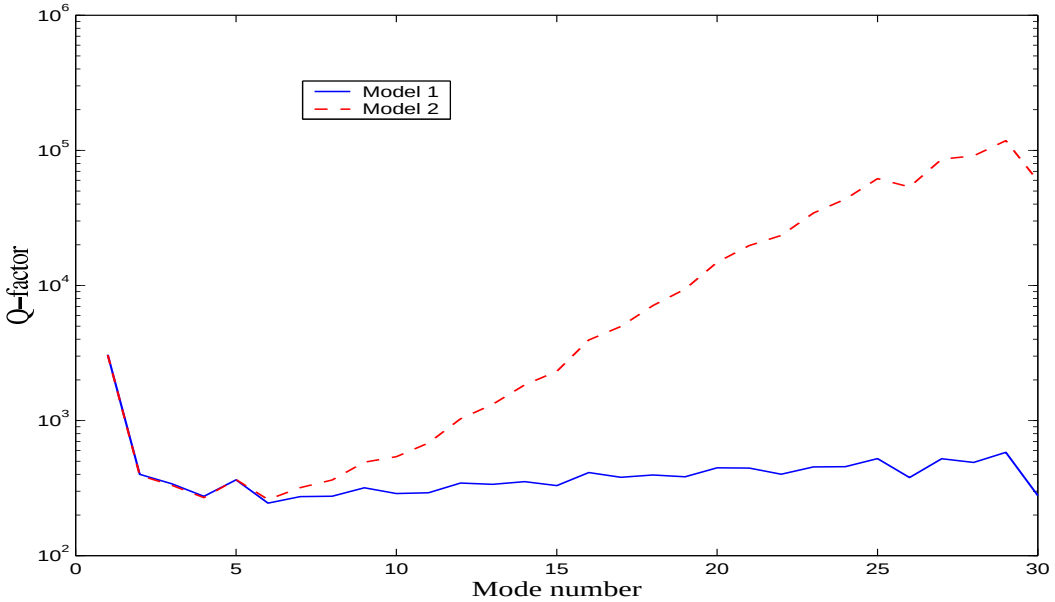

Figure 5.13: Modal Q-factors for the non-local case, $\gamma = 0.5$

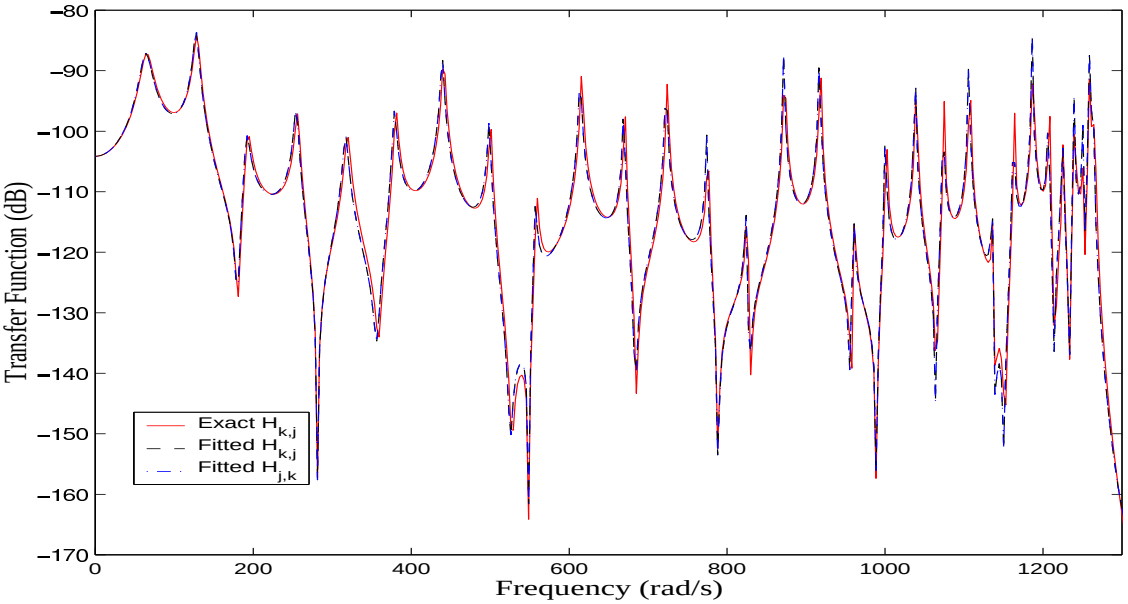

Figure 5.14: Transfer functions for the local case, $\gamma = 0.5$, damping model 1, $k = 11$, $j = 24$

5.5 Conclusions

In this chapter a method has been proposed to identify a non-proportional viscous damping matrix in vibrating systems. It is assumed that damping is light so that the first order perturbation method is applicable. The method is simple, direct, and compatible with conventional modal testing procedures. The complex modes and natural frequencies are used, but the method does not require either the full set of modal data, or any knowledge of the mass and stiffness matrices. The validity of the proposed method has been explored by applying it to simulated data from a simple test problem, in which a linear array of spring-mass oscillators is damped by non-viscous elements over part of its length.

Numerical experiments have been carried out with a wide range of parameter values and different damping models. The main features of the results have been illustrated by two particular damping models and representative parameter values. It has been shown that the method generally predicts the spatial location of the damping with good accuracy, and also gives a good indication of whether the damping is locally-reacting or not. Whatever the nature of the fitted damping matrix **C**, the transfer functions obtained from the fitted viscous damping agree well with the exact transfer functions of the simulated system. Reciprocity of the transfer functions remains preserved within an acceptable accuracy although in some cases the fitted viscous damping **C** is not symmetric.

Symmetry breaking of the fitted viscous damping matrix **C** depends on the value of the characteristic time constants θ of the damping model, defined by equation (5.19). When θ is short compared with the natural periods of the vibration, the damping is effectively viscous and the fitting procedure gives a physically-sensible symmetric matrix. When θ is larger, though, the memory of the damping function influences the detailed behaviour. Although the poles and residues of the

transfer functions can still be fitted accurately with a model of viscous form, the underlying non-viscous behaviour manifests itself in a non-symmetrical matrix. If a correct physical description of the damping mechanism is needed, then a suitable non-viscous model must be selected and fitted. We take up this question in Chapter 6.

Chapter 6

Identification of Non-viscous Damping

6.1 Introduction

Linear systems must generally be expected to exhibit non-viscous damping. In the last chapter it was shown that when a system is non-viscously damped, it is possible to fit a viscous damping model to the set of measured transfer functions but that the fitted damping matrix will be non-symmetrical. The fitted model may also be misleading in other ways: for example it may predict the wrong spatial distribution of damping over the structure. Of course, *a priori* selection of viscous damping in the identification procedure rules out any possibility of recognizing other damping behaviour present in the structure. In this chapter we consider the identification of certain non-viscous damping models in the context of general multiple degrees-of-freedom linear systems.

A key issue in identifying non-viscous damping is to decide on an appropriate damping model to consider. A brief review on available damping models may be found in Section 1.2. There have been detailed studies of material damping and of specific structural components. Lazan (1968), Bert (1973) and Ungar (1973) have given excellent accounts of different mathematical methods for modelling damping in (solid) material and their engineering applications. The book by Nashif *et al.* (1985) presents more recent studies in this area. Other than material damping a major source of energy dissipation in a vibrating structure is the structural joints. Here, energy loss can take place through air-pumping and local frictional effects. The air-pumping phenomenon is associated with air trapped in pockets in the vicinity of a vibrating surface. In these situations, the air is squeezed in and out through any available gap, leading to viscous dissipation of energy. Damping behaviour associated with joints has been studied by many authors. For example Earls (1966) has obtained the energy dissipation in a lap joint over a cycle under different clamping pressure. Beards and Williams (1977) have noted that significant damping can be obtained by suitably choosing the fastening pressure to allow some interfacial slip in joints. In many cases these damping mechanisms turn out be locally non-linear, requiring an equivalent linearization technique for a global analysis (Bandstra, 1983). These studies provide useful physical insights into damping mechanisms, but due to their very specific nature it is not possible to formulate a general procedure for identification of such mechanisms by simple vibration measurement.

In Section 1.6 it was pointed out that methodologies of identification of non-viscous damping in the context of general MDOF systems is not well developed. Banks and Inman (1991) have proposed a somewhat general approach for identification of non-viscous damping models in Euler-Bernoulli beams. They have considered four different models of damping: viscous air damping, Kelvin-Voigt damping, time hysteresis damping and spatial hysteresis damping, and used a spline inverse procedure to form a least-square fit to the experimental data. It was observed that the spatial hysteresis model combined with a viscous air damping model gave the best quantitative agreement with the experimental time histories. A procedure for obtaining hysteretic damping parameters in free-hanging pipe systems is given by Fang and Lyons (1994). Assuming material damping to be the only source of damping they have given a theoretical expression for the loss factor of the n-th mode. The system-specific nature of these methods means that they cannot be extended in a simple way to more general multiple degrees-of-freedom systems.

In Section 1.2.3 it was mentioned that convolution integral models are most general class of linear non-viscous damping models in the context of multiple degrees-of-freedom systems. In Chapter 3 it was shown that such damping models can be handled in a very similar way to viscous models. These results motivate us to develop procedures for identification this type of general damping models from standard vibration testing data. A wide variety of mathematical expressions, as shown in Table 1.1, could be used for the kernel functions. Of these, the exponential function seems a particularly promising candidate. Cremer and Heckl (1973) have written 'Of the many after-effect functions that are possible in principle, only one — the so-called relaxation function — is physically meaningful.' They go on to give a physical justification for this model, by which they mean the exponential case. The argument applies most convincingly to the case of material damping, rather than joint damping. An alternative mathematical rationalization can be given in terms of exponential contributions from the poles of frequency-response functions when the Fourier transform is inverted (see Muravyov, 1997). With this motivation, we concentrate here on fitting exponential damping models to vibration data.

The analysis in this chapter is restricted to linear system behaviour and it is assumed that the damping is light. In Section 6.2 we outline the expressions of complex frequencies and modes based on the first-order perturbation method when the system is non-viscously damped. Using these perturbation results, a method for identification of non-viscous damping models using complex modes and natural frequencies is proposed. We assume that the mass matrix of the structure is known — either directly from a finite element model or by means of modal updating based on experimental measurements. Having the mass matrix we try to identify an exponential damping model consistent with the measured complex modes. In Section 6.3 a procedure to obtain the *relaxation parameter* of an exponential damping model is outlined. Identification of the associated *damping coefficient matrix* is discussed in Section 6.5. The proposed method is illustrated using simulated numerical examples directly comparable to those in the last chapter. Finally Section 6.6 summarizes the main findings of this chapter.

6.2 Background of Complex Modes

Dynamics of non-viscously damped systems has been discussed in details in Chapter 3. As mentioned earlier, only elastic modes will be considered because non-viscous modes are not measurable within the scope of traditional modal analysis. Thus, in the context of non-viscously damped systems 'complex modes' implies complex elastic modes. Expressions of complex modes can be obtained from the analysis presented in Section 3.2.1. One special case of this general analysis in considered in Section 3.2.3 when the damping is lightly non-proportional. In this section we consider a further special case when the damping is light so that the first-order perturbation method can be applied. First-order perturbation results can be obtained from the results in Section 3.2.3 as follows.

Suppose $\lambda_j, \mathbf{z}_j$ is j-th complex natural frequency and and complex mode shape. In the context of the notations used in Section 3.2.3, $s_j = \mathrm{i}\lambda_j$. Using this, from equation (3.33) approximate expression for the complex natural frequencies can be obtained as

$$\lambda_j \approx \pm\omega_j + \mathrm{i}G'_{jj}(\pm\omega_j)/2 \tag{6.1}$$

where $G'_{kl}(\omega_j) = \mathbf{x}_k^T \mathbf{G}(\omega_j)\mathbf{x}_l$ is the frequency dependent damping matrix expressed in normal coordinates and $\mathbf{G}(\omega)$ is the Fourier transform of the matrix of kernel functions $\boldsymbol{\mathcal{G}}(t)$. Since the inverse Fourier transform of $\mathbf{G}(\omega)$ must be real it must satisfy the condition $\mathbf{G}(-\omega) = \mathbf{G}(\omega)^*$, where $(\bullet)^*$ denotes complex conjugation. It follows that the eigenvalues of the generally damped system appear in pairs λ and $-\lambda^*$ (unless λ is purely imaginary). The first-order approximate expression for the complex eigenvectors can be obtained as a special case of equation (3.35). The result is

$$\mathbf{z}_j \approx \mathbf{x}_j + \mathrm{i}\sum_{\substack{k=1 \\ k\neq j}}^{N} \frac{\omega_j G'_{kj}(\omega_j)}{(\omega_j^2 - \omega_k^2)}\mathbf{x}_k. \tag{6.2}$$

Equations (6.1) and (6.2) were first obtained by Woodhouse (1998). Note that the eigenvectors also appear in complex conjugate pairs. Since in general $G'_{kj}(\omega_j)$ will be complex, in contrast to the viscously damped case the real part of complex natural frequencies and complex mode shapes do not coincide with the undamped ones. This fact will complicate the problem of fitting model parameters to experimental complex modes.

It is natural to consider first the idealized problem in which just one relaxation function is used for identification purposes. In that case the general form of the kernel function in equation (3.1) reduces to

$$\boldsymbol{\mathcal{G}}(t) = \mathbf{C}\, g(t) \tag{6.3}$$

where $g(t)$ is some damping function and $\mathbf{C}$ is a positive-definite coefficient matrix. The admissible form of $g(t)$ is restricted by the condition of non-negative energy loss given in equation (1.33). The damping model in equation (6.3) is physically realistic if the real part of the Fourier transform of the kernel function is non-negative within the driving frequency range, that is $\Re[G(\omega)] \geq 0, \forall\, \omega$.

This can be easily shown. Rewriting equation (1.33) in the frequency domain and using (6.3), the rate of energy dissipation can be expressed as

$$F(\omega) = \frac{\omega^2}{2} \Re \left\{ \bar{\mathbf{q}}^{*^T} \mathbf{C}\, \bar{\mathbf{q}} G(\omega) \right\} \tag{6.4}$$

where $\Re(\bullet)$ represents the real part of $(\bullet)$ and $F(\omega)$, $\bar{\mathbf{q}}$ and $G(\omega)$ are the Fourier transform of $\mathcal{F}(t)$, $\mathbf{q}(t)$ and $g(t)$ respectively. For a physically realistic model of damping we must have

$$\begin{aligned} & F(\omega) \geq 0 \\ \text{or} \quad & \frac{\omega^2}{2} \Re \left\{ \bar{\mathbf{q}}^{*^T} \mathbf{C}\, \bar{\mathbf{q}} G(\omega) \right\} \geq 0 \\ \text{or} \quad & \Re \left\{ G(\omega) \right\} \geq 0 \end{aligned} \tag{6.5}$$

since for a real value of driving frequency $\omega^2 \geq 0$ and $\bar{\mathbf{q}}$ can be chosen in a way that $\Re \left\{ \bar{\mathbf{q}}^{*^T} \mathbf{C}\, \bar{\mathbf{q}} \right\} \geq 0$ as $\mathbf{C}$ is positive definite.

6.3 Fitting of the Relaxation Parameter

As has been mentioned earlier, from the wide range of non-viscous damping models the exponential function seems a particularly good candidate. It satisfies the condition (6.5) at all frequencies. In this section we outline a general method to fit the relaxation parameter of an exponential damping model using measured modal data.

6.3.1 Theory

We assume that the damping has only one relaxation function, so that the matrix of kernel functions is of the form

$$\boldsymbol{\mathcal{G}}(t) = \mu e^{-\mu t}\, \mathbf{C} \tag{6.6}$$

where μ is the relaxation parameter and $\mathbf{C}$ is the associated coefficient matrix. The factor μ serves to normalize the kernel function: see Section 6.3.2. Complex natural frequencies and mode shapes for systems with this kind of damping can be obtained from equations (6.1) and (6.2). In view of the expression for damping given in equation (6.6) it is easy to see that the term $G'_{kj}(\omega_j)$ appearing in these equations can be expressed as

$$G'_{kj}(\omega_j) = \frac{\mu}{\mu + \mathrm{i}\omega_j} C'_{kj} = \left[\frac{\mu^2}{\mu^2 + \omega_j^2} - \mathrm{i} \frac{\mu \omega_j}{\mu^2 + \omega_j^2} \right] C'_{kj} \tag{6.7}$$

where $C'_{kj} = \mathbf{x}_k^T \mathbf{C} \mathbf{x}_j$. Using this expression in equation (6.1), the j-th complex natural frequency is given by

$$\lambda_j \approx \omega_j + \mathrm{i} \frac{C'_{jj}}{2} \left[\frac{\mu^2}{\mu^2 + \omega_j^2} - \mathrm{i} \frac{\mu \omega_j}{\mu^2 + \omega_j^2} \right]. \tag{6.8}$$

Similarly from equation (6.2) the j-th complex mode can be expressed as

$$\mathbf{z}_j \approx \mathbf{x}_j + \sum_{\substack{k=1 \\ k\neq j}}^{N} \frac{\mu\omega_j}{(\mu^2+\omega_j^2)} \frac{\omega_j C'_{kj}}{(\omega_j^2-\omega_k^2)} \mathbf{x}_k + \mathrm{i} \sum_{\substack{k=1 \\ k\neq j}}^{N} \frac{\mu^2}{(\mu^2+\omega_j^2)} \frac{\omega_j C'_{kj}}{(\omega_j^2-\omega_k^2)} \mathbf{x}_k. \tag{6.9}$$

Suppose that $\hat{\lambda}_j$ and $\hat{\mathbf{z}}_j$ for $j = 1, 2, \cdots m$ are the *measured* complex natural frequencies and modes. Write

$$\hat{\mathbf{z}}_j = \hat{\mathbf{u}}_j + \mathrm{i}\hat{\mathbf{v}}_j. \tag{6.10}$$

Here $\hat{\mathbf{z}}_j \in \mathbb{C}^N$ where N denotes the number of measurement points on the structure and the number of modes considered in the study is m. In general $m \neq N$, usually $N \geq m$. Assume that $\hat{\mathbf{x}}_j \in \mathbb{R}^N$ are the *undamped modes* and $\hat{\mu}$ is the relaxation parameter to be estimated from the experiment. In order to fit a damping model of the form (6.6), equations (6.8) and (6.9) must be valid in conjunction with the experimental measurements $\hat{\lambda}_j$ and $\hat{\mathbf{z}}_j$. As an initial approximation we may suppose the real part of the complex natural frequencies to be the same as the undamped natural frequencies:

$$\hat{\omega}_j^{(0)} = \Re\left(\hat{\lambda}_j\right). \tag{6.11}$$

For most practical cases it turns out that the above value of $\hat{\omega}_j^{(0)}$ is sufficiently accurate to carry out further analysis. However, we present later an iterative method which may be used to update the value of $\hat{\omega}_j$ and remove the need for this approximation (see Section 6.5.2 for details).

In view of equations (6.9) and (6.10) and considering that only m modes are measured, separating real and imaginary parts of $\hat{\mathbf{u}}_j$ gives

$$\hat{\mathbf{u}}_j = \Re(\hat{\mathbf{z}}_j) \approx \hat{\mathbf{x}}_j + \sum_{\substack{k=1 \\ k\neq j}}^{m} \widetilde{A}_{kj}\hat{\mathbf{x}}_k; \quad \text{where} \quad \widetilde{A}_{kj} = \frac{\hat{\mu}\hat{\omega}_j}{(\hat{\mu}^2+\hat{\omega}_j^2)} B_{kj} \tag{6.12}$$

and

$$\hat{\mathbf{v}}_j = \Im(\hat{\mathbf{z}}_j) \approx \sum_{\substack{k=1 \\ k\neq j}}^{m} \widetilde{B}_{kj}\hat{\mathbf{x}}_k; \quad \text{where} \quad \widetilde{B}_{kj} = \frac{\hat{\mu}^2}{(\hat{\mu}^2+\hat{\omega}_j^2)} B_{kj}. \tag{6.13}$$

Here the unknown constants B_{kj} are defined as

$$B_{kj} = \frac{\hat{\omega}_j C'_{kj}}{\hat{\omega}_j^2 - \hat{\omega}_k^2}. \tag{6.14}$$

It may be noted that in addition to B_{kj}, the relaxation constant $\hat{\mu}$ and the undamped modes $\hat{\mathbf{x}}_k$ are also unknown. Combining equations (6.12) and (6.13) one can write

$$\hat{\mathbf{u}}_j = \hat{\mathbf{x}}_j + \frac{\hat{\omega}_j}{\hat{\mu}}\hat{\mathbf{v}}_j. \tag{6.15}$$

From the preceding equation it is clear that if $\hat{\mu} \gg \hat{\omega}_j$, then $\hat{\mathbf{u}}_j \to \hat{\mathbf{x}}_j$. This implies that when the damping mechanism is near to viscous, the real part of each complex mode tends towards

the corresponding undamped mode. Since the undamped modes are orthonormal with respect to the mass matrix, from equation (6.13) it may be observed that the imaginary part of each complex mode $\hat{\mathbf{v}}_j$ is M-orthogonal to its corresponding undamped mode so that $\hat{\mathbf{v}}_j^T\mathbf{M}\hat{\mathbf{x}}_j = 0$. Premultiplying equation (6.15) by $\hat{\mathbf{v}}_j^T\mathbf{M}$ one can write

$$\hat{\mathbf{v}}_j^T\mathbf{M}\hat{\mathbf{u}}_j = \hat{\mathbf{v}}_j^T\mathbf{M}\hat{\mathbf{x}}_j + \frac{\hat{\omega}_j}{\hat{\mu}}\hat{\mathbf{v}}_j^T\mathbf{M}\hat{\mathbf{v}}_j \tag{6.16}$$

Now use of the orthogonality property of $\hat{\mathbf{v}}_j$ and $\hat{\mathbf{x}}_j$ leads to

$$\hat{\mu}_j = \frac{\hat{\omega}_j\hat{\mathbf{v}}_j^T\mathbf{M}\hat{\mathbf{v}}_j}{\hat{\mathbf{v}}_j^T\mathbf{M}\hat{\mathbf{u}}_j}. \tag{6.17}$$

We have used the notation $\hat{\mu}_j$ because for different choices of j on the right hand side one will in general obtain different values of $\hat{\mu}$. If in practice one obtained very similar values, this would confirm the initial assumption that the actual system has only one relaxation time. On the other hand, if significantly different values are obtained it would indicate that the assumed model needs to be extended. We show shortly that the pattern of variation of $\hat{\mu}_j$ can give some clues about the true underlying model. If one wished to choose a single value of $\hat{\mu}$ to best represent a range of values found by this procedure, one could consider several alternatives:

1. Simply *select* a value of j, say $j = k \leq m$, to obtain $\hat{\mu}$. For this choice

$$\hat{\mu} = \frac{\hat{\omega}_k\hat{\mathbf{v}}_k^T\mathbf{M}\hat{\mathbf{v}}_k}{\hat{\mathbf{v}}_k^T\mathbf{M}\hat{\mathbf{u}}_k}. \tag{6.18}$$

   How to select the value of k will be discussed in the next subsection.

2. Average the realizations of $\hat{\mu}$. For this choice

$$\hat{\mu} = \frac{1}{m_\mu}\sum_{j=1}^{m_\mu}\frac{\hat{\omega}_j\hat{\mathbf{v}}_j^T\mathbf{M}\hat{\mathbf{v}}_j}{\hat{\mathbf{v}}_j^T\mathbf{M}\hat{\mathbf{u}}_j}. \tag{6.19}$$

   where $m_\mu \leq m$ are the number of terms to be retained.

3. Sum the numerator and denominator separately and take their ratio to obtain $\hat{\mu}$. For this choice

$$\hat{\mu} = \frac{\sum_{j=1}^{m_\mu}\hat{\omega}_j\hat{\mathbf{v}}_j^T\mathbf{M}\hat{\mathbf{v}}_j}{\sum_{j=1}^{m_\mu}\hat{\mathbf{v}}_j^T\mathbf{M}\hat{\mathbf{u}}_j}. \tag{6.20}$$

We can best illustrate via a numerical example.

6.3.2 Simulation Method

Numerical studies have been carried out using simulated systems identical to those used in Chapter 5. Figure 6.1 shows the model systems together with the numerical values used. For these parameter values the resulting undamped natural frequencies range from near zero to approximately 200

Hz. The damping elements are associated with masses between the s-th and $(s+l)$-th ($N = 30$, $s = 8$ and $(s+l) = 17$ are taken for the numerical calculations). For the system shown in Figure 6.1(a) the damping force depends only on the absolute motion of the individual masses. Such damping will be described as 'locally reacting'. For the system shown in Figure 6.1(b), by contrast, dissipative elements are connected between certain adjacent pairs of masses. In this case the damping force depends on the relative motion of the two adjacent masses, and will be called 'non-locally reacting'. In the previous chapter, a viscous damping matrix was calculated from the complex modes and frequencies of these systems. Here we seek to identify the parameters of an exponential damping model using the same modal data.

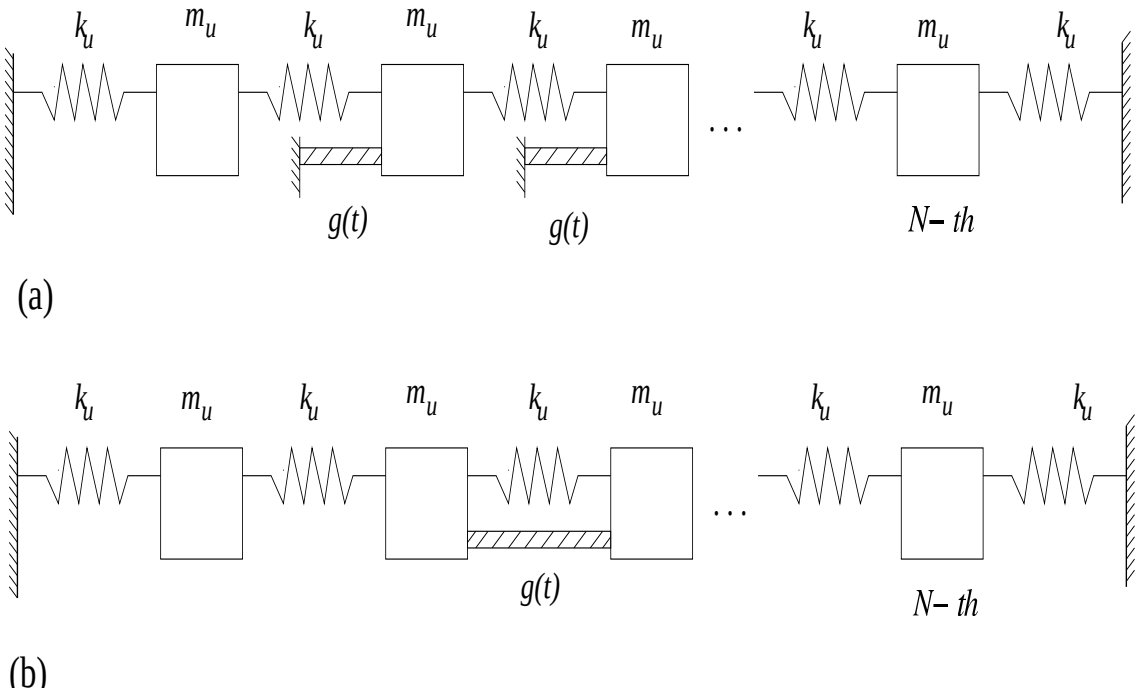

Figure 6.1: Linear array of N spring-mass oscillators, $N = 30$, $m_u = 1\,Kg$, $k_u = 4 \times 10^3 N/m$.

The dissipative elements shown in Figure 6.1 are taken to be linear non-viscous dampers so that the equations of motion are described by (5.16). Three damping models, two of which were considered in 5, are used: one with an exponential kernel function as assumed in the model being fitted, and two others with different functions to probe the limitations of the fitting procedure. They are determined by three different forms of $g(t)$ (defined in equation (6.3)):

- MODEL 1 (exponential):

$$g^{(1)}(t) = \mu_1 e^{-\mu_1 t} \tag{6.21}$$

- MODEL 2 (Gaussian):

$$g^{(2)}(t) = 2\sqrt{\frac{\mu_2}{\pi}} e^{-\mu_2 t^2} \tag{6.22}$$

- MODEL 3 (double exponential or GHM):

$$g^{(3)}(t) = \frac{\beta_1 \mu_3 e^{-\mu_3 t} + \beta_2 \mu_4 e^{-\mu_4 t}}{\beta_1 + \beta_2} \tag{6.23}$$

All the three damping models are normalized such that the damping functions have unit area when integrated to infinity, *i.e.*,

$$\int_0^\infty g^{(j)}(t)\,\mathrm{d}t = 1. \tag{6.24}$$

This will make them directly comparable with the viscous model, in which the corresponding damping function would be a unit delta function, $g(t) = \delta(t)$, and the coefficient matrix $\mathbf{C}$ would be the usual dissipation matrix. For each damping function a *characteristic time constant* can be defined via the first moment of $g^{(j)}(t)$:

$$\theta^{(j)} = \int_0^\infty t\, g^{(j)}(t)\,\mathrm{d}t. \tag{6.25}$$

For the three damping models considered here, evaluating this integral gives

$$\theta^{(1)} = \frac{1}{\mu_1} \tag{6.26}$$

$$\theta^{(2)} = \frac{1}{\sqrt{\pi \mu_2}} \tag{6.27}$$

$$\theta^{(3)} = \frac{\beta_1/\mu_3 + \beta_2/\mu_4}{\beta_1 + \beta_2}. \tag{6.28}$$

Note that for viscous damping $\theta = 0$. The characteristic time constant of a damping function gives a convenient measure of 'width': if it is close to zero the damping behaviour will be near-viscous, and vice versa. For comparability between the three damping models we take them all to have the same time constant.

Complex natural frequencies and modes of the systems are calculated using equations (6.1) and (6.2), then these are treated as if they were experimental data obtained from a modal testing procedure. The procedures described above can be applied to identify the relaxation parameter of an exponential damping model. We present results of the fitting procedure for both small and large values of the characteristic time constant, expressed in non-dimensional form as given by equation (5.20). When γ is small compared with unity the damping behaviour can be expected to be essentially viscous, but when γ is of order unity or bigger non-viscous effects are likely to be significant.

6.3.3 Numerical Results

Results for Small γ

We consider first $\gamma = 0.02$, so that damping models show near-viscous behaviour. Since the viscous model is a special case of the exponential model we might expect good fit quality in this

case. For the system shown in Figure 6.1(a) with locally reacting damping, Figure 6.2 shows the values of $\hat{\gamma}$ obtained from $\hat{\mu}$ (recall that $\hat{\gamma} = \frac{1}{T_{min}\hat{\mu}}$) for all $j = 1, \cdots, 30$ for Gaussian damping (model 2). In the same Figure the values of $\hat{\gamma}$ corresponding to equations (6.19) and (6.20) using $m_\mu = 30$ are also shown. Because the damping mechanism is near to viscous the fitted values of $\hat{\gamma}$ are quite small, and in fact agree well with the assumed $\gamma = 0.02$ for all values of j. To obtain a single 'best' value any one of the three relationships in equations (6.18) – (6.20) could be used. Similar features were observed (results not shown) when the fitting procedure was repeated for the non-locally damped case shown in Figure 6.1(b).

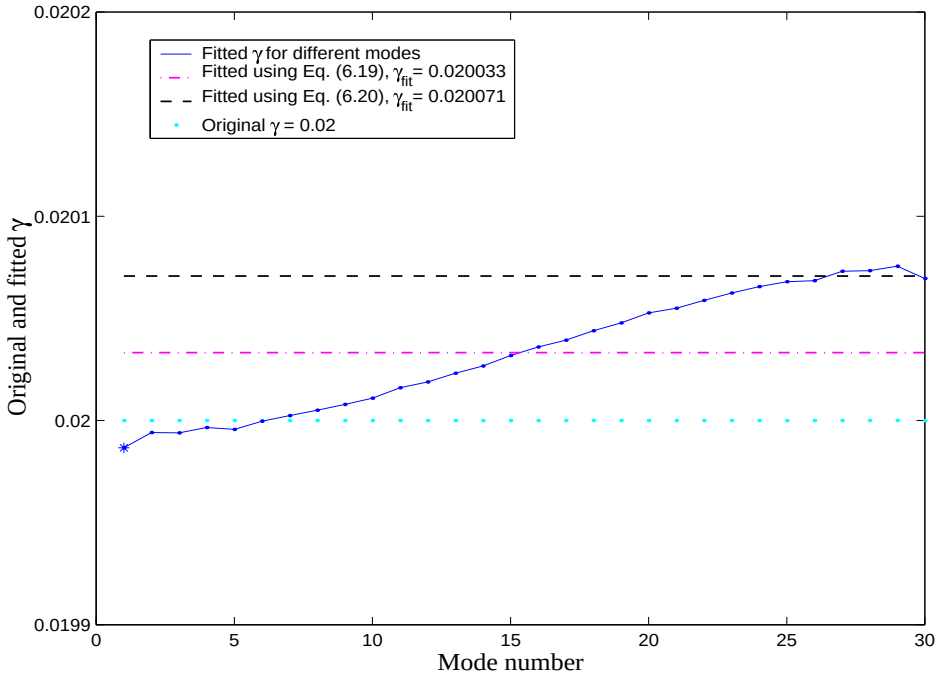

Figure 6.2: Values of $\hat{\gamma}$ obtained from different $\hat{\mu}$ calculated using equations (6.18)–(6.20) for the local case, damping model 2

Now we turn our attention to the systems with double exponential damping model (model 3). It is supposed that the two exponential functions combine to give a value $\gamma = 0.02$. In this case we consider $\beta_1 = 0.5, \gamma_3 = 0.01$ and $\beta_2 = 0.5, \gamma_4 = 0.03$. Values of $\hat{\gamma}$ obtained for different modes for the locally reacting case with this damping model is shown in Figure 6.3. In the same figure we also show the values of $\hat{\gamma}$ corresponding to equation (6.19) and (6.20). Again, as in the case of damping model 2 discussed above, the fitted values of $\hat{\gamma}$ are all very close to the correct value $\gamma = 0.02$. The only difference from the previous case is that values now decrease slightly with j rather than increasing. Similar features were observed (results not shown) when the fitting procedure is extended to non-locally damped systems with damping model 3. We conclude that, when the damping is near to viscous, regardless of the functional form or damping type, the fitting procedure gives a good estimate of the damping time constant and that any one of the relationship in equations (6.18) – (6.20) may be used to obtain the 'best' relaxation parameter.

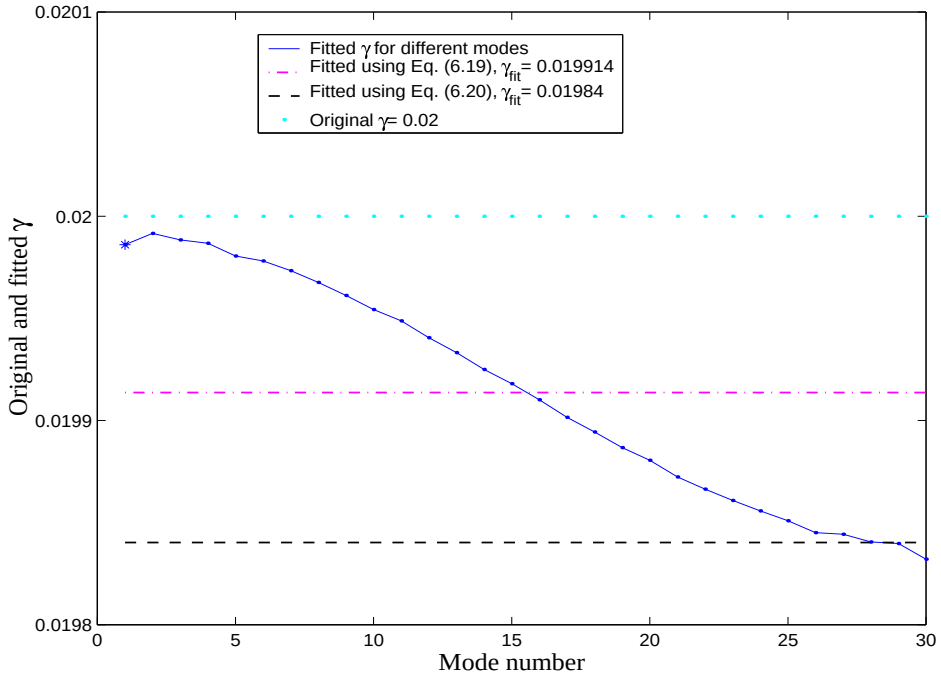

Figure 6.3: Values of $\hat{\gamma}$ obtained from different $\hat{\mu}$ calculated using equations (6.18)–(6.20) for the local case, damping model 3

Results for Larger γ

When γ is larger the three damping models depart more strongly from the viscous damping model each in its own way. Also, model 1, which is used for fitting purpose, differ form the other two damping models. We show typical results for the case $\gamma = 0.5$. When the fitting procedure is run for damping model 1, the calculation correctly reproduces the assumed γ value for all modes because the model being fitted is precisely the one assumed by the theory. This confirms the accuracy of the computer coding, but nothing further is to be learnt from displaying the results. Figure 6.4 shows the values of $\hat{\gamma}$ obtained for each mode for damping model 2 applied to the locally reacting system. The value of $\hat{\gamma}$ now vary considerably with j. This indicate, of course, that the assumption of a single kernel is not correct for this system. As will be discussed shortly, the variation of $\hat{\gamma}$ with j gives some clue as to the correct form of the kernel function. Estimates of $\hat{\gamma}$ obtained from equations (6.19) and (6.20) using $m_\mu = 30$ are also shown in Figure 6.4. Both these estimates are higher than the value of γ used for simulation and also the estimate obtained using equation (6.19) is higher than that obtained using equation (6.20). Observe that the value of $\hat{\gamma}$ obtained using equation (6.18) with $k = 1$ (marked by a *) is very close to the value of the original γ used in the simulation. An explanation of this behaviour is given in Section 6.4. It is shown there that under rather general circumstances, a value of $\hat{\gamma}$ obtained from equation (6.18) with $k = 1$ is likely to be a good estimate of the correct characteristic time constant defined via the first moment as in equation (5.20). Results for the non-local case are shown in Figure 6.5. A similar trend is seen to that in Figure 6.4. In this figure also we observe that the value of $\hat{\gamma}$ obtained

from equation (6.18) with $k = 1$ (marked by a *) is very close to the value of the original γ while those obtained from equations (6.19) and (6.20) differ significantly from the original one. Also observe that estimates of $\hat{\gamma}$ obtained from the two former equations are higher than the simulated value for both the local and nonlocal systems. However, unlike the case of Figure 6.4, here the value of $\hat{\gamma}$ obtained from equation (6.19) is lower than that obtained using equation (6.20).

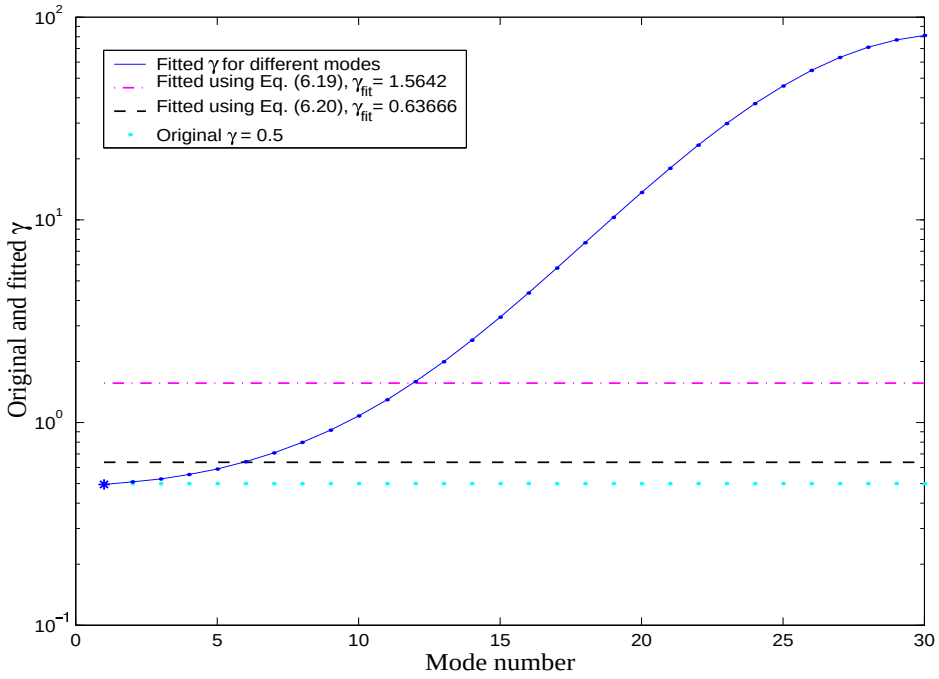

Figure 6.4: Values of $\hat{\gamma}$ obtained from different $\hat{\mu}$ calculated using equations (6.18)–(6.20) for the local case, damping model 2

Now consider damping model 3, consisting of two exponential functions. For the numerical values we take: $\beta_1 = 0.5, \gamma_3 = 0.2$ and $\beta_2 = 0.5, \gamma_4 = 0.8$. This results an equivalent γ for the model of 0.5, the same as for damping model 2 discussed above. Figure 6.6 shows the values of $\hat{\gamma}$ obtained for each mode for this damping model applied to the locally reacting system. This time $\hat{\gamma}$ decreases with j, in contrast to the Gaussian case. The range of variation is less dramatic, but still significant. Observe that, as with damping model 2, the value of $\hat{\gamma}$ obtained from equation (6.18) with $k = 1$ (marked by a *) is very close to the value of the original γ used in the simulation while that obtained from equations (6.19) and (6.20) differ significantly from the original one. However, unlike the case of damping model 2, here the estimates of $\hat{\gamma}$ obtained from the two former equations are lower than the simulated value. Behaviour analogous to this was also observed when the identification procedure is repeated for the nonlocally damped system.

6.4 Selecting the Value of $\hat{\mu}$

From equations (6.18) – (6.20) it is clear that different choices of j yield different values of $\hat{\mu}$, which contradicts our initial assumption that the system has only one relaxation time. Here it

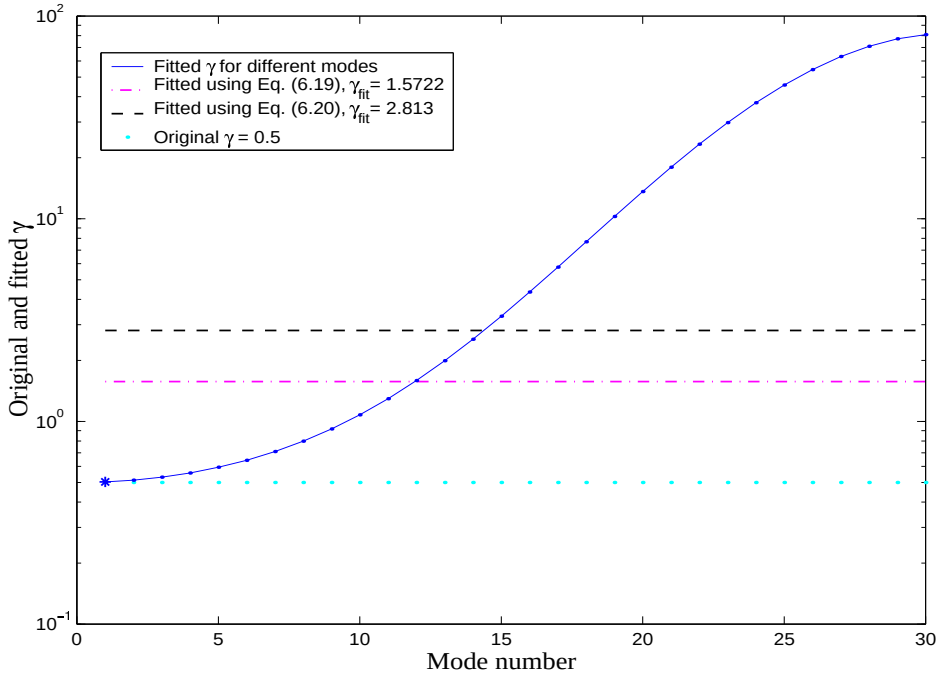

Figure 6.5: Values of $\hat{\gamma}$ obtained from different $\hat{\mu}$ calculated using equations (6.18)–(6.20) for the non-local case, damping model 2

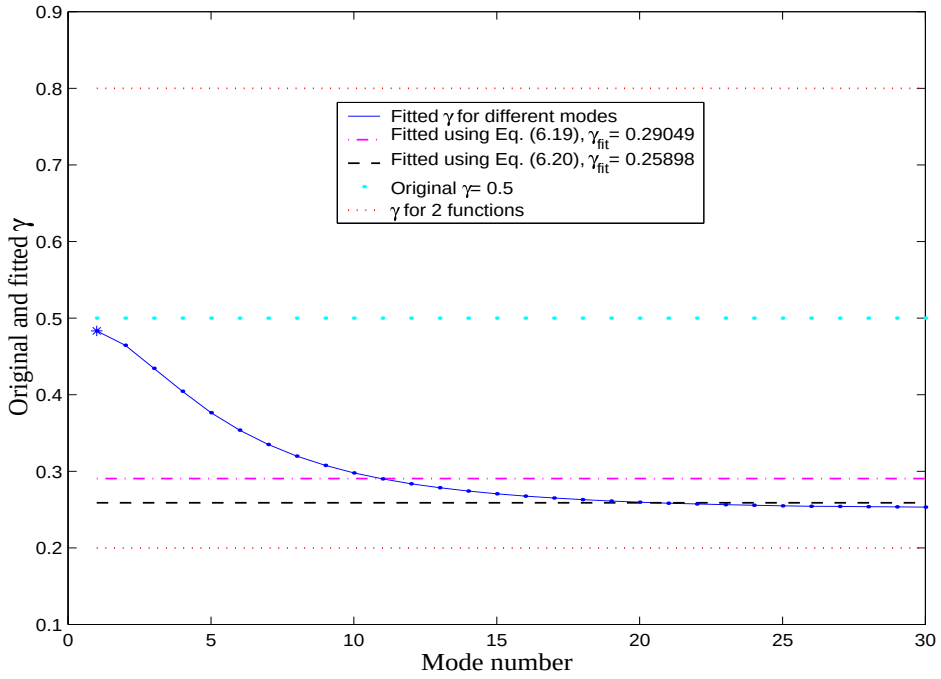

Figure 6.6: Values of $\hat{\gamma}$ obtained from different $\hat{\mu}$ calculated using equations (6.18)–(6.20) for the local case, damping model 3

will be shown that for systems with normalized damping functions similar to equations (6.21) and (6.22) the best estimate of $\hat{\mu}$ is given by equation (6.18) with $k = 1$.

Since the damping functions are normalized to have unit area when integrated to infinity they

can be written in the form

$$g(t) = \beta\, f(t); \quad \text{where} \quad \beta = \frac{1}{\int_0^\infty f(t)\mathrm{d}t}. \tag{6.29}$$

The characteristic time constant is obtained from equation (6.25) as

$$\theta = \frac{\int_0^\infty t\, f(t)\mathrm{d}t}{\int_0^\infty f(t)\mathrm{d}t}. \tag{6.30}$$

It is useful to express this result in the frequency domain. From the definition of the Fourier transform

$$F(\omega) = \int_0^\infty f(t)e^{-\mathrm{i}\omega t}\mathrm{d}t, \tag{6.31}$$

differentiating with respect to ω we have

$$F'(\omega) = \frac{\mathrm{d}F(\omega)}{\mathrm{d}\omega} = \int_0^\infty -\mathrm{i}t f(t)e^{-\mathrm{i}\omega t}\mathrm{d}t. \tag{6.32}$$

From equations (6.31) and (6.32) it is clear that

$$\begin{aligned} F(0) &= \int_0^\infty f(t)\mathrm{d}t \\ \text{and} \quad \mathrm{i}F'(0) &= \int_0^\infty t\, f(t)\mathrm{d}t \end{aligned} \tag{6.33}$$

so that from equation (6.30) the characteristic time constant may be represented as

$$\theta = \frac{\mathrm{i}F'(0)}{F(0)}. \tag{6.34}$$

Substituting $g(t)$ from (6.29) and taking the Fourier transform of equation (6.3) one obtains

$$\mathbf{G}(\omega) = \mathbf{C}\,\beta F(\omega) = \mathbf{C}\,\beta\,\left[F_R(\omega) + \mathrm{i}F_I(\omega)\right] \tag{6.35}$$

where

$$F(\omega) = F_R(\omega) + \mathrm{i}F_I(\omega) \tag{6.36}$$

where F_R and F_I are respectively the real and imaginary parts of F. Using this $\mathbf{G}(\omega)$ in the approximate expression for the complex modes in equation (6.2) and separating real and imaginary parts we have

$$\mathbf{u}_j = \Re(\mathbf{z}_j) \approx \mathbf{x}_j - \omega_j \beta F_I(\omega_j) \sum_{\substack{k=1 \\ k\neq j}}^{N} \frac{C'_{kj}}{(\omega_j^2 - \omega_k^2)}\mathbf{x}_k \tag{6.37}$$

and

$$\mathbf{v}_j = \Im(\mathbf{z}_j) \approx \omega_j \beta F_R(\omega_j) \sum_{\substack{k=1 \\ k\neq j}}^{m} \frac{C'_{kj}}{(\omega_j^2 - \omega_k^2)}\mathbf{x}_k. \tag{6.38}$$

From the above two equations it is easy to see that

$$\mathbf{u}_j = \mathbf{x}_j - \frac{F_I(\omega_j)}{F_R(\omega_j)}\mathbf{v}_j \tag{6.39}$$

It has been mentioned that $\hat{\mathbf{v}}_j$ is M-orthogonal to its corresponding undamped mode, *i.e.*, $\hat{\mathbf{v}}_j^T\mathbf{M}\hat{\mathbf{x}}_j = 0$. Using this relationship in equation (6.39) we have

$$\mathbf{v}_j^T\mathbf{M}\mathbf{u}_j = -\frac{F_I(\omega_j)}{F_R(\omega_j)}\mathbf{v}_j^T\mathbf{M}\mathbf{v}_j \quad \text{or} \quad \frac{\mathbf{v}_j^T\mathbf{M}\mathbf{u}_j}{\mathbf{v}_j^T\mathbf{M}\mathbf{v}_j} = -\frac{F_I(\omega_j)}{F_R(\omega_j)} \tag{6.40}$$

From this equation the expression for $\hat{\mu}$ may be rewritten as

$$\hat{\mu} = -\frac{\hat{\omega}_j F_R(\hat{\omega}_j)}{F_I(\hat{\omega}_j)}. \tag{6.41}$$

For the exponential function we have shown that the characteristic time constant $\theta = 1/\mu$. Thus using equation (6.34) one has

$$\mu = \frac{1}{\theta} = \frac{-\mathrm{i}F(0)}{F'(0)}. \tag{6.42}$$

This is an exact relationship. We now show why equation (6.41) is a good approximation to equation (6.42) when ω_j is small. Since $f(t)$ is a real function $F(\omega)$ can be expanded as a real polynomial in $(\mathrm{i}\omega)$. Thus

$$F(\omega) = F^{(0)} + (\mathrm{i}\omega)F^{(1)} + \frac{(\mathrm{i}\omega)^2}{2!}F^{(2)} + \cdots \tag{6.43}$$

where all $F^{(k)}$ are real. From this expansion we obtain

$$\begin{aligned} F(0) &= F^{(0)} \\ F'(0) &= \mathrm{i}F^{(1)} \end{aligned} \tag{6.44}$$

Now consider the case when ω is *small*. For this case the higher order terms in series (6.43) can be neglected to obtain

$$F(\omega) \approx F^{(0)} + \mathrm{i}\omega F^{(1)}. \tag{6.45}$$

Comparing above with equation (6.36) and in view of (6.44) one has

$$\begin{aligned} F_R(\omega) &\approx F(0) = F^{(0)} \\ \text{and} \quad F_I(\omega) &\approx \omega F^{(1)} = -\mathrm{i}\omega F'(0). \end{aligned} \tag{6.46}$$

Substituting in equation (6.42) we obtain

$$\mu \approx -\frac{\omega F_R(\omega)}{F_I(\omega)} \quad \text{when} \quad \omega \to 0. \tag{6.47}$$

This result is immediately comparable with the expression of $\hat{\mu}$ in (6.41). Observe that $\hat{\omega}_j$ is closest to zero when $j = 1$. For this reason the best estimate of $\hat{\mu}$ can be obtained by choosing $j = 1$ in (6.41). From equation (6.40) this in turn implies that

$$\hat{\mu} \approx -\frac{\hat{\omega}_1 F_R(\hat{\omega}_1)}{F_I(\hat{\omega}_1)} = \frac{\hat{\omega}_1 \hat{\mathbf{v}}_1^T\mathbf{M}\hat{\mathbf{v}}_1}{\hat{\mathbf{v}}_1^T\mathbf{M}\hat{\mathbf{u}}_1}. \tag{6.48}$$

6.4.1 Discussion

It should be noted that for all the cases in Figures 6.2, 6.4, 6.5 and Figures 6.3, 6.6 the values of $\hat{\gamma}$ evaluated for each mode show opposite trend: for system with damping model 2 the values of $\hat{\gamma}$ increases with increase of the mode number j whereas for system damping model 2 the values of $\hat{\gamma}$ decreases with increase of the mode number. This behaviour can give us further insight regarding the underlying damping function. Recall that after obtaining the complex modes and frequencies and having the mass matrix it is possible to obtain $\hat{\gamma}$ for different modes:

$$\hat{\gamma}_j = \frac{1}{T_{min}\hat{\mu}_j} \tag{6.49}$$

where $\hat{\mu}_j$ is given by equation (6.17). Because by equation (5.20) we know that $\hat{\gamma}_j$ is proportional to $\hat{\theta}_j$ it is sufficient if we understand the behaviour of the fitted $\hat{\theta}_j$. Using the expression of $\hat{\mu}_j$ in equation (6.41) one can express $\hat{\theta}_j$ as

$$\hat{\theta}_j = \frac{1}{\hat{\mu}_j} = -\frac{F_I(\hat{\omega}_j)}{\hat{\omega}_j F_R(\hat{\omega}_j)} \tag{6.50}$$

where F_R and F_I are respectively the real and imaginary parts of F, the Fourier transform of the (non-normalized) damping function $f(t)$ as defined in equation (6.29). Multiplying the numerator and denominator of equation (6.50) by the normalization constant β, the fitted $\hat{\theta}_j$ can be expressed in a more convenient form as

$$\hat{\theta}_j = -\frac{G_I(\hat{\omega}_j)}{\hat{\omega}_j G_R(\hat{\omega}_j)}. \tag{6.51}$$

Here $G(\omega)$, the Fourier transform of the normalized damping function $g(t)$, is defined as

$$G(\omega) = \int_0^\infty g(t) e^{-\mathrm{i}\omega t} \mathrm{d}t. \tag{6.52}$$

Expanding $e^{-\mathrm{i}\omega t}$ in the above expression gives

$$\begin{aligned} G(\omega) &= \int_0^\infty g(t) \left[1 - \mathrm{i}\omega t - \frac{\omega^2 t^2}{2!} + \frac{\mathrm{i}\omega^3 t^3}{3!} - \cdots\right] \mathrm{d}t \\ &= \mathcal{M}_0 - \mathrm{i}\omega\mathcal{M}_1 - \frac{\omega^2}{2}\mathcal{M}_2 + \frac{\mathrm{i}\omega^3}{6}\mathcal{M}_3 - \cdots \end{aligned} \tag{6.53}$$

where $\mathcal{M}_k$, the k-th moment of the damping function $g(t)$, is defined as

$$\mathcal{M}_k = \int_0^\infty t^k g(t) \mathrm{d}t; \quad k = 0, 1, 2, \cdots \tag{6.54}$$

For the three damping functions considered here in equations (6.21) – (6.22) the exact expressions for the k-th moment may be obtained as follows:

- MODEL 1:

$$\mathcal{M}_k = k!\, \mu_1^{-k}; \quad k = 0, 1, 2, \cdots \tag{6.55}$$

- MODEL 2:

$$\mathcal{M}_{2k} = \frac{(2k-1)!!}{2\mu_2^k}; \quad \mathcal{M}_{2k+1} = \frac{k!}{\sqrt{\pi}}\,\mu_2^{-(k+1/2)}; \qquad k = 0, 1, 2, \cdots \tag{6.56}$$

- MODEL 3:

$$\mathcal{M}_k = \frac{\beta_1\, k!\, \mu_3^{-k} + \beta_2\, k!\, \mu_4^{-k}}{\beta_1 + \beta_2}; \quad k = 0, 1, 2, \cdots \tag{6.57}$$

Clearly, for all the damping functions $\mathcal{M}_k > 0 \forall k$. In Figure 6.7 the first 6 moments of the three damping functions considered here are plotted when $\gamma = 0.5$. It is clear that although all $\mathcal{M}_k > 0$ their values approach zero as k increases. This ensures that omission of the higher order terms in equation (6.53) do not introduce much error for low values of ω. Now separating real and imaginary parts of $G(\omega)$ in equation (6.53) one has

$$\begin{aligned} G_R(\omega) &= \Re\left[G(\omega)\right] \approx \mathcal{M}_0 - \frac{\omega^2}{2}\mathcal{M}_2 \\ G_I(\omega) &= \Im\left[G(\omega)\right] \approx -\omega\mathcal{M}_1 + \frac{\omega^3}{6}\mathcal{M}_3. \end{aligned} \tag{6.58}$$

Using these relationships, from equation (6.51) the value of $\hat{\theta}$ at any frequency can be obtained as

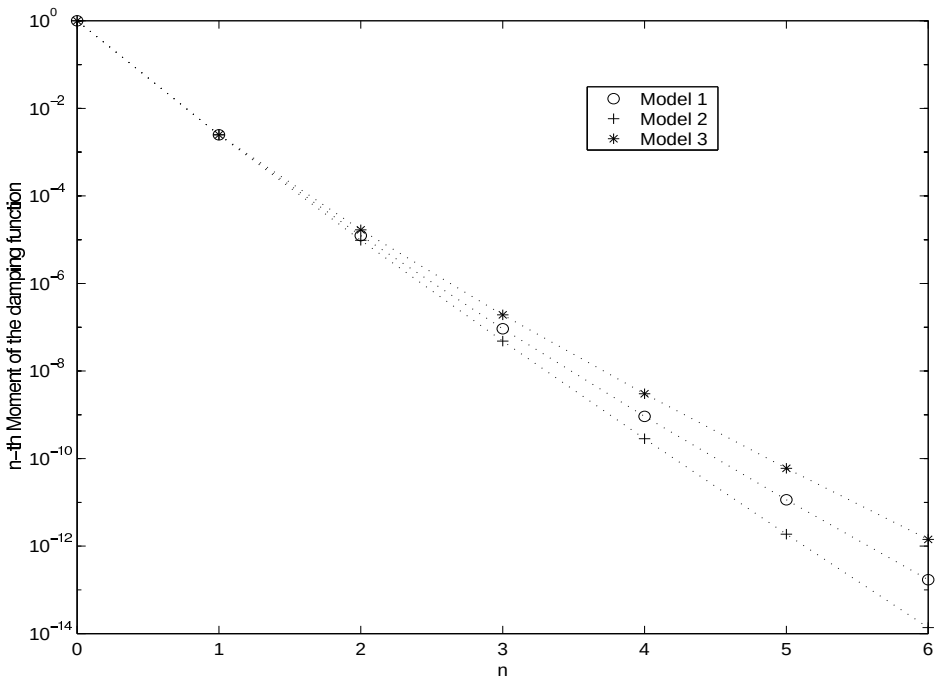

Figure 6.7: First six moments of the three damping functions for $\gamma = 0.5$

$$\hat{\theta}(\omega) \approx -\frac{-\omega\mathcal{M}_1 + \frac{\omega^3}{6}\mathcal{M}_3}{\omega\left(\mathcal{M}_0 - \frac{\omega^2}{2}\mathcal{M}_2\right)} = \frac{\mathcal{M}_1 - \frac{\omega^2}{6}\mathcal{M}_3}{\mathcal{M}_0 - \frac{\omega^2}{2}\mathcal{M}_2}. \tag{6.59}$$

From this we can further deduce

$$\hat{\theta}(\omega) \approx \frac{\left\{\mathcal{M}_1 - \frac{\omega^2}{6}\mathcal{M}_3\right\}}{\mathcal{M}_0}\left\{1 + \frac{\omega^2}{2}\left(\frac{\mathcal{M}_2}{\mathcal{M}_0}\right) + \frac{\omega^4}{4}\left(\frac{\mathcal{M}_2}{\mathcal{M}_0}\right)^2 + \cdots\right\} \tag{6.60}$$

Since ω is small and $\mathcal{M}_0 > \mathcal{M}_2$, higher order terms arising in this expression will be small. Thus, neglecting all the terms associated with higher power than ω^2 we obtain

$$\begin{aligned}\hat{\theta}(\omega) \approx & \frac{\left\{\mathcal{M}_1 - \frac{\omega^2}{6}\mathcal{M}_3\right\}}{\mathcal{M}_0}\left\{1 + \frac{\omega^2}{2}\frac{\mathcal{M}_2}{\mathcal{M}_0}\right\} \\ \approx & \frac{\mathcal{M}_1 + \omega^2\left\{\frac{1}{2}\frac{\mathcal{M}_1\mathcal{M}_2}{\mathcal{M}_0} - \frac{\mathcal{M}_3}{6}\right\}}{\mathcal{M}_0}\end{aligned} \tag{6.61}$$

The variation of the fitted θ_j in the low frequency region can now be deduced. The curve of fitted θ_j will increase, as for the system with damping model 2 shown in Figures 6.2, 6.4 and 6.5, if

$$\begin{aligned}&\frac{\mathcal{M}_1\mathcal{M}_2}{\mathcal{M}_0} - \frac{\mathcal{M}_3}{3} > 0; \quad \text{since } \omega, \mathcal{M}_0 > 0 \\ \text{or} \quad &3\frac{\mathcal{M}_2}{\mathcal{M}_3} - \frac{\mathcal{M}_0}{\mathcal{M}_1} > 0.\end{aligned} \tag{6.62}$$

Currently the curve of fitted θ_j will decrease if the above quantity is negative. This analysis gives some insight into the nature of the underlying damping function. Using the expressions for the moments given by equations (6.55) – (6.57) it may be verified that the damping functions considered here always satisfy this condition.

6.5 Fitting of the Coefficient Matrix

6.5.1 Theory

Once the relaxation parameter of the damping function is estimated our next step is to obtain the coefficient matrix $\mathbf{C}$ associated with the damping function as shown in equation (6.6). After obtaining $\hat{\mu}$, from the imaginary part of equation (6.8) the diagonal entries of $\mathbf{C}'$ can be obtained as

$$C'_{jj} = 2\Im(\hat{\lambda}_j)\frac{(\hat{\mu}^2 + \hat{\omega}_j^2)}{\hat{\mu}^2}. \tag{6.63}$$

This C'_{jj} and $\hat{\mu}$ can be substituted in equation (6.8) and subsequently an improved estimate value of $\hat{\omega}_j$ may be obtained from (6.11) by

$$\hat{\omega}_j^{(\text{new})} = \hat{\omega}_j + \frac{C'_{jj}}{2}\frac{\hat{\mu}\hat{\omega}_j}{\hat{\mu}^2 + \hat{\omega}_j^2}. \tag{6.64}$$

If all the $\hat{\omega}_j^{(\text{new})}$ are sufficiently close to $\hat{\omega}_j^{(0)}$ then we take the values of $\hat{\omega}_j^{(\text{new})}$ as the estimated values, *i.e.*, $\hat{\omega}_j = \hat{\omega}_j^{(\text{new})}$. Otherwise the process can be repeated by substituting $\hat{\omega}_j^{(\text{new})}$ in place of

$\hat{\omega}_j$ in one of the equations (6.18) – (6.20) to obtain $\hat{\mu}$, and subsequently obtaining a new set of $\hat{\omega}_j$ from (6.64). This iterative procedure may be continued until the differences between all new $\hat{\omega}_j$ and old $\hat{\omega}_j$ become sufficiently small. We select the final values of $\hat{\omega}_j$ and $\hat{\mu}$ as our estimated values.

Now $\hat{\mu}$ can be substituted in equation (6.15) to obtain an estimate of the undamped modes as

$$\hat{\mathbf{x}}_j = \hat{\mathbf{u}}_j - \frac{\hat{\omega}_j}{\hat{\mu}}\hat{\mathbf{v}}_j. \tag{6.65}$$

After obtaining $\hat{\mathbf{x}}_j$ in this way from equation (6.13), the constants $\widetilde{B}_{kj}$ can be derived using Galerkin error minimization as described in Section 5.3. Denoting $\widetilde{\mathbf{B}} \in \mathbb{R}^{m\times m}$ as the matrix of unknown $\widetilde{B}_{kj}$ one obtains

$$\widetilde{\mathbf{B}} = \left[\hat{\mathbf{X}}^T\hat{\mathbf{X}}\right]^{-1}\hat{\mathbf{X}}^T\hat{\mathbf{V}}. \tag{6.66}$$

where

$$\hat{\mathbf{X}} = [\hat{\mathbf{x}}_1, \hat{\mathbf{x}}_2, \cdots \hat{\mathbf{x}}_m] \in \mathbb{R}^{N\times m} \tag{6.67}$$

is the matrix of undamped modes. Now the off-diagonal terms C'_{kj} can be obtained from

$$C'_{kj} = \frac{(\hat{\omega}_j^2 - \hat{\omega}_k^2)}{\hat{\omega}_j}\frac{(\hat{\mu}^2 + \hat{\omega}_j^2)}{\hat{\mu}^2}\widetilde{B}_{kj} \quad \forall\ k, j = 1, \cdots m; k \neq j \tag{6.68}$$

The diagonal entries of $\mathbf{C}'$ have already been obtained in (6.63). Recall that C'_{kj} are constant coefficients of the damping matrix in the modal coordinates, with associated time function $e^{-\hat{\mu}t}$. The coefficients in the original coordinates can be calculated using the transformation

$$\mathbf{C} = \left[\left(\hat{\mathbf{X}}^T\hat{\mathbf{X}}\right)^{-1}\hat{\mathbf{X}}^T\right]^T\mathbf{C}'\left[\left(\mathbf{X}^T\hat{\mathbf{X}}\right)^{-1}\hat{\mathbf{X}}^T\right] \in \mathbb{R}^{m\times m}. \tag{6.69}$$

This coefficient matrix together with the relaxation parameter completely defines the fitted damping model for the structure. This fitting procedure has made use only of the complex natural frequencies, mode shapes and mass matrix to identify the best exponential damping model associated with the measurements.

It is easy to check that when $\hat{\mu}$ is large, *i.e.*, when the damping mechanism is near to viscous, this procedure reduces exactly to the procedure described in the earlier chapter 5 for identification of a viscous damping model. Thus, this method is a generalization of identification of viscous damping properties to the more general linear damping case described by an exponential model with a single relaxation time constant. One limitation of this method compared to the identification method of viscous damping matrix is that an estimate of the mass matrix is required. The extra information from the mass matrix also enables us to detect whether the correct damping model of the system is viscous/exponential or not.

6.5.2 Summary of the Identification Method

In summary, the procedure can be described by the following steps:

1. Measure a set of transfer functions $H_{ij}(\omega)$ at a set of N grid points. Fix the number of modes to be retained in the study, say m. Determine the complex natural frequencies $\hat{\lambda}_j$ and complex mode shapes $\hat{\mathbf{z}}_j$ from the transfer functions, for all $j = 1, \cdots m$. Denote by $\hat{\mathbf{Z}} = [\hat{\mathbf{z}}_1, \hat{\mathbf{z}}_2, \cdots \hat{\mathbf{z}}_m] \in \mathbb{C}^{N\times m}$ the complex mode shape matrix. Set $\hat{\mathbf{U}} = \Re\left[\hat{\mathbf{Z}}\right] = [\hat{\mathbf{u}}_1, \hat{\mathbf{u}}_2, \cdots \hat{\mathbf{u}}_m]$ and $\hat{\mathbf{V}} = \Im\left[\hat{\mathbf{Z}}\right] = [\mathbf{v}_1, \hat{\mathbf{v}}_2, \cdots \hat{\mathbf{v}}_m]$.

2. Obtain the first guess (*i.e.*, $r = 0$) of the 'undamped natural frequencies' as $\hat{\omega}_j^{(r)} = \Re(\hat{\lambda}_j)$.

3. Estimate the relaxation parameter $\hat{\mu}^{(r)} = \dfrac{\hat{\omega}_1^{(r)}\hat{\mathbf{v}}_1^T\mathbf{M}\hat{\mathbf{v}}_1}{\hat{\mathbf{v}}_1^T\mathbf{M}\hat{\mathbf{u}}_1}$ (or using a different estimate of $\hat{\mu}$ given by equations (6.19) or (6.20)).

4. Calculate the diagonal terms of the $\mathbf{C}'$ matrix as $C'^{(r)}_{jj} = 2\Im(\hat{\lambda}_j)\dfrac{(\hat{\mu}^{(r)^2} + \hat{\omega}_j^{(r)^2})}{\hat{\mu}^{(r)^2}}$ for all j.

5. Obtain new values of the undamped natural frequencies $\hat{\omega}_j^{(r+1)} = \hat{\omega}_j^{(r)} + \dfrac{C'^{(r)}_{jj}}{2}\dfrac{\hat{\mu}^{(r)}\hat{\omega}_j^{(r)}}{(\hat{\mu}^{(r)^2} + \hat{\omega}_j^{(r)^2})}$.

6. Select a value of ϵ, say $\epsilon = 0.001$. If $|\hat{\omega}_j^{(r+1)} - \hat{\omega}_j^{(r)}| < \epsilon \forall j$ then $\hat{\omega}_j = \hat{\omega}_j^{(r+1)}$, $C'_{jj} = C'^{(r)}_{jj}$ and $\hat{\mu} = \hat{\mu}^{(r)}$ and move to the next step. Otherwise increase r, set the final values of $\hat{\omega}_j$ as the current values, *i.e.*, $\hat{\omega}_j^{(r)} = \hat{\omega}_j^{(r+1)}$, and go back to step 3.

7. For all $j = 1, \cdots, m$ calculate the 'undamped mode shapes' $\hat{\mathbf{x}}_j = \left\{\hat{\mathbf{u}}_j - \dfrac{\hat{\omega}_j}{\hat{\mu}}\hat{\mathbf{v}}_j\right\}$. Set $\hat{\mathbf{X}} = [\hat{\mathbf{x}}_1, \hat{\mathbf{x}}_2, \cdots \hat{\mathbf{x}}_m] \in \mathbb{R}^{N\times m}$.

8. Evaluate the matrix $\widetilde{\mathbf{B}} = \left[\hat{\mathbf{X}}^T\hat{\mathbf{X}}\right]^{-1}\hat{\mathbf{X}}^T\hat{\mathbf{V}}$.

9. From the $\widetilde{\mathbf{B}}$ matrix get $C'_{kj} = \dfrac{(\hat{\omega}_j^2 - \hat{\omega}_k^2)}{\hat{\omega}_j}\dfrac{(\hat{\mu}^2 + \hat{\omega}_j^2)}{\hat{\mu}^2}\widetilde{B}_{kj}$ for $k, j = 1, 2\cdots m; k \neq j$.

10. Use $\mathbf{C} = \left[\left(\hat{\mathbf{X}}^T\mathbf{X}\right)^{-1}\hat{\mathbf{X}}^T\right]^T\mathbf{C}'\left[\left(\hat{\mathbf{X}}^T\hat{\mathbf{X}}\right)^{-1}\hat{\mathbf{X}}^T\right]$ to get the coefficient matrix in physical coordinates.

It may be observed that even if the measured transfer functions are reciprocal, from this procedure there is no reason why the fitted coefficient matrix $\mathbf{C}$ will always be symmetric. If we indeed detect a non-symmetric $\mathbf{C}$ then it may be guessed that the physical law behind the damping mechanism in the structure cannot be described by an exponential model. This possibility will be illustrated by considering numerical examples.

6.5.3 Numerical Results

Results for Small γ

Consider first $\gamma = 0.02$ so that all the damping models show near-viscous behaviour. For the system shown in Figure 6.1(a), with locally reacting damping, Figure 6.8 shows the fitted coefficient matrix of the exponential model for damping model 2, calculated using the complete set of 30 modes. The fitted matrix identifies the damping in the system very well. Equation (6.18) with $k = 1$ has been used to obtain the relaxation parameter. As has seen in Figure 6.2, the fitted relaxation parameter $\hat{\gamma} = 0.02$ so that the fitted characteristic time constant also agrees exactly with the original one, even though the underlying model was Gaussian rather than exponential. The high portion of the plot corresponds exactly to the spatial location of the dampers. The off-diagonal terms of the identified damping matrix are very small compared to the diagonal terms, indicating correctly that the damping is locally reacting.

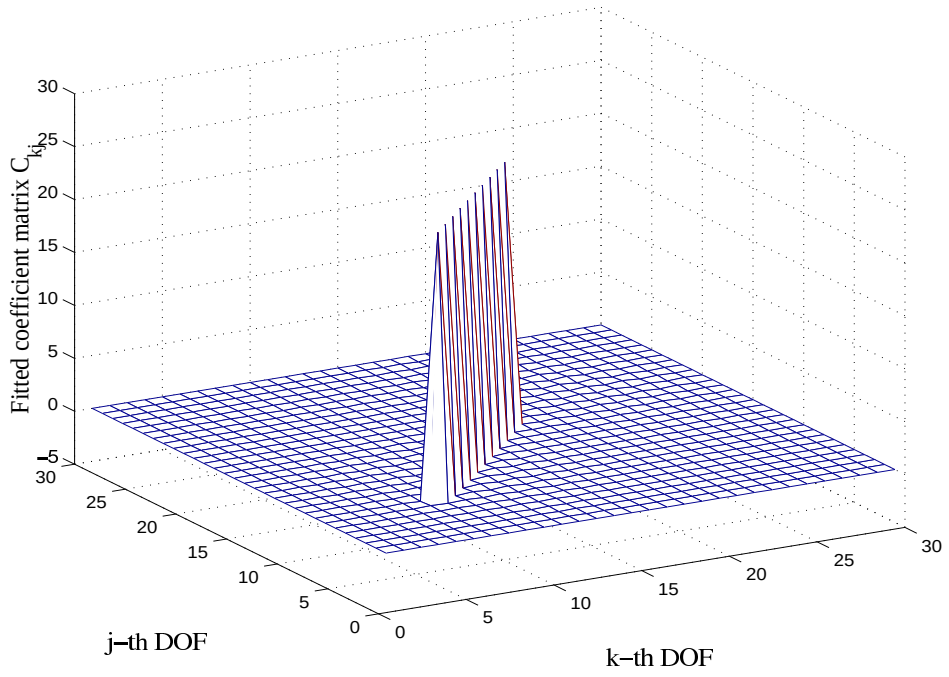

Figure 6.8: Fitted coefficient matrix of exponential model for the local case, $\gamma = 0.02$, damping model 2

Now consider the system shown in Figure 6.1(b) with non-locally reacting damping. Figure 6.9 shows the fitted coefficient matrix of an exponential model for damping model 2, using the full set of modes. Again the high portion of the plot corresponds to the spatial location of the dampers. Now the negative off-diagonal terms in the identified damping matrix indicate that the damping is non-locally reacting. We conclude that in both cases the proposed method extracts accurate information from the complex frequencies and modes. In practice, one might expect to be able to use only the first few modes of the system to identify the damping matrix. The proposed method can be applied using a smaller number of modes, and it is found that the result behaves in a very

similar way to the case of identification of a viscous damping matrix as discussed in Chapter 5 — the spatial resolution of the identified coefficient matrix gradually deteriorates as the number of modes used to fit the damping matrix is reduced, but still the identified coefficient matrix shows a reasonable approximation to the true behaviour.

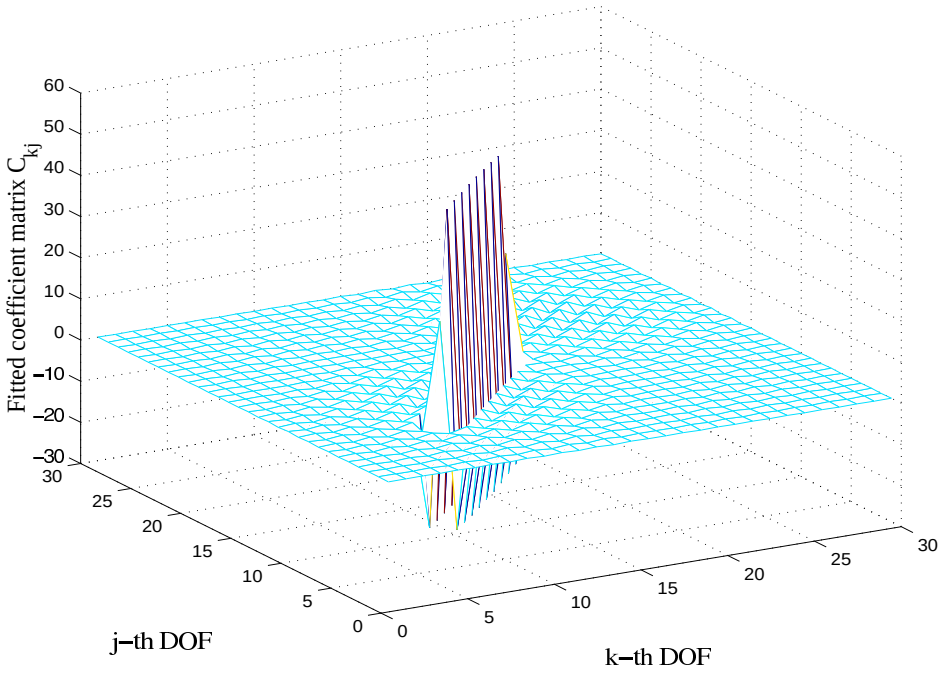

Figure 6.9: Fitted coefficient matrix of exponential model for the non-local case, $\gamma = 0.02$, damping model 2

When the fitting procedure is repeated using other damping models with a similarly short characteristic time constant, the result are very similar. The detailed difference in their functional behaviour does not influence the results significantly. It may be observed that the results obtained here are quite similar to those obtained by fitting a viscous damping model for the corresponding case discussed in Section 5.4.1. In summary, we can say that when the time constant for a damping model is small the proposed identification method seems to work well regardless of the functional form of the damping mechanism. The spatial location of damping is revealed clearly and the associated relaxation parameter is accurately estimated whether damping is locally or non-locally reacting. Modal truncation blurs the fitted coefficient matrix, but does not degrade the estimate of the relaxation parameter and overall the identification process remains valid.

Results for Larger γ

When γ is larger the two non-exponential damping models depart from the exponential damping model, each in its own way. For the value $\gamma = 0.5$, Figure 5.7 shows the result of fitting a viscous damping matrix, using the procedure described in Chapter 5, for damping model 1 (equation (6.21)) with locally-reacting damping and the full set of 30 modes. Note that although we have

started with a locally reacting damping model, which means the true coefficient matrix is non-zero only along the diagonal, non-zero values in the off-diagonal terms show that the fitted viscous damping is, in a sense, not locally reacting. Figure 6.10 shows the corresponding result of fitting the exponential model for this problem. This result clearly demonstrates the improvement of fitting over the result in Figure 5.7. Since the damping model is 'identified' correctly in this case, the correct value of the relaxation parameter is obtained, and the coefficient matrix corresponds to the exact coefficient matrix for the problem. Thus, even if the characteristic time constant of the damping mechanism present in a system is large, a correctly identified damping model can represent the true damping behaviour.

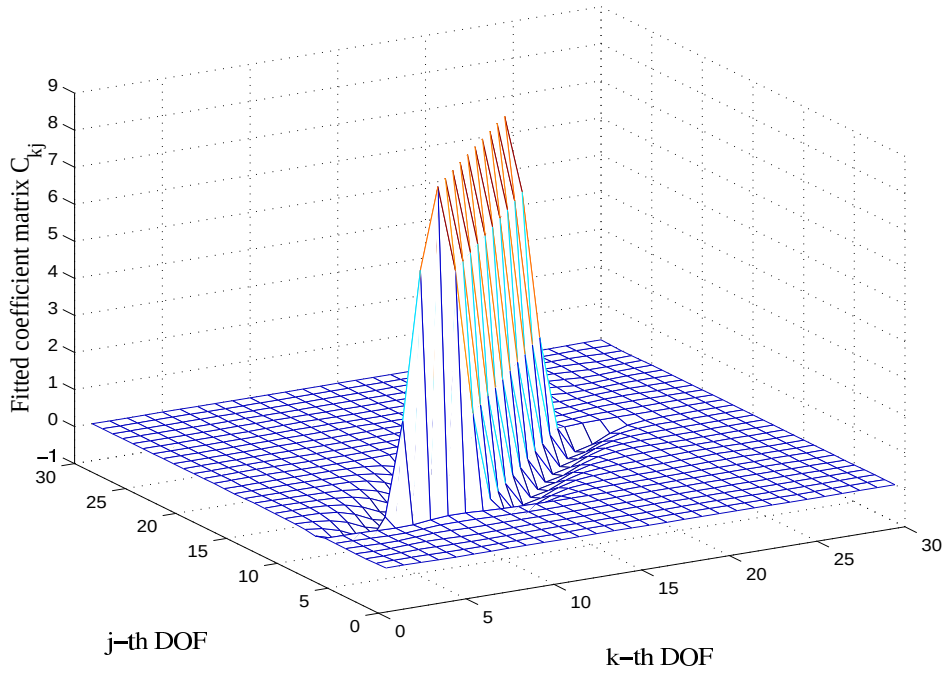

Figure 6.10: Fitted coefficient matrix of exponential model for the local case, $\gamma = 0.5$, damping model 1

Figure 6.11 shows the fitted coefficient matrix of the exponential function similar to Figure 6.10 but with damping model 2 (equation (6.22)). The fitted matrix has some negative off-diagonal values which wrongly gives the impression that the damping type is non-local. For this result equation (6.18) with $k = 1$ has been used to estimate the relaxation parameter. Figure 6.12 compares the original damping time function (Gaussian) with the fitted exponential function. It may be observed that although the fitted coefficient matrix does not match the original one very accurately the time functions agree with reasonable accuracy. Since $\hat{\gamma} = 0.4951$ the characteristic time constant of the fitted exponential model is surprisingly close to the exact γ of the simulated model. This remains true with even larger values of the characteristic time constant for systems with damping model 2.

The identification results show somewhat different behaviour for systems with damping model 3. Figure 6.13 shows the fitted coefficient matrix of the exponential function with $\gamma = 0.5$ for damping model 3 with two exponential functions as considered in subsection 6.3.3. Compared

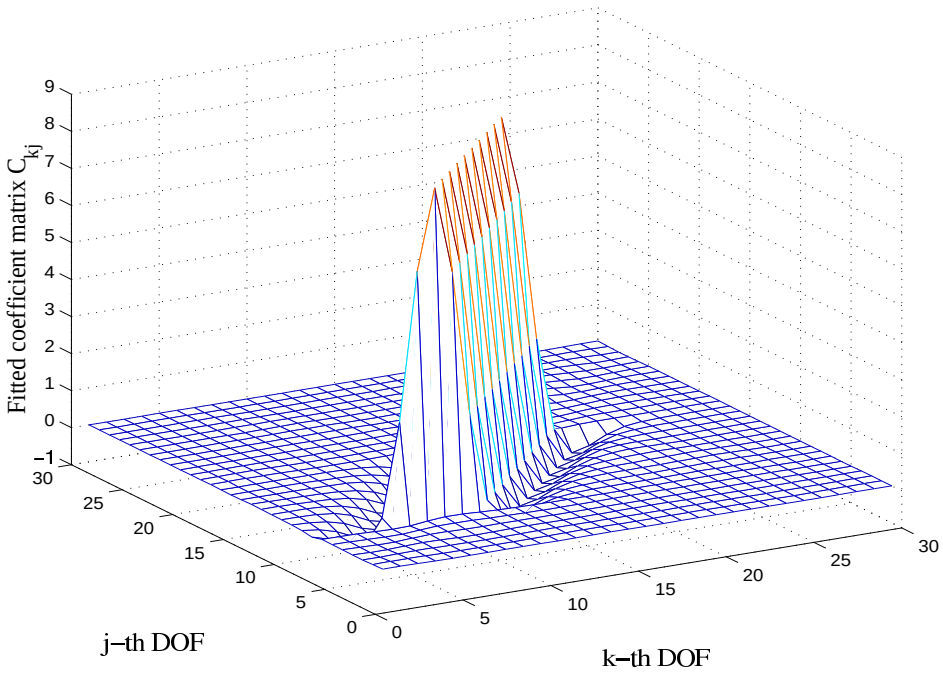

Figure 6.11: Fitted coefficient matrix of exponential model for the local case, $\gamma = 0.5$, damping model 2

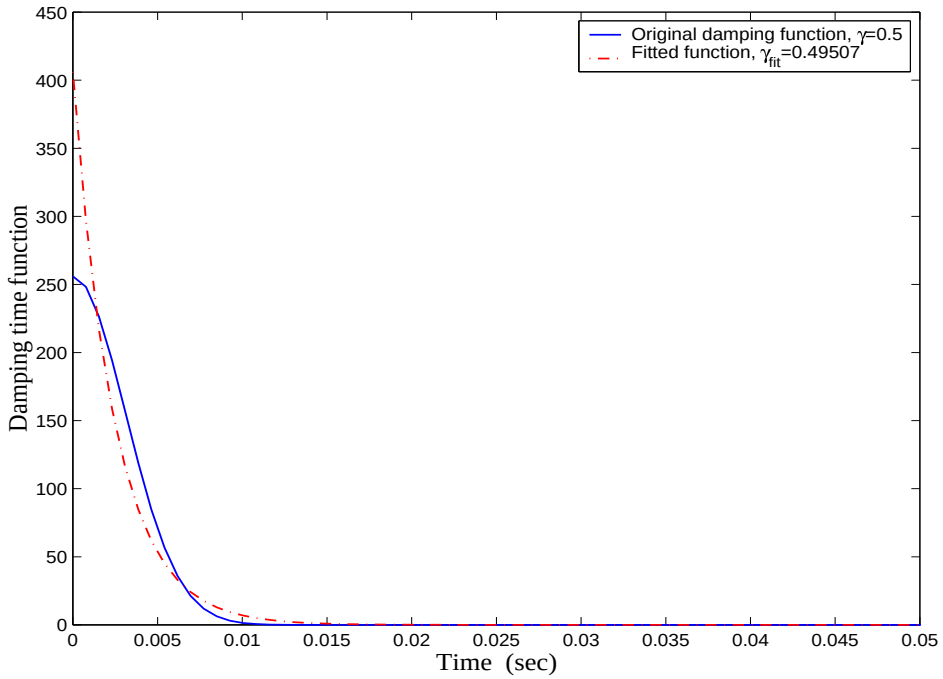

Figure 6.12: Original and fitted damping time function for the local case with damping model 2

to the case of damping model 2 (Figure 6.11), the fitted coefficient matrix is much closer to the original coefficient matrix used for simulation. However, we note that for the fitted exponential function $\hat{\gamma} = 0.4834$, less close to the correct value compared to that with damping model 2. Explanation of this fact lies in values of $\hat{\gamma}_j$ shown in Figures 6.5 and 6.6 for damping model 2 and 3 respectively. For damping model 2 variation of $\hat{\gamma}_j$ is much more compared to that for damping

model 3. Thus the fitted (exponential) damping model is 'closer' to model 3 compared to model 2. This is expected because $\hat{\gamma}_j$ always lies between extremum of all the γ used in simulation.

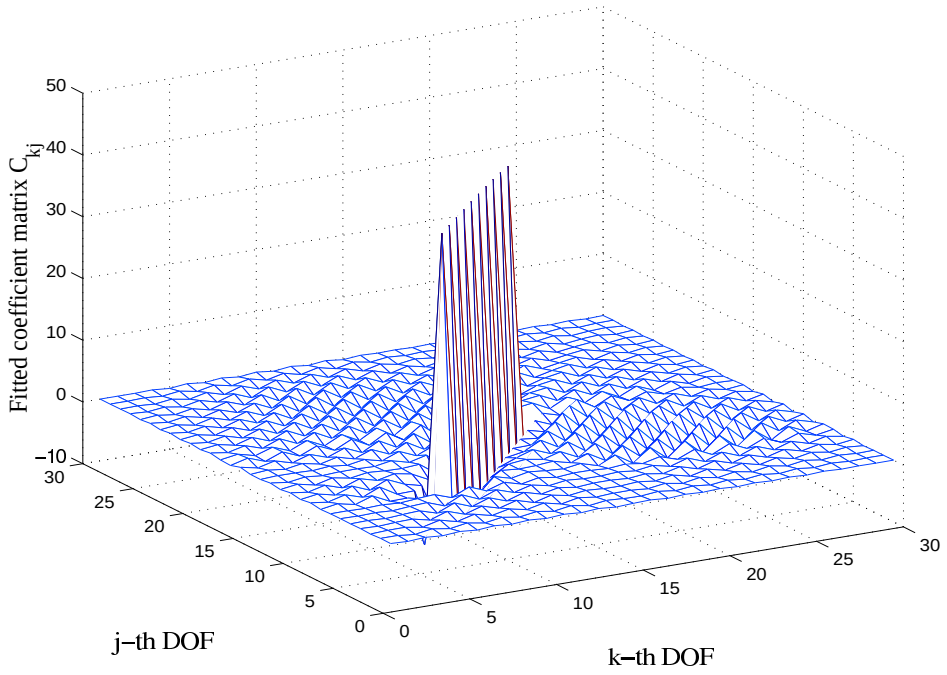

Figure 6.13: Fitted coefficient matrix of exponential model for the local case, $\gamma = 0.5$, damping model 3

In Chapter 5 it was shown that the features of the fitted viscous model were quite similar in the case of non-viscous damping models 1 and 2. Now, however, the features of fitting the exponential model with damping model 2 (Figure 6.11) are clearly different from those with model 1 (Figure 6.10) and model 3 (Figure 6.13). This is due to the fact that a viscous damping model was incorrect for both model 1 and 2, whereas when fitting the exponential model, it is correct for damping model 1 and close for damping model 3. For damping model 2, since the original damping function is Gaussian while the fitted function is exponential, the coefficient matrix does not correspond to the exact coefficient matrix of the problem. For damping model 3, since the fitted exponential function is a reasonable approximation of the original multiple exponential function, the coefficient matrix does not differ from the original function. From these results we conclude that when the characteristic time constant of a damping model is large an incorrect damping model (no matter whether it is viscous or non-viscous) may not accurately indicate the actual damping behaviour of a structure.

Now we turn our attention to the non-local case shown in Figure 6.1(b). As has just been shown with locally-reacting damping, the proposed method can identify the exact coefficient matrix and damping function for the system with damping model 1 because the fitted model is the same as the original model. Figure 6.14 shows the fitted coefficient matrix for damping model 2, using the full set of 30 modes. For these results equation (6.18) with $k = 1$ has been used to calculate $\hat{\gamma} = 0.5033$. Thus although the fitted coefficient matrix does not match very well with the original one,

we find once again that the value of the characteristic time constant is quite accurately predicted. For damping model 3 it was observed (results not shown) that, as in the locally-reacting case, the identified coefficient matrix is very close to the original one.

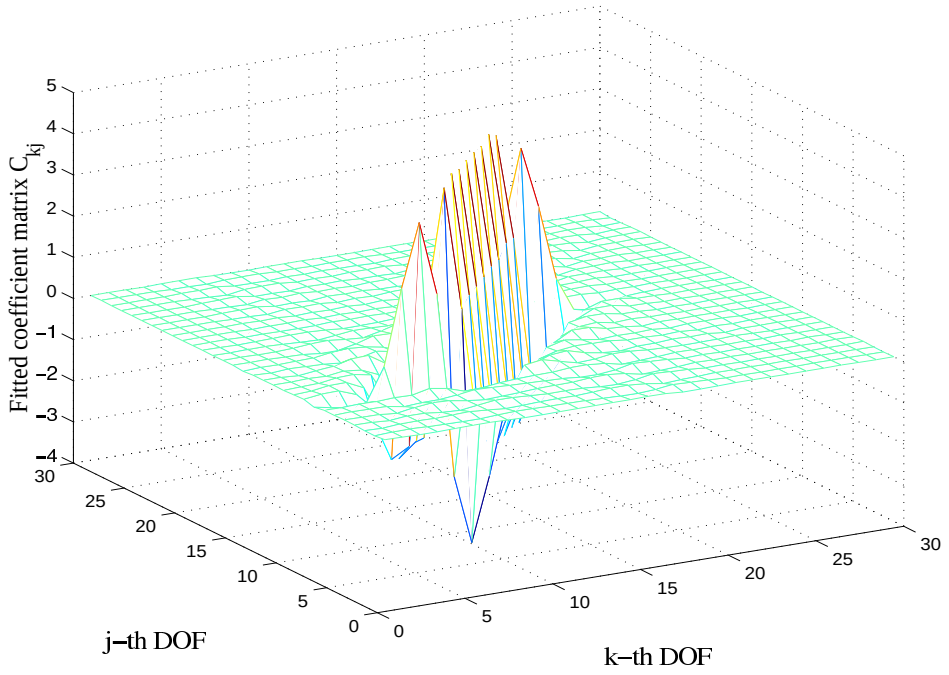

Figure 6.14: Fitted coefficient matrix of exponential model for the non-local case, $\gamma = 0.5$, damping model 2

It might be thought that a useful check on the accuracy of the fitting method could be made by comparing the 'measured' and reconstructed transfer functions. However, little information is gained from such a comparison. The reason is that, for both viscous and non-viscous fitting procedures, the poles and corresponding residues of all transfer functions are fitted correctly. It follows from Liouville's theorem that the transfer functions are always well reproduced. This demonstrates that there is a fundamental ambiguity in damping identification: two different damping models (*eg*., the viscous model and the exponential model) with different spatial distributions and different sets of parameters can reproduce accurately the full set of transfer functions of a system with an entirely different damping model (*eg*., the Gaussian model) with different spatial distributions and parameters. This in turn implies that *just by measuring the transfer functions it is not possible to identify uniquely the governing damping mechanism*. However, it should be noted that in cases like Figures 6.11, 6.14 *etc*., the fitted coefficient matrix is not symmetric. This is a non-physical result, which can be regarded as evidence that the true damping behaviour is not in fact described by an exponential function. In Chapter 5 similar features were also observed while fitting a viscous damping matrix.

6.6 Conclusions

In this chapter a method has been proposed to identify a non-proportional non-viscous damping model in vibrating systems. It is assumed that damping is light so that the first-order perturbation method is applicable. The method is simple, direct, and compatible with conventional modal testing procedures. The complex modes and natural frequencies are used together with the system mass matrix. The method does not require the full set of modal data. The damping behaviour is assumed to be described by an exponential relaxation function, and the relaxation time constant is found as part of the fitting procedure. Identification of the familiar viscous damping model is a special case of the general method proposed here. The validity of the proposed method has been explored by applying it to simulated data from a simple test problem, in which a linear array of spring-mass oscillators is damped by non-viscous elements over part of its length.

Numerical experiments have been carried out with a wide range of parameter values and different damping models. The main features of the results have been illustrated by two particular damping models and representative parameter values. It has been shown that the method generally predicts the spatial location of the damping with good accuracy, and also gives a good indication of whether the damping is locally-reacting or not. In general, the relaxation time constant was fitted well, even when the coefficient matrix was less accurate. The transfer functions obtained from the fitted exponential damping model agree well with the exact transfer functions of the simulated system. Reciprocity of the transfer functions is preserved within an acceptable accuracy, although in some cases the fitted coefficient matrix is not symmetric, indicating that the true damping model differs from the assumed exponential model.

When the time constant is short compared with the periods of all modes retained in the analysis, the damping is close to viscous and the fitting procedure gives a physically-sensible symmetric coefficient matrix and an accurate value of the relaxation parameter. When the time constant is larger, though, the memory of the damping function influences the detailed behaviour. If the identified model matches the true model then the fitting procedure gives a correct physical description of the damping. When the models are different, the poles and residues of the transfer functions are still fitted accurately with a model of the form considered, but the underlying different functional behaviour manifests itself in a non-symmetrical coefficient matrix and significant variation of fitted relaxation parameter with mode number. A correct physical description of the damping mechanism can be obtained only if a correct model is selected and fitted.

From equation (6.2) we can deduce that, within the approximation of small damping, each frequency function $G'_{kj}(\omega)$ can be observed at only two frequencies, ω_j and ω_k. This fact imposes a fundamental restriction on identification of an exact damping function using this approach. When the fitted coefficient matrix turns out to be non-symmetric, this indicates that it was not possible to fit the assumed function through both ‘measured’ frequency points, and two different coefficients were needed. To correct this problem it would be necessary to fit a different damping model,

able to pass through both measured points while retaining symmetric coefficients. The function cannot be uniquely determined by this requirement, of course. There can be two possible ways to tackle this problem. One can ‘invent’ different physically plausible damping models and try to fit their parameters using the approach outlined in this chapter and see which model fits the measured data most convincingly. Alternatively, one might use the viscous or exponential model and put constraints on the coefficients such that they yield symmetric coefficient damping matrix. This approach is explored in the next chapter.

Chapter 7

Symmetry Preserving Methods for Damping Identification

7.1 Introduction

In the preceding two chapters (Chapter 5 and Chapter 6) methods were proposed to identify viscous and non-viscous damping models from modal data. Some general conclusions emerging from these studies are

1. Whenever the fitted damping model (whether viscous or non-viscous) is not close to the original damping model of the system, the identified coefficient matrix becomes asymmetric.

2. Once the poles and residues of transfer functions are obtained, several damping models can be fitted. In other words, more than one damping model can reproduce some measured set of transfer functions exactly.

An asymmetric fitted damping matrix is a non-physical result because the original system is reciprocal. Thus, result 1 above may be regarded as an indication of the fact that the selected model is incorrect. Whereas, result 2 indicates that if one's interest is reconstructing the transfer functions within a given frequency band, then it does not matter even if a wrong damping model is assumed. This is the justification of widespread use of the viscous damping model. Motivated by these facts, in this chapter we consider fitting of viscous and exponential damping models so that reciprocity of the system is preserved. Unless the identified damping matrix is symmetric, the model may have poor predictive power for changes to the system.

Like the previous two chapters, analysis in this chapter is restricted to linear systems with light damping. Based on first-order perturbation results, a method for identification of a symmetry preserving viscous damping model using complex modes and natural frequencies is outlined in Section 7.2. In Section 7.3 this method is extended to identify the coefficients of an exponential damping model with a single relaxation parameter. Applications of these methods are illustrated by considering a few numerical examples. Finally Section 7.4 summarizes the main findings of this chapter.

7.2 Identification of Viscous Damping Matrix

7.2.1 Theory

In Chapter 5 we have proposed a method to identify a viscous damping matrix from measured complex frequencies and modes using a Galerkin type error minimization approach. This method does not guarantee symmetry of the identified damping matrix. In a numerical simulation study it was observed that in some cases the identified viscous damping matrix becomes asymmetric. This is a non-physical result since the viscous damping matrix by its definition (through the Rayleighs dissipation function) is symmetric. For this reason we now develop a method so that the identified damping matrix is always symmetric. A Lagrange multiplier based constrained optimization method is adopted for this purpose.

Consider $\hat{\lambda}_j$ and $\hat{\mathbf{z}}_j$ for all $j = 1, 2, \cdots m$ to be the *measured* complex natural frequencies and modes. Here $\hat{\mathbf{z}}_j \in \mathbb{C}^N$ where N denotes the number of measurement points on the structure and the number of modes considered in the study is m. In general $m \neq N$, usually $N \geq m$. Denote the complex modal matrix

$$\hat{\mathbf{Z}} = [\hat{\mathbf{z}}_1, \hat{\mathbf{z}}_2, \cdots, \hat{\mathbf{z}}_m] \in \mathbb{C}^{N\times m}. \tag{7.1}$$

If the measured complex mode shapes are consistent with a viscous damping model then from equation (5.1) the real part of each complex natural frequency gives the undamped natural frequency:

$$\hat{\omega}_j = \Re\left(\hat{\lambda}_j\right). \tag{7.2}$$

Similarly from equation (5.2), the real part of the complex modes immediately gives the corresponding undamped modes and the usual mass orthogonality relationship will be automatically satisfied. Write

$$\hat{\mathbf{Z}} = \hat{\mathbf{U}} + \mathrm{i}\hat{\mathbf{V}} \tag{7.3}$$

where

$$\begin{aligned} \hat{\mathbf{U}} &= [\hat{\mathbf{u}}_1, \hat{\mathbf{u}}_2, \cdots, \hat{\mathbf{u}}_m] \in \mathbb{R}^{N\times m} \\ \text{and} \quad \hat{\mathbf{V}} &= [\hat{\mathbf{v}}_1, \hat{\mathbf{v}}_2, \cdots, \hat{\mathbf{v}}_m] \in \mathbb{R}^{N\times m} \end{aligned} \tag{7.4}$$

are respectively the matrices of real and imaginary parts of the measured complex modes. Now in view of equation (5.2), expand the imaginary part of $\hat{\mathbf{z}}_j$ as a linear combination of $\hat{\mathbf{u}}_j$:

$$\hat{\mathbf{v}}_j = \sum_{k=1}^{m} B_{kj}\hat{\mathbf{u}}_k; \quad \text{where } B_{kj} = \frac{\hat{\omega}_j C'_{kj}}{\hat{\omega}_j^2 - \hat{\omega}_k^2}. \tag{7.5}$$

The constants B_{kj} should be calculated such that the error in representing $\hat{\mathbf{v}}_j$ by the above sum is minimized while the resulting damping matrix remains symmetric. Note that in the above sum we have included the $k = j$ term although in the original sum in equation (5.2) this term was absent. This is done to simplify the mathematical formulation to be followed, and has no effect on the

result. Our interest lies in calculating C'_{kj} from B'_{kj} through the relationship given by the second part of the equation (7.5), and indeed for $k = j$ we would obtain $C'_{kj} = 0$. The diagonal terms C'_{jj} are instead obtained from the imaginary part of the complex natural frequencies:

$$C'_{jj} = 2\Im(\hat{\lambda}_j). \tag{7.6}$$

For symmetry of the identified damping matrix $\mathbf{C}$, it is required that $\mathbf{C}'$ is symmetric, that is

$$C'_{kj} = C'_{jk}. \tag{7.7}$$

Using the relationship given by the second part of the equation (7.5) the above condition reads

$$B_{kj}\frac{\hat{\omega}_j^2 - \hat{\omega}_k^2}{\hat{\omega}_j} = B_{jk}\frac{\hat{\omega}_k^2 - \hat{\omega}_j^2}{\hat{\omega}_k}. \tag{7.8}$$

Simplification of equation (7.8) yields

$$\frac{B_{kj}}{\hat{\omega}_j} = -\frac{B_{jk}}{\hat{\omega}_k} \quad \text{or} \quad B_{kj}\hat{\omega}_k + B_{jk}\hat{\omega}_j = 0; \quad \forall k \neq j. \tag{7.9}$$

For further calculations is it convenient to cast the above set of equations in a matrix form. Consider $\mathbf{B} \in \mathbb{R}^{m\times m}$ to be the matrix of unknown constants B_{kj} and define

$$\hat{\mathbf{\Omega}} = \text{diag}(\hat{\omega}_1, \hat{\omega}_2, \cdots, \hat{\omega}_m) \in \mathbb{R}^{m\times m} \tag{7.10}$$

to be the diagonal matrix of the measured undamped natural frequencies. From equation (7.9) for all $k, j = 1, 2, \cdots, m$ (including $k = j$ for mathematical convenience) we have

$$\hat{\mathbf{\Omega}}\mathbf{B} + \mathbf{B}^T\hat{\mathbf{\Omega}} = \mathbf{0} \tag{7.11}$$

This equation must be satisfied by the matrix $\mathbf{B}$ in order to make the identified viscous damping matrix $\mathbf{C}$ symmetric. The error from representing $\hat{\mathbf{v}}_j$ by the series sum (7.5) can be expressed as

$$\boldsymbol{\varepsilon}_j = \hat{\mathbf{v}}_j - \sum_{k=1}^{m} B_{kj}\hat{\mathbf{u}}_k \in \mathbb{R}^N \tag{7.12}$$

We need to minimize the above error subject to the constraints given by equation (7.9). The standard inner product norm of $\boldsymbol{\varepsilon}_j$ is selected to minimize the error. Considering the Lagrange multipliers ϕ_{kj} the objective function may be constructed as

$$\chi^2 = \sum_{j=1}^{m} \boldsymbol{\varepsilon}_j^T\boldsymbol{\varepsilon}_j + \sum_{j=1}^{m}\sum_{k=1}^{m} \left(B_{kj}\hat{\omega}_k + B_{jk}\hat{\omega}_j\right)\phi_{kj} \tag{7.13}$$

To obtain B_{jk} by the error minimization approach set

$$\frac{\partial\chi^2}{\partial B_{rs}} = 0; \quad \forall r, s = 1, \cdots, m. \tag{7.14}$$

Substituting ε_j from equation (7.12) one has

$$\begin{aligned} &-2\hat{\mathbf{u}}_r^T\left(\hat{\mathbf{v}}_s-\sum_{k=1}^{m}B_{ks}\hat{\mathbf{u}}_k\right)+\left[\phi_{rs}+\phi_{sr}\right]\hat{\omega}_r=0 \\ \text{or}\quad &\sum_{k=1}^{m}\left(\hat{\mathbf{u}}_r^T\hat{\mathbf{u}}_k\right)B_{ks}+\frac{1}{2}\left[\hat{\omega}_r\phi_{rs}+\hat{\omega}_r\phi_{sr}\right]=\hat{\mathbf{u}}_r^T\hat{\mathbf{v}}_s;\quad \forall r,s=1,\cdots,m. \end{aligned} \tag{7.15}$$

The above set of equations can be represented in a matrix form as

$$\mathbf{WB}+\frac{1}{2}\left[\hat{\mathbf{\Omega}}\mathbf{\Phi}+\hat{\mathbf{\Omega}}\mathbf{\Phi}^T\right]=\mathbf{D} \tag{7.16}$$

where

$$\begin{aligned} \mathbf{W}=&\hat{\mathbf{U}}^T\hat{\mathbf{U}}\in\mathbb{R}^{m\times m} \\ \mathbf{D}=&\hat{\mathbf{U}}^T\hat{\mathbf{V}}\in\mathbb{R}^{m\times m} \end{aligned} \tag{7.17}$$

and $\mathbf{\Phi}\in\mathbb{R}^{m\times m}$ is the matrix of ϕ_{rs}. Note that both $\mathbf{B}$ and $\mathbf{\Phi}$ are unknown, so there are in total $2m^2$ unknowns. Equation (7.16) together with the symmetry condition (7.11) provides $2m^2$ equations. Thus both $\mathbf{B}$ and $\mathbf{\Phi}$ can be solved exactly provided their coefficient matrix is not singular or badly scaled. We follow the following procedure to obtain $\mathbf{B}$ and $\mathbf{\Phi}$.

Because in this study $\mathbf{\Phi}$ is not a quantity of interest, we try to eliminate it. Recalling that $\hat{\mathbf{\Omega}}$ is a diagonal matrix taking transpose of (7.16) one has

$$\mathbf{B}^T\mathbf{W}^T+\frac{1}{2}\left[\mathbf{\Phi}^T\hat{\mathbf{\Omega}}+\mathbf{\Phi}\hat{\mathbf{\Omega}}\right]=\mathbf{D}^T \tag{7.18}$$

Now postmultiplying equation (7.16) by $\hat{\mathbf{\Omega}}$ and premultiplying equation (7.18) by $\hat{\mathbf{\Omega}}$ and subtracting one has

$$\begin{aligned} &\mathbf{WB}\hat{\mathbf{\Omega}}+\frac{1}{2}\hat{\mathbf{\Omega}}\mathbf{\Phi}\hat{\mathbf{\Omega}}+\frac{1}{2}\hat{\mathbf{\Omega}}\mathbf{\Phi}^T\hat{\mathbf{\Omega}}-\hat{\mathbf{\Omega}}\mathbf{B}^T\mathbf{W}^T-\frac{1}{2}\hat{\mathbf{\Omega}}\mathbf{\Phi}^T\hat{\mathbf{\Omega}}-\frac{1}{2}\hat{\mathbf{\Omega}}\mathbf{\Phi}\hat{\mathbf{\Omega}}=\mathbf{D}\hat{\mathbf{\Omega}}-\hat{\mathbf{\Omega}}\mathbf{D}^T \\ \text{or}\quad &\mathbf{WB}\hat{\mathbf{\Omega}}-\hat{\mathbf{\Omega}}\mathbf{B}^T\mathbf{W}^T=\mathbf{D}\hat{\mathbf{\Omega}}-\hat{\mathbf{\Omega}}\mathbf{D}^T. \end{aligned} \tag{7.19}$$

This way $\mathbf{\Phi}$ has been eliminated. However, note that since the above is a rank deficient system of equations it cannot be used to obtain $\mathbf{B}$ and here we need to use the symmetry condition (7.11). Rearranging equation (7.11) we have

$$\mathbf{B}^T=-\hat{\mathbf{\Omega}}\mathbf{B}\hat{\mathbf{\Omega}}^{-1} \tag{7.20}$$

Substituting $\mathbf{B}^T$ in equation (7.19) and premultiplying by $\hat{\mathbf{\Omega}}^{-1}$ results in

$$\hat{\mathbf{\Omega}}^{-1}\mathbf{WB}\hat{\mathbf{\Omega}}+\hat{\mathbf{\Omega}}\mathbf{B}\hat{\mathbf{\Omega}}^{-1}\mathbf{W}^T=\hat{\mathbf{\Omega}}^{-1}\mathbf{D}\hat{\mathbf{\Omega}}-\mathbf{D}^T. \tag{7.21}$$

Observe from equation (7.17) that $\mathbf{W}$ is a symmetric matrix. Now denote

$$\begin{aligned} \mathbf{Q}=&\hat{\mathbf{\Omega}}^{-1}\mathbf{W}=\hat{\mathbf{\Omega}}^{-1}\mathbf{W}^T \\ \mathbf{P}=&\hat{\mathbf{\Omega}}^{-1}\mathbf{D}\hat{\mathbf{\Omega}}-\mathbf{D}^T. \end{aligned} \tag{7.22}$$

Using the above definitions, equation (7.21) reads

$$\mathbf{QB}\hat{\mathbf{\Omega}} + \hat{\mathbf{\Omega}}\mathbf{BQ} = \mathbf{P}. \tag{7.23}$$

This matrix equation represents a set of m^2 equations and can be solved to obtain $\mathbf{B}$ (m^2 unknowns) uniquely. To ease the solution procedure let us define the operation vec: $\mathbb{R}^{m\times n} \rightarrow \mathbb{R}^{mn}$ which transforms a matrix to a long vector formed by stacking the columns of the matrix in a sequence one below other. It is known that (see Zhou *et al.*, 1995, page 25) for any three matrices $\mathbf{A} \in \mathbb{C}^{k\times m}$, $\mathbf{B} \in \mathbb{C}^{m\times n}$, and $\mathbf{C} \in \mathbb{C}^{n\times l}$, we have $\mathrm{vec}\,(\mathbf{ABC}) = \left(\mathbf{C}^T \otimes \mathbf{A}\right)\mathrm{vec}(\mathbf{B})$ where $\otimes$ denotes the *Kronecker product*. Using this relationship and taking vec of both side of equation (7.23) one obtains

$$\begin{aligned} &\left(\hat{\mathbf{\Omega}} \otimes \mathbf{Q}\right)\mathrm{vec}(\mathbf{B}) + \left(\mathbf{Q}^T \otimes \hat{\mathbf{\Omega}}\right)\mathrm{vec}\,(\mathbf{B}) = \mathrm{vec}\,(\mathbf{P}) \\ \text{or} \quad &[\mathbf{R}]\,\mathrm{vec}\,(\mathbf{B}) = \mathrm{vec}\,(\mathbf{P}) \end{aligned} \tag{7.24}$$

where

$$\mathbf{R} = \left(\hat{\mathbf{\Omega}} \otimes \mathbf{Q}\right) + \left(\mathbf{Q}^T \otimes \hat{\mathbf{\Omega}}\right) \in \mathbb{R}^{m^2\times m^2}. \tag{7.25}$$

Since $\mathbf{R}$ is square matrix equation (7.24) can be solved to obtain

$$\mathrm{vec}\,(\mathbf{B}) = [\mathbf{R}]^{-1}\,\mathrm{vec}\,(\mathbf{P})\,. \tag{7.26}$$

From $\mathrm{vec}\,(\mathbf{B})$ the matrix $\mathbf{B}$ can be easily obtained by the inverse operation. Obtaining $\mathbf{B}$ in such a way will always make the identified damping matrix symmetric. The coefficients of the modal damping matrix can be derived from

$$C'_{kj} = \frac{(\hat{\omega}_j^2 - \hat{\omega}_k^2)B_{kj}}{\hat{\omega}_j}; \qquad k \neq j \tag{7.27}$$

Once $\mathbf{C}'$ is obtained, the damping matrix in the original coordinates can be obtained from equation (5.14). In summary, this procedure can be described by the following steps:

1. Measure a set of transfer functions $H_{ij}(\omega)$ at a set of N grid points. Fix the number of modes to be retained in the study, say m. Determine the complex natural frequencies $\hat{\lambda}_j$ and complex mode shapes $\hat{\mathbf{z}}_j$ from the transfer function, for all $j = 1, \cdots m$. Denote $\hat{\mathbf{Z}} = [\hat{\mathbf{z}}_1, \hat{\mathbf{z}}_2, \cdots \hat{\mathbf{z}}_m] \in \mathbb{C}^{N\times m}$ the complex mode shape matrix.

2. Set the 'undamped natural frequencies' as $\hat{\omega}_j = \Re(\hat{\lambda}_j)$. Denote the diagonal matrix $\hat{\mathbf{\Omega}} = \mathrm{diag}(\hat{\omega}_1, \hat{\omega}_2, \cdots, \hat{\omega}_m) \in \mathbb{R}^{m\times m}$.

3. Separate the real and imaginary parts of $\hat{\mathbf{Z}}$ to obtain $\hat{\mathbf{U}} = \Re\left[\hat{\mathbf{Z}}\right]$ and $\hat{\mathbf{V}} = \Im\left[\hat{\mathbf{Z}}\right]$.

4. From these obtain the $m \times m$ matrices $\mathbf{W} = \hat{\mathbf{U}}^T\hat{\mathbf{U}}$, $\mathbf{D} = \hat{\mathbf{U}}^T\hat{\mathbf{V}}$, $\mathbf{Q} = \hat{\mathbf{\Omega}}^{-1}\mathbf{W}$ and $\mathbf{P} = \hat{\mathbf{\Omega}}^{-1}\mathbf{D}\hat{\mathbf{\Omega}} - \mathbf{D}^T$.

5. Now denote $\mathbf{p} = \text{vec}\,(\mathbf{P}) \in \mathbb{R}^{m^2}$ and calculate $\mathbf{R} = \left(\hat{\mathbf{\Omega}} \otimes \mathbf{Q}\right) + \left(\mathbf{Q}^T \otimes \hat{\mathbf{\Omega}}\right) \in \mathbb{R}^{m^2 \times m^2}$ (MATLAB^{TM} command `kron` can be used to calculate the Kronecker product).

6. Evaluate $\text{vec}\,(\mathbf{B}) = [\mathbf{R}]^{-1}\,\mathbf{p}$ and obtain the matrix $\mathbf{B}$.

7. From the $\mathbf{B}$ matrix get $C'_{kj} = \dfrac{(\hat{\omega}_j^2 - \hat{\omega}_k^2)B_{kj}}{\hat{\omega}_j}$ for $k \neq j$ and $C'_{jj} = 2\Im(\hat{\lambda}_j)$.

8. Finally, carry out the transformation $\mathbf{C} = \left[\left(\hat{\mathbf{U}}^T\mathbf{U}\right)^{-1}\hat{\mathbf{U}}^T\right]^T \mathbf{C}' \left[\left(\hat{\mathbf{U}}^T\hat{\mathbf{U}}\right)^{-1}\hat{\mathbf{U}}^T\right]$ to get the damping matrix in physical coordinates.

A numerical illustration of the proposed method is considered next.

7.2.2 Numerical Examples

Numerical studies have been carried out using simulated systems identical to those used in Chapters 5 and 6. Figure 7.1 shows the model systems together with the numerical values used. The

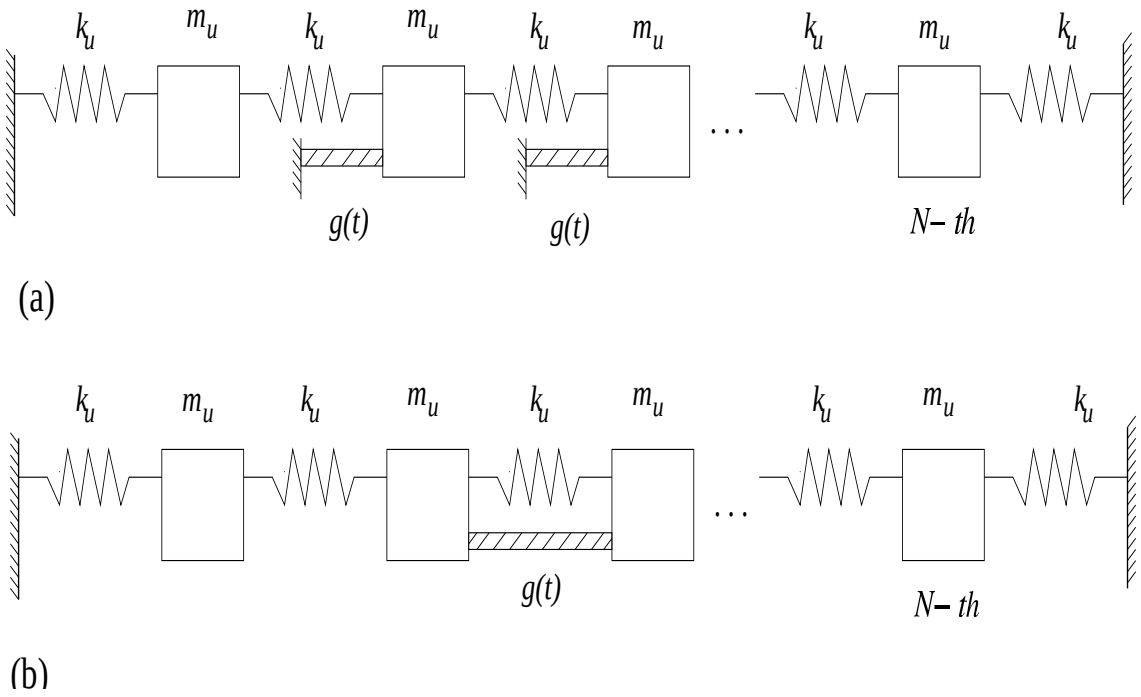

Figure 7.1: Linear array of N spring-mass oscillators, $N = 30$, $m_u = 1\,Kg$, $k_u = 4 \times 10^3 N/m$.

damping elements are associated with masses between the s-th and $(s+l)$-th ($N = 30$, $s = 8$ and $(s+l) = 17$ are taken for the numerical calculations). Damping shown in Figure 7.1(a) is described as 'locally reacting' and that in Figure 7.1(b) is called 'non-locally reacting'. The dissipative elements shown in Figure 7.1 are taken to be linear non-viscous dampers so that the equations of motion are described by (5.16). The two damping models considered in Chapter 5 are used. Here we seek to identify a symmetric viscous damping matrix using the modal data.

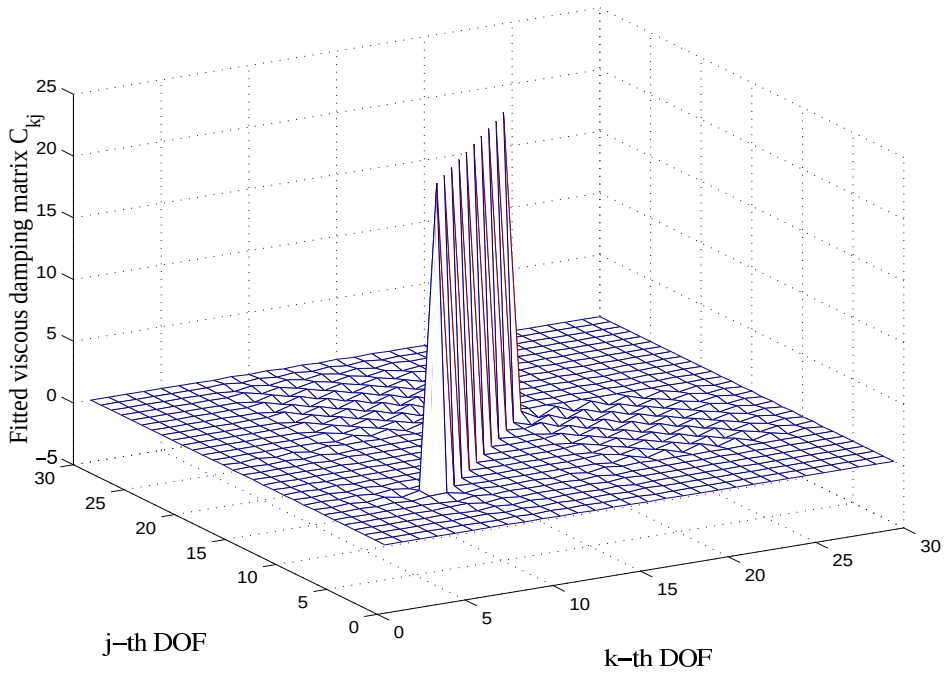

Figure 7.2: Fitted viscous damping matrix for the local case, $\gamma = 0.02$, damping model 2

Results for Small γ

When $\gamma = 0.02$ both damping models show near-viscous behaviour. In Section 5.4.1 it was shown that for this case the fitted viscous damping matrix is symmetric. For this reason, results obtained by using the symmetry preserving identification procedure developed in this paper must approach to the corresponding results obtained by using the procedure outlined in Chapter 5. Figure 7.2 shows the fitted viscous damping matrix for the local case using damping model 2. One immediately recognizes that this result is similar to its corresponding result shown in Figure 5.2. Figure 7.3 shows the fitted viscous damping matrix for non-local case using damping model 2. Again, the fitted matrix is similar to its corresponding case shown in Figure 5.5. Thus, when γ is small, the procure developed in the last section and that outlined in Chapter 5 yields similar result.

Results for Larger γ

When γ is larger the two non-viscous damping models depart from the viscous damping model. For this case, one obtains an asymmetric fitted viscous damping matrix following the procedure in Chapter 5. It is interesting to see how these results change when symmetry preserving method developed here is applied. Figure 7.4 shows the result of running the symmetry preserving fitting procedure for damping model 1 with locally-reacting damping and the full set of modes. The result of applying the usual viscous damping identification procedure corresponding to this case was shown before in Figure 5.7. Comparing the Figures 5.7 and 7.4 it may be observed that all the features of fitting in Figure 5.7, except asymmetry of the damping matrix, reappears in Figure 7.4. From the high non-zero values along the diagonal it is easy to identify the spatial location

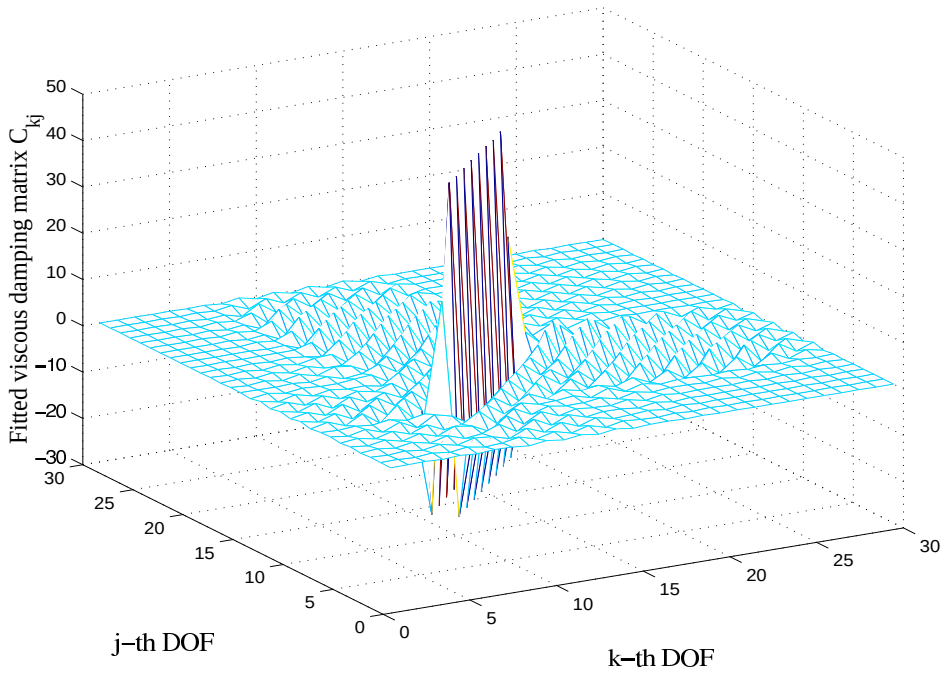

Figure 7.3: Fitted viscous damping matrix for the non-local case, $\gamma = 0.02$, damping model 2

of damping. Also observe that all non-zero off-diagonal elements have positive values. This implies that the damping mechanism maybe locally reacting. In order to understand what result the symmetry preserving fitting procedure yields when damping is significantly non-viscous we consider $\gamma = 2$ for damping model 1. Figure 7.5 shows the fitted viscous damping matrix for local case. The result corresponding to this without using the symmetry preserving method was before shown in Figure 5.9. Again, from Figure 7.5 the spatial distribution of damping can be guessed, however, the accuracy is reduced as the fitted model differs significantly from the actual damping model.

Figure 7.6 shows the symmetric fitted viscous damping matrix for damping model 2 corresponding to the case considered earlier in Figure 5.8. Comparing Figures 5.8 and 7.6, observations similar to the case of damping model 1 can be made. Consider now the effect of modal truncation on the symmetry preserving damping identification procedure. In practice, one might hope to be able to use only the first few modes of the system to identify the damping matrix. Figures 7.7 and 7.8 shows the fitted viscous damping matrix using, respectively, the first 20 and the first 10 modes only. The quality of the fitted damping matrix does not significantly deteriorate as the number of modes used to fit the damping matrix is reduced. This in turn implies that, if the fitted model (viscous in this case) is not close to the original one, then by using more modes in the symmetry preserving identification method does not significantly improve the result.

Figures 7.9 and 7.10 show the fitted symmetric viscous damping matrix for $\gamma = 0.5$ using the non-local damping model for damping model 1 and 2. Results corresponding to these obtained without the symmetry preserving method was shown in Figures 5.10 and 5.11. The spatial distri-

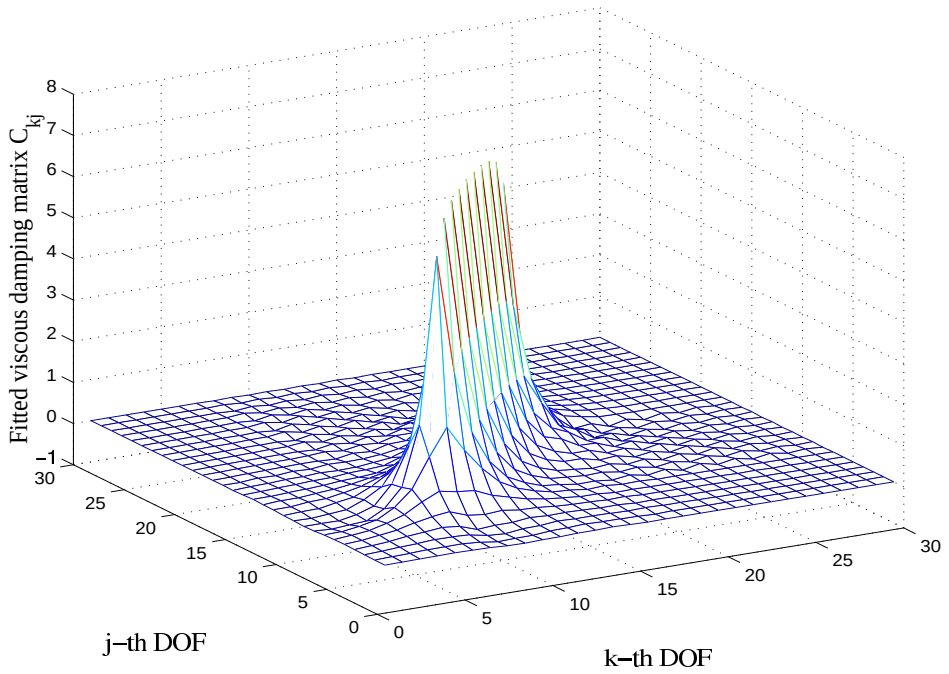

Figure 7.4: Fitted viscous damping matrix for the local case, $\gamma = 0.5$, damping model 1

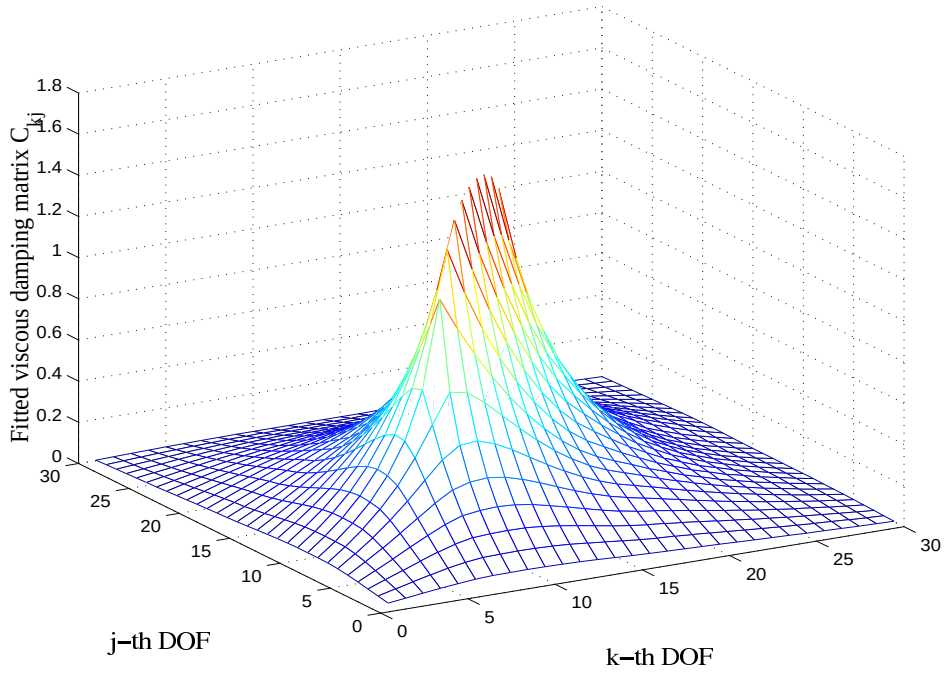

Figure 7.5: Fitted viscous damping matrix for the local case, $\gamma = 2.0$, damping model 1

bution of the damping is revealed quite clearly and correctly. In both cases, the non-local nature of the damping is hinted at by the strong negative values on either side of the main diagonal of the matrix.

Because the symmetry preserving method uses a constrained optimization approach, numerical accuracy of the fitting procedure might be lower compared to the procedure outlined in Chapter 5.

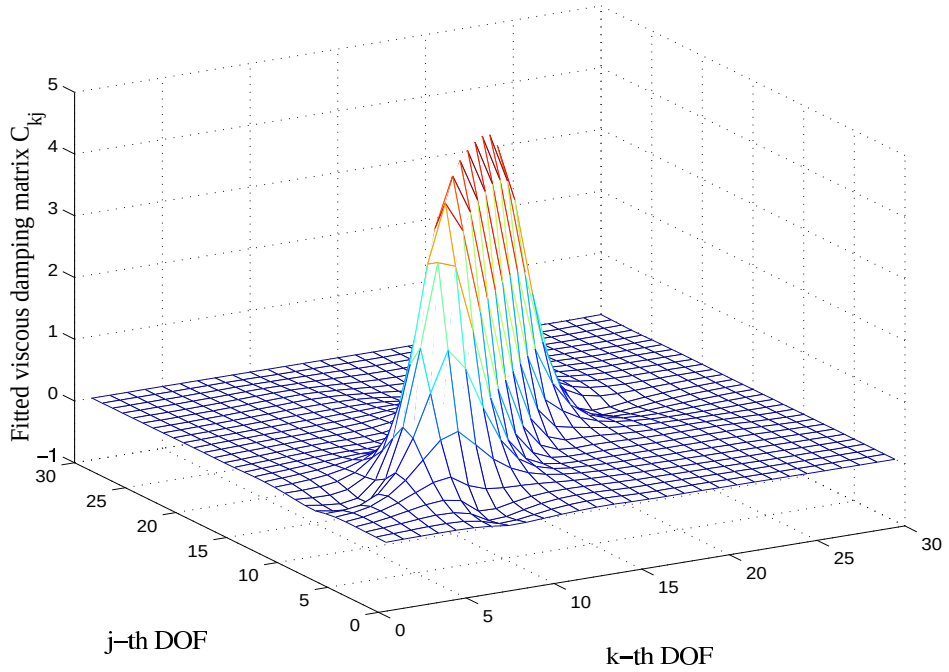

Figure 7.6: Fitted viscous damping matrix for the local case, $\gamma = 0.5$, damping model 2

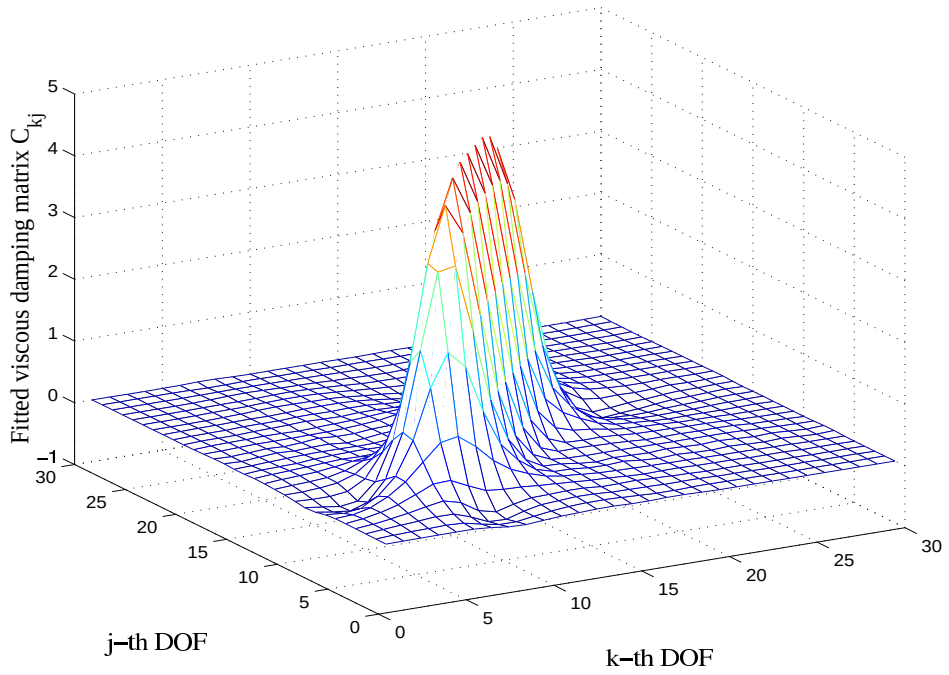

Figure 7.7: Fitted viscous damping matrix using first 20 modes for the local case, $\gamma = 0.5$, damping model 2

In order to check numerical accuracy we have reconstructed the transfer functions using the complex modes obtained by using the fitted viscous damping matrix. Comparison between a typical original and reconstructed transfer function $H_{kj}(\omega)$, for $k = 11$ and $j = 24$ is shown in Figure 7.11, based on locally-reacting damping using damping model 1. It is clear that the reconstructed

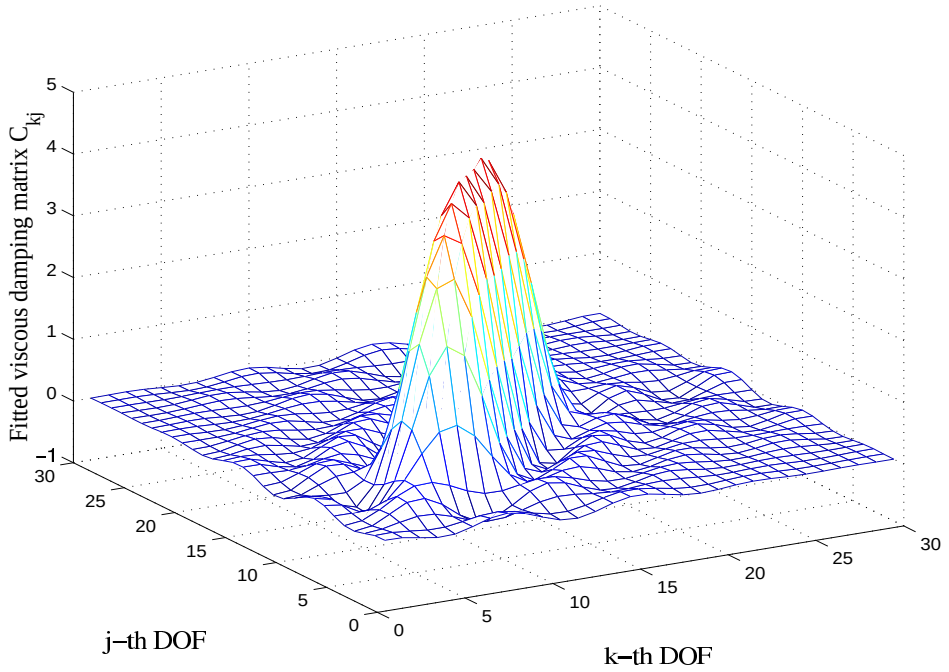

Figure 7.8: Fitted viscous damping matrix using first 10 modes for the local case, $\gamma = 0.5$, damping model 2

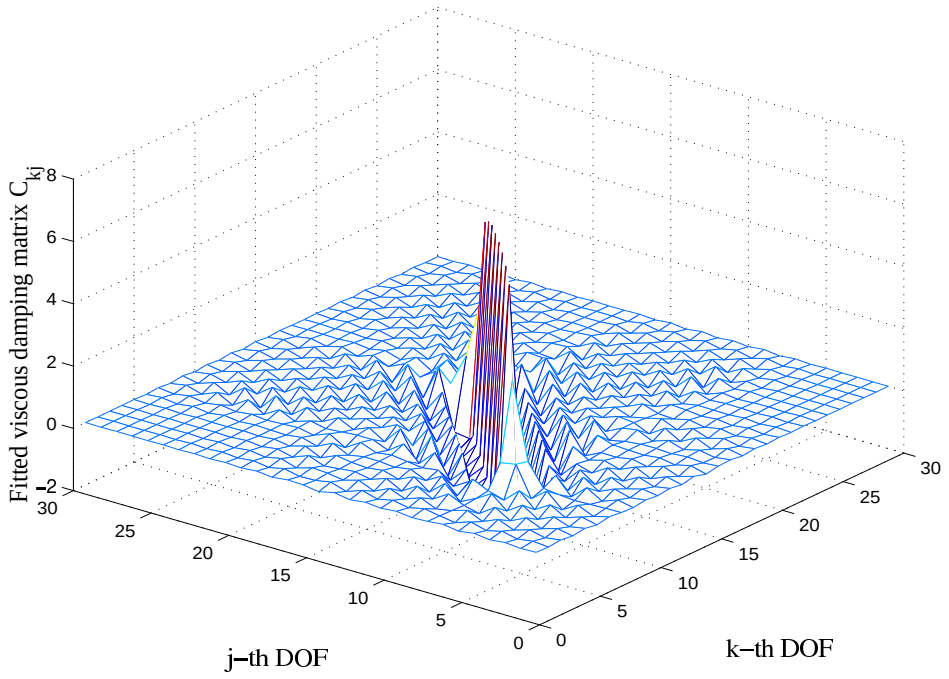

Figure 7.9: Fitted viscous damping matrix for the non-local case, $\gamma = 0.5$, damping model 1

transfer function agrees well with the original one. Thus the symmetry preserving viscous damping matrix identification method developed here does not introduce much error due to the applied constrains in the optimization procedure.

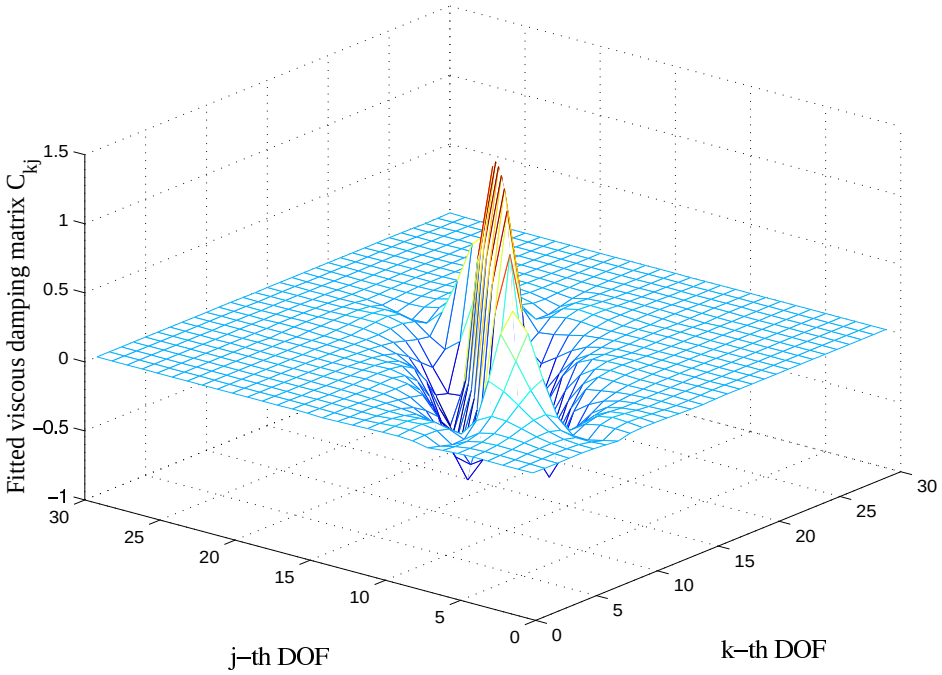

Figure 7.10: Fitted viscous damping matrix for the non-local case, $\gamma = 0.5$, damping model 2

7.3 Identification of Non-viscous Damping

7.3.1 Theory

As has been mentioned earlier, out of several non-viscous damping models the exponential function turns out to be the most plausible. In this section we outline a general method to fit an exponential model to measured data such that the resulting coefficient matrix remains symmetric. We assume that the mass matrix of the structure is known either directly from a finite element model or by means of modal updating. Also suppose that the damping has only one relaxation parameter, so that the matrix of the kernel functions is of the form

$$\boldsymbol{\mathcal{G}}(t) = \mu e^{-\mu t}\,\mathbf{C} \tag{7.28}$$

where μ is the relaxation parameter and $\mathbf{C}$ is the associated coefficient matrix. In Chapter 6 a method was proposed to obtain μ and $\mathbf{C}$ from measured complex modes and frequencies. This method may yield a $\mathbf{C}$ matrix which is not symmetric. In this section we develop a method which will always produce a symmetric $\mathbf{C}$ matrix.

The starting point of our discussion is equations (6.12) and (6.13), the expressions for the real and imaginary parts of the complex modes of a linear system with damping of the form (7.28). Assume that

$$\hat{\mathbf{X}} = [\hat{\mathbf{x}}_1, \hat{\mathbf{x}}_2, \cdots, \hat{\mathbf{x}}_m] \in \mathbb{R}^{N\times m} \tag{7.29}$$

is the matrix of *undamped mode shapes* and $\hat{\mu}$ is the relaxation parameter and m is the number of

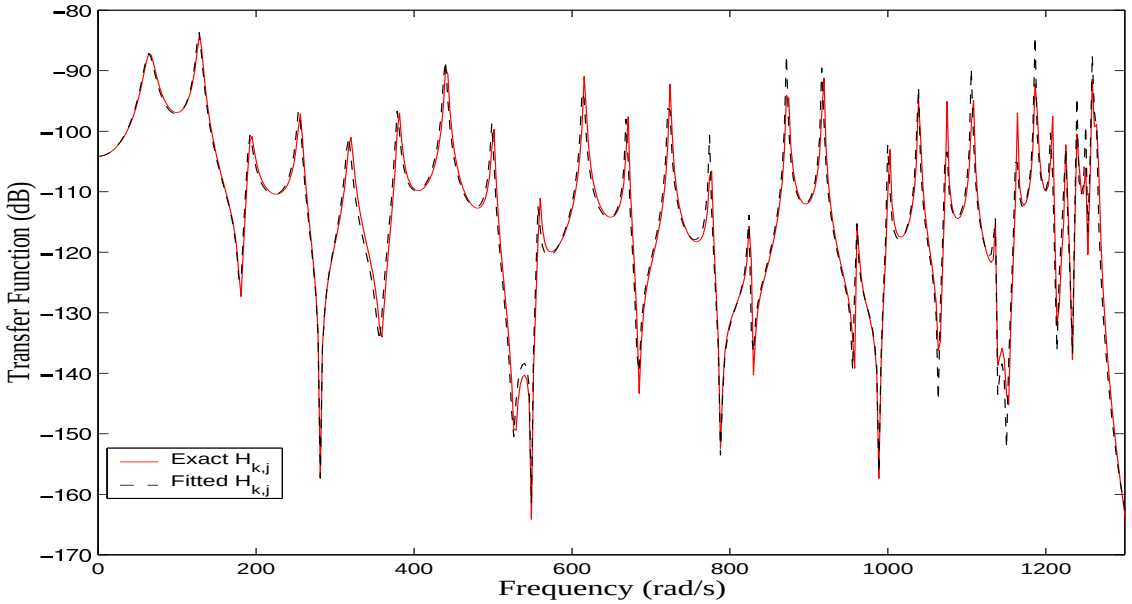

Figure 7.11: Transfer functions for the local case, $\gamma = 0.5$, damping model 1, $k = 11$, $j = 24$

modes retained in the study. Rewriting equations (6.12) and (6.13) one has

$$\hat{\mathbf{u}}_j = \Re(\hat{\mathbf{z}}_j) = \hat{\mathbf{x}}_j + \sum_{\substack{k=1 \\ k\neq j}}^{m} \frac{\hat{\mu}\hat{\omega}_j}{(\hat{\mu}^2 + \hat{\omega}_j^2)} B_{kj}\hat{\mathbf{x}}_k \tag{7.30}$$

and

$$\hat{\mathbf{v}}_j = \Im(\hat{\mathbf{z}}_j) = \sum_{\substack{k=1 \\ k\neq j}}^{m} f_j B_{kj}\hat{\mathbf{x}}_k; \quad \text{where} \quad f_j = \frac{\hat{\mu}^2}{(\hat{\mu}^2 + \hat{\omega}_j^2)}. \tag{7.31}$$

The unknown constants B_{kj} are defined before in equation (7.5). It may be noted that in addition to B_{kj}, the relaxation constant $\hat{\mu}$ and the undamped modes $\hat{\mathbf{x}}_k$ are also unknown. Combining the equations (7.30) and (7.31) one can write

$$\begin{aligned} \hat{\mathbf{x}}_j &= \hat{\mathbf{u}}_j - \frac{\hat{\omega}_j}{\hat{\mu}}\hat{\mathbf{v}}_j; \quad \forall j = 1, \cdots, m \\ \text{or} \quad \hat{\mathbf{X}} &= \hat{\mathbf{U}} - \frac{1}{\hat{\mu}}\left[\hat{\mathbf{V}}\hat{\mathbf{\Omega}}\right]. \end{aligned} \tag{7.32}$$

The relaxation constant $\hat{\mu}$ has to be calculated by following the procedure described in Chapter 6.

To ensure symmetry of the identified coefficient matrix the condition in (7.7) must hold. For this reason equations (7.9) and (7.11) are also applicable for this case. Now, the error from representing $\hat{\mathbf{v}}_j$ by the series sum (7.31) can be expressed as

$$\varepsilon_j = \hat{\mathbf{v}}_j - \sum_{k=1}^{m} f_j B_{kj}\hat{\mathbf{x}}_k \tag{7.33}$$

We need to minimize the above error subjected to the constraint in equation (7.9). The objective function can be formed using the Lagrange multipliers like equation (7.13). To obtain the unknown

coefficients B_{jk} using equation (7.14) one has

$$\begin{aligned} &-2\hat{\mathbf{x}}_r^T\left(\hat{\mathbf{v}}_s-\sum_{k=1}^{m} f_s B_{ks}\hat{\mathbf{x}}_k\right)++\left[\phi_{rs}+\phi_{sr}\right]\hat{\omega}_r=0 \\ \text{or}\quad &\sum_{k=1}^{m}\left(\hat{\mathbf{x}}_r^T\hat{\mathbf{x}}_k\right)f_s B_{ks}+\frac{1}{2}\left[\hat{\omega}_r\phi_{rs}+\hat{\omega}_r\phi_{sr}\right]=\hat{\mathbf{x}}_r^T\hat{\mathbf{v}}_s;\quad \forall r,s=1,\cdots,m \end{aligned} \tag{7.34}$$

The above set of equations can be combined in a matrix form and can be conveniently expressed as

$$\mathbf{W_1 B F}+\frac{1}{2}\left[\hat{\mathbf{\Omega}}\mathbf{\Phi}+\hat{\mathbf{\Omega}}\mathbf{\Phi}^T\right]=\mathbf{D_1}. \tag{7.35}$$

where the $m\times m$ matrices

$$\begin{aligned} \mathbf{W_1} =&\hat{\mathbf{X}}^T\hat{\mathbf{X}} \\ \mathbf{D_1} =&\hat{\mathbf{X}}^T\hat{\mathbf{V}} \\ \mathbf{F} =&\text{diag}(f_1,f_2,\cdots,f_m). \end{aligned} \tag{7.36}$$

Equation (7.35) needs to be solved with the symmetry condition (7.11). To eliminate $\mathbf{\Phi}$, postmultiplying (7.35) by $\hat{\mathbf{\Omega}}$ and premultiplying its transpose by by $\hat{\mathbf{\Omega}}$ and subtracting we obtain

$$\mathbf{W_1 B F}\hat{\mathbf{\Omega}}-\hat{\mathbf{\Omega}}\mathbf{F}^T\mathbf{B}^T{\mathbf{W_1}}^T=\mathbf{D_1}\hat{\mathbf{\Omega}}-\hat{\mathbf{\Omega}}{\mathbf{D_1}}^T. \tag{7.37}$$

Substitution of $\mathbf{B}^T$ from (7.20) in the above equation and premultiplication by $\hat{\mathbf{\Omega}}^{-1}$ results

$$\hat{\mathbf{\Omega}}^{-1}\mathbf{W_1 B F}\hat{\mathbf{\Omega}}+\mathbf{F}^T\hat{\mathbf{\Omega}}\mathbf{B}\hat{\mathbf{\Omega}}^{-1}{\mathbf{W_1}}^T=\hat{\mathbf{\Omega}}^{-1}\mathbf{D_1}\hat{\mathbf{\Omega}}-{\mathbf{D_1}}^T. \tag{7.38}$$

Observe from equation (7.36) that $\mathbf{W_1}$ is a symmetric matrix and $\mathbf{F}$ is diagonal matrix. Now denote

$$\begin{aligned} \mathbf{Q_1} =&\hat{\mathbf{\Omega}}^{-1}\mathbf{W_1}=\hat{\mathbf{\Omega}}^{-1}{\mathbf{W_1}}^T \\ \mathbf{P_1} =&\hat{\mathbf{\Omega}}^{-1}\mathbf{D_1}\hat{\mathbf{\Omega}}-{\mathbf{D_1}}^T \\ \mathbf{H} =&\mathbf{F}\hat{\mathbf{\Omega}}=\mathbf{F}^T\hat{\mathbf{\Omega}}. \end{aligned} \tag{7.39}$$

Using above definitions equation (7.38) reads

$$\mathbf{Q_1 B H}+\mathbf{H B Q_1}=\mathbf{P_1}. \tag{7.40}$$

This equation is similar to equation (7.23) obtained for the viscously damped case and can be solved using a similar procedure by taking vec of both sides. The procedures to be followed later to obtain the coefficient matrix $\mathbf{C}$ also remain similar to the viscously damped case. In summary the method can be implemented by the following steps:

1. Measure a set of transfer functions $H_{ij}(\omega)$ at a set of N grid points. Fix the number of modes to be retained in the study, say m. Determine the complex natural frequencies $\hat{\lambda}_j$ and complex mode shapes $\hat{\mathbf{z}}_j$ from the transfer function, for all $j=1,\cdots m$. Denote $\hat{\mathbf{Z}}=[\hat{\mathbf{z}}_1,\hat{\mathbf{z}}_2,\cdots\hat{\mathbf{z}}_m]\in\mathbb{C}^{N\times m}$ the complex mode shape matrix.

2. Set the 'undamped natural frequencies' as $\hat{\omega}_j = \Re(\hat{\lambda}_j)$. Denote the diagonal matrix $\hat{\mathbf{\Omega}} = \text{diag}(\hat{\omega}_1, \hat{\omega}_2, \cdots, \hat{\omega}_m) \in \mathbb{R}^{m\times m}$.
3. Separate the real and imaginary parts of $\hat{\mathbf{Z}}$ to obtain $\hat{\mathbf{U}} = \Re\left[\hat{\mathbf{Z}}\right]$ and $\hat{\mathbf{V}} = \Im\left[\hat{\mathbf{Z}}\right]$.
4. Obtain the relaxation parameter $\hat{\mu} = \dfrac{\hat{\omega}_1 \hat{\mathbf{v}}_1^T \mathbf{M} \hat{\mathbf{v}}_1}{\hat{\mathbf{v}}_1^T \mathbf{M} \hat{\mathbf{u}}_1}$.
5. Calculate the diagonal matrix $\mathbf{F} = \text{diag}\left(\frac{\hat{\mu}^2}{(\hat{\mu}^2+\hat{\omega}_j^2)}\right) \in \mathbb{R}^{m\times m}$.
6. Obtain the 'undamped modal matrix' $\hat{\mathbf{X}} = \hat{\mathbf{U}} - \dfrac{1}{\hat{\mu}}\left[\hat{\mathbf{V}}\hat{\mathbf{\Omega}}\right]$.
7. From these evaluate the $m \times m$ matrices $\mathbf{W_1} = \hat{\mathbf{X}}^T\hat{\mathbf{X}}$, $\mathbf{D_1} = \hat{\mathbf{X}}^T\hat{\mathbf{V}}$, $\mathbf{Q_1} = \hat{\mathbf{\Omega}}^{-1}\mathbf{W_1}$, $\mathbf{P_1} = \hat{\mathbf{\Omega}}^{-1}\mathbf{D_1}\hat{\mathbf{\Omega}} - \mathbf{D_1}^T$ and $\mathbf{H} = \mathbf{F}\hat{\mathbf{\Omega}}$.
8. Now denote $\mathbf{p_1} = \text{vec}\,(\mathbf{P_1}) \in \mathbb{R}^{m^2}$ and calculate $\mathbf{R_1} = (\mathbf{H} \otimes \mathbf{Q_1}) + \left(\mathbf{Q_1}^T \otimes \mathbf{H}\right) \in \mathbb{R}^{m^2\times m^2}$.
9. Evaluate $\text{vec}\,(\mathbf{B}) = [\mathbf{R_1}]^{-1}\,\mathbf{p_1}$ and obtain the matrix $\mathbf{B}$.
10. From the $\mathbf{B}$ matrix get $C'_{kj} = \dfrac{(\hat{\omega}_j^2 - \hat{\omega}_k^2)B_{kj}}{\hat{\omega}_j}$ for $k \neq j$ and $C'_{jj} = 2\Im(\hat{\lambda}_j)$.
11. Finally, carry out the transformation $\mathbf{C} = \left[\left(\hat{\mathbf{X}}^T\mathbf{X}\right)^{-1}\hat{\mathbf{X}}^T\right]^T \mathbf{C}' \left[\left(\hat{\mathbf{X}}^T\hat{\mathbf{X}}\right)^{-1}\hat{\mathbf{X}}^T\right]$ to get the damping matrix in physical coordinates.

7.3.2 Numerical Examples

We again consider the systems shown in Figure 7.1 to illustrate symmetry preserving fitting of exponential damping models outlined in last subsection. Three damping models, given by equations (6.21), (6.21) and (6.23) will be considered. Recall that the relaxation parameter has to be obtained by the procedure outlined in Chapter 6. So here we will only discuss fitting of the coefficient matrix.

Results for Small γ

It has been mentioned before that when γ is small, the ordinary viscous damping identification method (in Chapter 5), non-viscous damping identification method (in Chapter 6) and symmetry preserving viscous damping identification method (in Section 7.2) yields same result. This is because all the non-viscous damping models approach to a viscous damping model for small value of γ. Since the viscous damping model is a special case of the exponential damping model, we expect this method to produce results like the three previous methods. Figure 7.12 shows the fitted coefficient matrix of the exponential model for damping model 2, calculated using the complete set of 30 modes. It is clear that this result is similar to the corresponding result obtained in Figure 6.8

without using the symmetry preserving method. Figure 7.13 shows the fitted coefficient matrix for damping model 2 for the non-local case using the symmetry preserving method. Again, comparing it with Figure 6.9 one observes that they are similar. Thus, when γ is small the symmetry preserving method for fitting the coefficient matrix for the exponential function and the method described in Chapter 6 yields similar results.

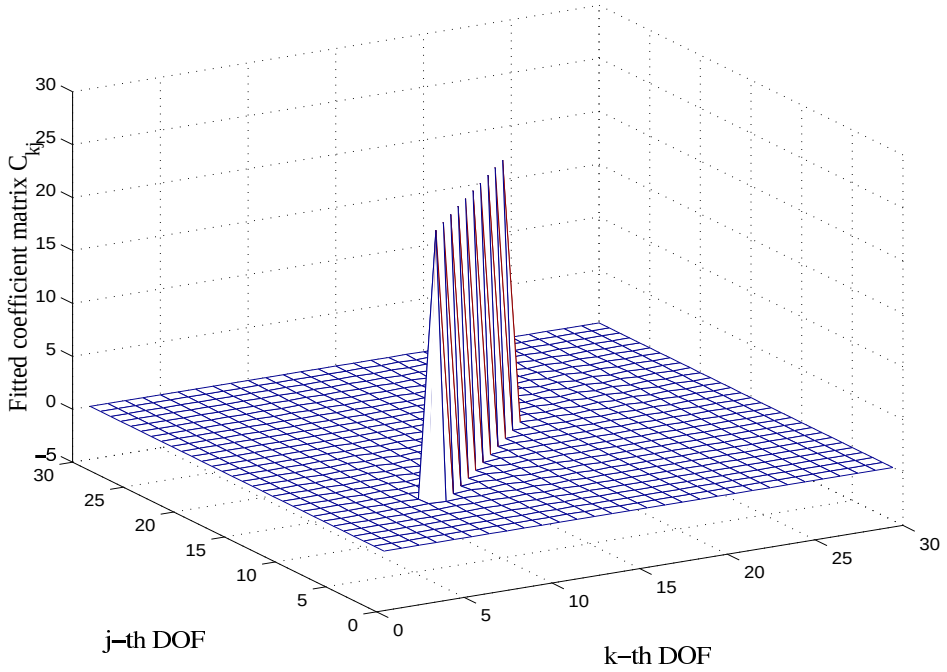

Figure 7.12: Fitted coefficient matrix of exponential model for the local case, $\gamma = 0.02$, damping model 2

Results for Larger γ

When γ is larger the two non-exponential damping models depart from the exponential damping model. Like previous examples, we consider $\gamma = 0.5$. For this case, in Chapter 6 it was observed that the identification method proposed there results an asymmetric coefficient matrix. The degree of asymmetry of the fitted coefficient depends on how much the original damping model deviates from the identified exponential model. Specifically, it was concluded that if variation of μ_j with j calculated using equation (6.17) is more, then the fitted coefficient matrix is likely to be more asymmetric. In this section we want to understand how the proposed method overcomes this problem and what one could tell from the identified coefficient matrix about the nature of damping. Figure 7.14 shows the fitted symmetric coefficient matrix for the local case with damping model 2. The result corresponding to this without using the symmetry preserving method was shown before in Figure 6.11. Comparison of these two figures clearly demonstrates the advantage of the proposed symmetry preserving method. The identified coefficient matrix is not only symmetric, but also the correct spatial location of damping can be deduced from the peak along the diagonal.

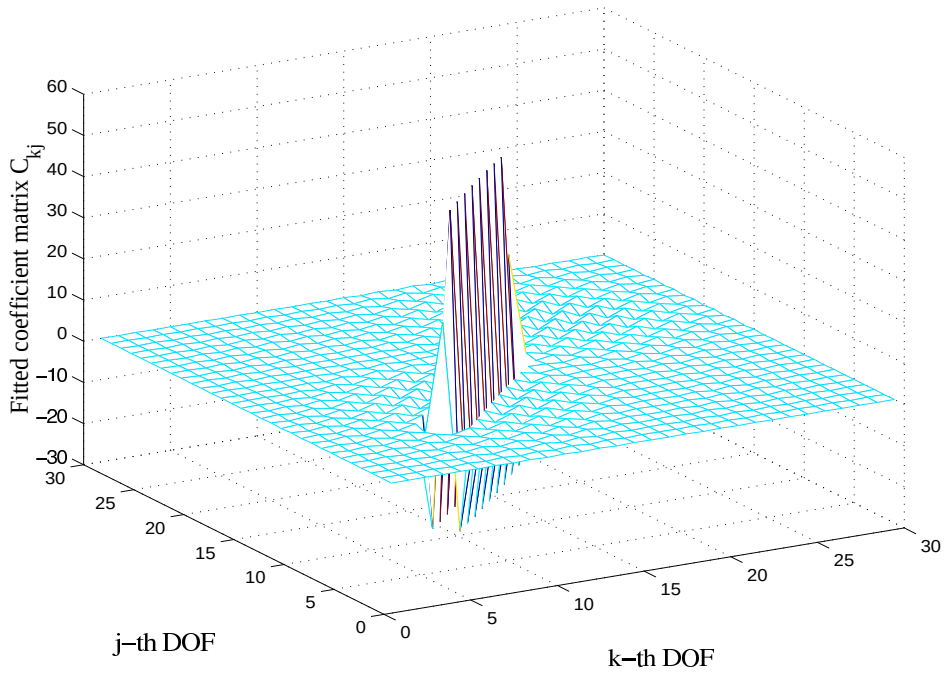

Figure 7.13: Fitted coefficient matrix of exponential model for the non-local case, $\gamma = 0.02$, damping model 2

Besides, predominantly positive values of the off-diagonal entries of the fitted coefficient matrix indicate that damping is locally reacting.

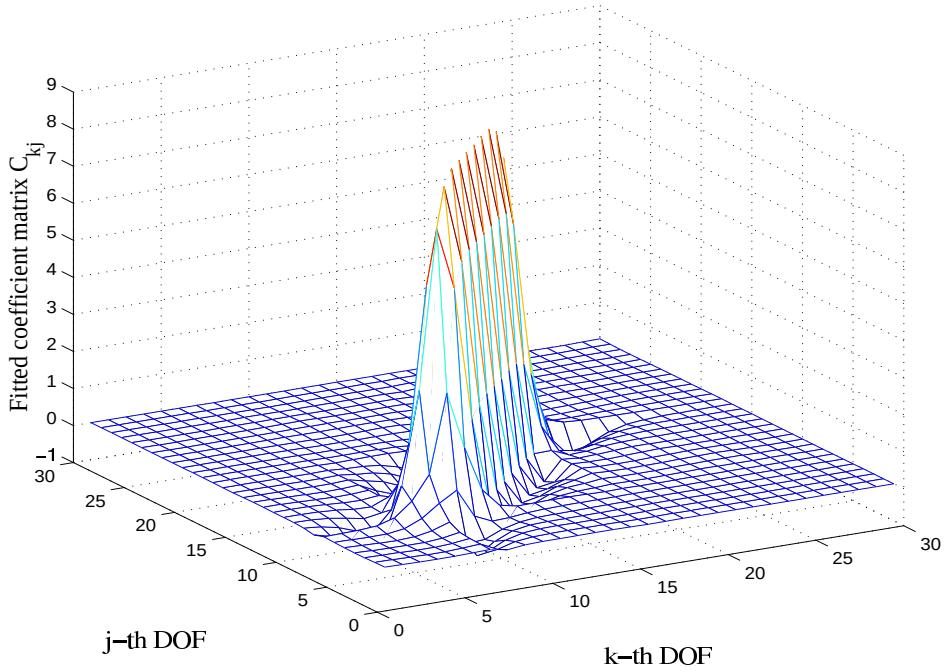

Figure 7.14: Fitted coefficient matrix of exponential model for the local case, $\gamma = 0.5$, damping model 2

To demonstrate the efficacy of the proposed method we consider a further larger value of γ.

Figure 7.15 shows the fitted coefficient matrix of the exponential function *without* using the symmetry preserving method for damping model 2 with $\gamma = 2.0$ and local case. Clearly, the large variation of μ_j with j, shown in Figure 7.16, is the reason for significant asymmetry of the fitted coefficient matrix. Application of the symmetry preserving method for this case is shown in Figure 7.17. In spite of large off-diagonal activity one can still guess about the position of damping. Again, like Figure 7.14, non-negative values of the off-diagonal entries indicate that damping is of local type.

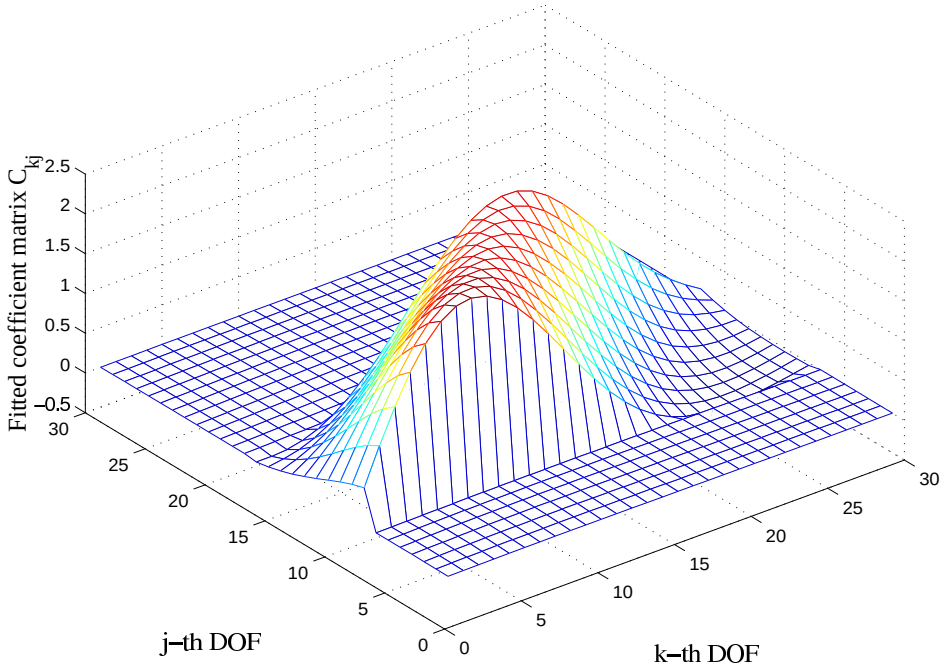

Figure 7.15: Fitted coefficient matrix of exponential model without using the symmetry preserving method for the local case, $\gamma = 2.0$, damping model 2

The fitted coefficient matrix for the local case with a double exponential damping model (model 3) with $\gamma = 0.5$ using the procedure outlined in Chapter 6 was shown in Figure 6.13. Observe that this matrix is not asymmetric as the corresponding variation of μ_j with j, shown in Figure 6.6, is small. Thus, application of the symmetry preserving method will not be significantly different from the result obtained using the procedure in Chapter 6 and may be verified from Figure 7.18.

Finally we turn our attention to the non-local case. Figure 7.19 shows the fitted coefficient matrix for non-local case with damping model 2 and $\gamma = 0.5$. Again, improvement of the fitted coefficient matrix may be observed by comparing it with Figure 6.14.

7.4 Conclusions

In this chapter a method is proposed to preserve symmetry of the identified damping matrix. Both viscous and non-viscous damping models are considered. For fitting a viscous damping model

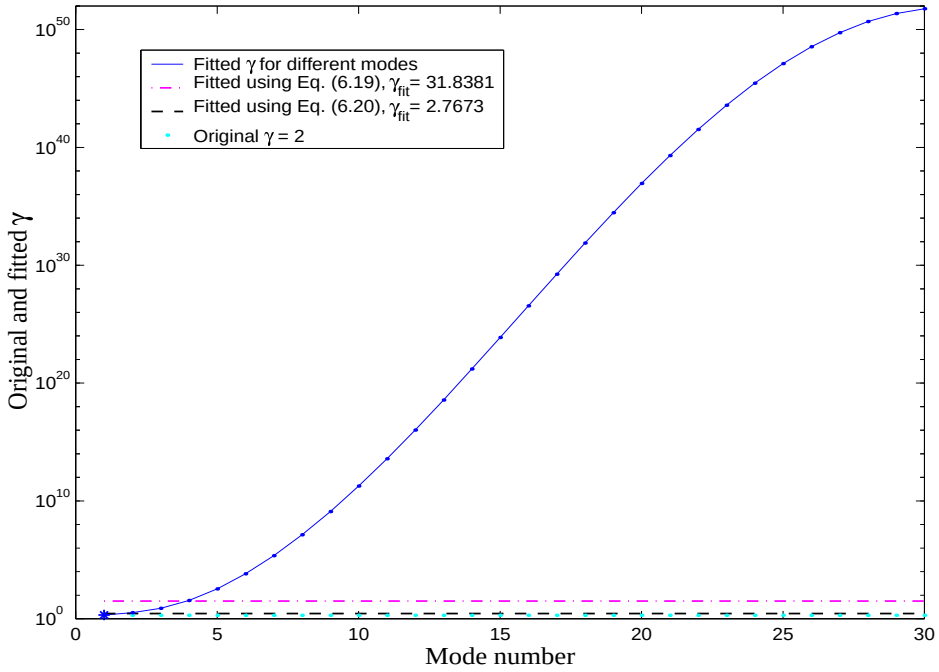

Figure 7.16: Values of $\hat{\gamma}$ obtained from different $\hat{\mu}$ calculated using equations (6.18)–(6.20) for the local case, damping model 2

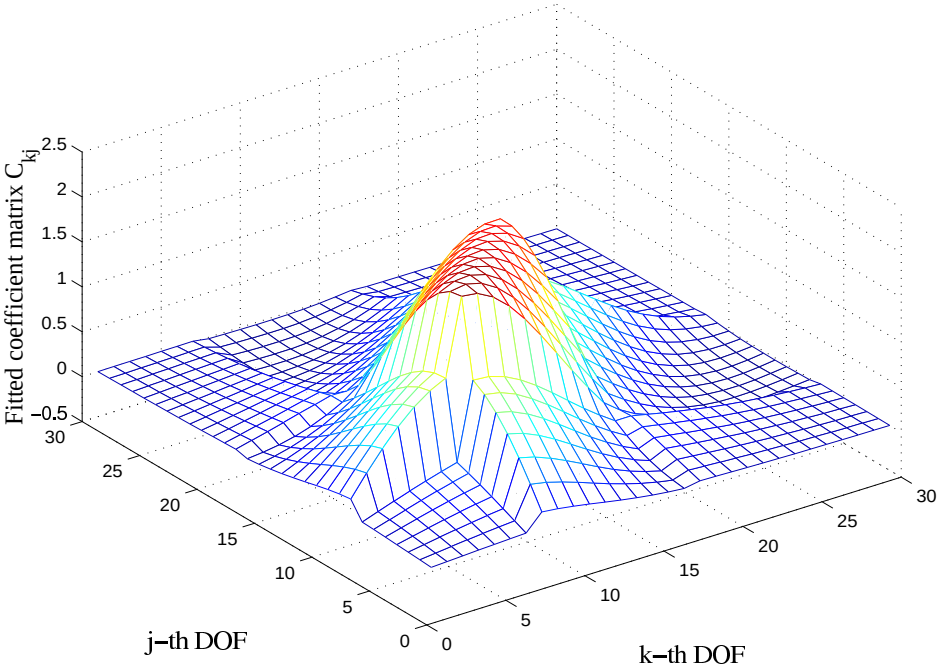

Figure 7.17: Fitted coefficient matrix of exponential model using the symmetry preserving method for the local case, $\gamma = 2.0$, damping model 2

only complex natural frequencies and mode shapes are required. To fit a non-viscous model, in addition to the modal data, knowledge of the mass matrix is also required. However, availability of the complete set of modal data is not a requirement of these methods. The proposed methods utilize a least-square error minimization approach together with a set of constraints which guaran-

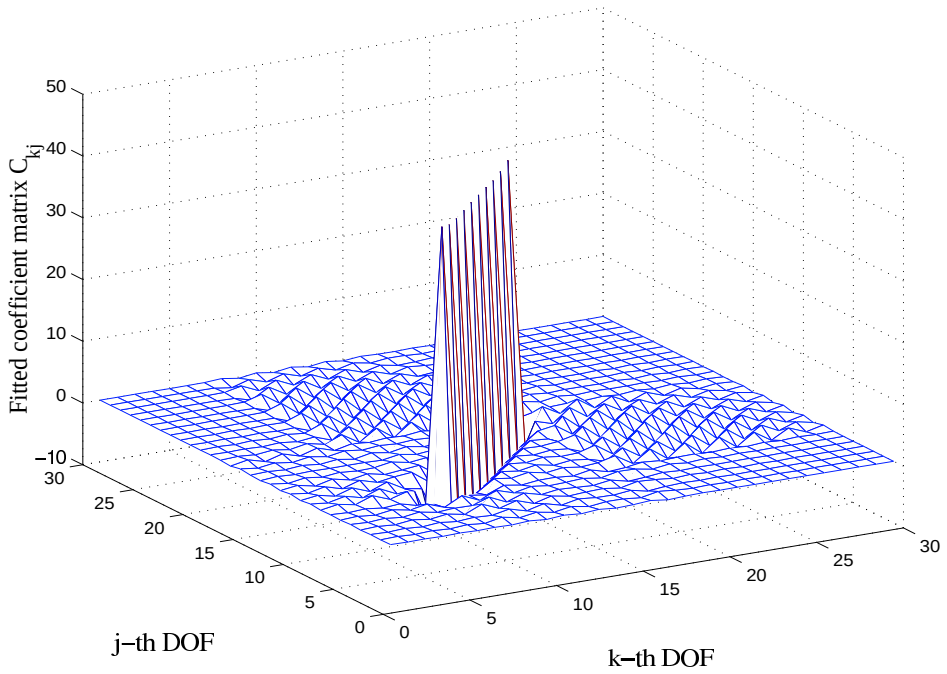

Figure 7.18: Fitted coefficient matrix of exponential model for the local case, $\gamma = 0.5$, damping model 3

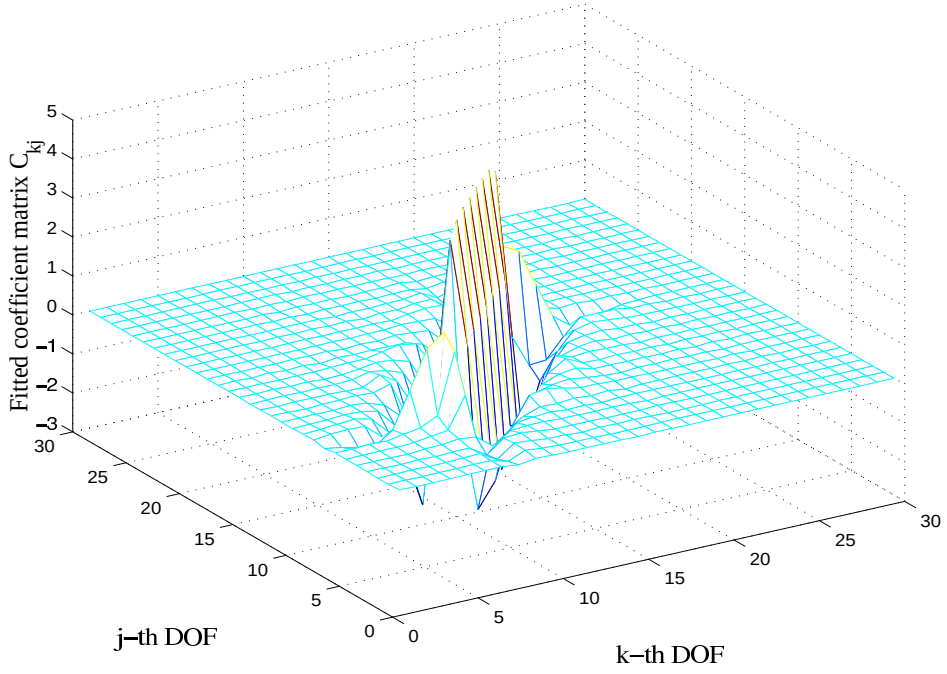

Figure 7.19: Fitted coefficient matrix of exponential model for the non-local case, $\gamma = 0.5$, damping model 2

tee symmetry of the fitted damping matrix. It was shown that, for the cases when application of the usual damping identification methods described in Chapters 5 and 6 produces an asymmetric matrix, this method not only fits a symmetric matrix but also all the other useful information about the systems damping properties are preserved.

Chapter 8

Experimental Identification of Damping

8.1 Introduction

In the last three Chapters several methods have been proposed to identify damping in a vibrating structure. The purpose of this Chapter is to verify some of the developed theories by conducting vibration experiments. Unlike mass and stiffness properties, damping is a purely dynamic property of a system, *i.e.*, damping can be measured only by conducting dynamic testing on a structure.

A description of a mechanical structure requires knowledge of the geometry, boundary conditions and material properties. The mass and stiffness matrices of a structure with complicated geometry, boundary conditions and material properties can be obtained experimentally or numerically (for example, using the finite-element method). Unfortunately, present knowledge of damping does not allow us to obtain the damping matrix like the mass and stiffness matrices for complicated systems. For this reason we consider simple systems for which geometry, boundary conditions and material properties are easy to determine. Specifically, a *free-free uniform beam* in bending vibration is considered in this Chapter to implement and verify the damping identification procedures developed so far in this dissertation. Details of the beam experiment will follow in Section 8.3.

The damping identification procedures developed in Chapters 5, 6 and 7 rely on complex natural frequencies and mode shapes. For lightly damped structures, complex natural frequencies can be expressed in terms of undamped natural frequencies and modal Q-factors. Natural frequencies, Q-factors and mode shapes are collectively called *modal parameters* or *modal data*. It should be noted that, in the context of general multiple-degree-of-freedom systems, these modal parameters can not be directly measured by conducting a vibration experiment. Typically one measures time histories of the responses at different degrees of freedom together with time histories of the input forces. The *transfer functions* of a system can be obtained by taking ratios of Fourier transforms of output time histories to that of corresponding input time histories. The modal parameters of a structure can be extracted from a set of transfer functions obtained in this way. The subject which deals with extraction of modal parameters is called *experimental modal analysis*. We refer to the books by Ewins (1984) and Maia and Silva (1997) for further details on experimental modal analysis. It

should be mentioned that the underlying theory behind experimental modal analysis explicitly or implicitly assumes that damping is viscous. It is legitimate to ask the question: what happens if the damping of the system is not viscous – does the conventional experimental modal analysis methodology extract correct modal parameters? In the next section we address this question and propose a generic method to extract modal parameters of generally damped multiple-degrees-of-freedom linear systems.

8.2 Extraction of Modal Parameters

It was mentioned that the starting point of extracting modal parameters is transfer functions. A transfer function $H_{jn}(\omega)$ is defined as

$$H_{jn}(\omega) = \frac{u_j(\omega)}{f_n(\omega)} \tag{8.1}$$

where $u_j(\omega)$ is the response at j-th degree of freedom and $f_n(\omega)$ is the applied force at n-th degree of freedom. A closed-form exact expression of the transfer function matrix of a generally damped N-degrees-of-freedom linear systems was obtained in Section 3.3. Taking the jn-th element of the transfer function matrix given by equation (3.65) one has

$$H_{jn}(\omega) = \sum_{k=1}^{N} \left[\frac{R_{k_{jn}}}{\mathrm{i}\omega - s_k} + \frac{R^*_{k_{jn}}}{\mathrm{i}\omega - s^*_k} \right] + \sum_{j=2N+1}^{m} \frac{R_{k_{jn}}}{\mathrm{i}\omega - s_k}. \tag{8.2}$$

In the above expression $R_{k_{jn}}$ is the jn-th element of the residue matrix corresponding to pole s_k. From equation (3.64) one obtains the relationship between residues $R_{k_{jn}}$ and mode shapes as

$$R_{k_{jn}} = \gamma_k z_{nk} z_{jk} \tag{8.3}$$

where z_{nk} is the n-th element of k-the mode shape and γ_k, the normalization constant of k-th mode, was defined in equation (3.66). The poles are related to natural frequencies λ_k by

$$s_k = \mathrm{i}\lambda_k. \tag{8.4}$$

In Chapter 3 it was mentioned that the first part of the right hand side of equation (8.2) corresponds to elastic modes and the second part corresponds to non-viscous modes. In general, elastic modes are complex in nature as damping is non-proportional. For an N-degree-of-freedom linear system, N elastic modes together with their complex conjugates correspond to N physical vibration modes. For lightly damped systems, the complex natural frequencies corresponding to the elastic modes have the form

$$\lambda_k \approx \omega_k + \mathrm{i}\frac{\omega_k}{2Q_k}. \tag{8.5}$$

In the above equation ω_k is the k-th undamped natural frequency and Q_k is the k-th Q-factor. The Q-factors or quality factors, reciprocal of twice the damping ratios, are expressed as

$$Q_k \approx \frac{\Re(\lambda_k)}{2\Im(\lambda_k)} = \frac{1}{2\zeta_k} \tag{8.6}$$

where ζ_k are damping ratios. If the damping is sufficiently light then all the elastic modes are sub-critically damped, *i.e.*, all of them are oscillatory in nature. In this case the transfer functions of a system has 'peaks' corresponding to all the elastic modes. The natural frequencies (ω_k) and the Q-factors (Q_k) can be obtained by examining each peak separately, for example using the circle fitting method (see Ewins, 1984). Estimation of ω_k and Q_k is likely to be good if the peaks are well separated.

For passive systems, the kind of systems we mostly encounter in practice, non-viscous modes are usually over-critically damped. Thus, in contrast to elastic modes, they do not produce any peaks in the transfer functions. As a consequence to this, the modal parameters corresponding to non-viscous modes cannot be obtained by usual techniques of experimental modal analysis as discussed above. This is the fundamental difficulty in applying conventional experimental modal analysis procedure to non-viscously damped systems. However, as shown through an example in Section 3.7.1, the non-viscous part of the response may be quite small compared to that of the elastic part. Thus, for practical purposes the second part of the right hand side of equation (8.2) may be neglected. In that case, the transfer functions of generally damped systems can be represented in way similar to viscously damped systems, that is,

$$H_{jn}(\omega) \approx \sum_{k=1}^{N} \left[\frac{R_{k_{jn}}}{\mathrm{i}\omega - s_k} + \frac{R^*_{k_{jn}}}{\mathrm{i}\omega - s^*_k} \right]. \tag{8.7}$$

Once equation (8.7) is assumed as the expression for transfer functions, conventional experimental modal analysis procedure may be applied to deal with non-viscously damped systems. This, analysis justifies that the conventional experimental modal analysis procedure, which *a priori* assumes the viscous damping model, indeed measures modal parameters of a system even when it is non-viscously damped. Next, assuming the validity of equation (8.7) a linear-nonlinear optimization approach is presented to extract complex modal parameters of non-viscously damped multiple-degrees-of-freedom linear systems.

8.2.1 Linear Least-Square Method

From equation (8.7) it is easy to observe that $H_{jn}(\omega)$ is a linear function of the residues while it is a nonlinear function of the poles. On the basis of this fact, it is legitimate to separate the extraction procedure for the poles and the residues. We propose a linear least-square approach to obtain the residues and a non-linear optimization approach to obtain the poles. Recently Duffour (1998) has proposed a similar method by considering all the residues to be real. His approach is equivalent to assuming that the systems is proportionally damped and consequently it yields real normal modes. In this section we extend this method to identify complex residues in order to extract complex modes.

Depending on what quantity is measured, the transfer functions can be (a) displacement transfer functions (receptance), (b) velocity transfer functions (mobility), and (c) acceleration transfer

functions (accelerance). Substituting s_k from equation (8.4), in a more general form, the transfer functions given by equation (8.7) may be expressed as

$$\begin{aligned} H_{jn}(\omega) &\approx (\mathrm{i}\omega)^r \sum_{k=1}^{N} \left[\frac{R_{k_{jn}}}{\mathrm{i}\omega - \mathrm{i}\lambda_k} + \frac{R^*_{k_{jn}}}{\mathrm{i}\omega + \mathrm{i}\lambda^*_k} \right] \\ &= (\mathrm{i}\omega)^r \sum_{k=1}^{N} \left[-\frac{\mathrm{i}R_{k_{jn}}}{\omega - \lambda_k} + \frac{\left(\mathrm{i}R_{k_{jn}}\right)^*}{\omega + \lambda^*_k} \right] \end{aligned} \tag{8.8}$$

where

- $r = 0$ corresponds to displacement transfer functions
- $r = 1$ corresponds to velocity transfer functions
- $r = 2$ corresponds to acceleration transfer functions.

Since the systems we consider are reciprocal, the transfer function matrix and consequently the residue matrix corresponding to each pole is symmetric, that is $R_{k_{jn}} = R_{k_{nj}}$. For this reason evaluation of the upper or lower half of the transfer function matrix is sufficient. However, most often only one row of the transfer matrix is measured in practice. For example, if one uses an impulse hammer for the excitation, then often the response measurement point is kept fixed while the excitation point varies according to an *a priori* selected grid on a structure. Thus, in equation (8.8) , j is fixed with its value equals to the degree of freedom of the response measurement point. Suppose the number of channels (*i.e.*, DOF of the system) is N and the number of modes retained in the study is m. Usually $m \leq N$. For brevity, omitting the subscript j, from equation (8.8) we obtain

$$H_n(\omega) \approx \sum_{k=1}^{m} \left[f_{1_k}(\omega) A_{kn} + f_{2_k}(\omega) A^*_{kn} \right]; \quad \forall\, n = 1, 2, \cdots, N \tag{8.9}$$

where

$$f_{1_k}(\omega) = -\frac{(\mathrm{i}\omega)^r}{\omega - \lambda_k} \tag{8.10}$$

$$f_{2_k}(\omega) = \frac{(\mathrm{i}\omega)^r}{\omega + \lambda^*_k} \tag{8.11}$$

$$A_{kn} = \mathrm{i}R_{k_{jn}}. \tag{8.12}$$

8.2.2 Determination of the Residues

Suppose $Y_n(\omega), \forall\, n = 1, 2, \cdots, N$ are set of the measured transfer functions corresponding to all the channels. We assume that initial estimates of $\omega_k, Q_k, \forall\, k = 1, 2, \cdots, m$ are known, for example using a circle fitting method. Thus, from equations (8.5), (8.10) and (8.11) it is clear that the complex functions $f_{1_k}(\omega)$ and $f_{2_k}(\omega)$ are known for all ω. Our aim is to obtain the matrix $\mathbf{A} : \{A_{kn}\} \in \mathbb{C}^{m \times N}$ such that the error in representing $Y_n(\omega)$ by equation (8.9) is minimized.

We define the frequency dependent error as

$$\varepsilon_n(\omega) = Y_n(\omega) - H_n(\omega). \tag{8.13}$$

Based on this, further define the *merit function* as

$$\begin{aligned}\chi^2 &= \sum_{n=1}^{N} \int_{\omega\in\Omega} |\varepsilon_n(\omega)|^2 \mathrm{d}\omega \\ &= \sum_{n=1}^{N} \int_{\omega\in\Omega} \varepsilon_n(\omega)\varepsilon_n^*(\omega)\mathrm{d}\omega\end{aligned} \tag{8.14}$$

where Ω is the range of frequency over which the transfer functions are obtained. To obtain A_{kn} by the error minimization approach, set

$$\frac{\partial \chi^2}{\partial A_{pq}} = 0; \quad \forall p = 1, \cdots, m; \;\; q = 1, \cdots, N. \tag{8.15}$$

Substituting ε_n from equation (8.13) the preceding equation can be expressed as

$$-\sum_{n=1}^{N} \int_{\omega\in\Omega} \left[\frac{\partial H_n(\omega)}{\partial A_{pq}} \{Y_n^*(\omega) - H_n^*(\omega)\} + \{Y_n(\omega) - H_n(\omega)\} \frac{\partial H_n^*(\omega)}{\partial A_{pq}} \right] \mathrm{d}\omega = 0. \tag{8.16}$$

Now, from the expression of $H_n(\omega)$ in equation (8.9) one obtains the following:

$$\frac{\partial H_n(\omega)}{\partial A_{pq}} = 0; \quad \forall n \neq q \tag{8.17}$$

$$\frac{\partial H_q(\omega)}{\partial A_{pq}} = f_{1_p}(\omega) \tag{8.18}$$

$$\frac{\partial H_q^*(\omega)}{\partial A_{pq}} = f_{2_p}^*(\omega). \tag{8.19}$$

Using the above three equations, (8.16) may be simplified to

$$\int_{\omega\in\Omega} \left[f_{1_p}(\omega) H_q^*(\omega) + f_{2_p}^*(\omega) H_q(\omega) \right] \mathrm{d}\omega = \int_{\omega\in\Omega} \left[f_{1_p}(\omega) Y_q^*(\omega) + f_{2_p}^*(\omega) Y_n(\omega) \right] \mathrm{d}\omega. \tag{8.20}$$

Substituting the expression of $H_n(\omega)$ in (8.9) for $n = q$, the preceding equation reduces to

$$\sum_{k=1}^{m} W_{pk} A_{kq} + E_{pk} A_{kq}^* = S_{pk} \tag{8.21}$$

where

$$W_{pk} = \int_{\omega\in\Omega} \left[f_{1_p}(\omega) f_{2_k}^*(\omega) + f_{2_p}^*(\omega) f_{1_k}(\omega) \right] \mathrm{d}\omega \tag{8.22}$$

$$E_{pk} = \int_{\omega\in\Omega} \left[f_{1_p}(\omega) f_{1_k}^*(\omega) + f_{2_p}^*(\omega) f_{2_k}(\omega) \right] \mathrm{d}\omega \tag{8.23}$$

$$S_{pk} = \int_{\omega\in\Omega} \left[f_{1_p}(\omega) Y_q^*(\omega) + f_{2_p}^*(\omega) Y_n(\omega) \right] \mathrm{d}\omega. \tag{8.24}$$

For $p = 1, \cdots, m$ and $q = 1, \cdots, N$ equation (8.21) can be rewritten in matrix form as

$$\mathbf{W}\mathbf{A} + \mathbf{E}\mathbf{A}^* = \mathbf{S} \tag{8.25}$$

where $\mathbf{W}, \mathbf{E} \in \mathbb{C}^{m\times m}$ and $\mathbf{S} \in \mathbb{C}^{m\times N}$. Since χ^2 is a real function we also have

$$\frac{\partial \chi^2}{\partial A^*_{pq}} = \left(\frac{\partial \chi^2}{\partial A_{pq}}\right)^*. \tag{8.26}$$

In view of the above, taking the complex conjugate of (8.25) one has

$$\begin{aligned} \mathbf{W}^*\mathbf{A}^* + \mathbf{E}^*\mathbf{A} &= \mathbf{S}^* \\ \text{or} \quad \mathbf{A}^* &= \mathbf{W}^{*^{-1}}\left[\mathbf{S}^* - \mathbf{E}^*\mathbf{A}\right] \end{aligned} \tag{8.27}$$

Substituting $\mathbf{A}^*$ from the above equation in (8.25) we finally obtain

$$\mathbf{A} = \left[\mathbf{W} - \mathbf{E}\mathbf{W}^{*^{-1}}\mathbf{E}^*\right]^{-1}\left[\mathbf{S} - \mathbf{E}\mathbf{W}^{*^{-1}}\mathbf{S}^*\right]. \tag{8.28}$$

Transfer function residues can be calculated from the above formula provided the matrix

$$\mathbf{W} - \mathbf{E}\mathbf{W}^{*^{-1}}\mathbf{E}^* \neq \mathbf{O}_m \tag{8.29}$$

where $\mathbf{O}_m$ is a $m \times m$ null matrix. Premultiplying the above equation by $\mathbf{E}^{-1}$ and defining

$$\mathbf{Q} = \mathbf{E}^{-1}\mathbf{W} \tag{8.30}$$

the condition for which $\mathbf{A}$ can be determined can be expressed as

$$\mathbf{Q} \neq \mathbf{Q}^{*^{-1}} \quad \text{or} \quad \mathbf{Q}^*\mathbf{Q} \neq \mathbf{I}_m. \tag{8.31}$$

Determination of the Complex Modes

Once the residues are obtained from equation (8.28), the complex modes can be calculated easily. Combining equations (8.12) and (8.3) one has

$$A_{kn} = \mathrm{i}\gamma_k z_{nk} z_{jk}. \tag{8.32}$$

In Chapter 4 it was mentioned that the normalization constants can be selected in various ways. The one which is consistent with conventional modal analysis is when $\gamma_k = 1/2\mathrm{i}\lambda_k$. Substituting this value of γ_k, equation (8.32) reads

$$A_{kn} = \frac{z_{nk} z_{jk}}{2\lambda_k}. \tag{8.33}$$

Note that in the above equation j is fixed (the response measurement point). For $n = j$, from equation (8.33) one has

$$z_{jk} = \sqrt{2\lambda_k A_{kj}}; \quad \forall k = 1, 2, \cdots, m \tag{8.34}$$

Substituting z_{jk} from the above into equation (8.33) the mode shapes are obtained as

$$\begin{aligned} z_{nk} &= \frac{2\lambda_k A_{kn}}{z_{jk}} \\ &= \sqrt{2\lambda_k}\frac{A_{kn}}{\sqrt{A_{kj}}}, \quad \forall \begin{array}{l} k = 1, 2, \cdots, m, \\ n = 1, 2, \cdots, N. \end{array} \end{aligned} \tag{8.35}$$

Thus, equation (8.35) together with (8.28), provides a closed-form expression for the complex modes extracted from a set of measured transfer functions.

8.2.3 Non-linear Least-Square Method

In the formulation presented before it was assumed that 'good' initial guesses of ω_k and Q_k are available. However, if substantially good initial values of ω_k and Q_k are not available then it is required to update them. Since $H_n(\omega)$ is a nonlinear function of ω_k and Q_k, a nonlinear optimization method needs to be employed for this purpose. We use a nonlinear least-square method outlined in Press *et al.* (1992, Section 15.5).

For convenience construct the parameter vector

$$\boldsymbol{\mathcal{V}} = \{\omega_1, \omega_2, \cdots, \omega_m, Q_1, Q_2, \cdots, Q_m\}^T \in \mathbb{R}^{2m}. \tag{8.36}$$

Suppose, for some current value of $\boldsymbol{\mathcal{V}}$, say $\boldsymbol{\mathcal{V}}_{\text{cur}}$, $\chi^2(\boldsymbol{\mathcal{V}})$ is sufficiently close to minimum. Expanding $\chi^2(\boldsymbol{\mathcal{V}})$ about $\boldsymbol{\mathcal{V}}_{\text{cur}}$ in a Taylor series and retaining quadratic terms we have

$$\chi^2(\boldsymbol{\mathcal{V}}) \approx \chi^2(\boldsymbol{\mathcal{V}} - \boldsymbol{\mathcal{V}}_{\text{cur}}) - (\boldsymbol{\mathcal{V}} - \boldsymbol{\mathcal{V}}_{\text{cur}})^T \boldsymbol{\nabla}\chi^2(\boldsymbol{\mathcal{V}}_{\text{cur}}) + \frac{1}{2}(\boldsymbol{\mathcal{V}} - \boldsymbol{\mathcal{V}}_{\text{cur}})^T \mathbf{D}(\boldsymbol{\mathcal{V}} - \boldsymbol{\mathcal{V}}_{\text{cur}}) \tag{8.37}$$

where $\boldsymbol{\nabla}(\bullet) = \left\{\dfrac{\partial(\bullet)}{\partial \mathcal{V}_j}\right\}$, $\forall j$ is the gradient vector and $\mathbf{D} \in \mathbb{R}^{2m\times 2m}$ is the Hessian matrix. Differentiating equation (8.37) one obtains

$$\boldsymbol{\nabla}\chi^2(\boldsymbol{\mathcal{V}}) = \boldsymbol{\nabla}\chi^2(\boldsymbol{\mathcal{V}}_{\text{cur}}) + \mathbf{D}(\boldsymbol{\mathcal{V}} - \boldsymbol{\mathcal{V}}_{\text{cur}}). \tag{8.38}$$

If the approximation is good, then by setting $\boldsymbol{\nabla}\chi^2(\boldsymbol{\mathcal{V}}) = 0$, the minimizing parameters $\boldsymbol{\mathcal{V}}_{\text{min}}$ can obtained from the current trial parameters $\boldsymbol{\mathcal{V}}_{\text{cur}}$ as

$$\boldsymbol{\mathcal{V}}_{\text{min}} = \boldsymbol{\mathcal{V}}_{\text{cur}} + \mathbf{D}^{-1}\left[-\boldsymbol{\nabla}\chi^2(\boldsymbol{\mathcal{V}}_{\text{cur}})\right]. \tag{8.39}$$

However, if (8.37) is a poor approximation, then the best we can do is to move down the gradient (steepest descent method), that is

$$\boldsymbol{\mathcal{V}}_{\text{next}} = \boldsymbol{\mathcal{V}}_{\text{cur}} - \text{constant} \times \boldsymbol{\nabla}\chi^2(\boldsymbol{\mathcal{V}}_{\text{cur}}) \tag{8.40}$$

Selection procedure of this constant will be discussed shortly. In order to use (8.39) or (8.40) we need to calculate the gradient of χ^2. Moreover, to use (8.39) calculation of the second derivative matrix (Hessian matrix) is also required. These issues are discussed next.

Calculation of the Gradient and Hessian

Differentiating the expression of χ^2 in equation (8.14) with respect to $\mathcal{V}_p$ the elements of the gradient vector can be obtained as

$$\begin{aligned}\frac{\partial \chi^2}{\partial \mathcal{V}_p} &= \sum_{n=1}^{N} \int_{\omega \in \Omega} \left[\frac{\partial \varepsilon_n(\omega)}{\partial \mathcal{V}_p} \varepsilon_n^*(\omega) + \varepsilon_n(\omega) \frac{\partial \varepsilon_n^*(\omega)}{\partial \mathcal{V}_p} \right] \mathrm{d}\omega \\ &= -\sum_{n=1}^{N} \int_{\omega \in \Omega} \left[\frac{\partial H_n(\omega)}{\partial \mathcal{V}_p} \varepsilon_n^*(\omega) + \varepsilon_n(\omega) \frac{\partial H_n^*(\omega)}{\partial \mathcal{V}_p} \right] \mathrm{d}\omega.\end{aligned} \tag{8.41}$$

The preceding equation can further be simplified as

$$\frac{\partial \chi^2}{\partial \mathcal{V}_p} = -2 \sum_{n=1}^{N} \int_{\omega \in \Omega} \Re \left[\varepsilon_n(\omega) \frac{\partial H_n^*(\omega)}{\partial \mathcal{V}_p} \right] \mathrm{d}\omega. \tag{8.42}$$

The term $\dfrac{\partial H_n^*(\omega)}{\partial \mathcal{V}_p}$ can be calculated following Appendix A. Taking an additional partial derivative of (8.41) with respect to $\mathcal{V}_q$ the elements of the Hessian matrix can be obtained as

$$\begin{aligned}&\frac{\partial^2 \chi^2}{\partial \mathcal{V}_p \partial \mathcal{V}_q} \\ &= -\sum_{n=1}^{N} \int_{\omega \in \Omega} \left[\frac{\partial^2 H_n(\omega)}{\partial \mathcal{V}_p \partial \mathcal{V}_q} \varepsilon_n^*(\omega) + \frac{\partial H_n(\omega)}{\partial \mathcal{V}_p} \frac{\partial \varepsilon_n^*(\omega)}{\partial \mathcal{V}_q} + \frac{\partial \varepsilon_n(\omega)}{\partial \mathcal{V}_q} \frac{\partial H_n^*(\omega)}{\partial \mathcal{V}_p} + \varepsilon_n(\omega) \frac{\partial^2 H_n^*(\omega)}{\partial \mathcal{V}_p \partial \mathcal{V}_q} \right] \mathrm{d}\omega.\end{aligned} \tag{8.43}$$

Substituting ε_n from equation (8.13) the preceding equation can be expressed as

$$\frac{\partial^2 \chi^2}{\partial \mathcal{V}_p \partial \mathcal{V}_q} = 2 \sum_{n=1}^{N} \int_{\omega \in \Omega} \Re \left[\frac{\partial H_n(\omega)}{\partial \mathcal{V}_p} \frac{\partial H_n^*(\omega)}{\partial \mathcal{V}_q} - \varepsilon_n(\omega) \frac{\partial^2 H_n^*(\omega)}{\partial \mathcal{V}_p \partial \mathcal{V}_q} \right] \mathrm{d}\omega. \tag{8.44}$$

It is customary to neglect the second term in the above expression because $\varepsilon_n(\omega)$ and $\dfrac{\partial^2 H_n^*(\omega)}{\partial \mathcal{V}_p \partial \mathcal{V}_q}$ are both small quantities. Thus, the elements of the Hessian matrix can be obtained from

$$\frac{\partial^2 \chi^2}{\partial \mathcal{V}_p \partial \mathcal{V}_q} \approx 2 \sum_{n=1}^{N} \int_{\omega \in \Omega} \Re \left[\frac{\partial H_n(\omega)}{\partial \mathcal{V}_p} \frac{\partial H_n^*(\omega)}{\partial \mathcal{V}_q} \right] \mathrm{d}\omega. \tag{8.45}$$

For convenience, removing the factors 2 from equations (8.42) and (8.45) we define a vector $\boldsymbol{\beta} \in \mathbb{R}^{2m}$ and a matrix $\boldsymbol{\alpha} \in \mathbb{R}^{2m \times 2m}$ such that

$$\beta_p = -\frac{1}{2} \frac{\partial \chi^2}{\partial \mathcal{V}_p} \tag{8.46}$$

$$\alpha_{pq} = \frac{1}{2} \frac{\partial^2 \chi^2}{\partial \mathcal{V}_p \partial \mathcal{V}_q}. \tag{8.47}$$

The matrix $\boldsymbol{\alpha} = \dfrac{1}{2}\mathbf{D}$ is often known as the curvature matrix. Using these relationships, equation (8.39) can be rewritten as the set of linear equations

$$\boldsymbol{\alpha}\, \delta \boldsymbol{\mathcal{V}} = \boldsymbol{\beta}. \tag{8.48}$$

Solving the above set of equations the increments $\delta\boldsymbol{\mathcal{V}} = \boldsymbol{\mathcal{V}}_{\text{min}} - \boldsymbol{\mathcal{V}}_{\text{cur}}$ can be obtained. These increments can be added to the current approximation to obtain the new values. Similarly, the steepest descent formula can be rewritten as

$$\delta\mathcal{V}_q = \nu_q \beta_q. \tag{8.49}$$

The constants ν_q can be selected using the Levenberg-Marquardt method.

Levenberg-Marquardt Method

The Levenberg-Marquardt method varies smoothly between the extreme of the inverse-Hessian method (8.48) and the steepest descent method (8.49). The latter method is used far from the minimum, switching continuously to the former as the minimum is approached. The Levenberg-Marquardt method assumes $\nu_q = \dfrac{1}{\kappa\alpha_{qq}}$, where κ is known as the *fudge factor* with the possibility of setting $\kappa \ll 1$. Using this, one can rewrite equation (8.49) as

$$\delta\mathcal{V}_q = \frac{1}{\kappa\alpha_{qq}}\beta_q \quad \text{or} \quad \kappa\alpha_{qq}\delta\mathcal{V}_q = \beta_q. \tag{8.50}$$

In view of the above equation, (8.48) and (8.49) can be combined into a single equation as

$$\boldsymbol{\alpha}'\,\delta\boldsymbol{\mathcal{V}} = \boldsymbol{\beta} \tag{8.51}$$

where the matrix $\boldsymbol{\alpha}'$ is defined as

$$\boldsymbol{\alpha}' = \boldsymbol{\alpha} + \kappa\mathbf{I}_{2m} \tag{8.52}$$

where $\mathbf{I}_{2m}$ is an identity matrix of size $2m$. If κ is very large, the matrix $\boldsymbol{\alpha}'$ becomes strictly diagonally dominant so that equation (8.52) reduces to the steepest descent method in equation (8.50). On the other hand, for small values of κ equation (8.52) reduces to the inverse-Hessian method in equation (8.48). Overall, the method can be performed by following these steps:

- Calculate $\chi^2(\boldsymbol{\mathcal{V}})$.
- Select a modest value of κ, say $\kappa = 0.001$.
- (‡) Solve the linear equations (8.51) for $\delta\mathcal{V}_q$ and calculate $\chi^2(\boldsymbol{\mathcal{V}} + \delta\boldsymbol{\mathcal{V}})$
- If $\chi^2(\boldsymbol{\mathcal{V}} + \delta\boldsymbol{\mathcal{V}}) \geq \chi^2(\boldsymbol{\mathcal{V}})$ *increase* κ by a factor of 10 (or any other substantial factor) and go back to (‡).
- If $\chi^2(\boldsymbol{\mathcal{V}} + \delta\boldsymbol{\mathcal{V}}) < \chi^2(\boldsymbol{\mathcal{V}})$ *decrease* κ by a factor of 10, update the trial solution $\boldsymbol{\mathcal{V}} \leftarrow \boldsymbol{\mathcal{V}} + \delta\boldsymbol{\mathcal{V}}$ and go back to (‡).

A stopping condition for the above iteration scheme has to be selected by choosing some acceptable value of χ^2.

8.2.4 Summary of the Method

In the last two sections a linear least-square and a nonlinear least-square method have been proposed to obtain the modal parameters. For practical purposes these two methods can unified to construct a single linear-nonlinear optimization method. Figure 8.1 shows the steps to followed in order to apply this method. A set of MATLAB^{TM} programs have been developed to implement this method. Several authors, for example Balmès (1995), Cole *et al.* (1995), Lin and Ling (1996), Balmès (1996) and Rosa *et al.* (1999) have proposed modal identification methods in frequency domain. Application of the approach developed in this study to a beam in bending vibration is considered next.

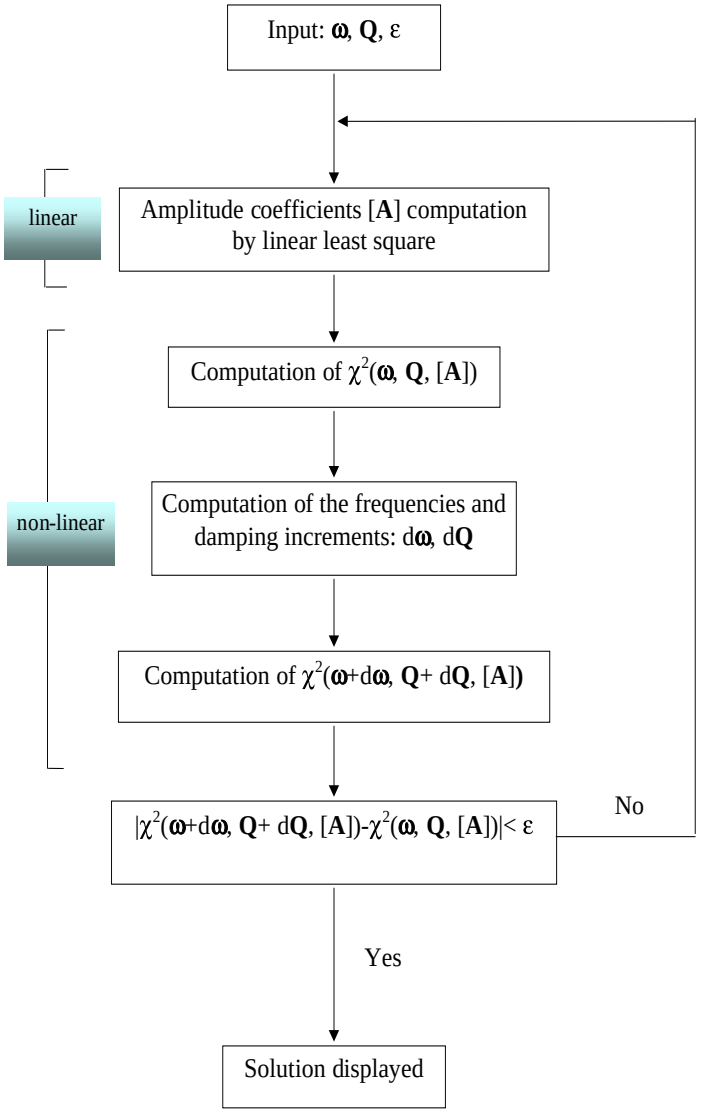

Figure 8.1: The general linear-nonlinear optimization procedure for identification of modal parameters

8.3 The Beam Experiment

We consider a free-free beam for experimental verification of the procedures developed so far in this dissertation. The physical properties of the beam, the arrangement of the damping mechanism and the scheme for the grid points will be discussed in Section 8.3.2. In the next section, the details of the equipment used for the experiment are explained.

8.3.1 Experimental Set-up

A schematic diagram of the experimental set-up is shown in Figure 8.2 while the details of the measuring equipment are given in Table 8.1. Figure 8.2 shows three main components of the measurement technique implemented:

- Excitation of the structure
- Sensing of the response
- Data acquisition and processing

Details of the above components of the experiment are discussed next.

Excitation of the Structure

A mechanical structure can be excited mainly in two ways, (a) using an exciter or shaker, and (b) using an impulse hammer. Shaker attachments have the advantage of providing any known waveform as the driving signal to a structure. This allows one to control the frequency content of the excitation and consequently to excite the modes in a chosen frequency-band. In addition, the steady-state sinusoidal driving is probably the only efficient way to measure the frequency response at different frequencies directly. However, a major disadvantage of attaching shakers as the driving mechanism is that it becomes a part of the vibrating structure and as a result the stiffness, and more importantly the damping behaviour, which we want to identify from this experiment, get changed. Beside this, there are some practical difficulties, for example:

- it not always convenient to mount a shaker to access all the excitation points we choose;
- to obtain a set of transfer functions with high frequency resolution and covering several modes is very time consuming.

For these reasons, the possibility of using shakers has been ruled out for this experiment.

It is much easier to excite a structure by hitting it with an instrumented hammer. The instrumented hammer essentially consists of three main components: a handle, a force transducer and a hammer tip. With experience it was found that the impulse excitation provided by an instrumented hammer gave the most reliable results for the present purpose. Impulse excitation using a hammer has the following advantages:

- the location of excitation point can be chosen arbitrarily;
- once an impulse has been struck and the hammer separated, the response obtained thereafter is free from any undesirable interaction with the excitation apparatus;
- depending on the nature of the hammer tip (that is soft or hard) the frequency range can be selected as desired.

For the hammer used in this experiment, the force transducer was a PCB A218 and a hard plastic tip was used. With this hard plastic tip we can go up to 2.5KHz.

Sensing of the Response

Response sensors have to be selected on the basis of what quantity one wants to measure and the size of the structure under test. The relative size and mass of the response transducers have influence on the vibrational behaviour of the test structure. It is very much desirable that a transducer has minimum effect on the structure so that one can avoid the corrections required at a later stage to discard the effect of the transducer.

The response of a structure may be defined in terms of displacement, velocity or acceleration. Accelerometers are the most widely used form of response transducer although, as laser vibrometers are more readily available, velocity transducers are also gaining popularity. The main advantage of the laser vibrometer is that the response measurement technique is 'non-contact'. Thus, questions of interactions between the response measurement apparatus and the structure do not arise for laser vibrometers. Beside, laser vibrometers can be used to measure response at points where accelerometers can not be attached. However, for the simple beam considered in this experiment it was found that traditional piezoelectric accelerometers are sufficient. A DJB piezoelectric accelerometer is used for the experiment. We have measured the acceleration response at only one point in the structure (detail will follow in Section 8.3.2). A small hole of 3mm diameter was drilled into the beam and the accelerometer was attached by screwing it through the hole.

Data Acquisition and Processing

(a) Amplifiers

Signals from the impulse hammer and the accelerometer give small charges. As a result the signals need to be amplified by using a charge amplifier. For this purpose in-house charge amplifiers were designed. The acceleration signal was amplified by using a charge amplifier with a sensitivity of 14mV/pc while the impulse signal was amplified by using a charge amplifier with a sensitivity of 2.0mV/pc. Both these amplifiers had a frequency range of 0.44Hz to 10KHz.

(b) Data-logging system

A National Instruments DAQCard 1200 was used to log the impulse force and the acceleration response. This card gives analog-to-digital conversion in 12 bits. The maximum sampling rate was set to 20kHz, which was sufficient for the frequency bandwidth of interest (*i.e.*, 0-2.5KHz).

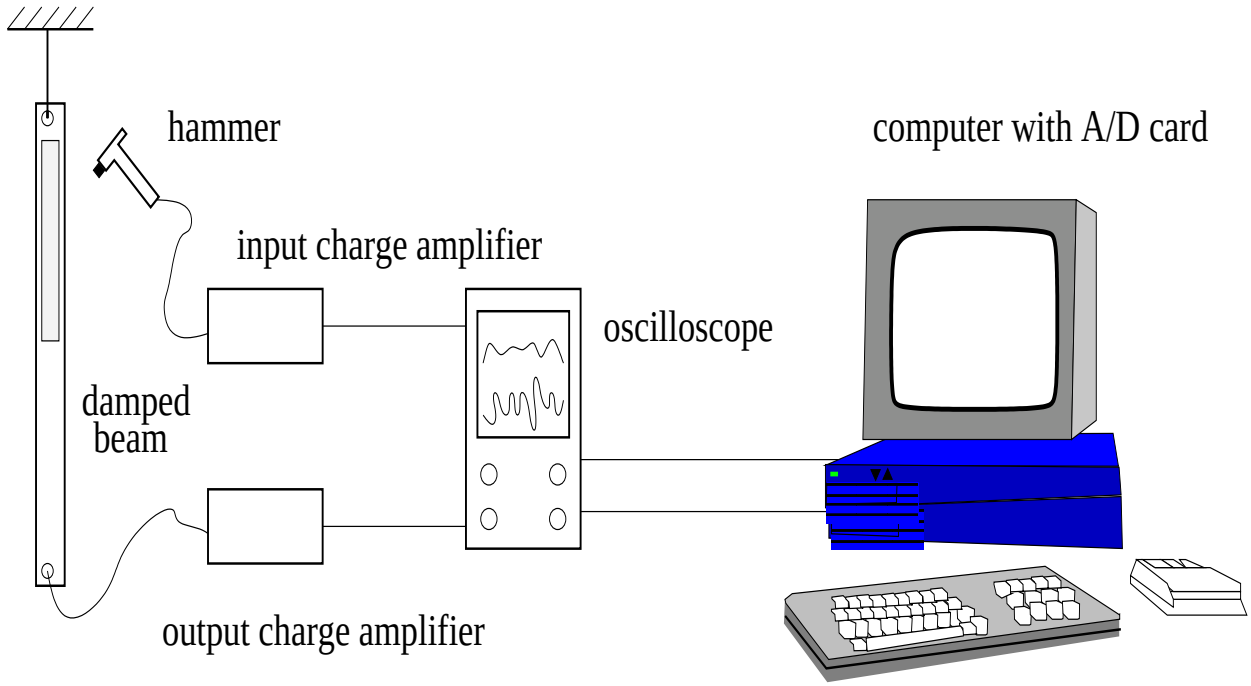

Figure 8.2: Schematic representation of the test set-up

A Visual Basic program running on a Daytek desktop computer controlled the DAQCard. This program was used to start data logging, set sampling frequencies, check sample saturation and save the data. After the raw data were measured and saved they were then opened using MATLAB™ and checked as to whether they were suitable or not by calculating the FRFs.

Item	Use
DJB Accelerometers	Measuring the acceleration response of the beam
PCB modal hammer	Measuring the force applied using the impulse hammer
Impulse charge amplifier	Amplifying the impulse force exerted on the structure
Response charge amplifier	Amplifying the acceleration response
National Instruments DAQCard 1200 data acquisition personal computer card	Sampling transducer time signals
Daytek Desktop Computer	Control of DAQCard 1200, data storage and analysis

Table 8.1: Summary of the equipment used

8.3.2 Experimental Procedure

A steel beam with uniform rectangular cross-section is considered for the experiment. Figure 8.3 shows the beam with details of the grid and damping mechanism. The physical and geometrical properties of the steel beam are shown in Table 8.2. The damping mechanism of the beam is through constrained layers (see Ungar, 2000, for a recent review on this topic). For the purpose of

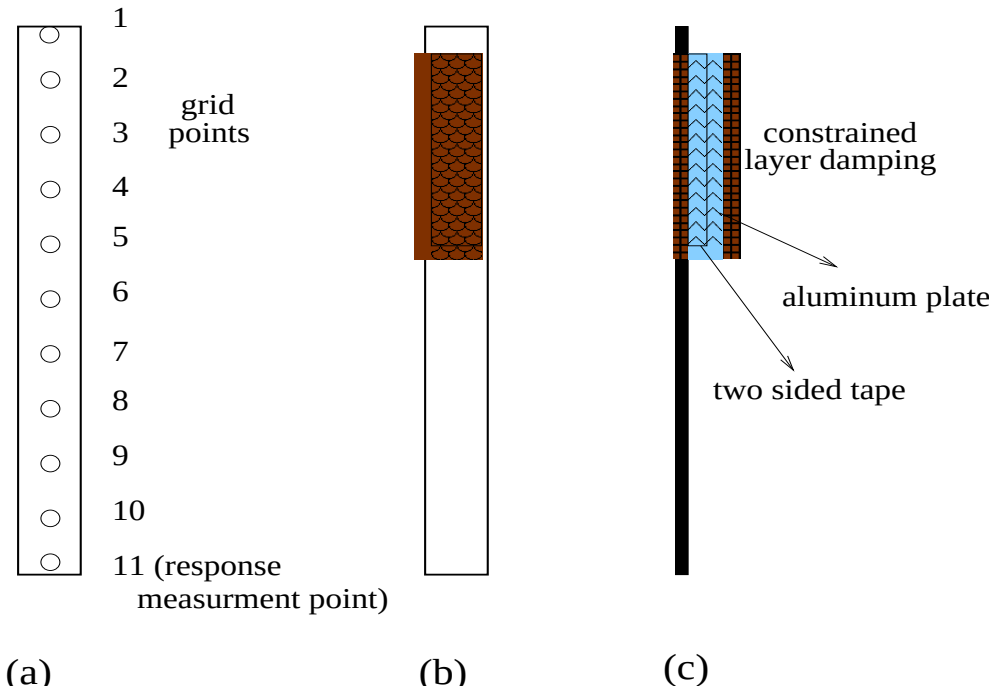

Figure 8.3: Details of the beam considered for the experiment; (a) Grid arrangement, (b) Back view showing the position of damping, (c) Side view of the constrained layer damping

Beam Properties	Numerical values
Length (L)	1.00 m
Width (b)	39.0 mm
Thickness (t_h)	5.93 mm
Mass density (ρ)	7800 Kg/m^3
Youngs modulus (E)	2.0×10^5 GPa
Cross sectional area ($a = bt_h$)	2.3127×10^{-4} m^2
Moment of inertia ($I = 1/12bt_h^3$)	6.7772×10^{-10} m^4
Mass per unit length (ρ_l)	1.8039 Kg/m
Bending rigidity (EI)	135.5431 Nm^2

Table 8.2: Material and geometric properties of the beam considered for the experiment

with boundary conditions, for example, the kind of problems one often encounters with clamped or pinned boundary conditions. For the purpose of the present experiment a 3mm hole was drilled in the beam and it was hung by a thread. The thread was chosen thin and long (one and half times the length of the beam) so as to produce minimum damping to the beam.

Results from initial testing on the 'undamped beam', that is without the damping layer, showed that damping is extremely light (Q-factors in the order of 1000). In fact, the damping is so light that for most of the modes the measurement of the Q-factor was not possible using the conventional circle fitting method and an alternative sonogram method was used. This ensures that the significant part of the damping comes from the localized constrained damping layer only. In a recent paper Ungar (2000) has mentioned that such damping is likely to be viscoelastic rather that viscous. This case is thus analogous to the numerical systems considered in the previous three

chapters, and we hope to obtain results close to that obtained from the numerical studies. Before discussing the results we briefly outline the theory of bending vibration of Euler-Bernoulli beams.

8.4 Beam Theory

The equation of motion describing free vibration of an undamped uniform Euler-Bernoulli beam in bending vibration can be expressed by

$$EI\frac{\partial^4 Y(x,t)}{\partial x^4} + \rho_l \frac{\partial^2 Y(x,t)}{\partial t^4} = 0. \tag{8.53}$$

Assuming harmonic motion, that is $Y(x,t) = y(x)e^{\mathrm{i}\omega t}$, the above equation can be expressed as

$$EI\frac{\mathrm{d}^4 y(x)}{\mathrm{d}x^4} - \beta^4 y(x) = 0, \quad \text{where} \quad \beta^4 = \frac{\omega^2 \rho_l}{EI}. \tag{8.54}$$

The natural frequencies and the mode shapes can be obtained by solving the differential eigenvalue problem (8.54) subjected to appropriate boundary conditions. For a free-free beam, the boundary conditions are expressed as

$$\frac{\mathrm{d}^2 y(x)}{\mathrm{d}x^2}|_{x=0} = 0, \qquad \frac{\mathrm{d}^3 y(x)}{\mathrm{d}x^3}|_{x=0} = 0, \tag{8.55}$$

$$\frac{\mathrm{d}^2 y(x)}{\mathrm{d}x^2}|_{x=L} = 0, \qquad \frac{\mathrm{d}^3 y(x)}{\mathrm{d}x^3}|_{x=L} = 0. \tag{8.56}$$

(8.57)

Solving the eigenvalue problem (see Meirovitch, 1997 Section 7.7) the natural frequencies are obtained approximately as

$$\omega_j \approx \left(\frac{(2j+1)\pi}{2}\right)^2 \sqrt{\frac{EI}{\rho_l L^4}}. \tag{8.58}$$

The mode shapes corresponding to the above natural frequencies are approximately

$$\begin{aligned}\phi_j(x) \approx & b_j \left[(\sin\alpha_j L - \sinh\alpha_j L)(\sin\alpha_j x - \sinh\alpha_j x)\right. \\ & \left. +(\cos\alpha_j L + \cosh\alpha_j L)(\cos\alpha_j x - \cosh\alpha_j x)\right], \quad \text{where} \quad \alpha_j = \frac{(2j+1)\pi}{2L}\end{aligned} \tag{8.59}$$

and b_j are normalization constants.

In Chapter 6 it was mentioned that in order to fit a non-viscous damping model, the mass matrix of the system is required. Note that for a continuous system, like the beam as considered here, a mass matrix of finite dimension essentially requires discretization of the equation of motion. This discretization can be performed in several ways, for example using the finite element method. However, for the simple uniform beam considered in the experiment, a discretized mass matrix can be obtained by following the simple procedure outlined in Appendix B.

8.5 Results and Discussions

In this section, results obtained from modal testing of the beam are described. All the results are for the case when damping is attached between the points 2 and 6 (see figure 8.3). First, some measured transfer functions and extracted modal properties are shown. Later, results on damping identification obtained using the procedures developed in the previous chapters are shown.

8.5.1 Measured and Fitted Transfer Functions

The frequency range for the experiment has to be selected based on the number of modes to be retained in the study. Because there are eleven grid points along the length of the beam we consider only the first eleven modes in this study. Table 8.3 shows the natural frequencies corresponding to the first eleven modes of the beam obtained from equation (8.58). These values give an indication

Mode number	Natural frequency (Hz)
1	30.6361
2	85.1004
3	166.7968
4	275.7253
5	411.8860
6	575.2788
7	765.9037
8	983.7608
9	1228.8499
10	1501.1713
11	1800.7247

Table 8.3: Natural frequencies using beam theory

of the frequency range to be selected for the experiment. We use a hard plastic tip for the hammer which produces frequency range of $0 - 2.5$ KHz. The sampling frequency was selected to be 20KHz and 65536 samples are used for logging the time response data. The transfer functions corresponding to input forces at the eleven points shown in Figure 8.3(a) are calculated by taking the Fourier transform of the logged time histories. In-house software was used for handling the data. The measured transfer functions are fitted using the modal identification procedure developed in Section 8.2. Figures 8.4 to 8.14 show amplitude and phase of the measured and fitted transfer functions obtained by hitting the hammer at points one to eleven respectively. It may be observed that the fitting of all the transfer functions is in general good. Results on the identified modal parameters obtained by this fitting procedure are discussed next.

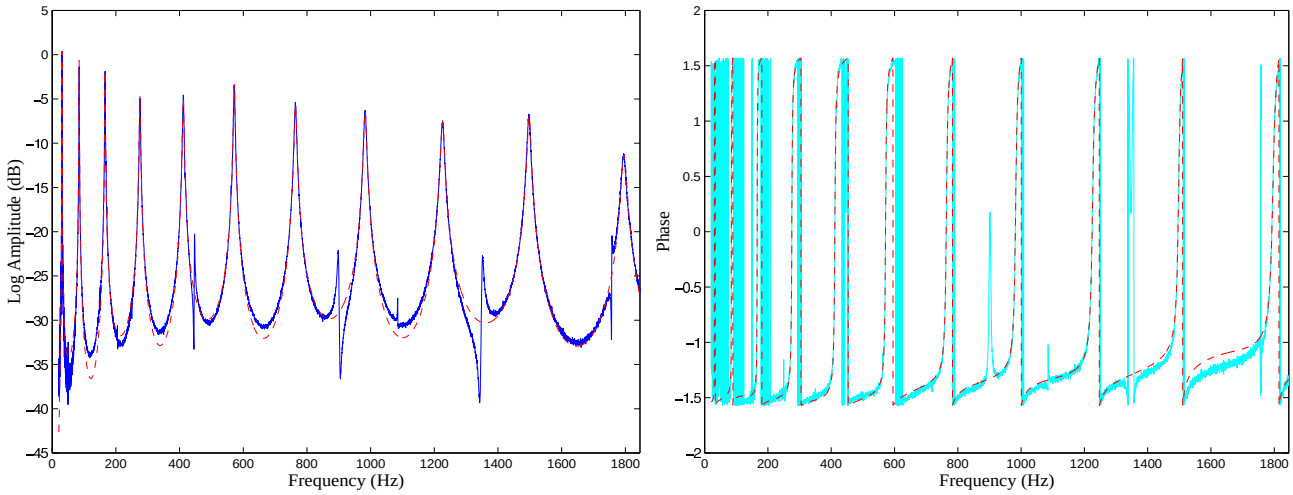

Figure 8.4: Amplitude and phase of transfer function $H_1(\omega)$,'—' measured, '−−' fitted

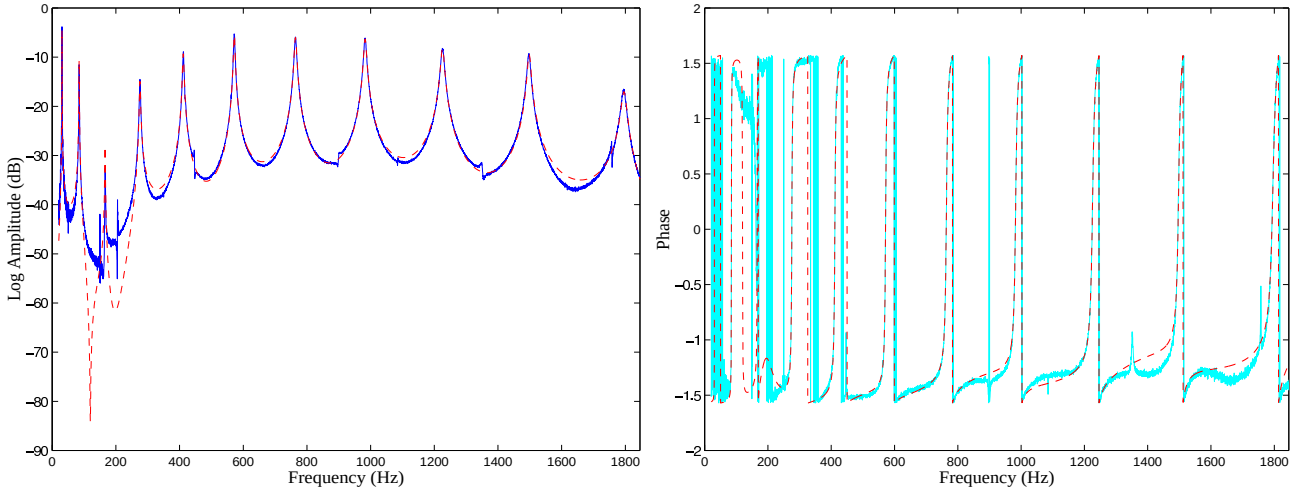

Figure 8.5: Amplitude and phase of transfer function $H_2(\omega)$,'—' measured, '−−' fitted

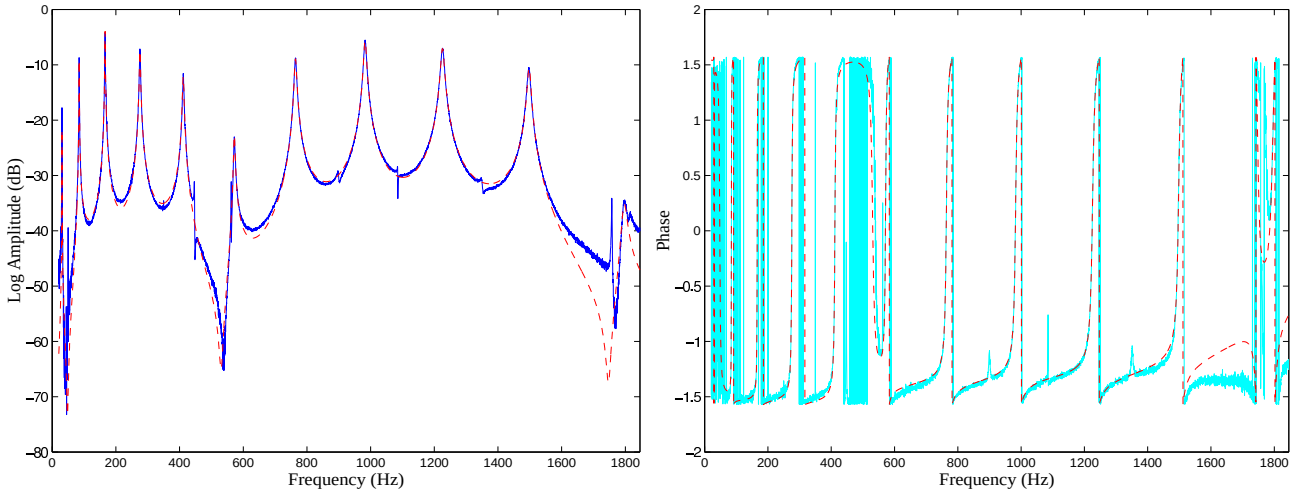

Figure 8.6: Amplitude and phase of transfer function $H_3(\omega)$,'—' measured, '−−' fitted

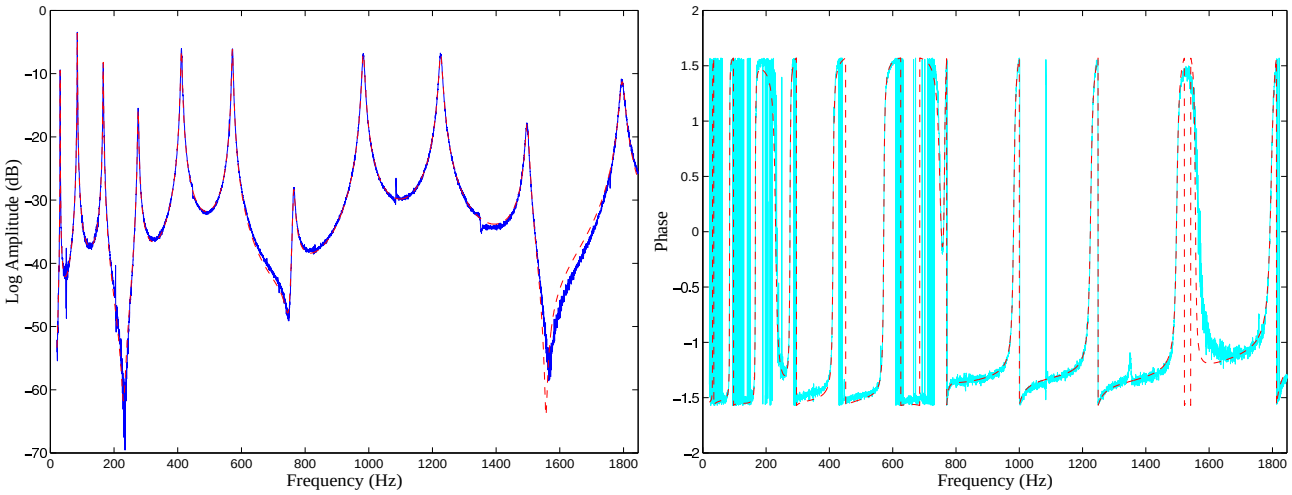

Figure 8.7: Amplitude and phase of transfer function $H_4(\omega)$,'—' measured, '– –' fitted

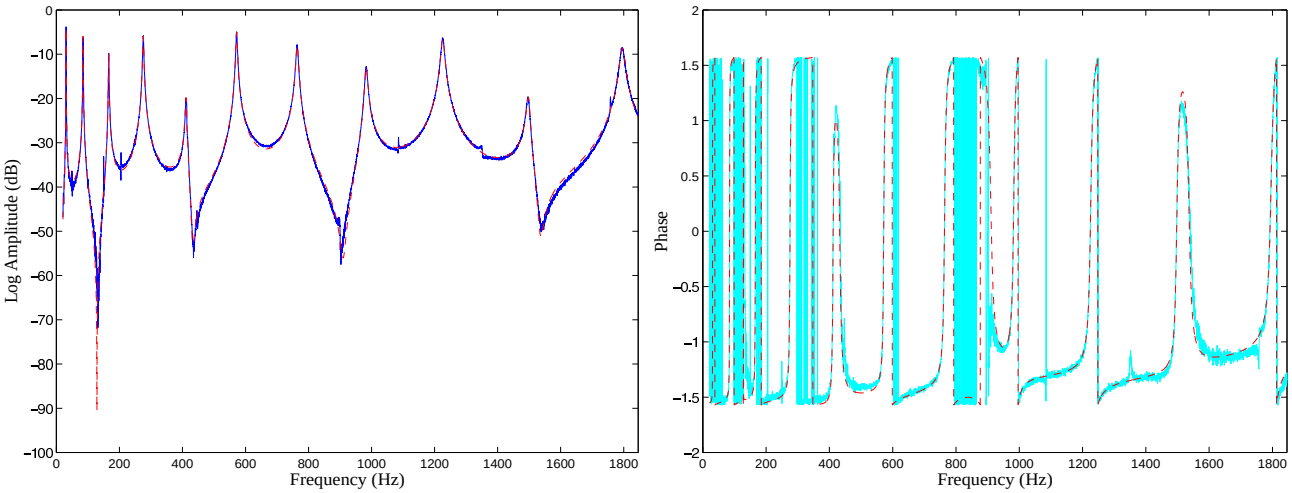

Figure 8.8: Amplitude and phase of transfer function $H_5(\omega)$,'—' measured, '– –' fitted

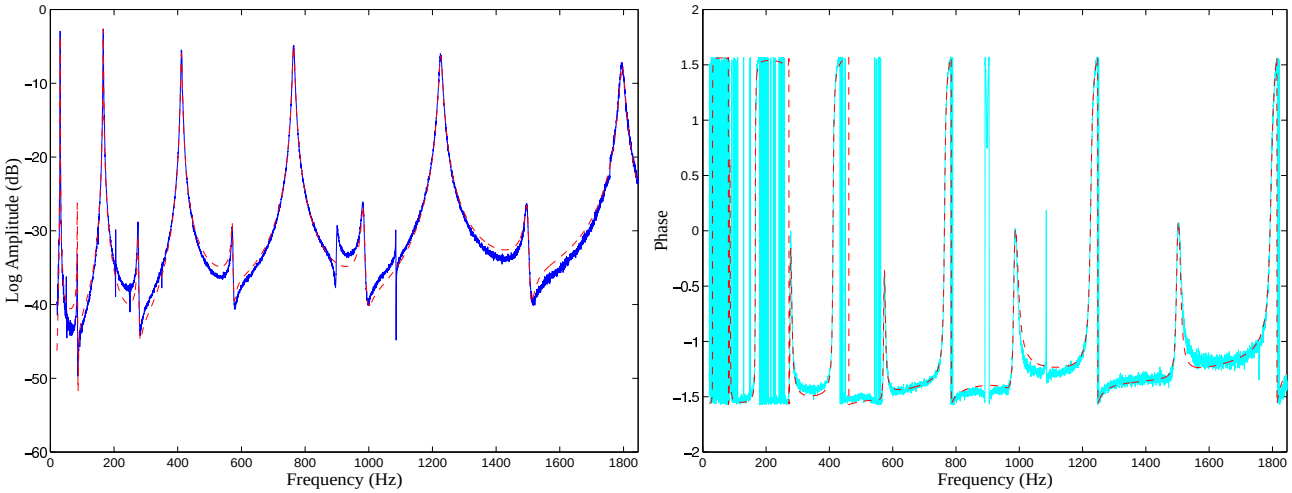

Figure 8.9: Amplitude and phase of transfer function $H_6(\omega)$,'—' measured, '– –' fitted

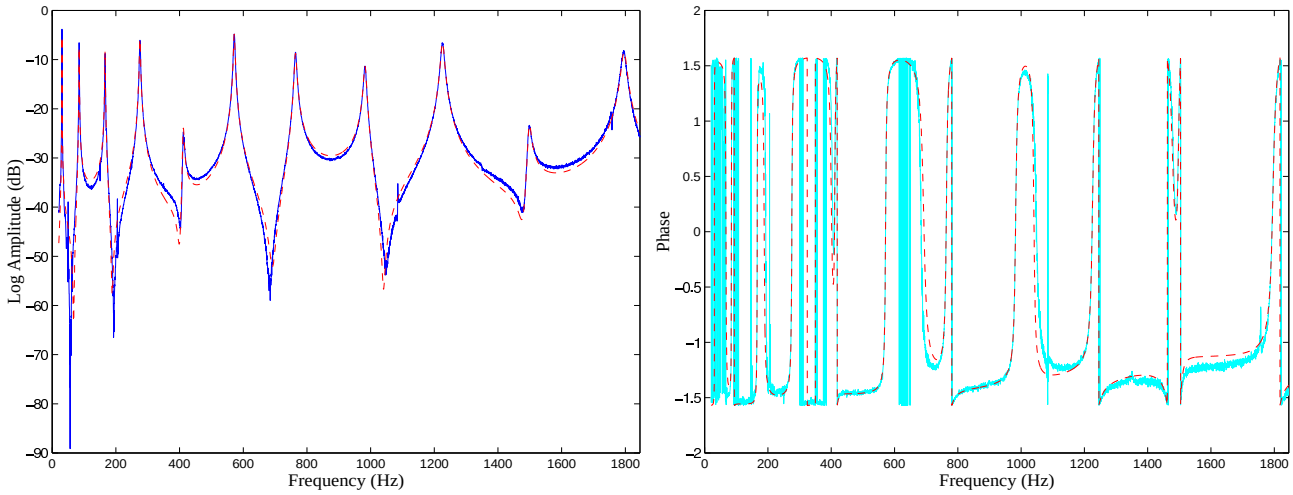

Figure 8.10: Amplitude and phase of transfer function $H_7(\omega)$,'—' measured, '−−' fitted

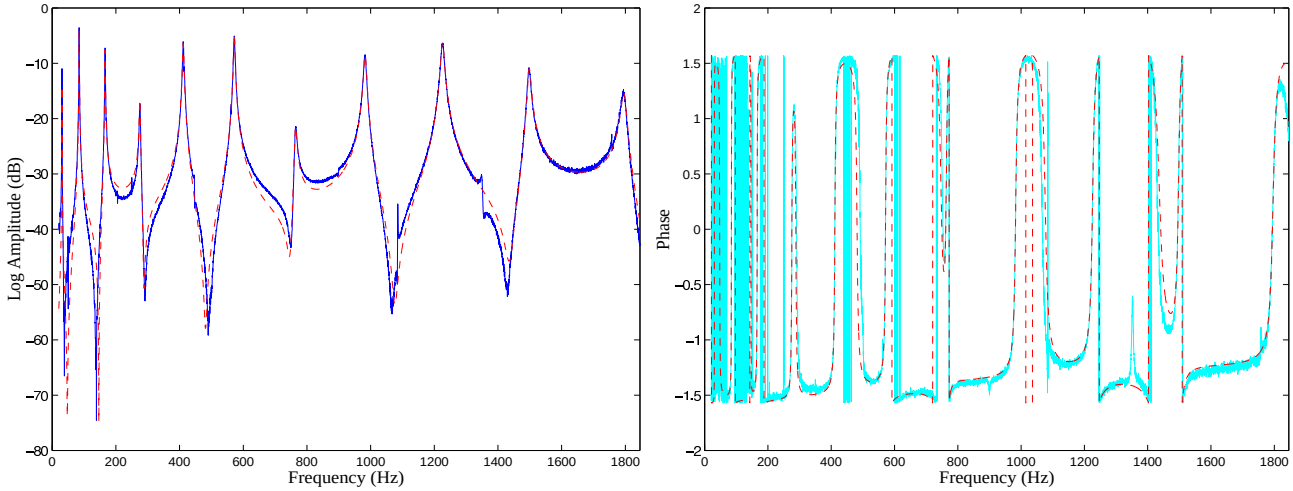

Figure 8.11: Amplitude and phase of transfer function $H_8(\omega)$,'—' measured, '−−' fitted

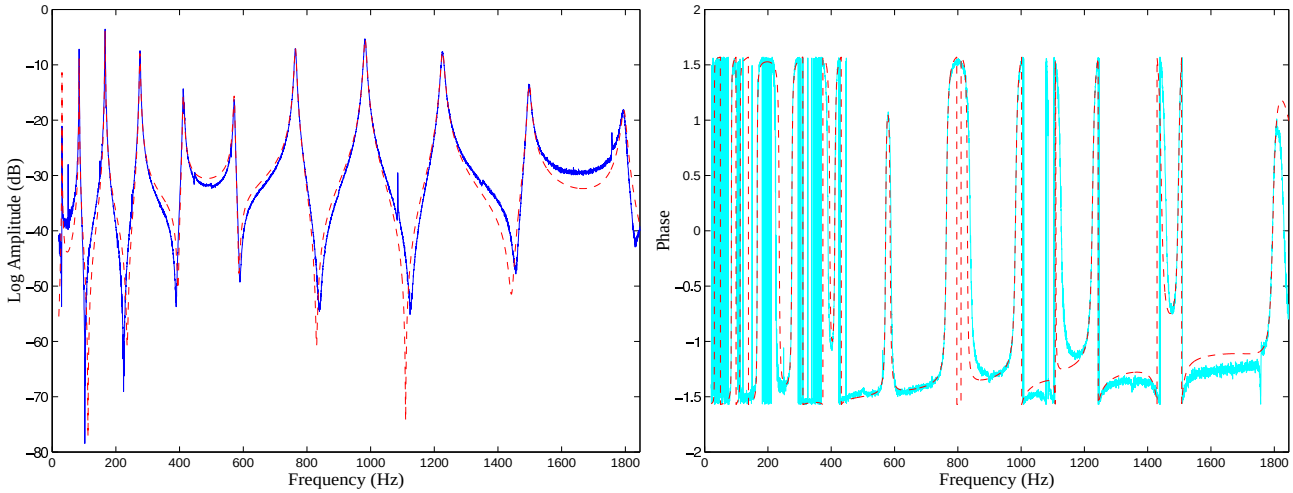

Figure 8.12: Amplitude and phase of transfer function $H_9(\omega)$,'—' measured, '−−' fitted

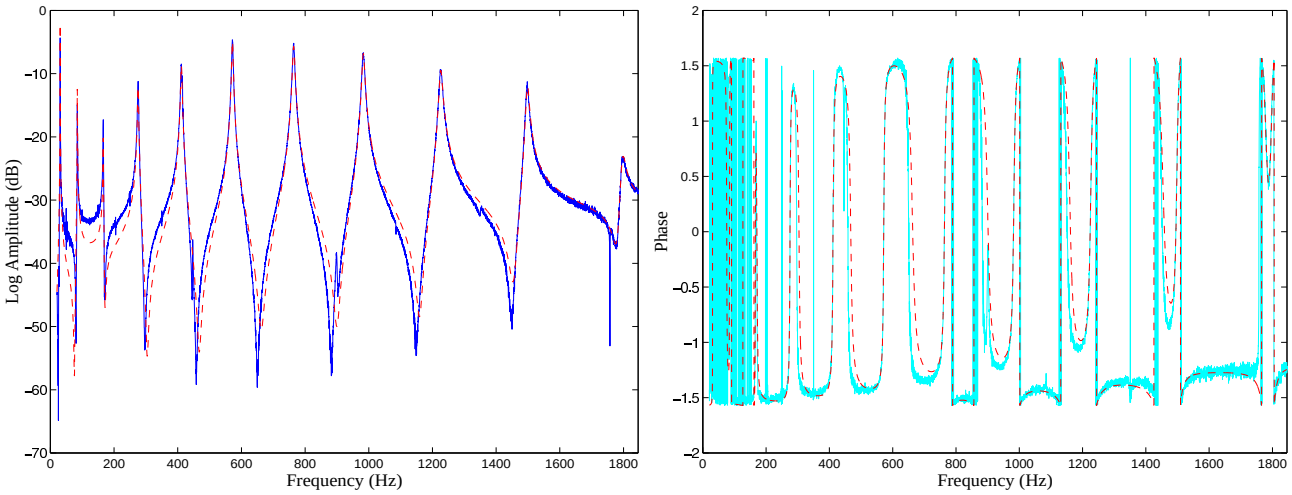

Figure 8.13: Amplitude and phase of transfer function $H_{10}(\omega)$,'—' measured, '−−' fitted

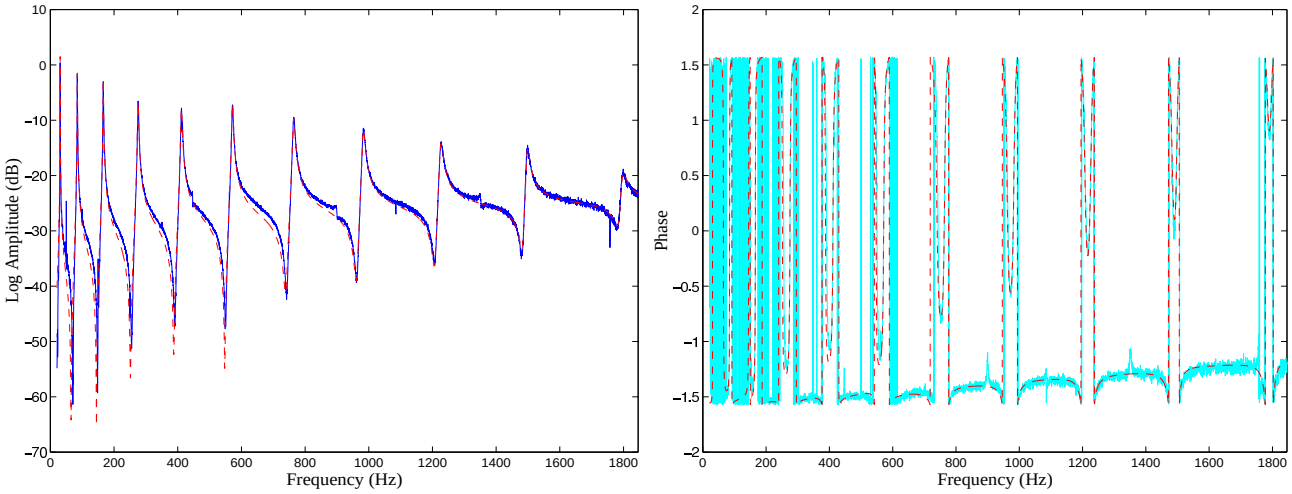

Figure 8.14: Amplitude and phase of transfer function $H_{11}(\omega)$,'—' measured, '−−' fitted

8.5.2 Modal Data

Figure 8.15 compares the measured natural frequencies (extracted using the non-linear optimization method described in Section 8.2.3) and the analytical natural frequencies as shown in Table 8.3. From this diagram it is clear that the natural frequencies obtained from the experiment match very well to the analytical natural frequencies obtained using simple beam theory. This gives us the confidence to compare the mode shape associated with each natural frequency.

The modal Q-factors obtained from the experiment are shown in Figure 8.16. The values of the Q-factors lie between 80 and 140. This implies that the beam is moderately damped and the damping identification procedures developed in the previous three chapters may be applied to this system.

Mode shapes can be obtained from the identified transfer function residues by using equation (8.35). It has been mentioned that if the damping is small then the real part of the complex modes

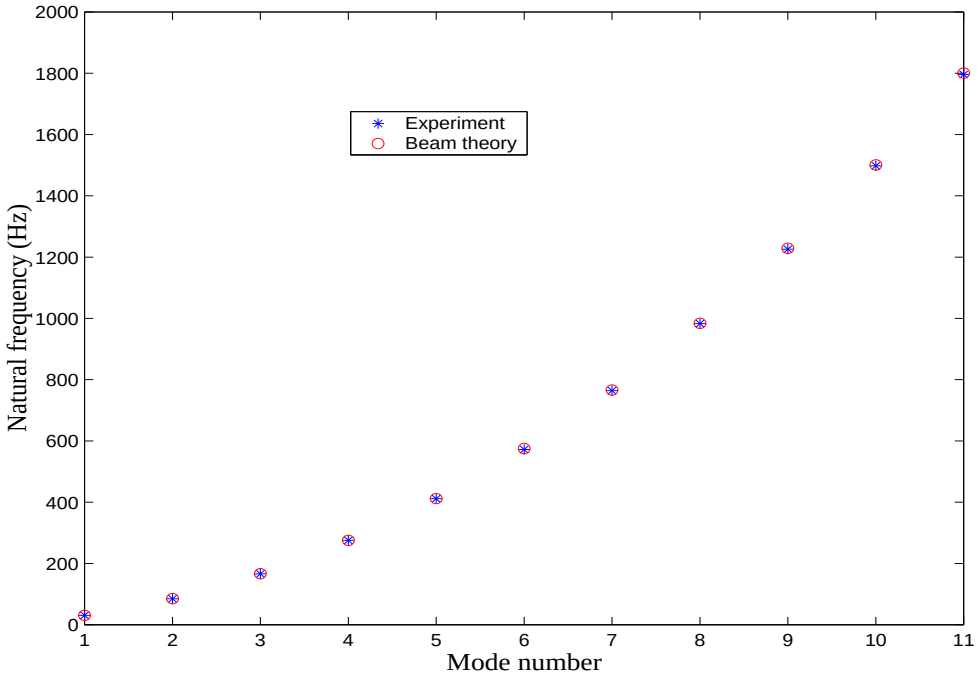

Figure 8.15: Comparison of measured and analytical natural frequencies

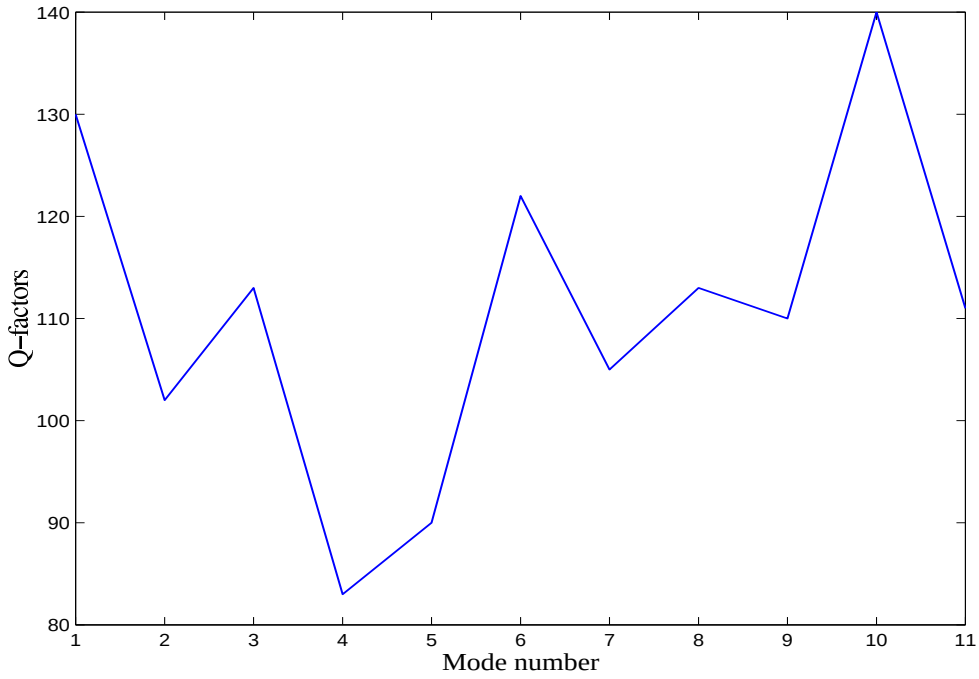

Figure 8.16: Modal Q-factors obtained from the experiment

obtained from equation (8.35) would be close to the undamped mode shapes. The undamped mode shapes of the free-free beam under consideration can be obtained from equation (8.59) sampled at the points corresponding to the grid points shown in Figure 8.3(a). In Figures 8.17 to 8.27 the real and imaginary parts of extracted complex modes and the undamped modes obtained from the beam theory are shown. From these figures it may be observed that the real parts of the

extracted complex modes ($\mathbf{u}_j$) match very well with the undamped modes obtained from the beam theory ($\mathbf{x}_j$). This agreement confirms the accuracy of the experimental procedure and the computer program developed to implement the mode extraction method described in Section 8.2.

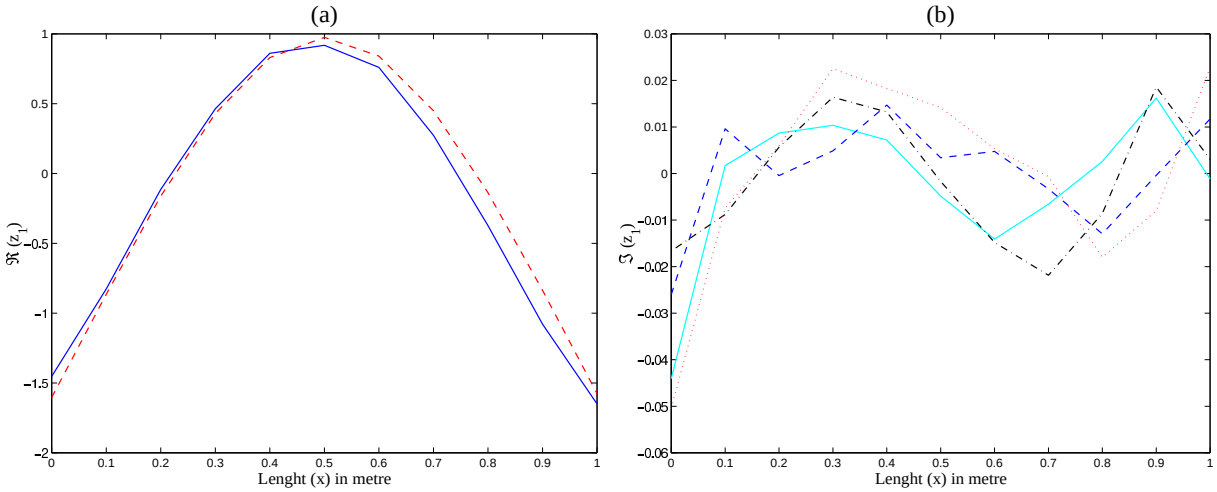

Figure 8.17: (a) The real part of complex mode $\mathbf{z}_1$,'—' experiment, '– –' theory; (b) The imaginary part of complex mode $\mathbf{z}_1$ for four sets of experimental data

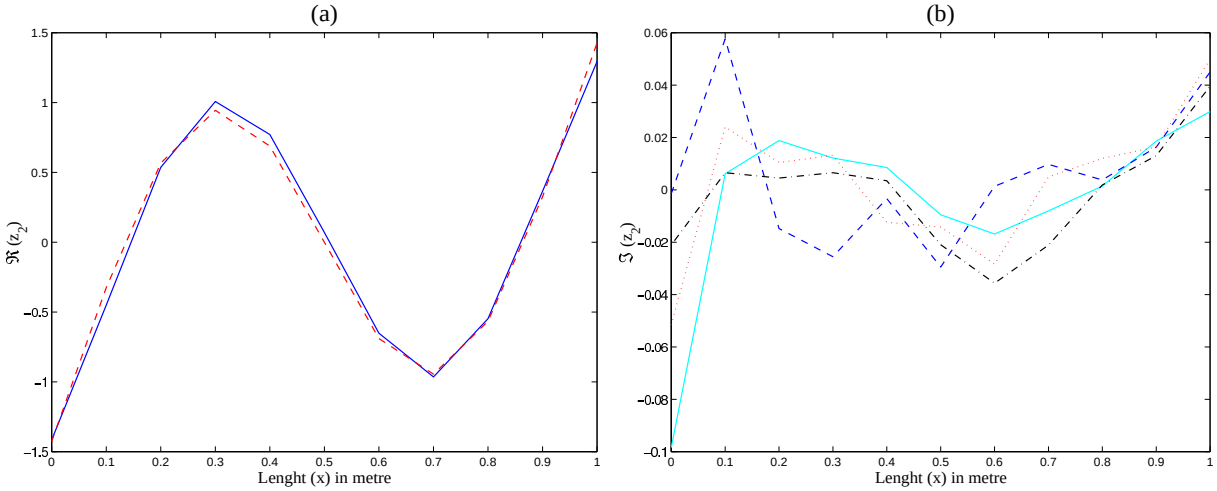

Figure 8.18: (a) The real part of complex mode $\mathbf{z}_2$,'—' experiment, '– –' theory; (b) The imaginary part of complex mode $\mathbf{z}_2$ for four sets of experimental data

It is useful to check the mass orthogonality relationship satisfied by the real parts of extracted complex modes and the undamped modes obtained from the beam theory. The (tri-diagonal) mass matrix is obtained using equation (B.8) derived in Appendix B. Figure 8.28 shows the mass matrix in the modal coordinates ($\mathbf{M}'$) using analytical undamped modes. The 'ridge' along the diagonal indicates that the matrix $\mathbf{M}'$ is diagonally dominant. Also note that the modes are normalized such that $\mathbf{M}'$ is an identity matrix or close to that. From this figure it is clear that the real parts of extracted complex modes satisfy the mass orthogonality relationship with good accuracy. In

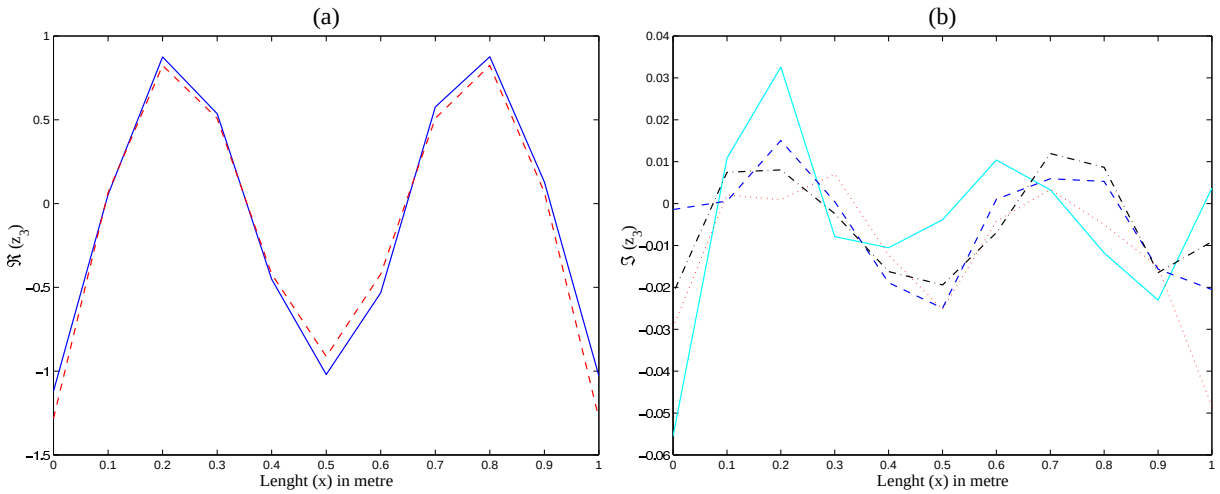

Figure 8.19: (a) The real part of complex mode $\mathbf{z}_3$,'—' experiment, '−−' theory; (b) The imaginary part of complex mode $\mathbf{z}_3$ for four sets of experimental data

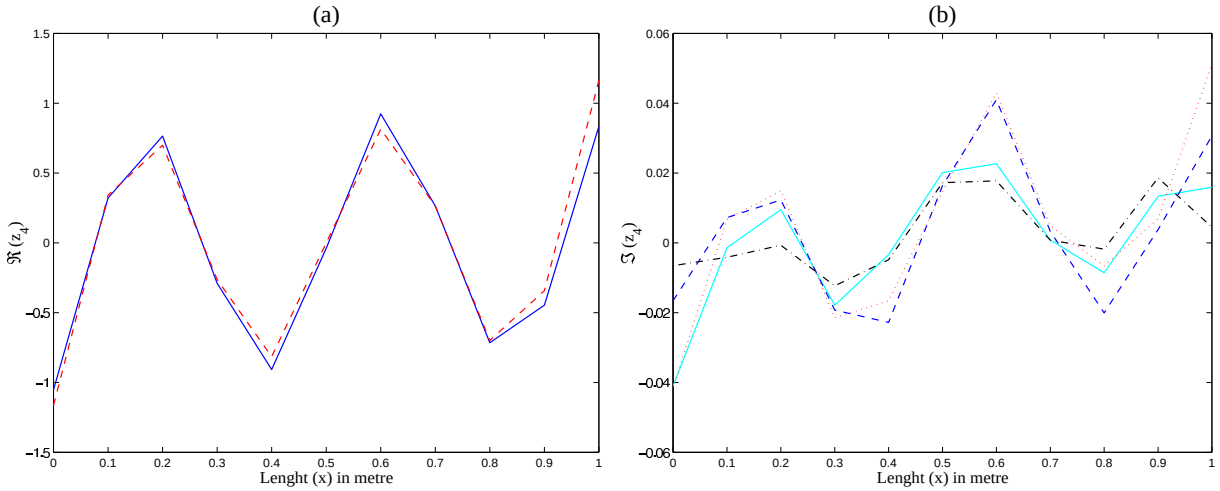

Figure 8.20: (a) The real part of complex mode $\mathbf{z}_4$,'—' experiment, '−−' theory; (b) The imaginary part of complex mode $\mathbf{z}_4$ for four sets of experimental data

Figure 8.29 the matrix $\mathbf{M}'$ obtained using the real parts of extracted complex modes is shown.

The imaginary parts of extracted complex modes cannot be compared with 'theory' because a correct theoretical damping model is required in order to produce the imaginary parts of complex modes. Thus, unlike the real parts of extracted complex modes, there is no simple way in which one can verify the accuracy of the imaginary parts. Unfortunately, it is the imaginary parts of the extracted complex modes which are more likely to get affected by any experimental noise because their magnitudes are much smaller compared to the corresponding real parts (see Figures 8.17 to 8.27).

Besides numerical accuracy, it also not known if the shapes of the imaginary parts of the extracted complex modes are at all correct. For the purpose of this study the experiment was repeated several times and from Figures 8.17 to 8.27 it may be verified that the imaginary parts of the ex-

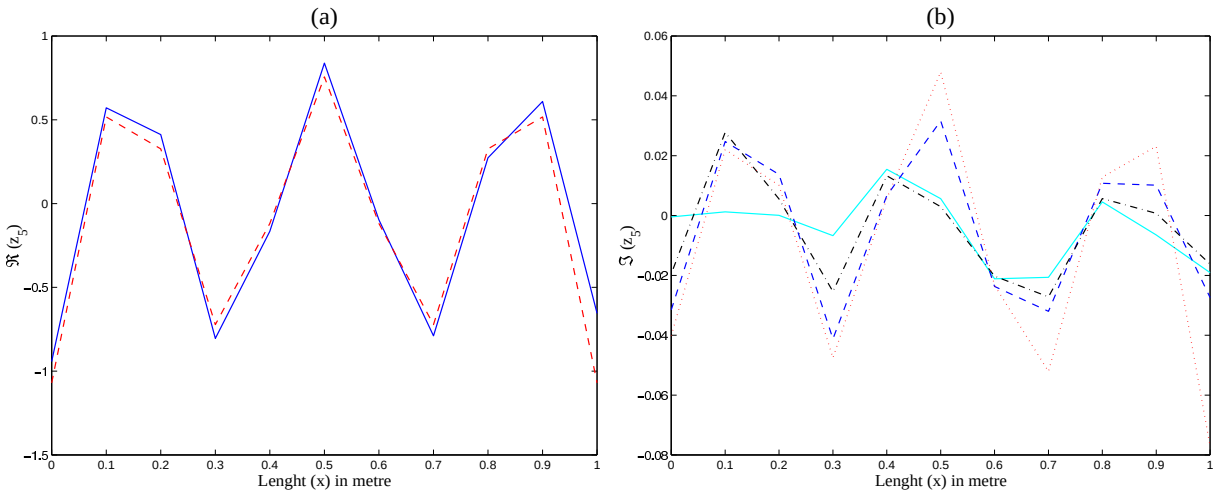

Figure 8.21: (a) The real part of complex mode $\mathbf{z}_5$,'—' experiment, '−−' theory; (b) The imaginary part of complex mode $\mathbf{z}_5$ for four sets of experimental data

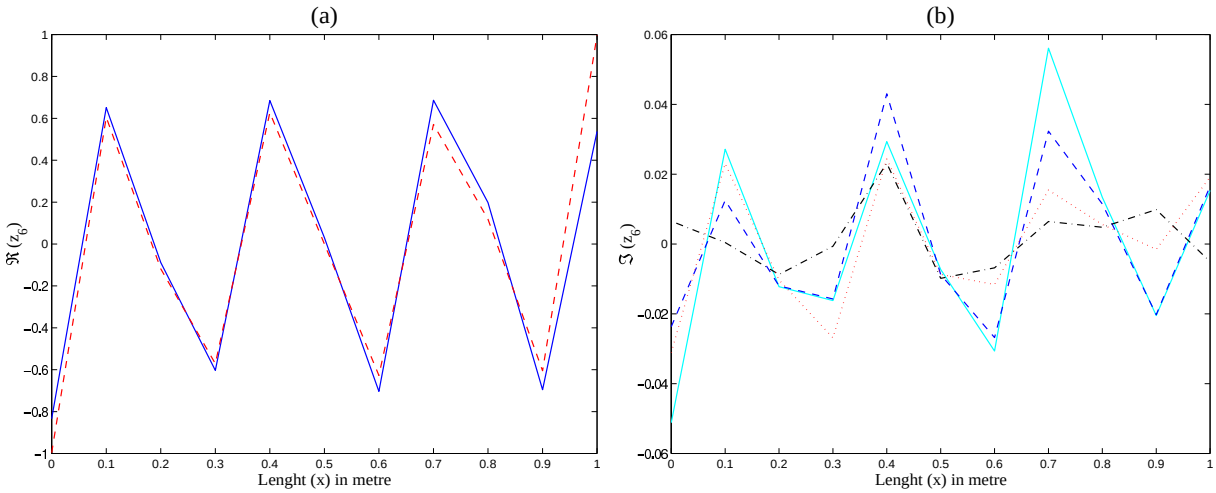

Figure 8.22: (a) The real part of complex mode $\mathbf{z}_6$,'—' experiment, '−−' theory; (b) The imaginary part of complex mode $\mathbf{z}_6$ for four sets of experimental data

tracted complex modes are reasonably accurately repeatable. This confirms that although they are small, these quantities are not random noise, but possibly arise due to the physics of the damping mechanism. Results on identification of the damping properties using the real and imaginary parts of complex modes are discussed next.

8.5.3 Identification of the Damping Properties

Fitting of the Viscous Damping Model

First, we consider fitting of a viscous damping matrix to the extracted modal data. The procedure for fitting the viscous damping matrix developed in Chapter 5 is applied. Figure 8.30 shows the fitted viscous damping matrix of the beam. Observes that this matrix is not symmetric. The

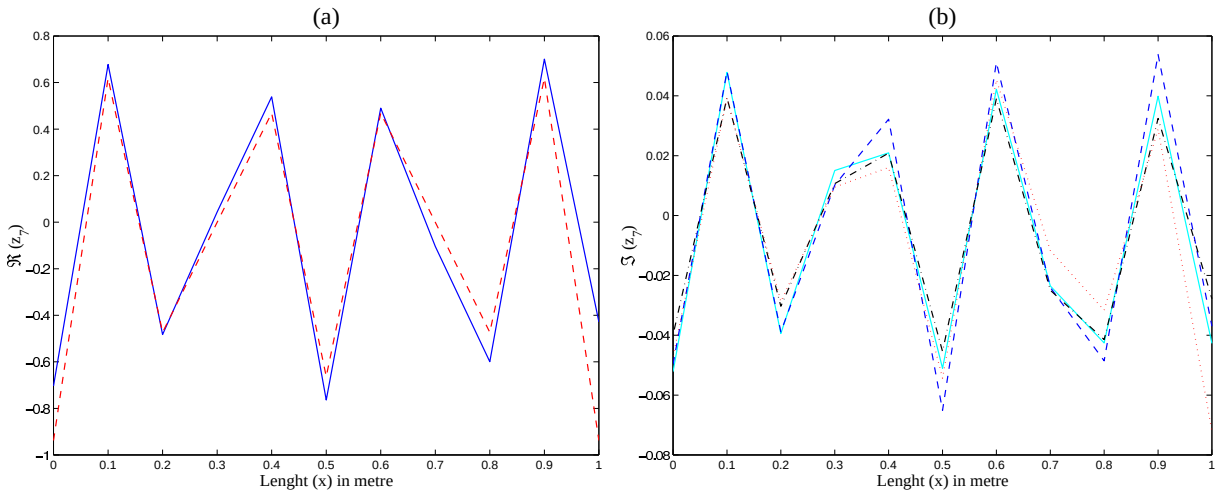

Figure 8.23: (a) The real part of complex mode $\mathbf{z}_7$,'—' experiment, '−−' theory; (b) The imaginary part of complex mode $\mathbf{z}_7$ for four sets of experimental data

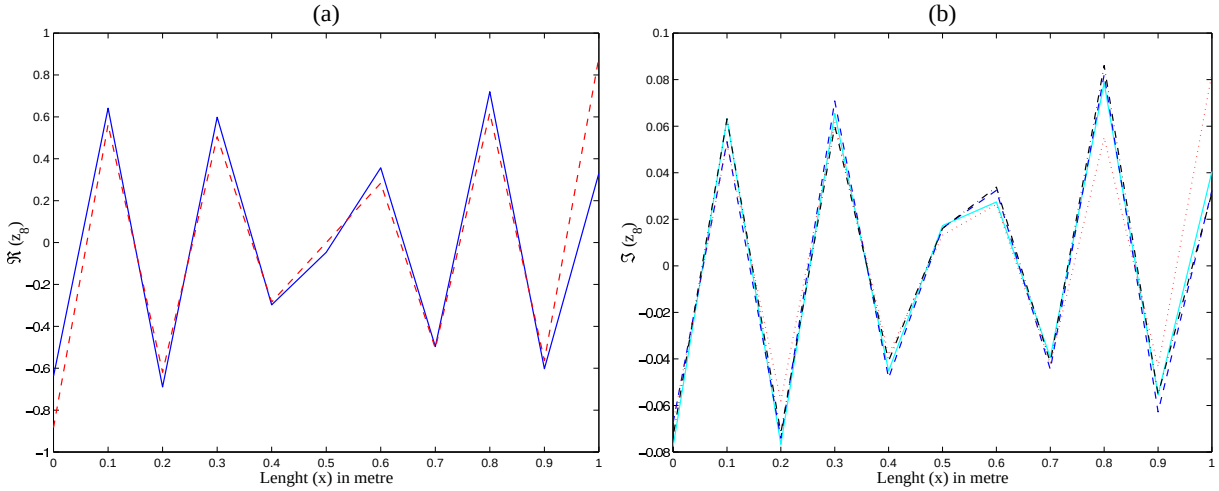

Figure 8.24: (a) The real part of complex mode $\mathbf{z}_8$,'—' experiment, '−−' theory; (b) The imaginary part of complex mode $\mathbf{z}_8$ for four sets of experimental data

negative off-diagonal terms in some places indicate that the damping is not local. However, it is encouraging that the high portion in the diagram roughly corresponds to the position of the damping layer used in the beam. This fact is more evident if one takes the diagonal of the fitted viscous damping matrix as shown in Figure 8.31. The features of fitting the viscous damping matrix observed here are quite similar to the cases discussed in Chapter 5 when the damping in the original system is significantly non-viscous (see, for example Figures 5.7,5.8 and 5.9).

According to the conclusions drawn in Chapter 5, we may regard the asymmetry of the fitted viscous damping matrix as an indication that a wrong damping model has been chosen for fitting. This indicates that the damping mechanism of the constrained layer damped beam used here is not viscous. This results also illustrates that the viscous damping model commonly used in the literature is not correct for this system. Next we consider fitting of an exponential damping model

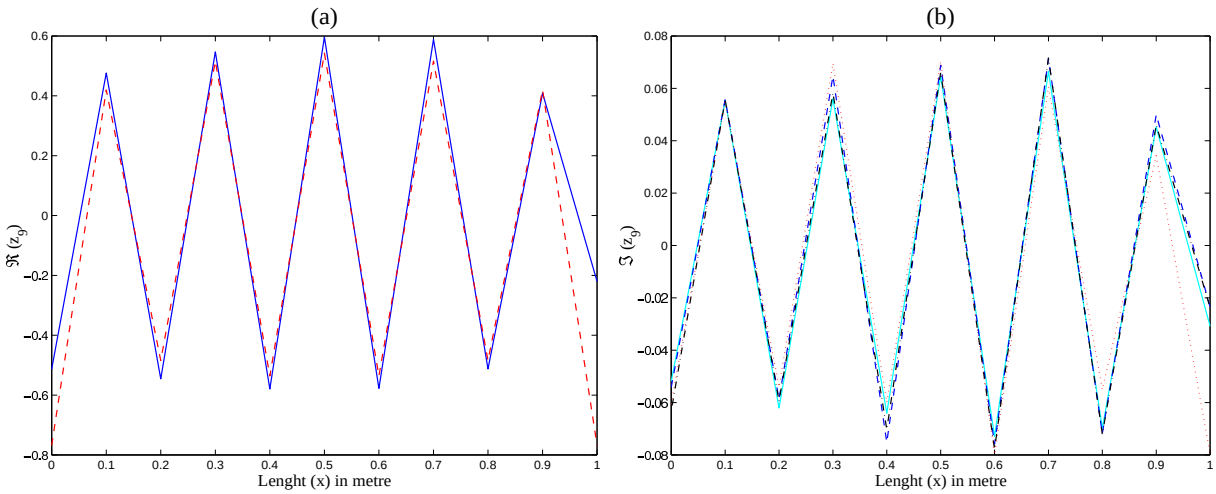

Figure 8.25: (a) The real part of complex mode $\mathbf{z}_9$,'—' experiment, '– –' theory; (b) The imaginary part of complex mode $\mathbf{z}_9$ for four sets of experimental data

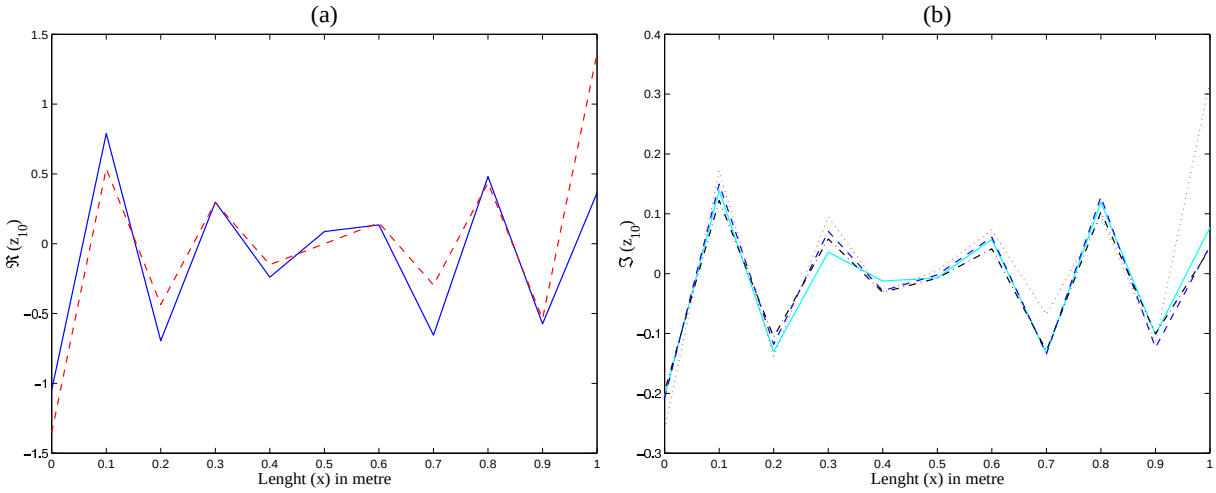

Figure 8.26: (a) The real part of complex mode $\mathbf{z}_{10}$,'—' experiment, '– –' theory; (b) The imaginary part of complex mode $\mathbf{z}_{10}$ for four sets of experimental data

to the measured modal data.

Fitting of Non-Viscous Damping

A procedure for fitting of a non-viscous damping model was developed in Chapter 6. In this section we apply this method to the damped beam considered here. Figure 8.32 shows the values of $\hat{\gamma}$ obtained from different $\hat{\mu}$ calculated using equations (6.18)–(6.20). The trend of this plot is similar to the one corresponding to the double-exponential model (GHM model) shown in Figure 6.6. The values of fitted γ approximately vary from 53 to 0.9. In view of the discussions in Chapter 6, we select the value of γ corresponding to the value at the first mode (marked by a $*$). For this value of γ, the damping time function is shown in Figure 8.33. The fitted coefficient matrix corresponding to this function is shown in Figure 8.34. The high portion near one end roughly indicates the

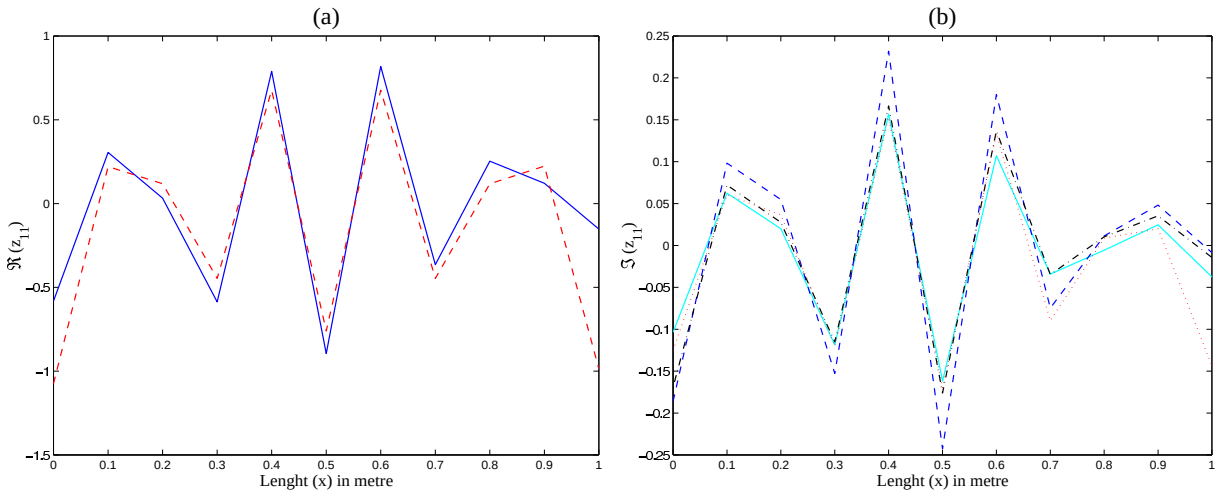

Figure 8.27: (a) The real part of complex mode $\mathbf{z}_{11}$,'—' experiment, '−−' theory; (b) The imaginary part of complex mode $\mathbf{z}_{11}$ for four sets of experimental data

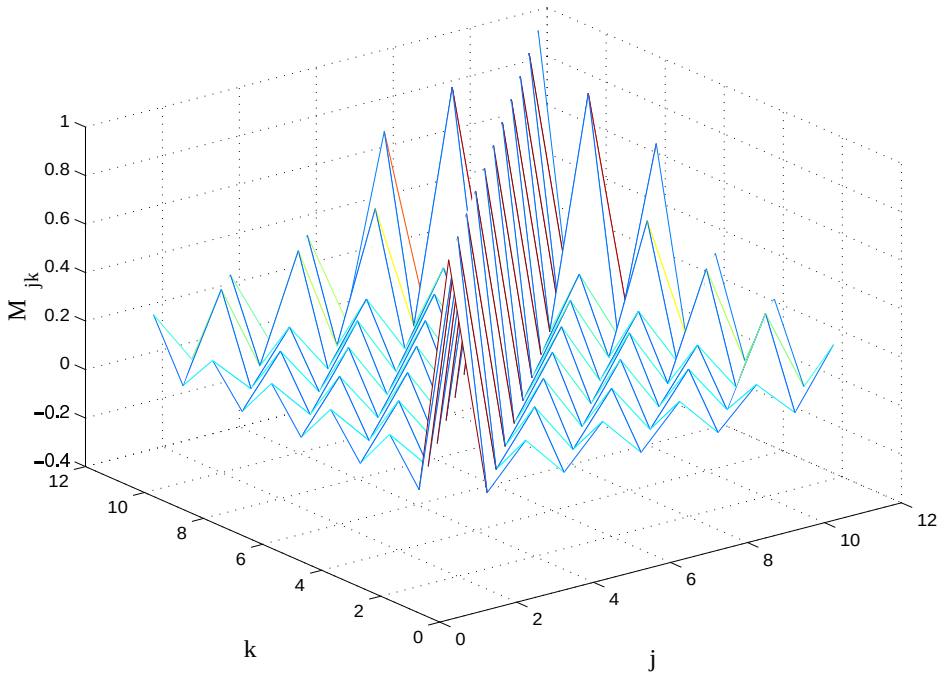

Figure 8.28: Mass matrix in the modal coordinates using the modes obtained from the beam theory

position of the damping in the beam. The diagonal of the fitted coefficient matrix shown in Figure 8.35 clearly reveals this fact. Off-diagonal elements are present in the fitted coefficient matrix, but since they are all positive, this may indicate that the damping mechanism is approximately local. Interestingly, observe that the fitted coefficient matrix is symmetric which indicates that the fitted model might be correct. This is, in a way, contradictory to the result shown in Figure 8.32 for the fitted values of γ. If the original damping model is truly exponential then the values of fitted γ for all the modes would have been the same, that is, a straight line would be obtained rather than a line with downward slope as obtained here. In spite of this, the fitted coefficient matrix turns

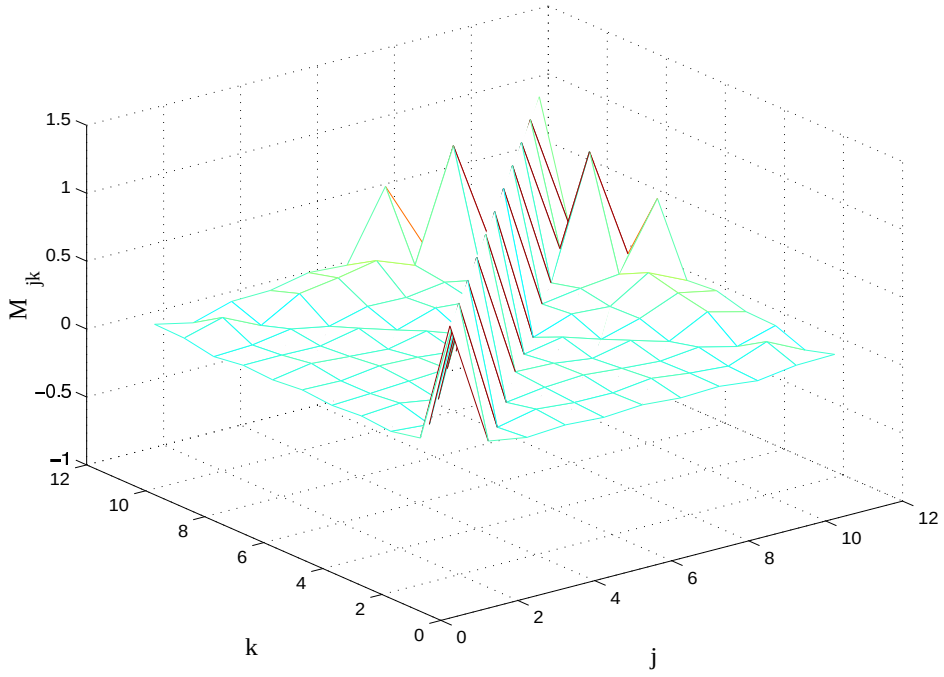

Figure 8.29: Mass matrix in the modal coordinates using the modes obtained from measurement

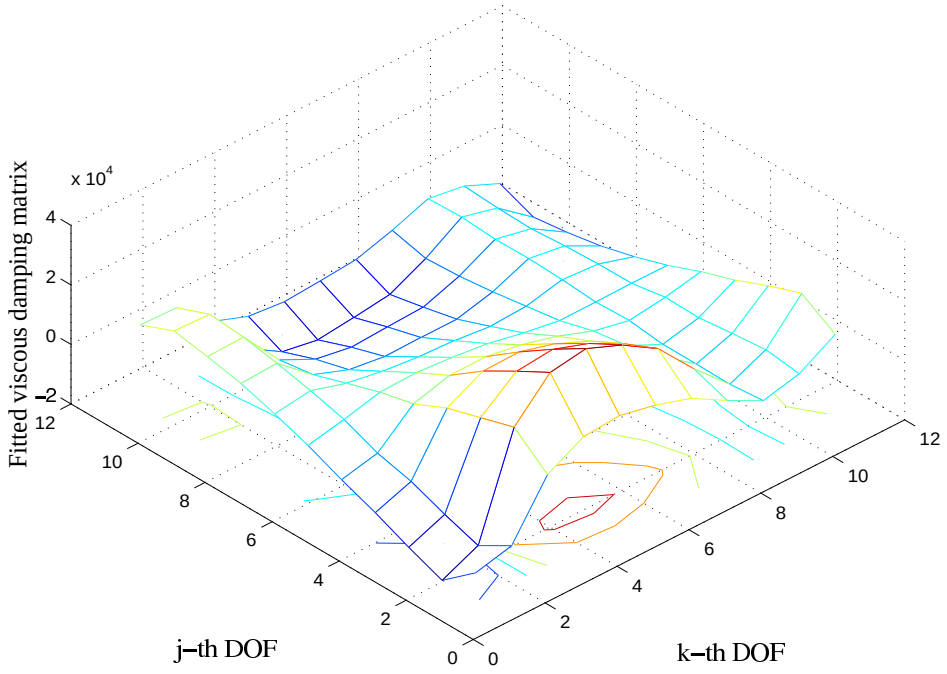

Figure 8.30: Fitted viscous damping matrix for the beam

out to be symmetric. This is due to the fact that the values of γ are not very high (in the order of 50). Recall that similar features were also observed in the simulation studies, see Figures 6.6 and 6.13. From these results we conclude that the damping mechanism of the constrained layer damped beam considered here is perhaps close to a single exponential model. This is consistent with the fact that constrained layer damping is often viscoelastic (see Ungar, 2000).

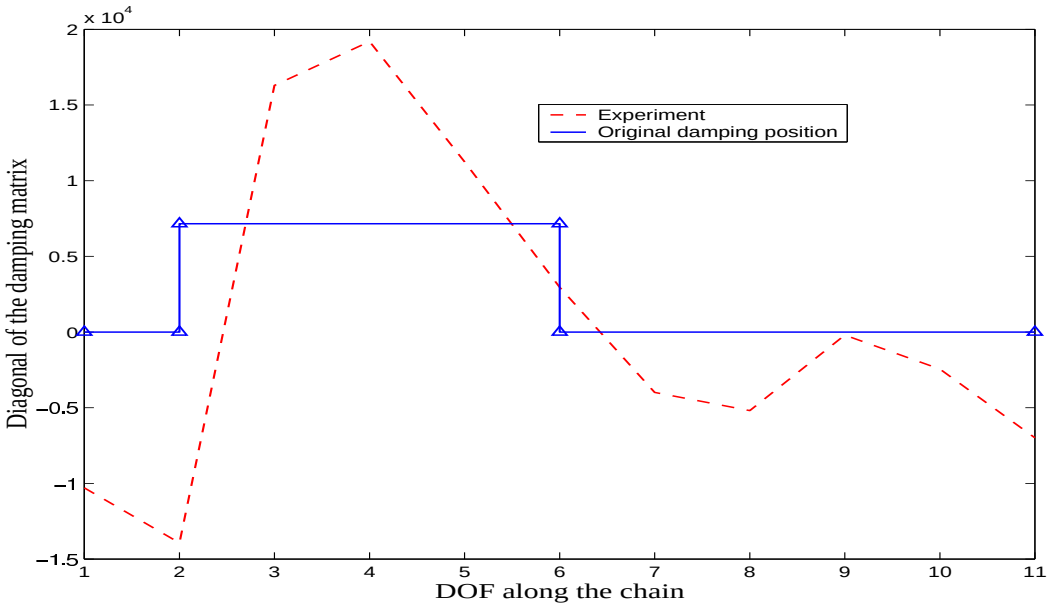

Figure 8.31: Diagonal of the fitted viscous damping matrix

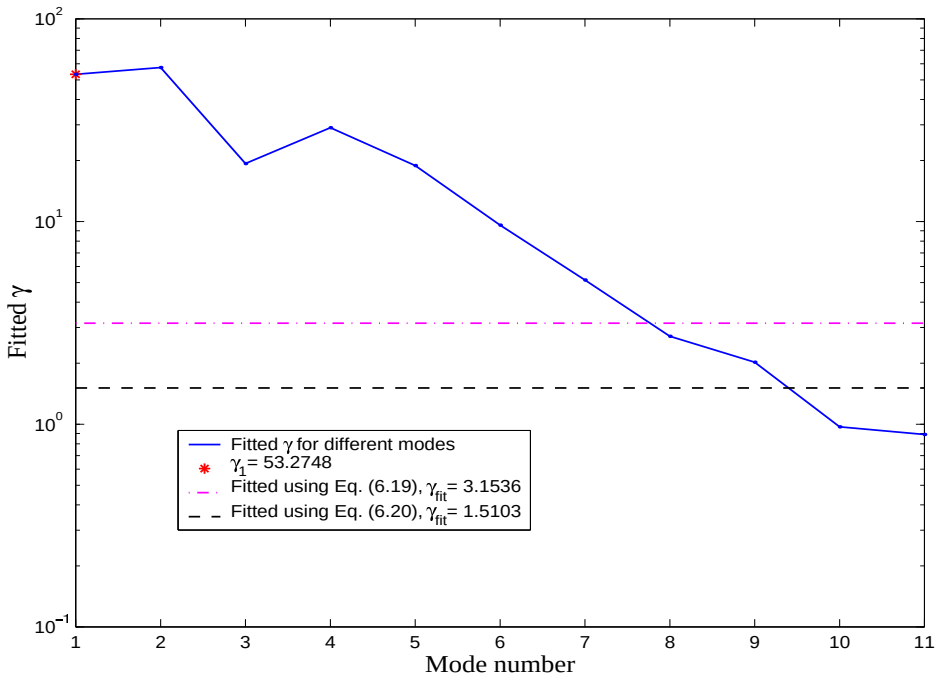

Figure 8.32: Values of $\hat{\gamma}$ obtained from different $\hat{\mu}$ calculated using equations (6.18)–(6.20)

Symmetry-Preserving Fitting

In this section the symmetry-preserving damping identification method developed in Chapter 7 is applied to the modal data extracted for the damped beam. Because the coefficient matrix of the identified exponential damping function is symmetric, the symmetry preserving method is applied to identification of the viscous damping model only. Figure 8.36 shows the fitted symmetric viscous damping matrix. The high portion corresponds to the position of the damping layer in the

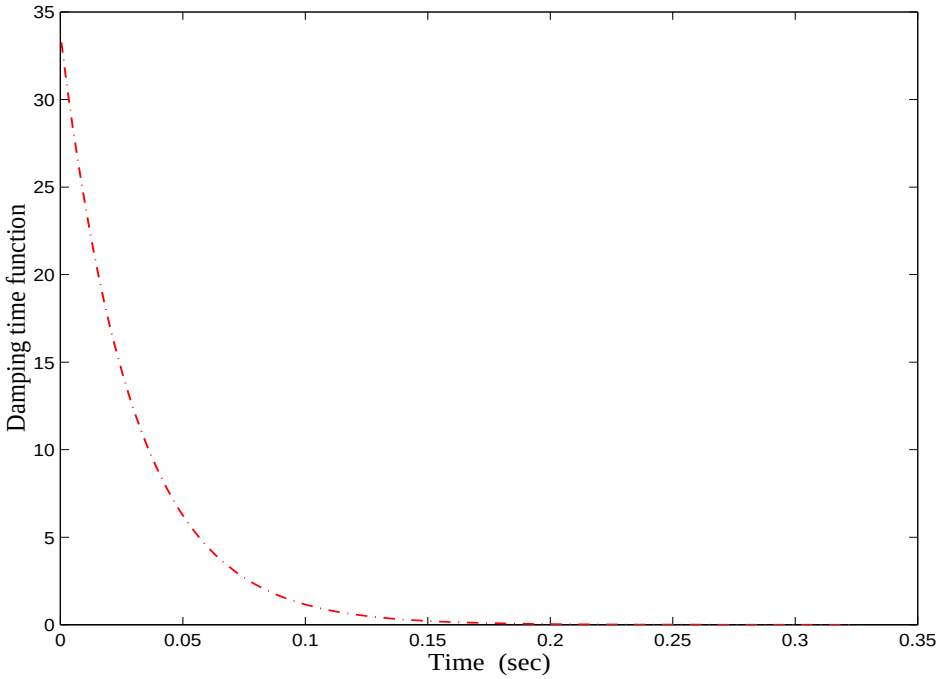

Figure 8.33: Fitted damping time function for the beam

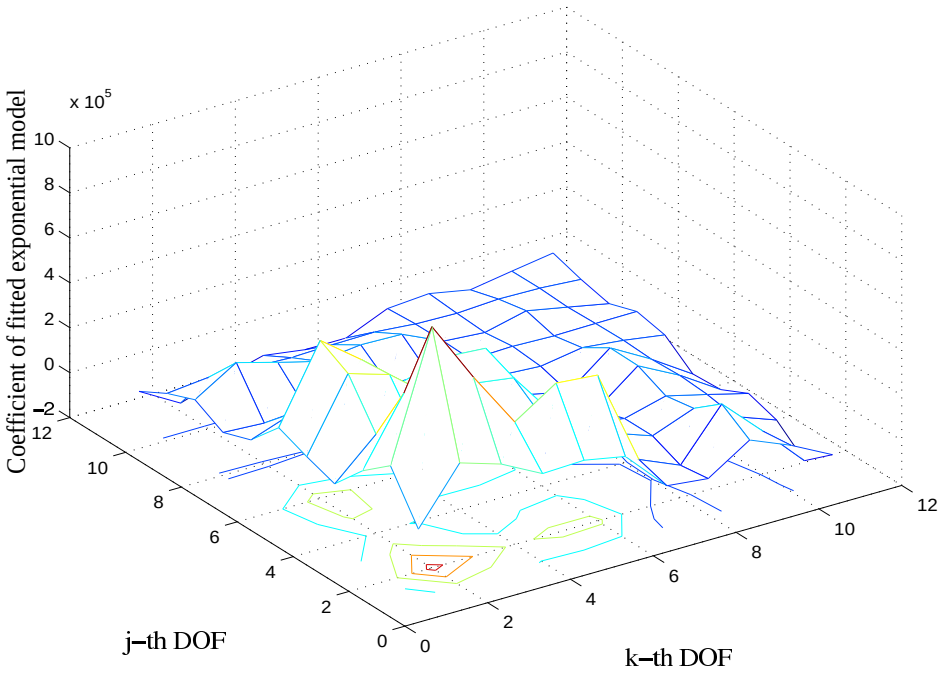

Figure 8.34: Fitted coefficient matrix of exponential model

beam. Comparison of Figures 8.36 and 8.30 clearly demonstrates improvement of the fitted viscous damping matrix for the latter case.

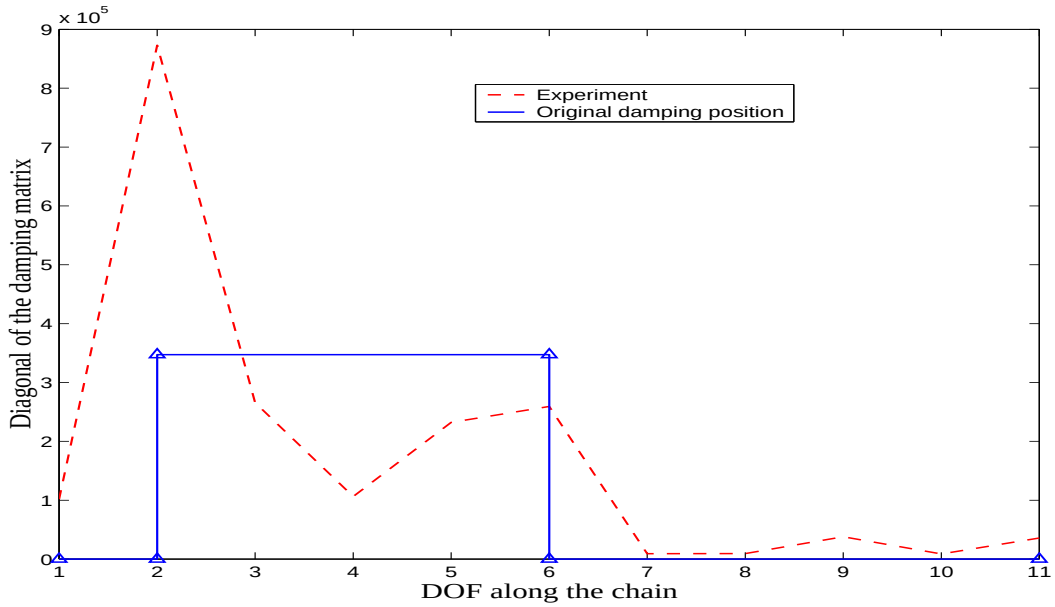

Figure 8.35: Diagonal of the fitted coefficient matrix of exponential model

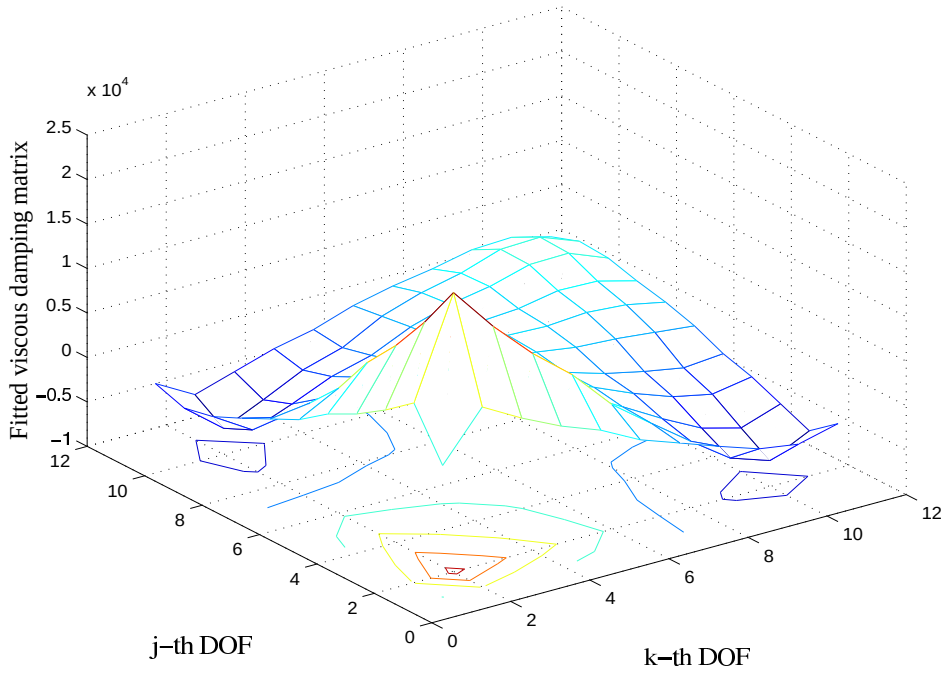

Figure 8.36: Fitted symmetric viscous damping matrix

Discussions

From the results shown so far it may be concluded that the damping characteristics of the beam considered in study is best represented by the exponential damping model. Application of the usual method of fitting the viscous damping matrix yields an asymmetric damping matrix. This indicates that the damping mechanism of the beam is non-viscous. However, recall that both the damping models are fitted from the same set of poles and residues extracted from the measured transfer

functions. This demonstrates that two different damping models with different spatial distributions and parameters can be fitted to the measured transfer functions. On the one hand, this result is negative because it says that by conducting conventional modal testing it is not possible to identify unique damping model. On the other hand, this result is positive as any damping model can be fitted to reconstruct the measured set of poles and residues.

It is now the analyst's choice to decide on which approach should be adopted. If the interest lies in understanding the true damping mechanism of a system then a model should be fitted for which the coefficient matrix is symmetric. If, however, the interest is only to reconstruct a set of measured transfer functions, then either a viscous or a non-viscous model can be fitted. The choice of viscous or non-viscous model in this case depends on whether an accurate mass matrix of the system is available or not. If the identified coefficient matrix is found to be asymmetric, the symmetry preserving methods can be applied. As shown here, the damping matrix obtained using the symmetry preserving method can give a reasonable account of the spatial distribution of damping even for the case when the fitted model is incorrect.

Modal testing of the beam was conducted several times and the results shown so far correspond to just one set of data. It was observed that in some cases the results on damping identification were not very good. Figure 8.37 shows fitted values of γ for a different set of measurements. The identified coefficient matrix using the value of γ_1 is shown in Figure 8.38. Although general trends

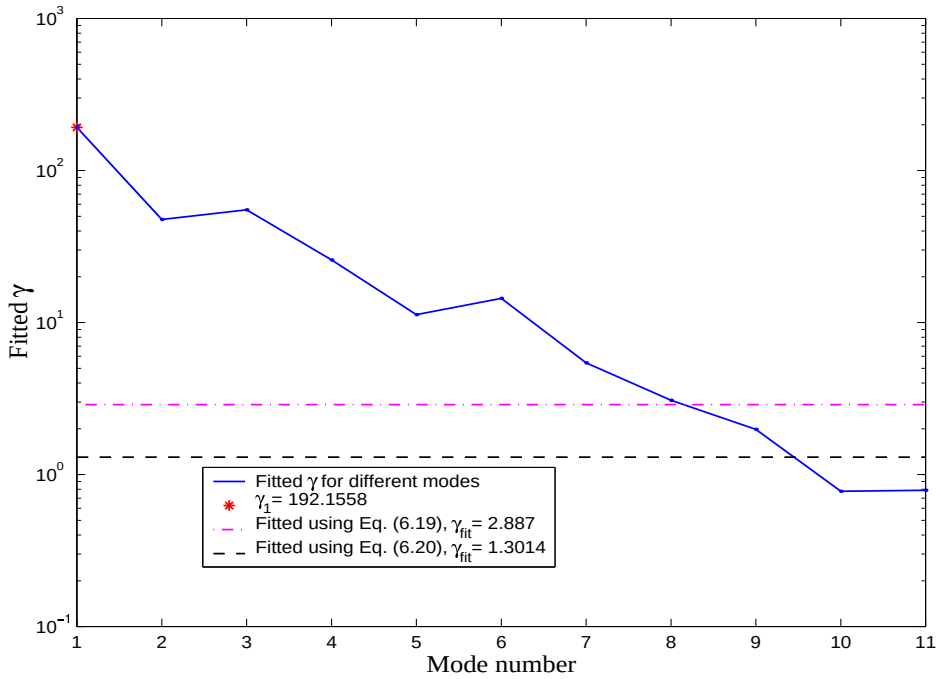

Figure 8.37: Values of $\hat{\gamma}$ obtained from different $\hat{\mu}$ calculated using equations (6.18)–(6.20)

of these two figures are similar to Figures 8.32 and 8.34, the numerical values are quite different. The value of γ_1 is much higher in Figure 8.37 compared to that in Figure 8.32. Also observe that the spatial distribution of damping shown in Figure 8.38 is less accurate than that in Figure 8.34.

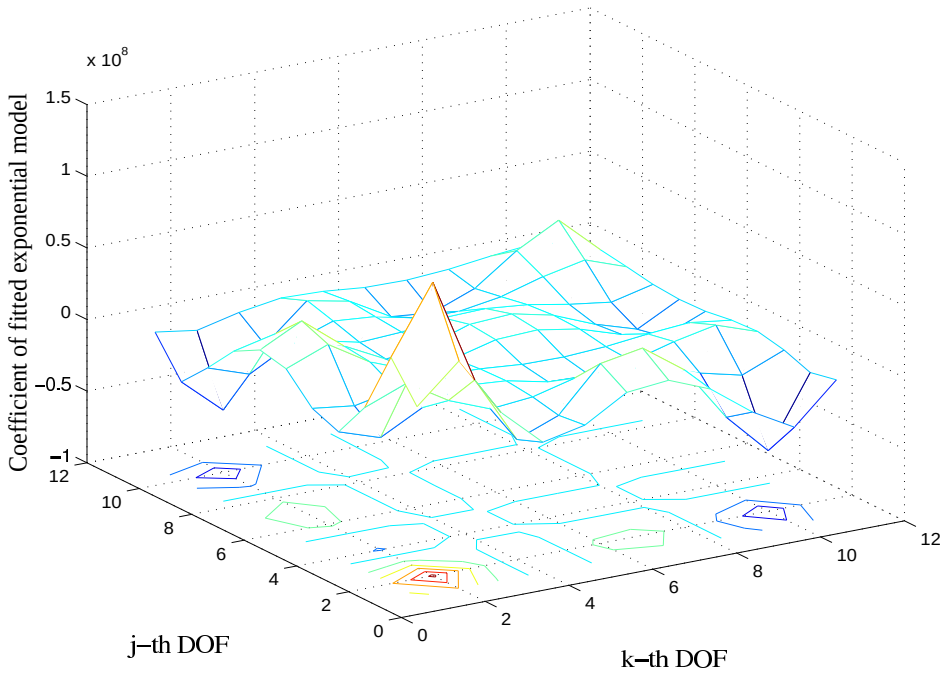

Figure 8.38: Fitted coefficient matrix of exponential model

This raises the question – how sensitive are the damping identification procedures to measurement noise? We take up this issue in the next section.

8.6 Error Analysis

In this section we consider the effects of measurement noise on the identified damping matrix. Due to the presence of noise or random errors, the measured transfer functions become noisy. This in turn makes the poles and residues, and consequently the complex natural frequencies and modes erroneous. Further, recall that for lightly damped systems the imaginary parts of the complex modes are small compared to their corresponding real parts. Thus, the presence of random errors is likely to affect the imaginary parts more than the real parts. The effect of errors in the modal data on identification of viscous and non-viscous damping is considered in the next two sections.

8.6.1 Error Analysis for Viscous Damping Identification

In Chapter 5, the method for viscous damping identification was developed by assuming that the complex natural frequencies as well as the complex modes are obtained exactly. In this section, how the identified viscous damping matrix behaves due to the presence of errors in the modal data is investigated. This can be done best by considering the numerical example used in Section 5.4.

In order to simulate the effect of noise, we perturb the modal data by adding zero-mean Gaussian random noise to them. Numerical experiments have been performed by adding different levels of noise to the following four quantities:

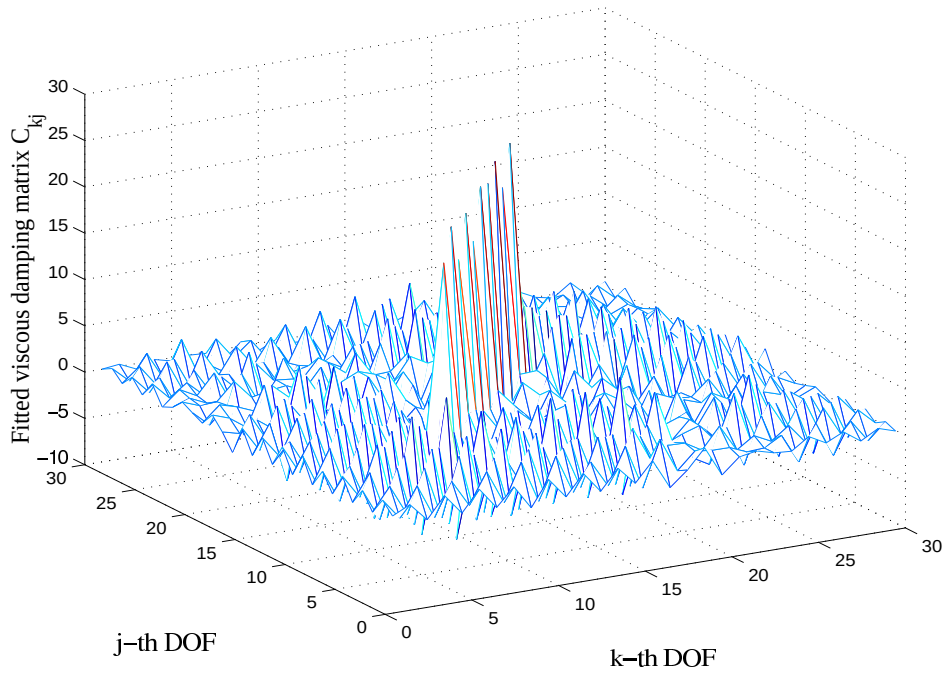

Figure 8.39: Fitted viscous damping matrix for the local case, $\gamma = 0.02$, damping model 2, noise case (a)

1. Real parts of complex natural frequencies (r_ω)
2. Imaginary parts of complex natural frequencies (r_η)
3. Real parts of complex modes (r_u)
4. Imaginary parts of complex modes (r_v).

Levels of noise, denoted by the quantities r_ω, r_η, r_u and r_v, are expressed as a percentage of their corresponding original values. In practice we hope to obtain the natural frequencies and Q-factors with good accuracy. So, in what follows next, we assume $r_\omega = r_\eta = 2\%$ for all the modes. The following cases are considered regarding noise levels r_u and r_v for all the modes:

(a) $r_u = 2\%$ and $r_v = 10\%$

(b) $r_u = 10\%$ and $r_v = 2\%$

(c) $r_u = 2\%$ and $r_v = 30\%$.

Figures 8.39, 8.40 and 8.41 show fitted viscous damping matrix for damping model 2 corresponding to the noise cases (a), (b) and (c) respectively. The locally reacting damping model shown in Figure 5.1(a) is considered and $\gamma = 0.02$ is assumed. Observe that for the noise case (a), the fitted coefficient matrix is not very different from the exact one shown in Figure 5.2. This indicates that 2% noise in the real parts of complex modes and 10% noise in the imaginary parts of complex modes do not effect the fitting result significantly. However, as observed from Figure

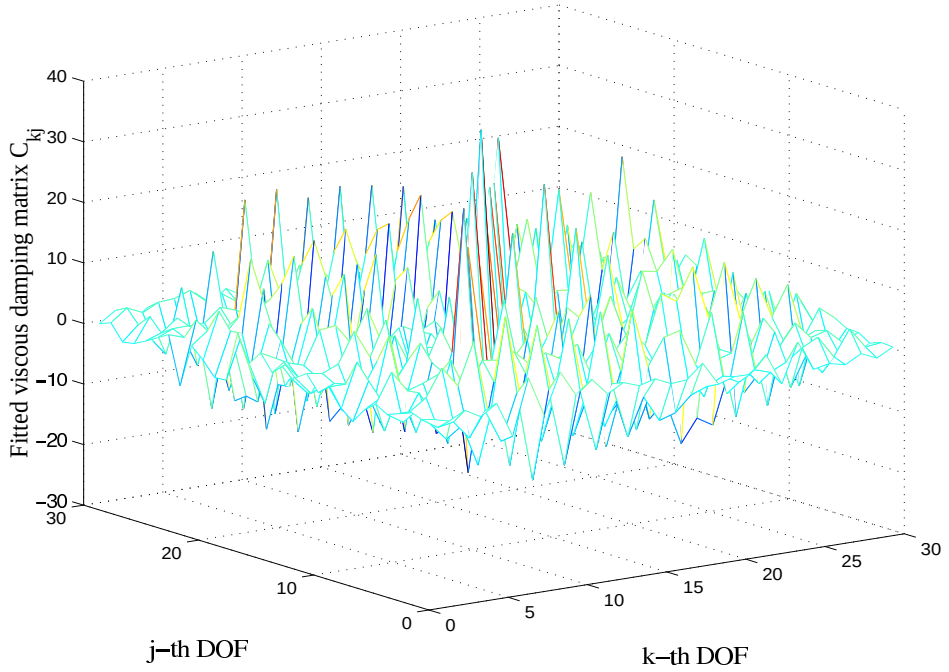

Figure 8.40: Fitted viscous damping matrix for the local case, $\gamma = 0.02$, damping model 2, noise case (b)

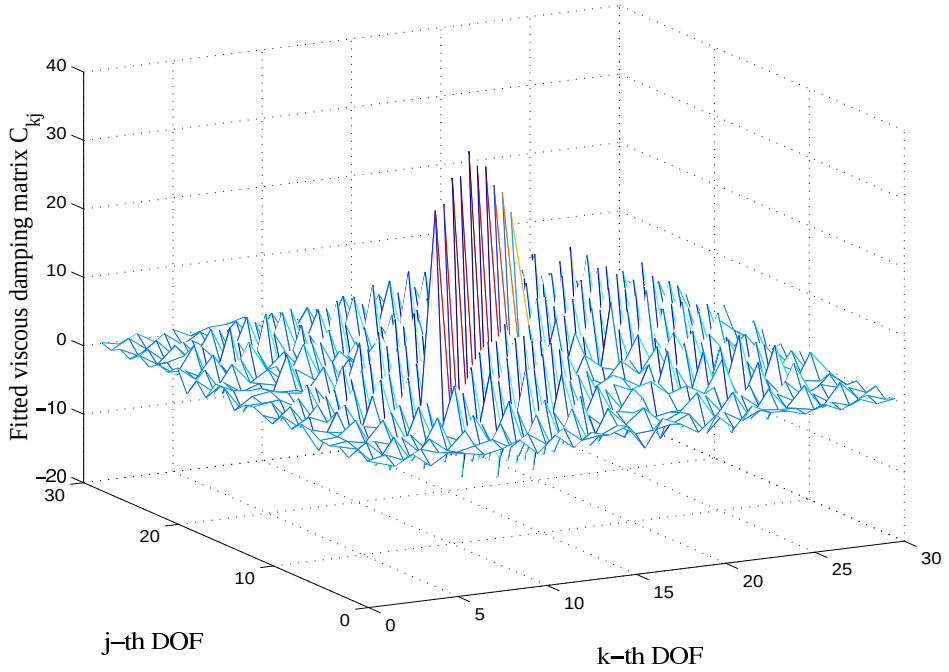

Figure 8.41: Fitted viscous damping matrix for the local case, $\gamma = 0.02$, damping model 2, noise case (c)

8.40, the story becomes completely different for the noise case (b) when the values of r_u and r_v are swapped. This clearly shows that the proposed viscous damping identification procedure is much more sensitive to errors in the real parts of complex modes than to errors in the imaginary parts. To illustrate this fact further, noise case (c) is considered where the noise level in the imaginary parts of complex modes is 30%. From Figure 8.41 observe that even for this high value of r_v, the fitted viscous damping matrix is close to the noise-free case as shown before in Figure 5.2.

Numerical experiments have been carried out using different damping models and parameter sets. The results are in general quite similar. From this simulation study we conclude that errors in the real parts of complex modes affect the damping fitting procedure much more than errors in the imaginary parts of complex modes. This fact makes the proposed method very suitable for practical purposes because the real parts of complex modes can be obtained more accurately and reliably than their corresponding imaginary parts.

A semi-analytical explanation of this fact may be given by a perturbation analysis. Suppose, the real and imaginary parts of the complex modal matrix can be expressed as

$$\begin{aligned} \mathbf{U} &= \mathbf{U}_0 + \boldsymbol{\Delta}\mathbf{U} \\ \mathbf{V} &= \mathbf{V}_0 + \boldsymbol{\Delta}\mathbf{V} \end{aligned} \tag{8.60}$$

where $\boldsymbol{\Delta}(\bullet)$ denotes the 'error part' and $(\bullet)_0$ denotes the 'error-free part'. Note that, in general $\mathbf{U}$ and $\mathbf{V}$ are *not* square matrices. From equation (5.12), one obtains the matrix of constants

$$\begin{aligned} \mathbf{B} &= \left[\mathbf{U}^T\mathbf{U}\right]^{-1}\mathbf{U}^T\mathbf{V} \\ &= \left[\left(\mathbf{U}_0 + \boldsymbol{\Delta}\mathbf{U}\right)^T\left(\mathbf{U}_0 + \boldsymbol{\Delta}\mathbf{U}\right)\right]^{-1}\left(\mathbf{U}_0 + \boldsymbol{\Delta}\mathbf{U}\right)^T\left(\mathbf{V}_0 + \boldsymbol{\Delta}\mathbf{V}\right) \\ &= \left[\mathbf{I} - \left(\mathbf{U}_0^T\mathbf{U}_0\right)^{-1}\left(\boldsymbol{\Delta}\mathbf{U}^T\mathbf{U}_0 + \mathbf{U}_0^T\boldsymbol{\Delta}\mathbf{U} + \boldsymbol{\Delta}\mathbf{U}^T\boldsymbol{\Delta}\mathbf{U}\right)\right]^{-1} \\ &\qquad \left(\mathbf{U}_0^T\mathbf{U}_0\right)^{-1}\left(\mathbf{U}_0 + \boldsymbol{\Delta}\mathbf{U}\right)^T\left(\mathbf{V}_0 + \boldsymbol{\Delta}\mathbf{V}\right) \end{aligned} \tag{8.61}$$

Neglecting second or higher order terms involving $\boldsymbol{\Delta}$, the above relationship can be approximated as

$$\begin{aligned} \mathbf{B} \approx \mathbf{B}_0 + \left[\left(\mathbf{U}_0^T\mathbf{U}_0\right)^{-1}\boldsymbol{\Delta}\mathbf{U}^T\mathbf{V}_0 - \left(\mathbf{U}_0^T\mathbf{U}_0\right)^{-1}\left(\boldsymbol{\Delta}\mathbf{U}^T\mathbf{U}_0 + \mathbf{U}_0^T\boldsymbol{\Delta}\mathbf{U}\right)\left(\mathbf{U}_0^T\mathbf{U}_0\right)^{-1}\mathbf{U}_0^T\mathbf{V}_0\right] \\ + \left[\left(\mathbf{U}_0^T\mathbf{U}_0\right)^{-1}\mathbf{U}^T\boldsymbol{\Delta}\mathbf{V}\right] \end{aligned} \tag{8.62}$$

where

$$\mathbf{B}_0 = \left(\mathbf{U}_0^T\mathbf{U}_0\right)^{-1}\mathbf{U}_0^T\mathbf{V}_0. \tag{8.63}$$

From equation (8.62) observe that there is only one term which contains $\boldsymbol{\Delta}\mathbf{V}$ in the approximate expression of $\mathbf{B}$. Also recall that the steps to be followed in order to obtain $\mathbf{C}'$ and $\mathbf{C}$ do not involve $\mathbf{V}$. For this reason the effect of $\boldsymbol{\Delta}\mathbf{V}$ is much less than that of $\boldsymbol{\Delta}\mathbf{U}$. This simple analysis explains why errors in the real parts of complex modes effect the viscous damping fitting procedure much more than errors in the imaginary parts of complex modes.

8.6.2 Error Analysis for Non-viscous Damping Identification

For identification of the exponential damping model we need to obtain the relaxation parameter and the coefficient damping matrix. The three noise cases introduced before have been considered. Again, the locally reacting damping model shown in Figure 5.1(a) is used and $\gamma = 0.02$ is assumed.

Figure 8.42 shows the values of fitted γ for the noise case (a). The fitted coefficient matrix

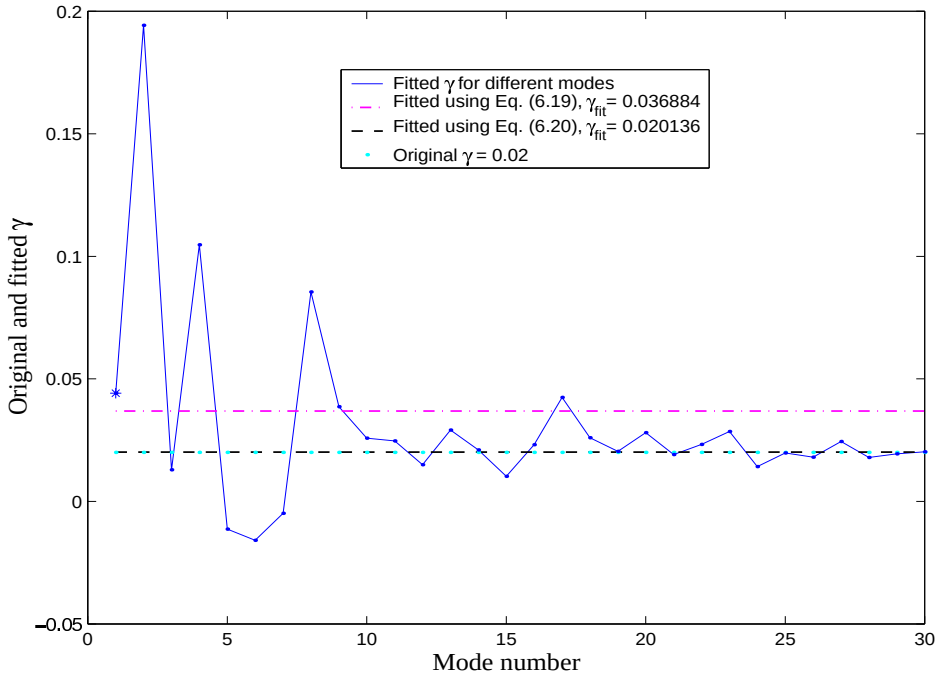

Figure 8.42: Values of $\hat{\gamma}$ obtained from different $\hat{\mu}$ calculated using equations (6.18)–(6.20) for the local case, damping model 2, noise case (a)

corresponding to this case is shown in Figure 8.43. Note that, the pattern of fitted γ for different modes shown in Figure 8.42 is quite different from its corresponding noise-free case shown in Figure 6.2. However, the fitted coefficient matrix in Figure 8.43 is not very different from the noise-free case as shown in Figure 6.8 except that the matrix become noisy. The spatial distribution of damping and that the damping is local type is clear from this diagram.

Figure 8.44 shows the values of fitted γ for the noise case (b). The fitted coefficient matrix corresponding to this case is shown in Figure 8.45. Like the noise case (a), the pattern of fitted γ for different modes shown in Figure 8.44 is quite different from its corresponding noise-free case and also variation in the values of fitted γ is more now. However, unlike noise case (a), the fitted coefficient matrix in Figure 8.45 is quite noisy and getting useful information from it becomes very difficult.

Figure 8.42 shows the values of fitted γ for the noise case (c). The fitted coefficient matrix corresponding to this case is shown in Figure 8.47. Like the two previous noise cases, the pattern of fitted γ for different modes shown in Figure 8.46 is quite different from its corresponding noise-free case and the values of fitted γ varies to a greater extent now. In spite of this, the fitted coefficient

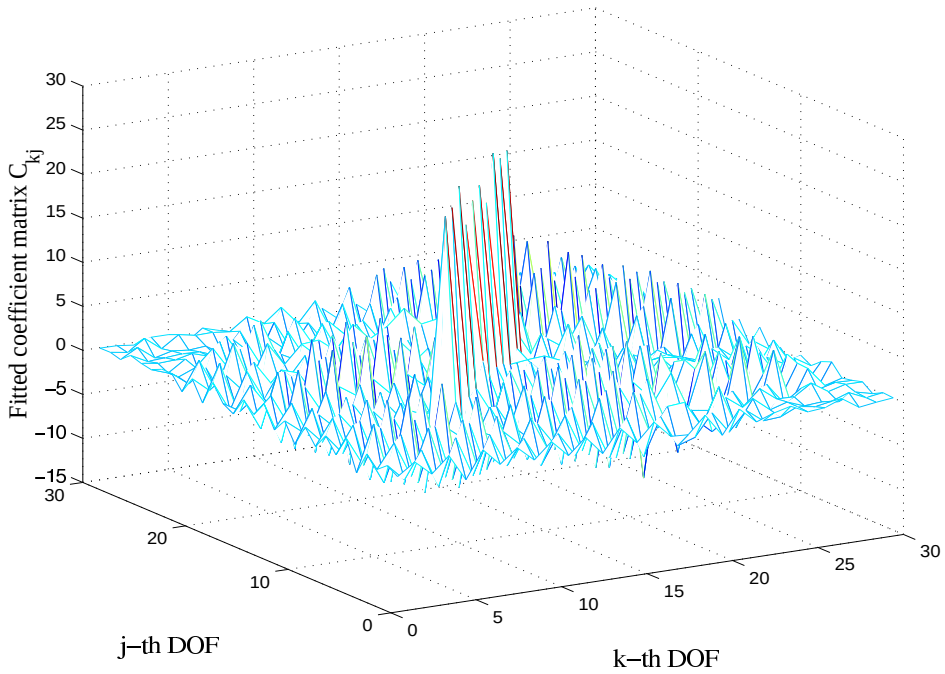

Figure 8.43: Fitted coefficient matrix of exponential model for the local case, $\gamma = 0.02$, damping model 2, noise case (a)

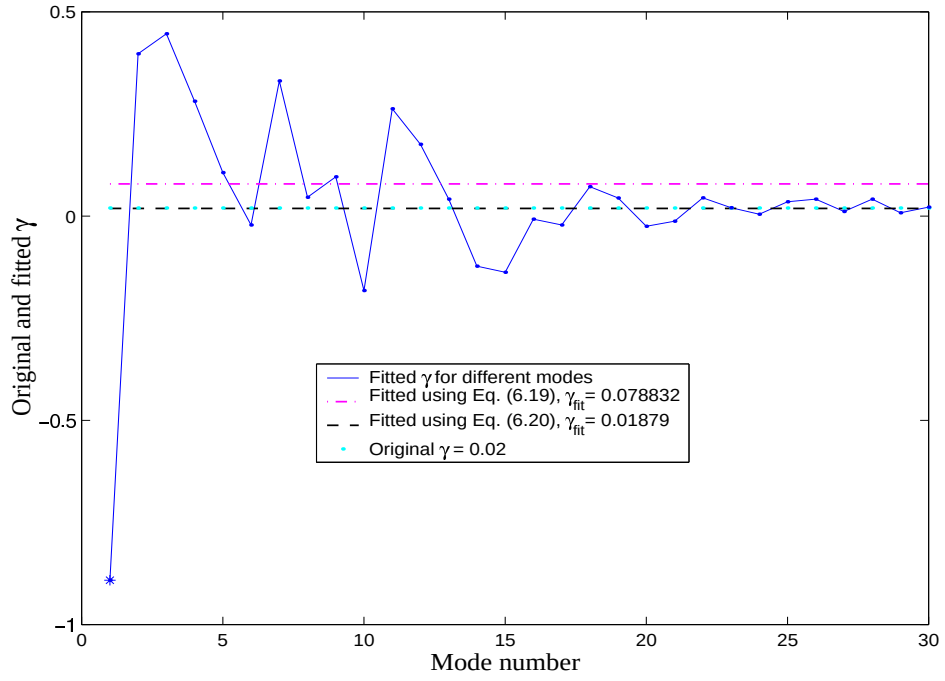

Figure 8.44: Values of $\hat{\gamma}$ obtained from different $\hat{\mu}$ calculated using equations (6.18)–(6.20) for the local case, damping model 2, noise case (b)

matrix in Figure 8.47 is not very different from the noise-free case shown in Figure 6.8. The spatial distribution of damping and that the damping is local type can be recognized from this diagram.

From these results we conclude that the values of relaxation parameter are sensitive to errors in both the real and imaginary parts of complex modes. However, the fitted coefficient matrix is

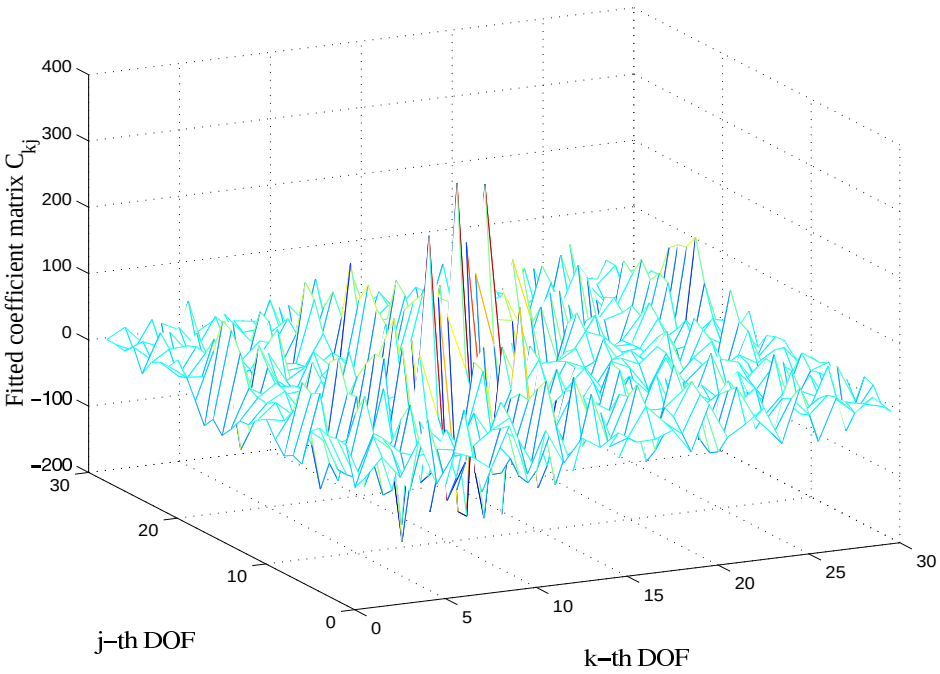

Figure 8.45: Fitted coefficient matrix of exponential model for the local case, $\gamma = 0.02$, damping model 2, noise case (b)

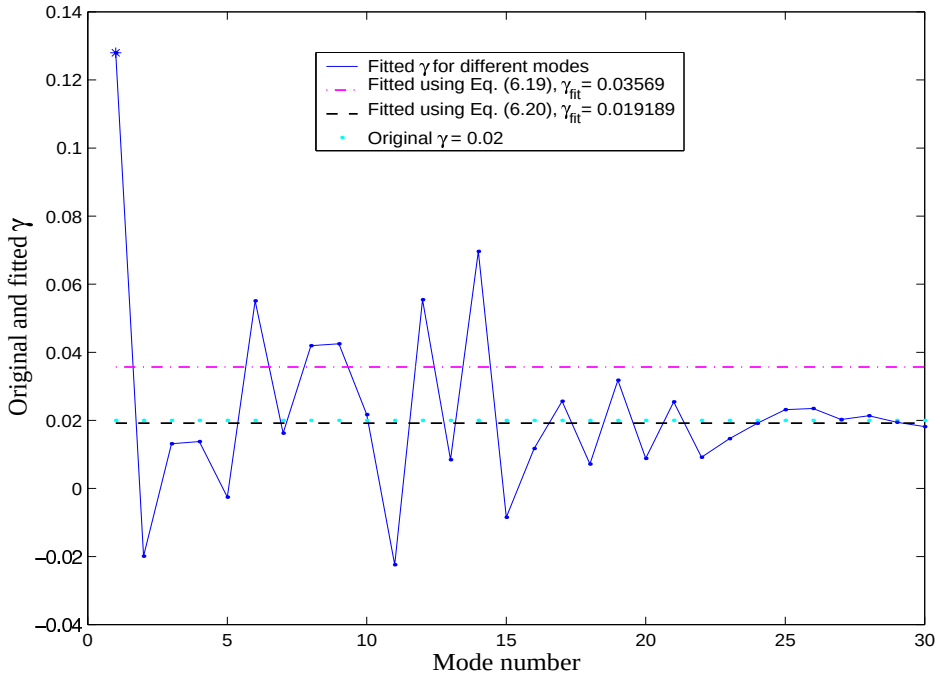

Figure 8.46: Values of $\hat{\gamma}$ obtained from different $\hat{\mu}$ calculated using equations (6.18)–(6.20) for the local case, damping model 2, noise case (c)

more sensitive to errors in the real parts of complex modes than the imaginary parts as observed for identification of the viscous damping matrix.

Explanation of these facts can again be given by a simple perturbation analysis. Since the the procedure for fitting of the coefficient matrix is similar to that of the viscous damping matrix, we

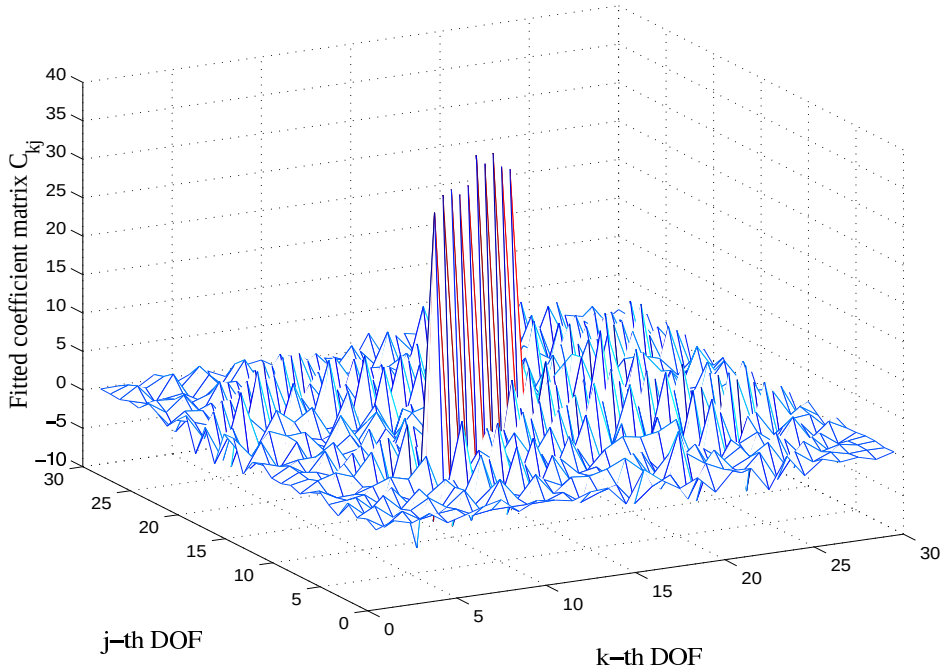

Figure 8.47: Fitted coefficient matrix of exponential model for the local case, $\gamma = 0.02$, damping model 2, noise case (c)

will discuss sensitivity analysis for the relaxation parameter only. Suppose for any j-th mode

$$\begin{aligned} \mathbf{u}_j &= \mathbf{u}_{0_j} + \boldsymbol{\Delta}\mathbf{u}_j \\ \mathbf{v}_j &= \mathbf{v}_{0_j} + \boldsymbol{\Delta}\mathbf{v}_j \\ \omega_j &= \omega_{0_j} + \Delta\omega_j \end{aligned} \tag{8.64}$$

Now, from equation (6.17), the expression of the relaxation parameter for j-th mode, μ_j can be written as

$$\begin{aligned} \mu_j &= \omega_j \frac{\mathbf{v}_j^T \mathbf{M} \mathbf{v}_j}{\mathbf{v}_j^T \mathbf{M} \mathbf{u}_j} \\ &= \left(\omega_{0_j} + \Delta\omega_j\right) \frac{\left(\mathbf{v}_{0_j} + \boldsymbol{\Delta}\mathbf{v}_j\right)^T \mathbf{M} \left(\mathbf{u}_{0_j} + \boldsymbol{\Delta}\mathbf{u}_j\right)}{\left(\mathbf{v}_{0_j} + \boldsymbol{\Delta}\mathbf{v}_j\right)^T \mathbf{M} \left(\mathbf{v}_{0_j} + \boldsymbol{\Delta}\mathbf{v}_j\right)} \end{aligned} \tag{8.65}$$

Neglecting all terms of second or higher order involving $\boldsymbol{\Delta}$, the above expression may be approximated as

$$\mu_j \approx \mu_{0_j} - \mu_{0_j} \frac{\boldsymbol{\Delta}\mathbf{v}_j^T \mathbf{M} \mathbf{u}_{0_j} + \mathbf{v}_{0_j}^T \mathbf{M} \boldsymbol{\Delta}\mathbf{u}_j}{\mathbf{v}_{0_j}^T \mathbf{M} \mathbf{u}_{0_j}} + \mu_{0_j} \frac{\boldsymbol{\Delta}\mathbf{v}_j^T \mathbf{M} \mathbf{v}_{0_j} + \mathbf{v}_{0_j}^T \mathbf{M} \boldsymbol{\Delta}\mathbf{v}_j}{\mathbf{v}_{0_j}^T \mathbf{M} \mathbf{v}_{0_j}} + \mu_{0_j} \frac{\Delta\omega_j}{\omega_{0_j}} \tag{8.66}$$

where

$$\mu_{0_j} = \omega_{0_j} \frac{\mathbf{v}_{0_j}^T \mathbf{M} \mathbf{v}_{0_j}}{\mathbf{v}_{0_j}^T \mathbf{M} \mathbf{u}_{0_j}} \tag{8.67}$$

Equation (8.66) describes how approximately the values of μ_j get effected due to error in the modal data. Observe that error in the real and imaginary parts of complex modes as well as error in the natural frequencies introduces error in the estimate of the relaxation parameter.

8.7 Conclusions

Identification of damping properties by conducting dynamic testing of structures has been discussed. It was shown that conventional modal testing theory, the basis of which is viscously damped linear systems, can be applied to generally damped linear systems with reasonable accuracy. A linear-nonlinear optimization method is proposed to extract complex modal parameters from a set of measured transfer functions.

A free-free beam with constrained layer damping is considered to illustrate the damping identification methods developed in the previous chapters of this dissertation. Modal parameters of the beam were extracted using the newly developed method. It was shown that the transfer functions can be reconstructed with very good accuracy using this modal extraction procedure. The real parts of complex frequencies and modes show good agreement with the undamped natural frequencies and modes obtained from beam theory. It was shown that, in contrast to the traditional viscous damping assumption, the damping properties of the beam can be adequately represented by an exponential (non-viscous) damping model. This fact emphasizes the need to incorporate non-viscous damping models in structural systems.

The effects of noise in the modal data on the identified damping properties has been investigated. For the case of viscous damping matrix identification, it was observed that the result is very sensitive to small errors in the real parts of complex modes while it is not very sensitive to errors in the imaginary parts. For the identification of non-viscous damping model, the relaxation parameter is sensitive to errors in both the real and imaginary parts, however the associated coefficient damping matrix is not very sensitive to errors in the imaginary parts. This fact makes the proposed method more suitable for practical problems because the real parts of complex modes can be obtained more accurately that the imaginary parts.

With this chapter the work taken up in this dissertation comes to an end. The contributions made in the study are summarized in the next chapter and and a few suggestions for further work are also made.

Chapter 9

Summary and Conclusions

The studies taken up in this dissertation have developed fundamental methods for analysis and identification of damped linear systems. Summary and detailed discussions have been taken up at the end of relevant chapters. The purpose of this chapter is to recapitulate the main findings, unifying them and to suggest some further research directions.

9.1 Summary of the Contributions Made

Modal analysis, the most popular tool for solving engineering vibration problems, is based on dynamics of undamped systems. However, all real-life structural systems exhibit vibration damping. The presence of damping give rise to two major problems. Firstly, the classical modal analysis procedure cannot be applied directly to generally damped systems. Secondly, and possibly more importantly, unlike the stiffness and inertia forces which have strong theoretical as well as experimental basis, knowledge of the damping forces is largely empirical in nature. For this reason, it is not obvious what equations of motion should be used at the first place, let alone how to proceed with a solution procedure. The studies reported in this dissertation address these two problems.

Viscous damping model is the most common form of damping normally considered in the context of general multiple degree-of-freedom systems. This dissertation considers a more general non-viscous damping model in which the damping forces depend on the past history of motion via convolution integrals. The importance of considering such general damping models has been brought out. It was shown that classical modal analysis can be extended to incorporate general non-viscous damping models, at least when the damping is light. General methodologies for identification of damping properties have been proposed and through an experimental investigation it was further shown that the damping mechanism of a system is indeed likely to be non-viscous.

The answer to the question, whether classical modal analysis is directly applicable to a damped system or not, comes from the concept of existence of classical normal modes in that system. In this line, classical damping or proportional damping was proposed for viscously damped systems. In this dissertation, the concept of proportional damping is generalized to non-viscously damped systems. This result demonstrates that, contrary to the traditional beliefs, the damping mechanism

need not be viscous in order to apply classical modal analysis. This was the initial motivation for considering more general non-viscous damping models. It was shown that, general non-viscously damped systems possess two kinds of modes: (a) elastic modes, and (b) non-viscous modes. Elastic modes are counterparts of the 'modes' of viscously damped systems, while non-viscous modes are intrinsic to the non-viscous damping mechanism and do not appear in viscously damped systems. For underdamped systems, elastic modes appear in complex conjugate pairs and are oscillatory in nature. Non-viscous modes are real and not oscillatory in nature. It was shown that the system response can be expressed exactly in terms of these modes in a manner similar to that used for undamped or viscously damped systems. Classical mode orthogonality relationships known for undamped systems were generalized to non-viscously damped systems. It was shown that there exist unique relationships which relate the system matrices to the natural frequencies and modes of non-viscously damped systems. These relationships, in turn, enable us to reconstruct the system matrices from full set of modal data.

The above mentioned results give a strong footing to pursue more fundamental studies regarding damping mechanisms in general vibrating systems. Assuming that the damping is small, a method is proposed to obtain a viscous damping matrix from complex modes and complex natural frequencies. It was observed that when the actual damping mechanism of the structure is not viscous, this method fits a viscous damping matrix which is asymmetric, therefore non-physical[1]. If, however, the damping mechanism is viscous or close to viscous, this method identifies the correct viscous damping matrix. Thus, using this method it is possible to tell whether the damping mechanism of a structure is effectively viscous or not. This fact makes this method particularly useful because currently there are no methods available in the literature which address this question, most of them *a priori* assume the damping mechanism to be viscous and then try to fit a viscous model. This study also indicates that when the damping mechanism of a structure is non-viscous, some particular non-viscous damping model must be used for fitting. As a first step towards this, we have considered the simplest non-viscous damping model, namely a single relaxation parameter model, for fitting purposes. Identification of the damping properties using this model offers a greater flexibility than that of the conventional viscous damping model. However, when the original damping model of the system is not close to the fitted one, the method again yields a non-physical result. Thus, using this method also, it is possible to understand whether the damping mechanism of the original system is close to what was considered for the fitting. Another important result to emerge from these studies is that, when the damping is light, several damping models can be fitted to reproduce some measured set of transfer functions exactly. In other words, the identified damping model is non-unique. On the one hand, this result is encouraging and serves as a kind of justification of the widespread use of the viscous damping model. On the other hand, it demonstrates that by conducting conventional modal testing procedure in general it is *not* possible to identify the true damping model. Motivated by this fact, some methods were developed to identify damping

[1] According to the definition of Rayleighs dissipation function, see Section 1.2.3

models which will preserve the symmetry of the system. These methods in general yield physically realistic damping matrix and reconstruct the transfer functions with good accuracy. The symmetry preserving methods should be used when both the viscous and non-viscous damping identification method fail to yield a symmetric damping matrix. However, the disadvantage is that the identified models may have poor predictive power for changes to the system as the actual damping model is incorrect.

It must be noted that complex modes and frequencies can not be measured directly in order to apply the damping identification methods developed here. A linear-nonlinear optimization method was proposed to extract the complex modal data from the measured transfer functions. This method was applied experimentally to a beam with constrained layer damping and quite good agreement between the measured and the reconstructed transfer functions was obtained. It was observed that the damping mechanism of the beam considered for the experiment was not viscous but could be adequately represented by an exponential damping model. This result clearly demonstrates the need to use non-viscous damping modes in linear dynamic systems.

In summary, the work conducted in this dissertation achieves the following:

- Redefinition of the concept of proportional damping and generalization of it to the non-viscous case (Chapter 2).
- Extension of modal analysis to deal with non-classical and non-viscously damped linear systems by introducing the concept of *elastic modes* and *non-viscous modes* (Chapter 3).
- Generalization of the classical mode orthogonality and normalization relationships known for undamped systems to non-classical and non-viscously damped systems (Chapter 4).
- Identification of the full non-proportional viscous damping matrix from incomplete and noisy modal data (Chapters 5 and 8).
- Identification of non-viscous damping functions from incomplete and noisy modal data together with the mass matrix (Chapters 6 and 8).
- A method for preserving symmetry in damping identification procedures (Chapter 7).
- A general procedure for extraction of complex natural frequencies and modes from the measured transfer functions in the context of non-viscously damped systems (Chapter 8).

9.2 Suggestions for Further Work

The study conducted in this dissertation throws open several questions on generally damped vibrating systems. The following are some important areas of research which emerge immediately from this study:

- *Multiple parameter exponential models for damping identification*: The non-viscous damping identification method proposed in Chapter 6 considers only single parameter exponential model for fitting purposes. It was observed that this simple model becomes inadequate when the true damping mechanism is different from the exponential model. In order to overcome this problem, it is required to fit a multiple parameter exponential model to measured complex modes and frequencies. Currently there has been very little study in this direction. The multiple parameter exponential model has several advantages. From a mathematical point of view, having more parameters offers more flexibility for fitting purposes. From the point of view of the physics of the damping mechanism, it is perfectly possible that the damping mechanism of a structure comprises of a linear combination of several relaxation functions. Thus, there are good physical as well as mathematical reasons to pursue a systematic study on fitting of multiple parameter exponential models to measured complex modes and frequencies.

- *Analysis of complex modes*: In spite of extensive research efforts, the nature of complex modes is not quite clear. Although the results derived in Chapter 4 clarify some of the important theoretical issues, *eg*., normalization, orthogonality *etc*., there are several topics which need further attention. Upon proper normalization, the real parts of the complex modes can be understood from our usual knowledge of normal modes (for example, see Figures 8.17 to 8.27). However, nothing so simple can be said about the imaginary parts. Beside this there are several general questions of interest:

  1. How should one quantify the amount of 'complexity' in a given complex mode?
  2. Does the amount of 'complexity' have a direct relationship with the amount of non-proportionality?
  3. What should we except the shape of the imaginary parts of the complex modes to look like? What are the parameters which govern these shapes?

  Some of these questions have been addressed to some extent in the literature for viscously damped systems. It is required to extend these results to generally damped systems.

- *Numerical and experimental study on 2D systems*: The experimental and numerical studies on damping identification conducted here were on one dimensional (1D) systems. It is required to extend these works to more general two dimensional (2D) systems (plates, for example). Some preliminary numerical studies were conducted by the author (although the results are not reported) and it was observed that the methods proposed here can be applied to such general 2D systems. Further studies are required to exploit the generality of the proposed damping identification methods.

- *Stability and Criticality of non-viscously damped systems*: In Chapter 3, the nature of the

eigenvalues of non-viscously damped systems were discussed under simplified assumptions. Clearly, these assumptions are not valid under general circumstances. For viscously damped systems, based on the nature of the eigenvalues, there are well established works on when the damping become critical or the system become unstable. It is important to obtain analogous results for non-viscously damped systems.

- *Asymmetric systems*: The studies conducted in Chapters 2, 3 and 4 are self-contained as long as systems with symmetric coefficient matrices are considered. However, the dynamical behaviour of some systems encountered in practice cannot be expressed in terms of symmetric coefficient matrices or self-adjoint linear operators. Some examples are – gyroscopic and circulatory systems (Huseyin and Liepholz, 1973), aircraft flutter (Fawzy and Bishop, 1977), ship motion in sea water (Bishop and Price, 1979), contact problems (Soom and Kim, 1983) and many actively controlled systems (Caughey and Ma, 1993). Therefore, for the sake of generality, it is required to extend the formulation in Chapters 2, 3 and 4 to linear asymmetric MDOF systems.

- *Distributed parameter systems*: In this dissertation we have considered only discrete parameter systems or discretized model of distributed parameter systems. Modelling of mechanical systems through distributed parameters (inertia, stiffness and damping) offers more accurate treatment of the problem. In this case the equations of motion can be expressed by partial differential equations. The difficulty in adopting such an approach is that the exact solutions can be obtained for only very special cases with simple geometry and boundary conditions. There have been some studies on viscously damped distributed parameter systems but very little is available in the literature on non-viscously damped distributed parameter systems. It will be useful to extend the works reported in Chapters 2, 3 and 4 to distributed parameter systems.

Appendix A

Calculation of the Gradient and Hessian of the Merit Function

The gradient and Hessian of the merit function χ^2 can be obtained from equations (8.42) and (8.45) respectively. Since $\boldsymbol{\mathcal{V}}$ is a real vector, $\dfrac{\partial H_n^*(\omega)}{\partial \mathcal{V}_p} = \left(\dfrac{\partial H_n(\omega)}{\partial \mathcal{V}_p}\right)^*$. Thus, it is sufficient to obtain an expression of the term $\dfrac{\partial H_n(\omega)}{\partial \mathcal{V}_p}$ only.

First note that, from the definition of $\boldsymbol{\mathcal{V}}$ in equation (8.36) we have

$$\frac{\partial H_n(\omega)}{\partial \mathcal{V}_p} = \frac{\partial H_n(\omega)}{\partial \omega_p}, \quad \forall p = 1, 2, \cdots, m \tag{A.1}$$

$$\text{and} \quad \frac{\partial H_n(\omega)}{\partial \mathcal{V}_p} = \frac{\partial H_n(\omega)}{\partial Q_{(p-m)}}, \quad \forall p = m+1, m+2, \cdots, 2m. \tag{A.2}$$

Consider the expression of $H_n(\omega)$ in equation (8.9). Since the residue matrix $\mathbf{A}$ is independent of $\boldsymbol{\mathcal{V}}$, from (8.9) we further have

$$\frac{\partial H_n(\omega)}{\partial \omega_j} = \frac{\partial f_{1_j}(\omega)}{\partial \omega_j} A_{jn} + \frac{\partial f_{2_j}(\omega)}{\partial \omega_j} A_{jn}^* \tag{A.3}$$

$$\text{and} \quad \frac{\partial H_n(\omega)}{\partial Q_j} = \frac{\partial f_{1_j}(\omega)}{\partial Q_j} A_{jn} + \frac{\partial f_{2_j}(\omega)}{\partial Q_j} A_{jn}^*, \quad \forall j = 1, 2, \cdots, m \tag{A.4}$$

because, for $l = 1, 2$, $\dfrac{\partial f_{l_k}(\omega)}{\partial \omega_j} = \dfrac{\partial f_{l_k}(\omega)}{\partial Q_j} = 0, \forall k \neq j$.

Using equation (8.5), the functions $f_{1_j}(\omega)$ and $f_{2_j}(\omega)$ can be expressed in terms of ω_j and Q_j as

$$f_{1_j}(\omega) = -\frac{(\mathrm{i}\omega)^r}{d_{1_j}(\omega)}, \quad \text{where} \quad d_{1_j}(\omega) = \omega - \left(\omega_j + \mathrm{i}\frac{\omega_j}{2Q_j}\right) \tag{A.5}$$

$$\text{and} \quad f_{2_j}(\omega) = \frac{(\mathrm{i}\omega)^r}{d_{2_j}(\omega)}, \quad \text{where} \quad d_{2_j}(\omega) = \omega + \left(\omega_j - \mathrm{i}\frac{\omega_j}{2Q_j}\right). \tag{A.6}$$

Differentiating equations (A.5) and (A.6) with respect to ω_j and Q_j we have

$$\frac{\partial f_{1_j}(\omega)}{\partial \omega_j} = -\left(1 + \mathrm{i}/2Q_k\right) \frac{(\mathrm{i}\omega)^r}{d_{1_j}^2(\omega)} \tag{A.7}$$

$$\frac{\partial f_{2_j}(\omega)}{\partial \omega_j} = -\left(1 - \mathrm{i}/2Q_k\right) \frac{(\mathrm{i}\omega)^r}{d_{2_j}^2(\omega)} \tag{A.8}$$

$$\frac{\partial f_{1_j}(\omega)}{\partial Q_j} = \left(\mathrm{i}\omega_j/2Q_k^2\right) \frac{(\mathrm{i}\omega)^r}{d_{1_j}^2(\omega)} \tag{A.9}$$

$$\frac{\partial f_{2_j}(\omega)}{\partial Q_j} = -\left(\mathrm{i}\omega_j/2Q_k^2\right) \frac{(\mathrm{i}\omega)^r}{d_{2_j}^2(\omega)}, \quad \forall j = 1, 2, \cdots, m \tag{A.10}$$

Appendix B

Discretized Mass Matrix of the Beam

Suppose that the displacement field of the beam is sampled at n points. All the points are equally spaced with a spacing distance of a and denoted by $0, a, 2a, \cdots, (n-1)a$ as shown in Figure B.1. The values of displacement at these points are denoted by $u_1, n_2, \cdots, u_n$. Consider the first

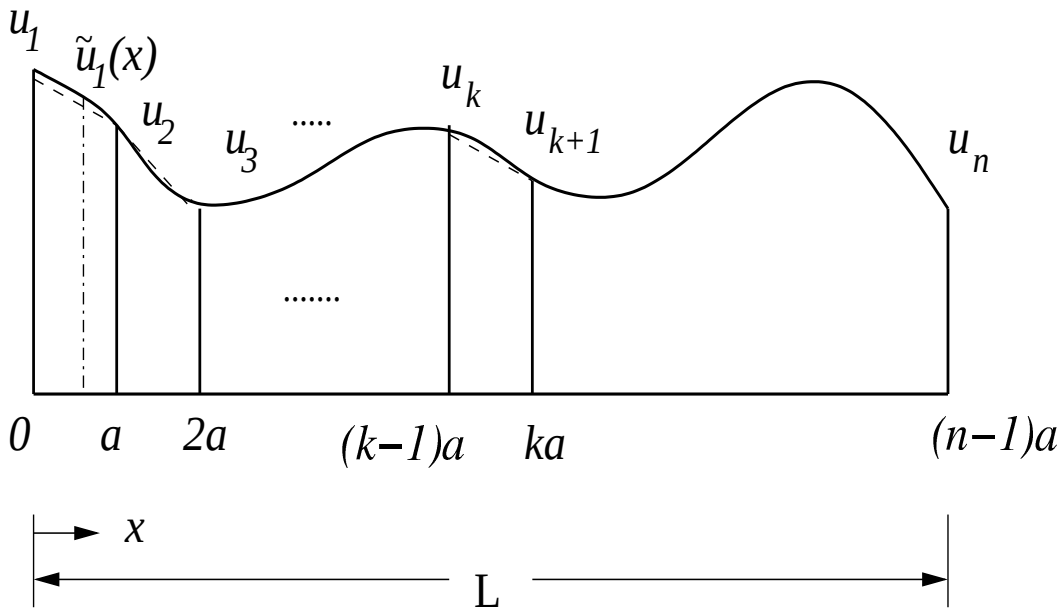

Figure B.1: Discretization of the displacement field

segment and denote $\tilde{u}_1(x)$ as the value of the displacement in $0 \leq x \leq a$. Assuming *linear* variation of $\tilde{u}_1(x)$ between u_1 and u_2, one has

$$\frac{u_1 - u_2}{a} = \frac{\tilde{u}_1(x) - u_2}{a - x} \quad \text{or} \quad \tilde{u}_1(x) = \frac{u_2 x + u_1(a - x)}{a}. \tag{B.1}$$

Similar expressions can be obtained for other segments also. To obtain the mass matrix, first consider the kinetic energy of the beam in the frequency domain given by

$$\mathcal{T} = \omega^2 \frac{1}{2} \int_o^L m(x) u^2(x) \mathrm{d}x. \tag{B.2}$$

In the above expression L denote the length of the beam, $m(x)$ is the mass distribution and $u(x)$ is the displacement function. Equation (B.2) can be expressed in a discretized form as

$$\mathcal{T} = \omega^2 \frac{1}{2} \sum_{k=0}^{n-1} \int_o^a m_k \tilde{u}_k^2(x) \mathrm{d}x. \tag{B.3}$$

Assuming uniform mass density and denoting M as the total mass of the beam, the above equation can be expressed as

$$\mathcal{T} = \omega^2 \frac{1}{2} \frac{M}{(n-1)} \sum_{k=0}^{n-1} \int_o^a \tilde{u}_k^2(x) \mathrm{d}x. \tag{B.4}$$

Substituting $\tilde{u}_1(x)$ from (B.1), the first term of the above series reads

$$\int_o^a \tilde{u}_1^2(x) \mathrm{d}x = \int_o^a \left[\frac{u_2 x + u_1(a-x)}{a} \right]^2 \mathrm{d}x = \frac{a}{3}[u_1^2 + u_2^2 + u_1 u_2]. \tag{B.5}$$

Similarly, considering all the terms, from (B.4) the kinetic energy of the beam can be expressed as

$$\mathcal{T} = \omega^2 \frac{1}{2} \mathbf{u}^T \mathbf{M} \mathbf{u} \tag{B.6}$$

$$\text{where} \quad \mathbf{u} = \{u_1, u_1, \cdots, u_n\}^T \tag{B.7}$$

$$\text{and} \quad \mathbf{M} = m_u \begin{bmatrix} 1 & 1/2 & & & & & \\ 1/2 & 2 & 1/2 & & & & \\ & \ddots & \ddots & \ddots & & & \\ & & 1/2 & 2 & 1/2 & & \\ & & & & \ddots & \ddots & \\ & & & & & 1/2 & 1 \end{bmatrix} \quad \text{with} \quad m_u = \frac{Ma}{3(n-1)}. \tag{B.8}$$

Bibliography

Adhikari, S. (1998), *Energy Dissipation in Vibrating Structures*, First Year Report, Cambridge University Engineering Department, Cambridge, UK.

Adhikari, S. (1999), "Rates of change of eigenvalues and eigenvectors in damped dynamic systems", *AIAA Journal*, **37** (11), pp. 1152–1158.

Adhikari, S. (2000), "Calculation of derivative of complex modes using classical normal modes", *Computer and Structures*, **77** (6), pp. 625–633.

Adhikari, S. and Manohar, C. S. (1999), "Dynamic analysis of framed structures with statistical uncertainties", *International Journal for Numerical Methods in Engineering*, **44** (8), pp. 1157–1178.

Alvin, K. F., Peterson, L. D., and Park, K. C. (1997), "Extraction of normal modes and full modal damping from complex modal parameters", *AIAA Journal*, **35** (7), pp. 1187–1194.

Baburaj, V. and Matsukai, Y. (1994), "A study on the material damping of thin angle-ply laminated plates", *Journal of Sound and Vibration*, **172** (3), pp. 415–419.

Bagley, R. L. and Torvik, P. J. (1983), "Fractional calculus–a different approach to the analysis of viscoelastically damped structures", *AIAA Journal*, **21** (5), pp. 741–748.

Balmès, E. (1995), *Structural Dynamics Toolbox, User's Manual 2.0*, Sèrves, France: Scientific Software Group, France.

Balmès, E. (1996), "Frequency domain identification of structural dynamics using the pole/residue parametrization", in "Proceedings of the 14th International Modal Analysis Conference (IMAC)", Dearbon, MI, volume 1, (pp. 540–546).

Balmès, E. (1997), "New results on the identification of normal modes from experimental complex modes", *Mechanical System and Signal Processing*, **11** (2), pp. 229–243.

Bandstra, J. P. (1983), "Comparison of equivalent viscous damping in discrete and continuous vibrating system", *Transaction of ASME, Journal of Vibration, Acoustics, Stress and Reliability in Design*, **105**, pp. 382–392.

Banks, H. T. and Inman, D. J. (1991), "On damping mechanisms in beams", *Transaction of ASME, Journal of Applied Mechanics*, **58**, pp. 716–723.

Baruch, M. (1997), "Identification of the damping matrix", *Technical Report TAE No.803*, Technion, Israel, Faculty of Aerospace Engineering, Israel Institute of Technology, Haifa.

Beards, C. F. and Williams, J. L. (1977), "The damping of structural vibration by rotational slip in structural joint", *Journal of Sound and Vibration*, **53** (3), pp. 333–340.

Béliveau, J.-G. (1976), "Identification of viscous damping in structures from modal information", *Transaction of ASME, Journal of Applied Mechanics*, **43**, pp. 335–339.

Béliveau, J.-G. (1977), "Eigenrelations in structural dynamics", *AIAA Journal*, **15** (7), pp. 1039–1041.

Bellos, J. and Inman, D. J. (1990), "Frequency response of non-proportionally damped, lumped parameter, linear systems", *Transaction of ASME, Journal of Vibration and Acoustics*, **112**, pp. 194–201.

Bert, C. W. (1973), "Material damping: an introductory review of mathematical models, measure and experimental techniques", *Journal of Sound and Vibration*, **29** (2), pp. 129–153.

Bhaskar, A. (1992), *Damping in Mechanical Vibrations: New Methods of Analysis and Estimation*, Ph.D. thesis, Cambridge University Engineering Department, Cambridge, UK.

Bhaskar, A. (1995), "Estimates of errors in the frequency response of non-classically damped system", *Journal of Sound and Vibration*, **184** (1), pp. 59–72.

Bhaskar, A. (1999), "Mode shapes during asynchronous motion and non-proportionality indices", *Journal of Sound and Vibration*, **224** (1), pp. 1–16.

Biot, M. A. (1955), "Variational principles in irreversible thermodynamics with application to viscoelasticity", *Physical Review*, **97** (6), pp. 1463–1469.

Biot, M. A. (1958), "Linear thermodynamics and the mechanics of solids", in "Proceedings of the Third U. S. National Congress on Applied Mechanics", ASME, New York, (pp. 1–18).

Bishop, R. E. D. and Price, W. G. (1979), "An investigation into the linear theory of ship response to waves", *Journal of Sound and Vibration*, **62** (3), pp. 353–363.

Bishop, R. E. D. and Price, W. G. (1986), "A note on hysteretic damping of transient motion", in "Random Vibration Status and Recent Developments", edited by I. Elishakoff and R. H. Lyon, Elsevier, Amsterdam, (pp. 39–45).

Bland, D. R. (1960), *Theory of Linear Viscoelasticity*, Pergamon Press, London.

Buhariwala, K. J. (1982), *Dynamic Response of Viscoelastic Fibre Reinforced Composite Materials*, Master's thesis, University of Toronto, Institute for Aerospace Studies.

Caravani, P. and Thomson, W. T. (1974), "Identification of damping coefficients in multidimensional linear systems", *Transaction of ASME, Journal of Applied Mechanics*, **41**, pp. 379–382.

Caughey, T. K. (1960), "Classical normal modes in damped linear dynamic systems", *Transaction of ASME, Journal of Applied Mechanics*, **27**, pp. 269–271.

Caughey, T. K. and Ma, F. (1993), "Complex modes and solvability of non-classical linear systems", *Transaction of ASME, Journal of Applied Mechanics*, **60**, pp. 26–28.

Caughey, T. K. and O'Kelly, M. E. J. (1965), "Classical normal modes in damped linear dynamic systems", *Transaction of ASME, Journal of Applied Mechanics*, **32**, pp. 583–588.

Chakrabarti, S., Bhattacharyya, B. B., and Swamy, M. N. S. (1978), "On simultaneous diagonalization of a collection of hermitian matrices", *The Matrix and Tensor Quarterly*, **29** (2), pp. 35–54.

Chassiakos, A. G., F.Masri, S., Smyth, A. W., and Caughey, T. K. (1998), "On-line identification of hysteretic systems", *Transaction of ASME, Journal of Applied Mechanics*, **65**, pp. 194–203.

Chen, S. Y., Ju, M. S., and Tsuei, Y. G. (1996a), "Estimation of mass stiffness and damping matrices from frequency response function", *Transaction of ASME, Journal of Vibration and Acoustics*, **118**, pp. 78–82.

Chen, S. Y., Ju, M. S., and Tsuei, Y. G. (1996b), "Extraction of normal modes for highly coupled incomplete systems with general damping", *Mechanical System and Signal Processing*, **10** (1), pp. 93–106.

Chung, K. R. and Lee, C. W. (1986), "Dynamic reanalysis of weakly non-proportionally damped systems", *Journal of Sound and Vibration*, **111**, pp. 37–50.

Clough, R. W. and Mojtahedi, S. (1976), "Earthquake response analysis considering non-proportional damping", *Earthquake Engineering and Structural Dynamics*, **4**, pp. 489–496.

Cole, D. G., Saunders, W. R., and Robertshaw, H. H. (1995), "Modal parameter estimation for piezostructures", *Transaction of ASME, Journal of Vibration and Acoustics*, **117**, pp. 431–437.

Crandall, S. H. (1970), "The role of damping in vibration theory", *Journal of Sound and Vibration*, **11** (1), pp. 3–18.

Crandall, S. H. (1991), "The hysteretic damping model in vibration theory", *Journal of Mechanical Engineering Science*, **205**, pp. 23–28.

Cremer, L. and Heckl, M. (1973), *Structure-Brone Sound*, Springer-Verlag Berlin, Germany, second edition, translated by E. E. Ungar.

Crighton, D. G. (1985), "Acoustics of a stiff locally reacting structure", *Proceedings of the Royal Society of London, Series- A*, **397**, pp. 99–120.

Cronin, D. L. (1976), "Approximation for determining harmonically excited response of non-classically damped system", *ASME Journal of Engineering for Industry*, **98** (1), pp. 43–47.

Cronin, D. L. (1990), "Eigenvalue and eigenvector determination of non-classically damped dynamic systems", *Computer and Structures*, **36** (1), pp. 133–138.

Dalenbring, M. (1999), "Damping function estimation based on measured vibration frequency responses and finite-element displacement modes", *Mechanical System and Signal Processing*, **13** (4), pp. 547–569.

Duffour, P. (1998), *Modal Testing of Violin Bodies*, Master's thesis, Cambridge University Engineering Department, Cambridge, UK.

Duncan, P. E. and Taylor, R. E. (1979), "A note on the dynamic analysis of non-proportionally damped systems", *Earthquake Engineering and Structural Dynamics*, **7**, pp. 99–105.

Earls, S. W. E. (1966), "Theoretical estimation of frictional energy dissipation in a simple lap joint", *Journal of Mechanical Engineering Science*, **8** (2), pp. 207–214.

Ewins, D. J. (1984), *Modal Testing: Theory and Practice*, Research Studies Press, Taunton.

Fabunmi, J., Chang, P., and Vorwald, J. (1988), "Damping matrix identification using the spectral basis technique", *Transaction of ASME, Journal of Vibration, Acoustics, Stress and Reliability in Design*, **1110**, pp. 332–337.

Fang, J. and Lyons, G. J. (1994), "Material damping of free hanging pipes: Theoretical and experimental studies", *Journal of Sound and Vibration*, **172** (3), pp. 371–389.

Fawzy, I. (1977), "Orthogonality of generally normalize eigenvector and eigenrows", *AIAA Journal*, **15** (2), pp. 276–278.

Fawzy, I. and Bishop, R. E. D. (1976), "On the dynamics of linear non-conservative systems", *Proceedings of the Royal Society of London, Series- A*, **352**, pp. 25–40.

Fawzy, I. and Bishop, R. E. D. (1977), "On the nature of resonance in non-conservative systems", *Journal of Sound and Vibration*, **55** (4), pp. 475–485.

Felszeghy, S. F. (1993), "On uncoupling and solving the equations of motion of vibrating linear discrete systems", *Transaction of ASME, Journal of Applied Mechanics*, **60**, pp. 456–462.

Felszeghy, S. F. (1994), "Development of biorthonormal eigenvectors for modal analysis of linear discrete non-classically damped systems", *Journal of Sound and Vibration*, **176** (2), pp. 225–269.

Foss, K. A. (1958), "Co-ordinates which uncouple the equations of motion of damped linear dynamic systems", *Transaction of ASME, Journal of Applied Mechanics*, **25**, pp. 361–364.

Friswell, M. I. and Inman, D. J. (1999), "Reduced-order models of structures with viscoelastic components", *AIAA Journal*, **37** (10), pp. 1318–1325.

Friswell, M. I., Inman, D. J., and Lam, M. J. (1997), "On the realisation of GHM models in viscoelasticity", *Journal of Intelligent Material Systems and Structures*, **8** (11), pp. 986–993.

Fritzen, C.-P. (1986), "Identification of mass, damping and stiffness matrices of mechanical systems", *Transaction of ASME, Journal of Vibration, Acoustics, Stress and Reliability in Design*, **108**, pp. 9–16.

Fung, Y. C. (1965), *Foundations of Solid Mechanics*, Prentice-Hall Inc., Englewood Cliffs, New Jersey.

Garvey, S. D., Penny, J. E. T., and Friswell, M. I. (1995), "The relationship between the real and imaginary parts of complex modes", *Journal of Sound and Vibration*, **212** (1), pp. 75–83.

Gaul, L. (1999), "The influence of damping on waves and vibrations", *Mechanical System and Signal Processing*, **13** (1), pp. 1–30.

Gaul, L., Klein, P., and Kemple, S. (1991), "Damping description involving fractional operators", *Mechanical System and Signal Processing*, **5** (2), pp. 81–88.

Gawronski, W. and Sawicki, J. T. (1997), "Response errors of non-proportionally lightly damped structures", *Journal of Sound and Vibration*, **200** (4), pp. 543–550.

Géradin, M. and Rixen, D. (1997), *Mechanical Vibrations*, John Wiely & Sons, New York, NY, second edition, translation of: Théorie des Vibrations.

Golla, D. F. and Hughes, P. C. (1985), "Dynamics of viscoelastic structures - a time domain finite element formulation", *Transaction of ASME, Journal of Applied Mechanics*, **52**, pp. 897–906.

Halevi, Y. and Kenigsbuch, R. (1999), "Model updating of the complex modeshapes and the damping matrix", in "Inverse Problems in Engineering", edited by M. I. Friswell, J. E. Mottershead, and A. W. Lees, Swansea, Wales, UK, (pp. 251–260).

Hasselsman, T. K. (1972), "A method of constructing a full modal damping matrix from experimental measurements", *AIAA Journal*, **10** (4), pp. 526–527.

Hasselsman, T. K. (1976), "Modal coupling in lightly damped structures", *AIAA Journal*, **14**, pp. 1627–1628.

Huseyin, K. and Liepholz, H. H. E. (1973), "Divergence instability of multiple parameter circulatory systems", *Quarterly of Applied Mathematics*, **31**, pp. 185–197.

Hwang, J. H. and Ma, F. (1993), "On the approximate solution of non-classically damped linear systems", *Transaction of ASME, Journal of Applied Mechanics*, **60**, pp. 695–701.

Ibrahim, S. R. (1983a), "Computation of normal modes from identified complex modes", *AIAA Journal*, **21** (3), pp. 446–451.

Ibrahim, S. R. (1983b), "Dynamic modeling of structures from measured complex modes", *AIAA Journal*, **21** (6), pp. 898–901.

Ibrahim, S. R. and Sestieri, A. (1995), "Existence and normalization of complex modes in post experimental use in modal analysis", in "Proceedings of the 13th International Modal Analysis Conference (IMAC)", Nashville, TN, volume 1, (pp. 483–489).

Ibrahimbegovic, A. and Wilson, E. L. (1989), "Simple numerical algorithms for the mode superposition analysis of linear structural systems with non-proportional damping", *Computer and Structures*, **33** (2), pp. 523–531.

Imregun, M. and Ewins, D. J. (1995), "Complex modes - origin and limits", in "Proceedings of the 13th International Modal Analysis Conference (IMAC)", Nashville, TN, (pp. 496–506).

Lallement, G. and Inman, D. J. (1995), "A tutorial on complex eigenvalues", in "Proceedings of the 13th International Modal Analysis Conference (IMAC)", Nashville, TN, (pp. 490–495).

Lancaster, P. (1961), "Expression of damping matrices in linear vibration problems", *Journal of Aerospace Sciences*, **28**, p. 256.

Lancaster, P. (1966), *Lambda-matrices and Vibrating System*, Pergamon Press, London.

Lazan, B. J. (1959), "Energy dissipation mechanisms in structures with particular reference to material damping", in "Structural Dynamics", edited by J. E. Ruzcka, ASME Annual Meeting, Atlantic City, N. J.

Lazan, B. J. (1968), *Damping of Materials and Members in Structural Mechanics*, Pergamon Press, Oxford.

Lesieutre, G. A. and Mingori, D. L. (1990), "Finite element modeling of frequency-dependent material properties using augmented thermodynamic fields", *AIAA Journal of Guidance, Control and Dynamics*, **13**, pp. 1040–1050.

Liang, Z., Tong, M., and Lee, C. G. (1992), "Complex modes in damped linear systems", *International Journal of Analytical and Experimental Modal Analysis*, **7** (1), pp. 1–20.

Lin, R. M. and Ling, S. F. (1996), "New method for accurate and consistent identification of modal parameters", *AIAA Journal of Guidance, Control and Dynamics*, **19** (5), pp. 992–999.

Liu, K., Kujath, M. R., and Zheng, W. (2000), "Quantification of non-proportionality of damping in discrete vibratory systems", *Computer and Structures*, **77** (5), pp. 557–569.

Liu, Q. K. and Sneckenberger, J. E. (1994), "Free vibration analysis of linear vibrating deficient systems with arbitrary damping", *Journal of Sound and Vibration*, **177** (1), pp. 43–55.

Maia, N. M. M. and Silva, J. M. M. (Eds.) (1997), *Theoretical and Experimental Modal Analysis*, Engineering Dynamics Series, Research Studies Press, Taunton, England, series Editor, J. B. Robetrs.

Maia, N. M. M., Silva, J. M. M., and Ribeiro, A. M. R. (1997), "A contribution to understanding the identification of systems with general damping", in "Proceedings of the 17th International Modal Analysis Conference (IMAC)", volume 2, (pp. 1145–1151).

Maia, N. M. M., Silva, J. M. M., and Ribeiro, A. M. R. (1998), "On a general model for damping", *Journal of Sound and Vibration*, **218** (5), pp. 749–767.

Makris, N. (1999), "Frequency-independent dissipation and causality", in "Computational Stochastic Mechanics", edited by P. Spanos, Balkema, Rotterdam, (pp. 435–441).

Malone, D. P., Cronin, D. L., and Randolph, T. W. (1997), "Eigenvalue and eigenvector determination for damped gyroscopic systems", *Transaction of ASME, Journal of Applied Mechanics*, **64**, pp. 710–712.

Manohar, C. S. and Adhikari, S. (1998), "Dynamic stiffness of randomly parametered beams", *Probabilistic Engineering Mechanics*, **13** (1), pp. 39–51.

McTavis, D. J. and Hughes, P. C. (1993), "Modeling of linear viscoelastic space structures", *Transaction of ASME, Journal of Vibration and Acoustics*, **115**, pp. 103–110.

Meirovitch, L. (1967), *Analytical Methods in Vibrations*, Macmillan Publishing Co., Inc., New York.

Meirovitch, L. (1980), *Computational Methods in Structural Dynamics*, Sijthoff & Noordohoff, Netherlands.

Meirovitch, L. (1997), *Principles and Techniques of Vibrations*, Prentice-Hall International, Inc., New Jersey.

Meirovitch, L. and Ryland, G. (1985), "A perturbation technique for gyroscopic systems with small internal and external damping", *Journal of Sound and Vibration*, **100** (3), pp. 393–408.

Minas, C. and Inman, D. J. (1991), "Identification of a nonproportional damping matrix from incomplete modal information", *Transaction of ASME, Journal of Vibration and Acoustics*, **113**, pp. 219–224.

Mitchell, L. (1990), "Complex modes: a review", in "Proceedings of the 8th International Modal Analysis Conference (IMAC)", Kissimmee, Florida, volume 2, (pp. 891–899).

Mottershead, J. E. (1990), "Theory for the estimation of structural vibration parameters from incomplete data", *AIAA Journal*, **28** (3), pp. 559–561.

Muravyov, A. (1997), "Analytical solutions in the time domain for vibration problems of discrete viscoelastic systems", *Journal of Sound and Vibration*, **199** (2), pp. 337–348.

Muravyov, A. (1998), "Forced vibration responses of a viscoelastic structure", *Journal of Sound and Vibration*, **218** (5), pp. 892–907.

Nair, S. S. and Sing, R. (1986), "Examination of the validity of proportional damping approximations with two further numerical indices", *Journal of Sound and Vibration*, **104**, pp. 348–350.

Nashif, A. D., Jones, D. I. G., and Henderson, J. P. (1985), *Vibration Damping*, John Wiley, New York.

Naylor, V. D. (1970), "Some fallacies in modern damping theory", *Journal of Sound and Vibration*, **11**, pp. 278–280.

Nelson, H. D. and Glasgow, D. A. (1979), "Eigenrelations for general second-order systems", *AIAA Journal*, **17** (7), pp. 795–797.

Newland, D. E. (1987), "On the modal analysis of nonconservative linear systems", *Journal of Sound and Vibration*, **112** (1), pp. 69–96.

Newland, D. E. (1989), *Mechanical Vibration Analysis and Computation*, Longman, Harlow and John Wiley, New York.

Nicholson, D. W. (1987a), "Response bounds for non-classically damped mechanical systems under transient loads", *Transaction of ASME, Journal of Applied Mechanics*, **54**, pp. 430–433.

Nicholson, D. W. (1987b), "Stable response of non-classically damped mechanical systems", *Applied Mechanics Reviews, ASME*, **40** (6), pp. 733–740.

Nicholson, D. W. and Baojiu, L. (1996), "Stable response of non-classically damped mechanical systems - ii", *Applied Mechanics Reviews, ASME*, **49** (10, Part-2), pp. S49–S54.

Nigam, N. C. (1983), *Introduction to Random Vibration*, The MIT Press, Cambridge, Massachusetts.

Oliveto, G. and Santini, A. (1996), "Complex modal analysis of a continuous model with radiation damping", *Journal of Sound and Vibration*, **192** (1), pp. 15–33.

Park, C. H., Inman, D. J., and Lam, M. J. (1999), "Model reduction of viscoelastic finite element models", *Journal of Sound and Vibration*, **219** (4), pp. 619–637.

Park, I. W., Kim, J. S., and Ma, F. (1992a), "On the modal coupling in non-classically damped linear systems", *Mechanics Research Communications*, **13**, pp. 407–413.

Park, I. W., Kim, J. S., and Ma, F. (1994), "Characteristics of modal coupling in non-classically damped systems under harmonic excitation", *Transaction of ASME, Journal of Applied Mechanics*, **61**, pp. 77–83.

Park, S., Park, I. W., and Ma, F. (1992b), "Decoupling approximation of non-classically damped structures", *AIAA Journal*, **30** (9), pp. 2348–2351.

Parter, G. and Sing, R. (1986), "Quantification of the extent on non-proportional damping discrete vibratory systems", *Journal of Sound and Vibration*, **104** (1), pp. 109–125.

Peres-Da-Silva, S. S., Cronin, D. L., and Randolph, T. W. (1995), "Computation of eigenvalues and eigenvectors of nonclassically damped systems", *Computer and Structures*, **57** (5), pp. 883–891.

Pilkey, D. F. and Inman, D. J. (1997), "Iterative approach to viscous damping matrix identification", in "Proceedings of the 15th International Modal Analysis Conference (IMAC)", volume 2, (pp. 1152–1157).

Pilkey, D. P. and Inman, D. J. (1998), "Survey of damping matrix identification", in "Proceedings of the 16th International Modal Analysis Conference (IMAC)", volume 1, (pp. 104–110).

Placidi, F., Poggi, F., and Sestieri, A. (1991), "Real modes computation from identified modal parameters with estimate of general damping", in "Proceedings of the 9th International Modal Analysis Conference (IMAC)", London.

Prells, U. and Friswell, M. I. (2000), "A measure of non-proportional damping", *Mechanical System and Signal Processing*, **14** (2), pp. 125–137.

Press, W. H., Teukolsky, S. A., Vetterling, W. T., and Flannery, B. P. (1992), *Numerical Recipes in C*, Cambridge University Press, Cambridge.

Rayleigh, Lord (1877), *Theory of Sound (two volumes)*, Dover Publications, New York, reissued 1945, second edition.

Ren, G. and Zheng, Z. (1997), "A quasi-decoupling approach for nonclassical linear systems in state-space", *Transaction of ASME, Journal of Applied Mechanics*, **64**, pp. 946–950.

Roemer, M. J. and Mook, D. J. (1992), "Mass, siffness and damping matrix identification: an integrated approach", *Transaction of ASME, Journal of Vibration and Acoustics*, **114**, pp. 358–363.

Rosa, L. F. L., Magluta, C., and Roitman, N. (1999), "Estimation of modal parameters through a non-linear optimisation technique", *Mechanical System and Signal Processing*, **13** (4), pp. 593–607.

Rossikhin, Y. A. and Shitikova, M. V. (1997), "Applications of fractional calculus to dynamic problems of linear and nonlinear hereditary mechanics of solids", *Applied Mechanics Reviews, ASME*, pp. 15–67.

Scanlan, R. H. (1970), "Linear damping models and causality in vibrations", *Journal of Sound and Vibration*, **13** (4), pp. 499–503.

Sestieri, A. and Ibrahim, R. (1994), "Analysis of errors and approximations in the use of modal coordinates", *Journal of Sound and Vibration*, **177** (2), pp. 145–157.

Shahruz, S. M. (1990), "Approximate decoupling of the equations of motion of damped linear systems", *Journal of Sound and Vibration*, **136** (1), pp. 51–64.

Shahruz, S. M. (1995), "Comments on 'an index of damping non-proportionality for discrete vibrating systems"', *Journal of Sound and Vibration*, **186** (3), pp. 535–542, letters to the editor.

Shahruz, S. M. and Ma, F. (1988), "Approximate decoupling of the equations of motion of linear underdamped system", *Transaction of ASME, Journal of Applied Mechanics*, **55**, pp. 716–720.

Shahruz, S. M. and Srimatsya, P. A. (1997), "Approximate solutions of non-classically damped linear systems in normalized and physical coordinates", *Journal of Sound and Vibration*, **201** (2), pp. 262–271.

Slater, J. C., Belvin, W. K., and Inman, D. J. (1993), "A survey of modern methods for modeling frequency dependent damping in finite element models", in "Proceedings of the 11th International Modal Analysis Conference (IMAC)", (pp. 1508–1512).

Soom, A. and Kim, C. (1983), "Roughness-induced dynamic loading at dry boundary-lubricated sliding contacts", *ASME Journal of Lubrication Technology*, **105**, pp. 514–517.

Starek, L. and Inman, D. J. (1997), "A symmetric inverse vibration problem for nonproportional underdamped systems", *Transaction of ASME, Journal of Applied Mechanics*, **64**, pp. 601–605.

Suarez, L. E. and Sing, M. P. (1987), "Eigenproperties of nonclassically damped primary structure and oscillator systems", *Transaction of ASME, Journal of Applied Mechanics*, **54**, pp. 668–673.

Suarez, L. E. and Sing, M. P. (1989), "Dynamic synthesis of nonclassically damped substructures", *ASCE Journal of Engineering Mechanics*, **115** (1), pp. 52–70.

Tan, G. B. (1997), *Non-Linear Vibration of Cable-Deployed Space Structures*, Ph.D. thesis, Cambridge University Engineering Department, Cambridge, UK.

Thomson, W. T., Calkins, C., and Caravani, P. (1974), "A numerical study of damping", *Earthquake Engineering and Structural Dynamics*, **3**, pp. 97–103.

Tong, M., Liang, Z., and Lee, G. C. (1992), "On non-proportionality of generally damped systems", in "Proceedings of the 10th International Modal Analysis Conference (IMAC)", San Diego, CA, USA, (pp. 1302–1308).

Tong, M., Liang, Z., and Lee, G. C. (1994), "An index of damping non-proportionality for discrete vibrating systems", *Journal of Sound and Vibration*, **174**, pp. 37–55.

Torvik, P. J. and Bagley, R. L. (1987), "Fractional derivatives in the description of damping: materials and phenomena", in "The Role of Damping in Vibration and Noise Control", ASME DE-5, (pp. 125–135).

Udwadia, F. E. and Esfandiari, R. S. (1990), "Non-classically damped dynamic systems: An iterative approach", *Transaction of ASME, Journal of Applied Mechanics*, **57**, pp. 423–433.

Ungar, E. E. (1973), "The status of engineering knowledge concerning the damping of built-up structures", *Journal of Sound and Vibration*, **26**, pp. 141–154.

Ungar, E. E. (2000), "Damping by viscoelastic layers", *Applied Mechanics Reviews, ASME*, **53** (6), pp. R33–R38.

Ungar, E. E. and Kerwin, E. M. (1962), "Loss factors of viscoelastic systems in terms of energy concepts", *The Journal of the Acoustical Society of America*, **34** (7), pp. 954–957.

Veletsos, A. S. and Ventura, C. E. (1986), "Modal analysis of non-classically damped linear systems", *Earthquake Engineering and Structural Dynamics*, **14**, pp. 217–243.

Vigneron, F. R. (1986), "A natural modes model and modal identities for damped linear structures", *Transaction of ASME, Journal of Applied Mechanics*, **53**, pp. 33–38.

Warburton, G. B. and Soni, S. R. (1977), "Errors in response calculations for non-classically damped structures", *Earthquake Engineering and Structural Dynamics*, **5**, pp. 365–376.

Woodhouse, J. (1998), "Linear damping models for structural vibration", *Journal of Sound and Vibration*, **215** (3), pp. 547–569.

Yae, K. H. and Inman, D. J. (1987), "Response bounds for linear underdamped systems", *Transaction of ASME, Journal of Applied Mechanics*, **54**, pp. 419–423.

Yang, B. (1993), "Exact receptances of non-proportionally damped dynamic systems", *Transaction of ASME, Journal of Vibration and Acoustics*, **115**, pp. 47–52.

Yang, B. and Wu, X. (1998), "Modal expansion of structural systems with time delays", *AIAA Journal*, **36** (12), pp. 2218–2224.

Zhou, K., Doyle, J. C., and Glover, K. (1995), *Robust and Optimal Control*, Prentice-Hall Inc, Upper Saddle River, New Jersey 07458.

Zienkiewicz, O. C. and Taylor, R. L. (1991), *The Finite Element Method*, McGraw-Hill, London, fourth edition.